ABSTRACT

Title of Document: INTEGRATED METHODOLOGY FOR THERMAL-HYDRAULICS UNCERTAINTY ANALYSIS (IMTHUA)

MOHAMMAD POURGOL-MOHAMAD, DOCTOR OF PHILOSOPHY 2007

Directed By: PROFESSOR MOHAMMAD MODARRES, MECHANICAL ENGINEERING DEPARTMENT
PROFESSOR ALI MOSLEH, MECHANICAL ENGINEERING DEPARTMENT

This dissertation describes a new integrated uncertainty analysis methodology for "best estimate" thermal hydraulics (TH) codes such as RELAP5. The main thrust of the methodology is to utilize all available types of data and information in an effective way to identify important sources of uncertainty and to assess the magnitude of their impact on the uncertainty of the TH code output measures. The proposed methodology is fully quantitative and uses the Bayesian approach for quantifying the uncertainties in the predictions of TH codes. The methodology also uses the data and information for a more informed and evidence-based ranking and selection of TH phenomena through a modified PIRT method. The modification considers importance of various TH phenomena as well as their uncertainty importance. In identifying and assessing uncertainties, the proposed methodology treats the TH code as a white box, thus explicitly treating internal sub-model uncertainties, and propagation of such

model uncertainties through the code structure as well as various input parameters. A The TH code output is further corrected through a Bayesian updating with available experimental data from integrated test facilities. It utilizes the data directly or indirectly related to the code output to account *implicitly* for missed/screened out sources of uncertainties. The proposed methodology uses an efficient Monte Carlo sampling technique for the propagation of uncertainty using modified Wilks sampling criteria. The methodology is demonstrated on the LOFT facility for 200% cold leg LBLOCA transient scenario.

INTEGRATED METHODOLOGY FOR THERMAL-HYDRAULICS UNCERTAINTY ANALYSIS (IMTHUA)

By

Mohammad Pourgol-Mohammad

Dissertation submitted to the Faculty of the Graduate School of the
University of Maryland, College Park, in partial fulfillment
of the requirements for the degree of
Doctor of Philosophy
2007

Advisory Committee:
Professor Mohammad Modarres (Co-Advisor), Co-Chair
Professor Ali Mosleh (Co-Advisor), Co-Chair
Professor Marino di Marzo
Associate Professor Gary A. Pertmer
Professor Gregory Baecher

TABLE OF CONTENT

TABLES

FIGURES

DEDICATION

To my parents

,

To Farrin for your understanding and support throughout

and

To Our Beloved Children Amin and Sara

ACKNOWLEDGEMENTS

I hereby would like to thank everybody that has helped me through process of this dissertation. I would like to express my deepest appreciation to my advisors Professor Mohammad Modarres and Professor Ali Mosleh for their helpful guidance all through the research. Dr. Modarres supported the research with his engineering solution when research was stuck in some complicated conditions. Professor Mosleh supported the research with his modeling solutions. The research could not get to this point without his ideas. I am thankful to them for their patience with me, technical guidance, academic stimulation, insightful comments and interest in my personal welfare throughout the course of my graduate study at the University of Maryland.

I also greatly appreciate the technical and financial support provided by the United States Nuclear Regulatory Commission (NRC), and express my gratitude for the technical support of many individuals from NRC, particularly Mr. Todd Hilsmeier, Dr. Joe Kelley, Dr. Stephan Bajorek, Dr. Arthur Buslik and Dr. Mirela Gavrila.

I am grateful to the members of my dissertation committee for consenting to serve. A special thanks to Dr. di Marzo. He has been extremely supportive throughout and has contributed significantly to my understanding of the Thermal-Hydraulics phenomena. Professor Bilal Ayyub provided guidance in understanding modeling, and uncertainty analysis, especially non-probabilistic approaches. Special thanks also to Dr. Chris Alison and Mr. Richard Wagner from, ISS INC, Idaho Falls for helping to understand RELAP5 code structure. Thanks to Dr. Birol Baktas from ISL Inc (currently with GE Nuclear) for the opportunity to become familiar with TRACE

code. Thanks to my fellow friend Reza Azarkhail for his helps. He was always patient to listen to the problem and his solutions helped a lot.

Above all I thank God whose goodness and love enabled me to achieve this important milestone. My family prayed for me throughout and the difficulties that we have faced have made us stronger. To Farrin, Amin and Sara I love you all and look forward to playing a more fulsome role in your lives once again.

NOMENCLATURE & ABBREVATIONS

AHP	Analytic Hierarchical Process
BWR	Boiling Water Reactor
CABUE	Code Accuracy Based Uncertainty Methodology
CSAU	Code Scaling, Applicability and Uncertainty Evaluation
CFT	Critical Flow Test
ECCS	Emergency Core Cooling System
EES	Engineering Equation Solver
FFTBM	Fast Fourier Transform Based Method
GRS	Gesellschat Fur Anlagen- und Reaktorsicherheit
HPIS	High Pressure Injection System
HTC	Heat Transfer Coefficient
IMTHUA	Thermal-Hydraulics Uncertainty Study
INEEL	Idaho National Engineering Laboratory
ISP	International Standard Problems
ITF	Integrated Test Facility
LBLOCA	Large Break Loss of Coolant Accident
LOCA	Loss of Coolant Accident
LOFT	Loss-of-Fluid Test
LPIS	Low Pressure Injection System
MCMC	Markov Chain Monte Carlo

NPP	Nuclear Power Plant
PCT	Peak Clad Temperature
PDF	Probability Distribution Function
PIRT	Phenomena Identification and ranking Table
PWR	Pressurized Water Reactor
RELAP	Reactor Excursion and Leak Analysis Program
SBLOCA	Small Break Loss of Coolant Accident
SET	Separate Effect Test
TH	Thermal-Hydraulics
TRAC	Transient Reactor Analysis Code
TRACE	TRAC/RELAP Advanced Computational Engine
UMAE	Uncertainty Analysis Methodology based on Accuracy Extrapolation
USNRC	United States Nuclear Regulatory Commission

CHAPTER 1: INTROCTION

1.1 Problem Statement

The USNRC has revised the ECCS licensing rules in 1989 to allow the use of "best estimate" (USNRC 1988, USNRC 1989) computer codes such as Relap5, TRAC, and recently consolidated TRACE code. This requires explicit quantitative assessment of the uncertainties of the TH calculations in the licensing and regulatory processes. Properly integrating various types of information available (input, code structure, and output of the code) leads to TH best-estimates along with formal characterization of associated uncertainties. In a risk-informed regulatory environment, such a best-estimate and formal characterization of all available information helps the decision makers to better appreciate the ranges of uncertainty, given all available information, and the impact it might have on the decision. Uncertainty analysis methodology in complex system models requires a comprehensive treatment of many uncertainty sources. All sources of uncertainties should be ideally considered in the analysis explicitly, but this is not practical considering complexities. The nature and availability of various types of information and data, and variety of uncertainty sources, add more complexity to the uncertainty assessment.

The aim of this research is to develop an integrated methodology for TH uncertainty quantification with effective utilization of available knowledge and information in qualified and quantified format. Among the TH uncertainty methodologies developed over last two decades, several include integrated methodologies for uncertainty analysis (Technical Program Group 1989, Glaeser 1998, D'Auria 1998a), while

others have focused either on improving specific aspects of an existing methodology or have added new features (D'Auria et al. 1998, D'Auria et al. 2006) As part of the research leading to the development of the method proposed in this dissertation, extensive literature review was conducted to evaluate the merits and limitation of the proposed methods with the objective of incorporating the best features into a new, more comprehensive method. An overview of specification of existing methodologies with a comparison with methodology developed in this research will be given in next chapter later.

1.2 Approaches to Managing Code Uncertainty in Safety Context

Different approaches in the context of safety analysis of the nuclear power plants can be divided into conservative and best estimate methodologies. In 1988, the NRC approved (USNRC 1988) a revised rule for the acceptance of ECCS followed by a guidance for the use of best estimate codes. The word uncertainty is connected with the use of best estimate codes. Experimental research and advanced computer code development brought enough confidence to USNRC to adopt such changes.

1.2.1 Conservative Methods

To assure the safety of the early reactors, safety analyses were based on what were considered very conservative assumptions for the analysis models used to calculate the thermal-hydraulic performance of the ECCS. This was done to be on the safe side given the large uncertainties in the computer models used for design and licensing (Wallis and Ransom 2002). Conservative codes such as RELAP4 were developed with such conservative boundary and initial condition and conservative assumptions

on systems availability. Examples of conservative assumptions are the requirements of Appendix K of 10CFR 50.46 of the USNRC (Code of Federal Regulation 2003). Appendix K prescribes required features and acceptable features of ECCS evaluation models for demonstrating conformance with 10CFR 50.46. These features in essence assure that the values of the ECCS performance figures of merit, such as peak cladding temperature (PCT) are bounded. (Orechwa 2004)

There are several problems using this type of analysis, including predicting unrealistic physical behavior, changed order of events, and unknown level of conservatism. From high experimental data collection experiences, and understanding abnormal behavior of nuclear facilities, the conservative approach is proven to be undesirable. Conservative-best Estimate (partially conservative) methods and pure best estimate became viable alternative as new information from operating experience and ECCS research accumulated and shed light on safety margins. Consequently revisions of the decision rules became possible. It was argued in the OECD/NEA (1994) that conservative assessment of uncertainties does not necessarily result in safer assessment of uncertainties. The reasons for switching to best-estimates approaches were summarized by Orechwa (2004).

1.2.2 Best-Estimate Methods

Best estimate analysis provides a good picture of the existing safety margins with best estimate system code, realistic initial/boundary conditions. Availability of information and data about every contributor in the simulation requires its consideration. This approach takes into account the new information in the form of best-estimate models and estimates uncertainty with which the code calculates the

true transient, the input and plant parameter uncertainties, and the nuclear parameter uncertainties. It requires considering all information about all parameters and variables. As such, research advances allow us to go beyond Appendix K procedures which result in highly conservative values for the PCT of the limiting transient.

Approach used in best estimate analysis is to compute for example peak cladding temperature BE-PCT that bounds a pre-specified list of all LOCAs for the reactor design at hand. The computation of the BE-PCT has three basic ingredients (Orechwa 2004).

1. The computation of PCT for the limiting transient with best estimate models, as opposed to Appendix K specified models, which we denote as PCT_{BE}.
2. An estimate of a systematic uncertainty associated with the BE models as opposed to Appendix K specified models. This uncertainty we compute as $\Delta PCT_{sys} = [PCT_{Realistic+Appendix\ K} - PCT_{BE}]$. The value of $PCT_{Realistic+Appendix\ K}$ uses realistic models augmented with the required features of Appendix K. This value is usually limited to values between LPCT and $PCT_{Appendix\ K}$.
3. An estimate of a random uncertainty due to uncertainties in the plant parameters, which we compute as $\Delta PCT_i = PCT_{i\text{-th perturbed parameter}} - PCT_{nominal}$. BE-PCT is then computed as $BE\text{-}PCT = PCT_{BE} + k[(\Delta PCT_{sys})^2 + \Sigma(\Delta PCT)^2]^{1/2}$, where k defines the fraction (usually 0.95) of all LOCAs with PCTs bounded by BE-PCT. This is the specific methodology based on surface response as implemented in original CSAU. IMTHUA found the BE method with realistic models and assumptions a superior way to represent uncertainties in the TH code results. The way of uncertainty propagation is differed from the original approach by

implementing a Monte Carlo based statistical method for propagation of uncertainties.

1.2.3 Best Estimate mixed with conservative assumptions

Use of best estimate code using full or partially conservative boundary/initial conditions (BIC) is the essence of this approach. This is the approach used by Westinghouse in their ASTRUM uncertainty analysis methodology. This methodology considers conservative assumption on some of BICs such as burn-up rate set to its highest value e.g., fresh fuel (Nissley et al. 2004)). Difficulties with pure best estimate approaches motivated utilities and licensees to use partially conservative methods. Difficulties with pure BE analysis are in quantifying code uncertainties sufficiently for every phenomenon, and all accident scenarios.

1.3 Efforts to Develop Formal TH Codes Uncertainty Analysis

Over the past 20 years a number of research and development efforts have lead to the development of half a dozen methods for more comprehensive treatment of uncertainties in TH codes. The major methods are briefly described in the following, and classified later.

1.3.1 GRS Methodology

The GRS methodology considers the effect of uncertainty of input parameters like code models coefficients, initial and boundary conditions, other application specific input data and solution algorithm on the calculation results. Detail of methodology was published in NEA-CSNI report (Glaeser et al 1998). Following steps describes the methodology:

1. Identification of all potentially important phenomena, modeling assumptions, and parameters.
2. Representation of all uncertainty sources by uncertain parameters.
3. Quantification of the state of knowledge of parameters by adequate probability distributions
4. Measures of dependence interpreted based on the subjectivist probability concept.
5. Generation of a random sample according to a joint probability distribution

   Performance of TH model runs
6. Each sample element generated under 4 is propagated through the thermal-hydraulics model. After the propagation of all sample elements, a random sample of TH model results is available.
7. The sample for each model result is from the unknown probability distribution of the model result.
8. Quantification of the uncertainty in the model results; Moments and quantiles of the unknown (subjective) probability distribution of the model result under 5. The uncertainty in the model result may be quantified in terms of Utilizing Wilks' Tolerance Interval Method. (Kloos 2006)

GRS methodology has a powerful statistical framework for uncertainty propagation through code calculation using through order statistics based tolerance limit known as Wilks formula. Most engineering methodologies developed recently by the industry such as by AREVA (Martin 2005) and Westinghouse (Nissley 2004) have adopted this methodology as part of their TH uncertainty analysis.

1.3.2 CSAU Methodology

Flow chart of USAU methodology is shown in Figure 1. It includes Element 1: requirement and code capabilities, Element 2: assessment and ranking of parameters, and Element 3: sensitivity and uncertainty analysis. The methodology considers various sources of uncertainty in TH codes such as use of one-dimensional models, time and space averaging (use of relatively big nodes dominating some microscopic scale phenomena,) input-related uncertainties. The methodology uses a systematic way (i.e., PIRT) to identify sources of uncertainty in conceptual phenomenological level. Uncertainty is treated qualitatively as well as quantitavely to consider all sources of information. Applicability of the TH code for a specific safety study of a particular scenario (Boyack B.E., at el 1990) and other qualified steps are part of model uncertainty treatment.

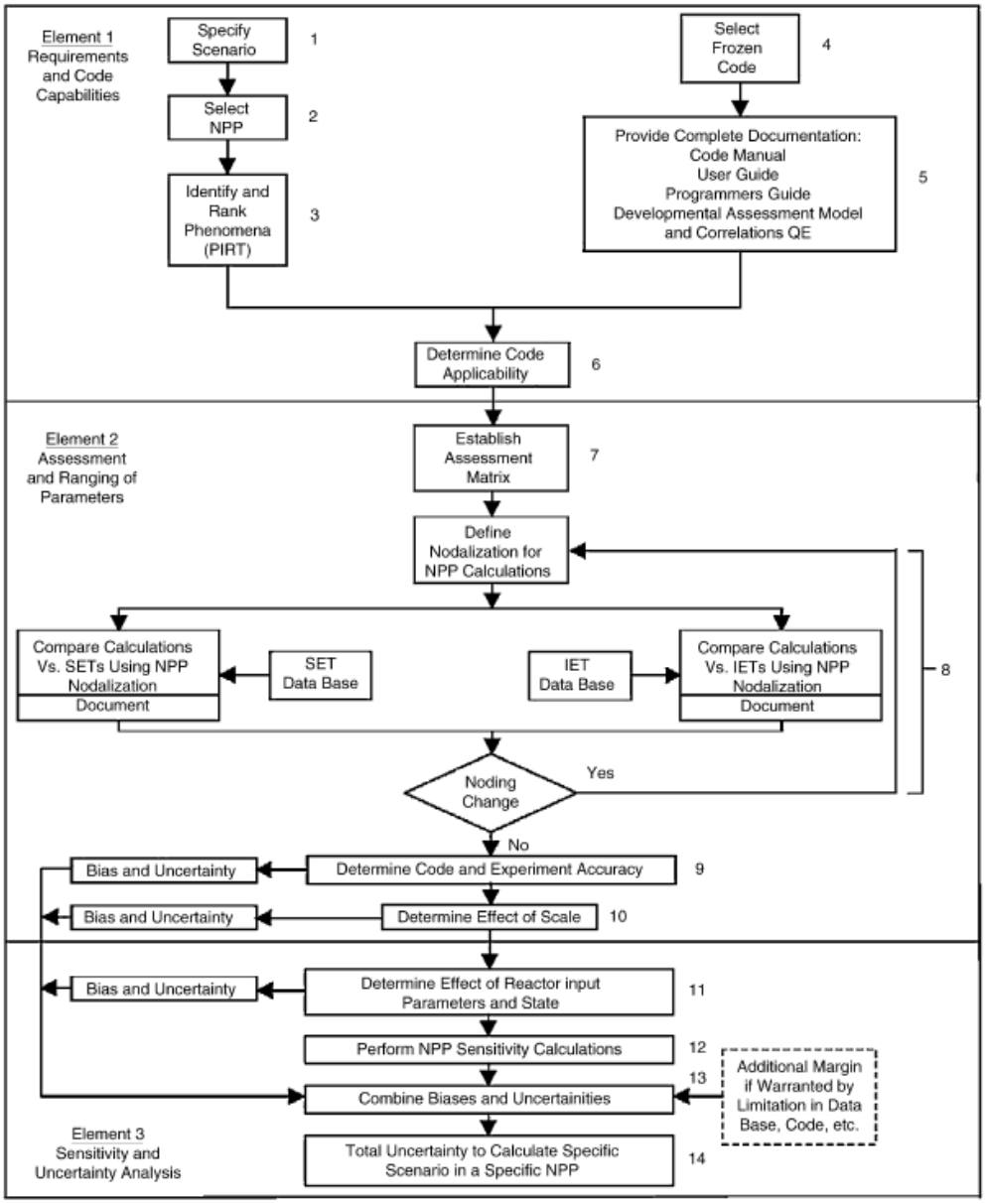

Figure 1: CSAU Methodology Flow Chart (Boyack at el 1990)

1.3.3 ASTRUM-Westinghouse

Steps of ASTRUM are listed in Table 1. As can be seen, ASTRUM is very similar to CSAU with the differences in statistical approach including Wilks tolerance limit method to propagation and inference about code output uncertainty.

Table 1: ASTRUM-Westinghouse Methodology Steps

Step 1: Scenario Specification
Step 2: Nuclear Power Plant Selection
Step 3: Phenomena Identification and Ranking
Step 4: Frozen Code Selection
Step 5: Provide Complete Documentation
Step 6: Code Applicability Determination
Step 8: Define Nodalization
Step 9: Determine Code and Experiment Accuracy
Step 10: Determine Effect of Scale
Step 11: Determine Effect of Reactor Input Parameters and State
Step 12: Perform NPP Sensitivity Calculations
Step 13: Combine Biases and Uncertainties
Step 14: Calculate Total Uncertainty

1.3.4 UMAE Methodology

As shown in Figure 2, basic idea of UMAE methodology is the use of the accuracy in output results from the comparison of measured and calculated trends of relevant experiments and calculations, respectively. The experiment must come from relevant facilities and the calculation results from qualified codes and nodalization (both in steady state and transient) based on the data base. The need for selection of input uncertainties is ignored with these qualifications. Results of accuracy based comparison between measured and calculated trends are extrapolated. UMAE

methodology was recently implemented on the Relap5 code enabling the code for internal uncertainty quantification. It is called CIAU (D'Auria and Marsini 2000, D'Auria and Giannotti 2000, and Madeira et al. 1999). Figure 2 shows the simplified flow chart for the UMAE methodology with emphasize on role of SET and ITF test data for qualification and calculation of accuracy values for different scales test facilities respectively.

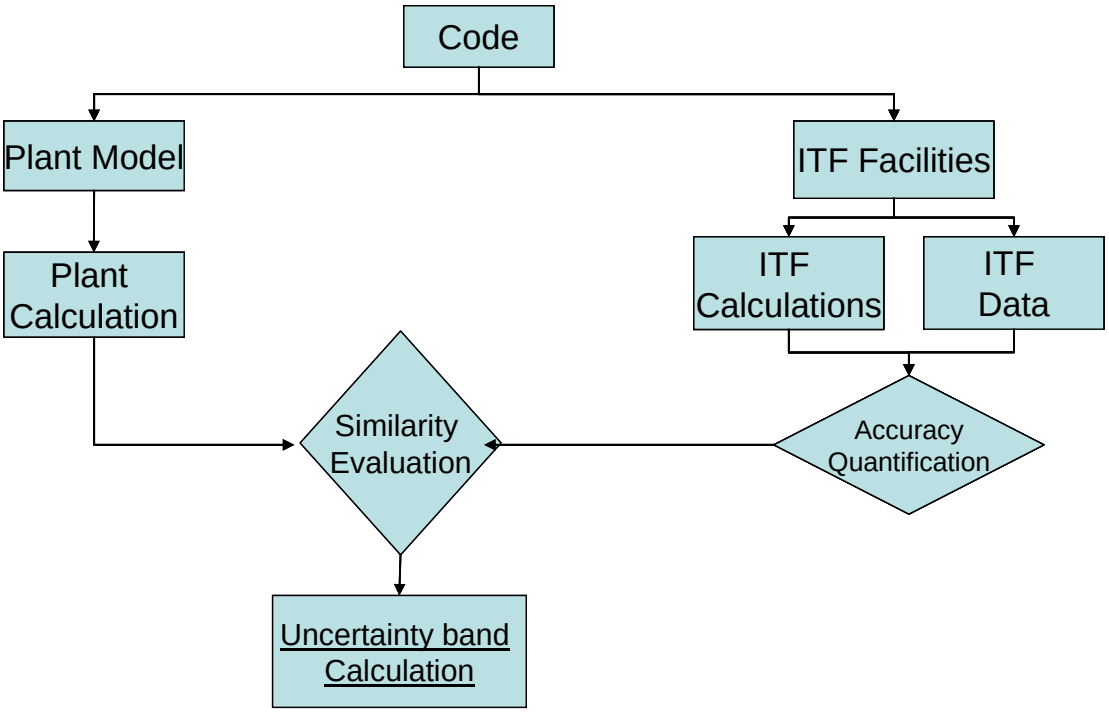

Figure 2: Flow Chart for UMAE methodology

Figure 3 demonstrates calculation of uncertainty bands based on time and magnitude errors. The temporal uncertainty is a desirable specification in this method and is recommended for other methodologies too.

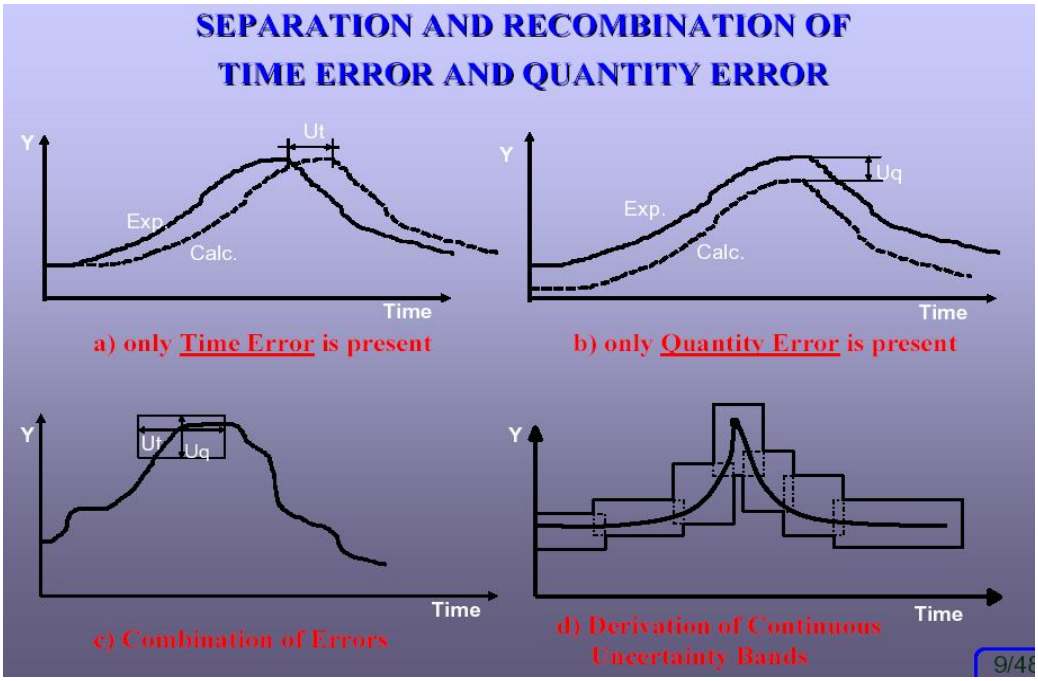

Figure 3: End Results of Uncertainty Quantification by UMAE (D'Auria and Giannotti 2000)

1.3.5 CABUE Methodology

CABUE is a systematic methodology (Lee and Han 2004) for comparison of data from integral and separate effect tests in determining the code uncertainty. CABUE methodology is based on the results of code accuracy to quantify code uncertainty. Code accuracy plays a role on the selection of code parameters and the determination of their ranges. Application of the methodology is demonstrated in reference (Lee and Han 2004) for a three loop Westinghouse nuclear power plant.

1.4 An Assessment of the Current Uncertainty Analysis Methodologies

A systematic uncertainty analysis provides insight into the level of confidence in model estimates. Comprehensive uncertainty analysis methodology in complex

system models require treatment of all, or at least important sources of uncertainty, considering available information. Complexity of systems and their models with dependency of processes and phenomena lead to insufficient understanding of simulation code behavior and predictions. The method should be general, applicable to wide range of scenarios, and efficient with respect to cost and resources. Availability of information and data plays an important role in quantifying uncertainty. Precise quantification of uncertainty given available evidence requires a formal and comprehensive analysis methodology. The methodology should consider uncertainties in input (broadly defined), models (individual models and sub-models and interaction between models) and uncertainty in the output based on integral performance information independent of the data used in assessing input variables.

As there are too many TH phenomena that can contribute to uncertainties, with limitation in resources and knowledge it is neither possible nor practical to explicitly factor the impact of all such phenomena on output uncertainty. Implementation of a screening procedure however raises some serious questions about influence of sources of uncertainties not considered. It is understood that plant behavior is not equally influenced by all processes and phenomena that occur during a transient. It is also obvious that different sources of uncertainties such as the user effects, operation conditions, and internal models do not have equal influence. CSAU and some other methodologies try to reduce the analysis effort to a manageable set of phenomena (e.g., from around 50 to 5-6). If each of the screened out phenomena has about 2-5% contribution to the total output uncertainty, their cumulative effect is almost equal to

that of the important ones. This is an issue that needs to be addressed in the methodology.

Available information should be manipulated precisely. Credibility, form, and relevance of data, should be considered in the analysis. Inference about physical models from experiments, credibility assessment, and value of parameters and relevance of information require fairly sophisticated methodologies such as Bayesian methods. The methodology should be applicable to a wide range of scenarios and applications, and not tightly linked to peculiarities of specific cases. Currently the broad applicability of available methodologies has not been demonstrated. Finally, method for the assessment and propagation of uncertainties must be efficient with reasonable demands on cost and available resources

Table 2 provides a characterization of the above TH uncertainty quantification methodologies, based on their treatment of input, propagation through models, and output. The methodology proposed by this dissertation is also assessed in this table.

Table 2: Comparison of IMTHUA, GRS, CSAU, UMAE, and W-House Methodologies

		IMTHUA	GRS	CSAU	UMAE	W-House
Input	Parameters	Use of Data Probabilistic Method	Expert Judgment	Use of Data Probabilistic Method	NA	Use of Data Probabilistic Method
	Models	Expert Judgment Corrective Factors/ Bias	Expert Judgment	Correction factors	NA	Correction factors
	Restriction on the No. of Input Parameters	N	N	Y	NA	N
	Dependency of No. of Code Runs to No. of	N	N	Y	NA	N
	Dependency Consideration	Y	N	N	NA	N
	Input Uncertainty Assignment	Maximum Entropy	Expert Judgment	Expert Judgment	NA	Expert Judgment
Propagation	Parameters	95|95 Wilks Tolerance Limit	95|95 Wilks Tolerance Limit	Response Surface	NA	95|95 Wilks Tolerance Limit
	Models	95|95 Wilks Tolerance Limit	95|95 Wilks Tolerance Limit	NA	NA	95|95 Wilks Tolerance Limit
Output	Parameters	NA	NA	NA	NA	NA
	Models	Use of Integral Data Bayesian Framework	NA	NA	Accuracy Based Uncertainty	NA
	Consideration for Missed/Screened Out Models	Y	N	N	Y	N

In an international benchmark exercise 5 methodologies including some of the methods reviewed above were applied for a specific problem (small break LOCA experiment in the LSTF test facility) and compared against actual experimental measurements (CSNI-NEA 1998). The results are shown in Figure 4. While in this particular exercise some methodologies performed better than others, defining the criteria for quality and performance of an uncertainty methodology is not a trivial matter. For instance one would need to have an assessment of the extent that a method uses the available information in all its forms and sources. In other words it is sufficient to use the size and location of uncertainty ranges generated by various methodologies as a performance measure since in some cases broader range of uncertainty may be more consistent with the available information. Addressing this question was one of the purposes of this research. .

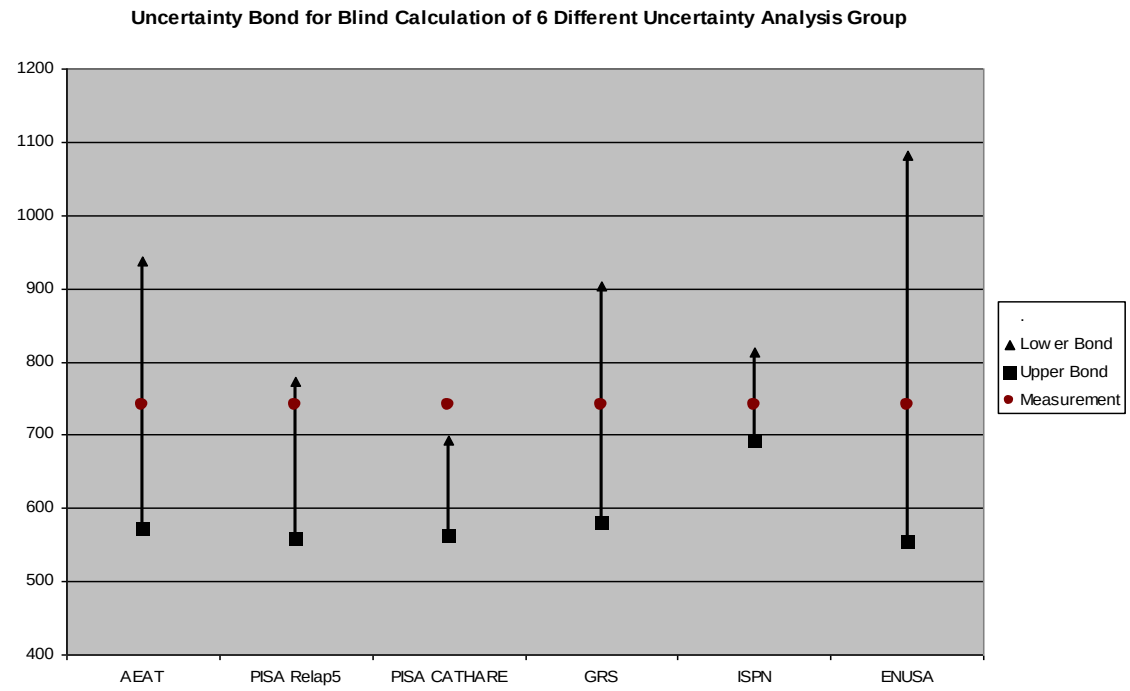

Figure 4: Comparison of Models End Results

With respect to the use of information and then stage at which uncertainty is quantified, the existing methodologies are either input-driven or output-driven or a mix. Figure 5 demonstrates schematically methodologies based on input sources of uncertainties.

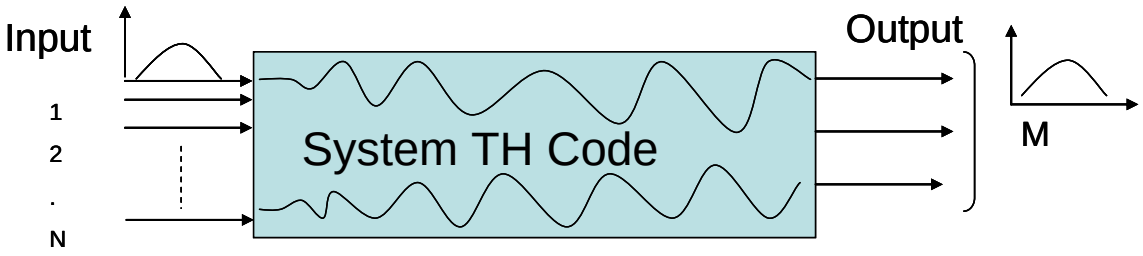

Figure 5: A Schematic Illustration of Input Based Uncertainty Analysis Methodologies

In output-driven methods inaccuracies of calculations are characterized by comparing measured and calculated output as shown schematically in Figure 6.

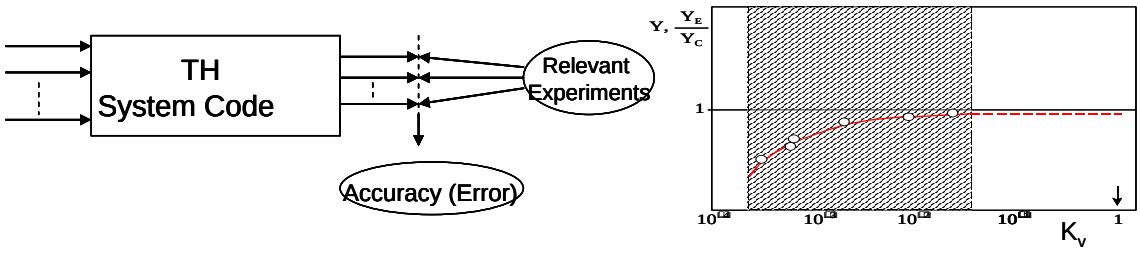

Figure 6: A Schematic Illustration of Output Based Uncertainty Analysis Methodologies

Examples of input-driven methods are CSAU (Technical Program Group 1989) and GRS (Glaeser 1998), while the UMAE method (D'Auria 1998) is essentially an output-driven method. Other methods are mainly variations of the basic ideas of the above approaches. D'Auria (1998, 2006) has compared different TH uncertainty analysis methodologies based on different features and their capabilities. Existing output-based methods can not distinguish uncertainty contribution of the individual uncertainty sources, require significant amount of experimental data, and do not provide a conceptual and methodic base for generalization beyond the cases studied. Input-based methods on the other hand may not be sufficient and comprehensive due to initial screening of phenomena and parameters, intentionally limiting the scope (e.g., not considering "user effects"), and the issue of unknown phenomena or incomplete spectrum of alternative models.

Among many technical challenges encountered in uncertainty analysis of TH computational codes are: (1) the use of various subjective information and experimental data to assess the uncertainty about performance of the internal models (sub-models and correlations), (2) the integration of sub-model uncertainties into an overall uncertainty of the predictions of the code, and (3) complexity of system code with too many dynamic models and correlations. For example in dealing with model

uncertainty (as opposed to parameter uncertainty), the typical "white box" decomposition approach will be inadequate without correction for "missing models" in addition to alternative models. There are other issues which have not also properly been addressed in the past. These include mixing of aleatory and epistemic uncertainties, and proper representation of uncertainty in the temporal output retaining physical meaning.

The existing methodologies suffer from some combination of the following limitations:

- Black Box approach (inability to explicitly consider internal sub-model uncertainties)
- Not capable of comprehensively using all available data and information
  - Prior knowledge and information
  - Test and field data from different sources

and specifically in case of CSAU (Technical Program Group 1998) and recently released ASTRUM methodology developed by Westinghouse (Nissley et al. 2004 and Young et al.):

- Ignoring the effect of nodalization and user effects on uncertainty
- Eliminating too many TH phenomena as sources of uncertainty in ranking process.
- Excessive use of biases to account for code deficiencies
- Reliance on holistic engineering judgment

1.5 Challenges for Uncertainty Analysis in Complex Computational Codes

While complex TH codes pose similar complexities as any other large computer codes, there are also technical challenges unique to them. Some of these are summarized below:

1. Averaging procedures mask the capability to resolve phenomena in a microscale sense. Thus phenomena such as turbulent fluctuations will either be ignored or integrated into correlations. Only the average three dimensional, time-varying characteristics of the flow over a scale dictated by the size of the mesh cells can be retained CSNI-NEA (1994).

2. In earlier two-phase models the fluid was treated as a homogeneous mixture of liquid and vapor and consequently only three conservation equations were needed to describe the two phase flow. In the homogeneous equilibrium model the phases are assumed to move with the same velocity and also exist at the same temperature. An extension to the mixture model is the drift flux model in which the relation between the phasic velocities is described through an algebraic equation, thus allowing for slip between the phases. In recent models the conservation equations are set up for each phase separately, and six equations are used (two-fluid two-phase flow models). Additional equations can be incorporated in the models to account for liquid solutes and non-condensable gases. The significant property of the two-fluid model is that it allows the two phases to have different velocities and temperatures. Consequently this type of model has the potential to calculate the effects of phase separation and thermal non-equilibrium.

3. The two-phase flow model is in most cases simplified to be a one-dimensional model whether it is a mixture or two-fluid model. Then possible three dimensional effects can not be taken into account, but have to be included by means of special process models (for example special models for simulating the phenomena associated with sub-cooled ECC injection into a voided pipe) and by simulating the actual flow path by the appropriate connections of a number of one-dimensional flow paths.

4. There are two-phase models that retain some three-dimensional characteristics, although simplifications in the equations are usually introduced in order to make system calculations practical. Despite of the simplifications, these models have the potential to simulate three-dimensional effects which can be most important, for example, in some time windows of a large break LOCA, where flow re-distributions are supposed to occur in the reactor vessel.

5. The numerical algorithms for solving the set of finite difference equations will in many cases influence the results of the solution. For instance it is well known that a first order upstream difference scheme that is used in many codes for the flux terms has a tendency to smooth out flow property changes along the flow direction (numerical diffusion). This type of influence from the numerics is not treated in this research but one has to realize its existence and be aware that the result of a simulation can be distorted by numerics shortcomings.

6. In order to solve the set of finite difference equations, closure or constitutive equations are required, along with relations describing the steam-water properties under different conditions. In this context the steam-water properties are assumed to be well known for most of the application ranges. Associated tables and functions are

supposed to be adequately programmed in any of the used codes. The same is also assumed to be true for needed derivatives of the properties.

-Scope and objectives for uncertainty analysis

-Difficulties in recognition between inputs, interim inputs and Latent data

-Difficulties in assessment of some inputs; they appear in some equations as input parameters and in other equations as dependent variables. Inter-dependencies between parameters in arrangement are shown in Figure 7.

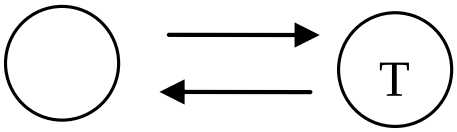

Figure 7: Interdependency between parameters and variables

The figure shows the relations of $f(T)$ and T $g(\ )$ where and T are two variables of the computational code. Many input variables of the code calculation are not independent inputs. Most of correlations coefficients have such nature and require special treatment.

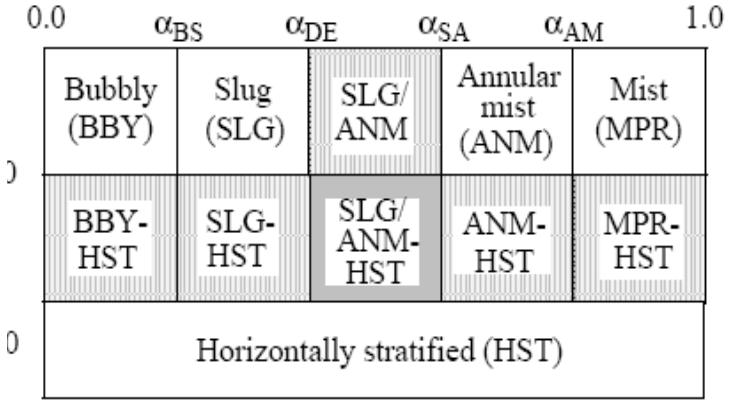

Figure 8: Horizontal flow phase change Based of void fraction and flow velocity

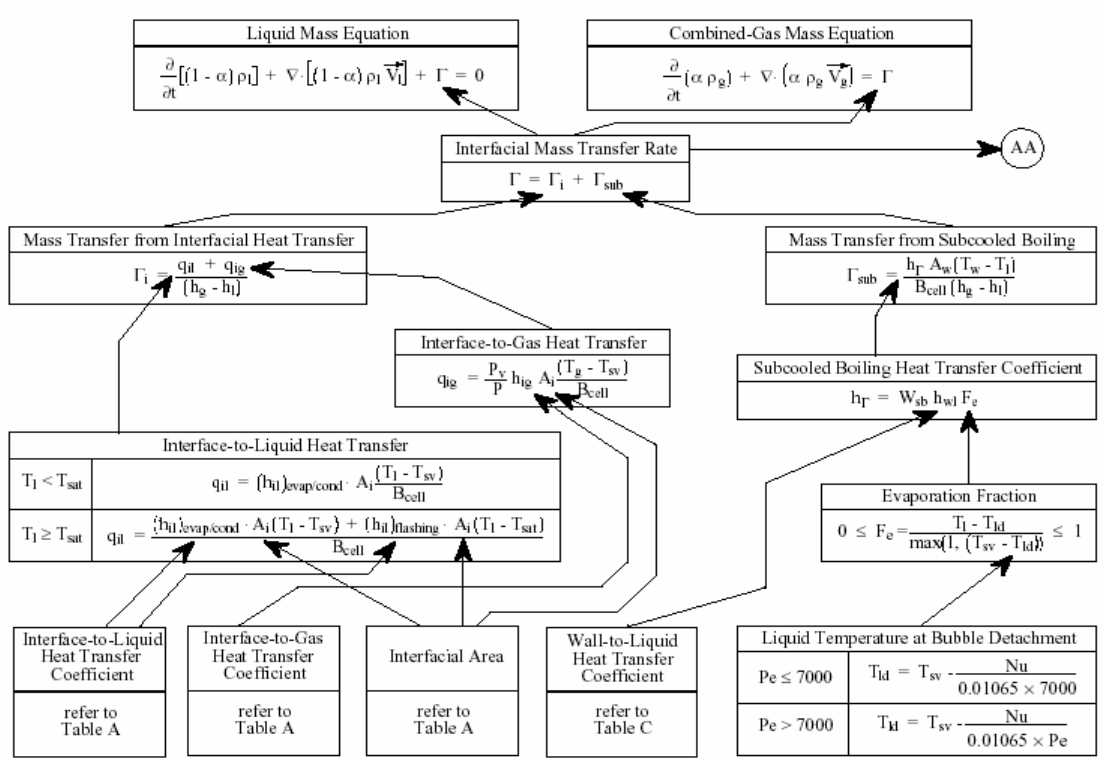

Figure 9: Code structure for Mass conservation equation with relevant constitution equations

It is clear that complex configuration as shown in Figure 9 for mass conservation equation solution (refer to code manuals Relap5 Code Development Team, 2001, for other conservation equation solution flowchart) and many other dependencies between parameters in dynamic environment influence uncertainty characterization in code calculation. Format of correlation and models for specific phenomenon is different by changing in flow regime as discussed for horizontal regimes in Figure 8. Finally, all of them result in a imperfect computational code with shortcomings in calculation. Some of those are shown in Table 3.

Table 3: Examples of Code Deficiencies (Relap5 Team 2003)

Reflood	Delayed quenching, high pressure spikes and oscillations during reflood, and incorrect void profile and vapor cooling in dispersed flow. Shortcomings in the description of the heat transfer within the liquid core, the use of certain correlations

	outside the range of there validity
Subcooled Boiling	Void fraction for the case of low pressures is overpredicted. The over prediction of the void fraction is attributed to a deficiency in the interphase heat transfer model ("umbrella" model)
Condensation (Wall and Interfacial)	Over prediction the number of relief valve cycles occurring during the transient (inadequacies in the wall and steam-water interface condensation model) (SGTR Case)
Interphase Drag	Deficiencies Associated with interphase drag model

Uncertainties come from different sources in TH calculation. Table 4 lists code model uncertainty-related sources affecting overall TH code calculations. Their impacts on the output results are different from scenario to scenario, plant to plant, as well as for a specific scenario. They also impact differently for different phases of scenario and figure of merits.

Table 4: Code Model Uncertainties

Plant Physical Description
Dimensions Uncertainties; Geometries
Code Input
Wall Surface Area, Cell Volume, Hydraulic Diameter, Power
Flow resistance; surface roughness
Problem Boundary Condition
Break Location
Break Type (DEGB or Split)
Break Size (Small, Medium, or Large)
Offsite Power
Safety Injection Flow
Safety Injection Temperature
Safety Injection Delay
Containment Pressure
Rod Drop Time

Code structure model uncertainties are classified in following 3 categories as:

a. Thermodynamic and Transport Fluid Properties

Density, Viscosity, Thermal conductivity , Internal energy

Enthalpy for the Liquid, Vapor, and Noncondensable components

Saturation properties for the Liquid and Vapor components

b. Material Properties

Code Library; Temperature-Dependent properties; mixed Water (light and Heavy), Air, Nitrogen, Oxide Fuel, Zircaloy, stainless steel

c. Local-Dependent (Closure Coefficients) Parameters

Interfacial Area (A_i); Interfacial Mass-Transfer Rate (Γ)

Interfacial Drag Coefficient (c_i)

Wall Drag Coefficients (c_{wl}, c_{wg})

Interfacial Heat-transfer Coefficients (h_{il}, h_{ig});

Heat-Transfer Coefficient (h_{gl})

Wall Heat-Transfer Coefficients (h_{wl}, h_{wg})

Local-dependent parameters appear in the code as closure coefficient. Because of complexity of interaction between conservation equations and these correlations, they have significant influence in uncertainty ranges for the outputs.

Additionally the cost of calculation in complex TH computational codes is high. This cost has been reduced with new advancements in computers but still is a considerable parameter of the analysis. Analysis of the code models and correlations is complicated and require analyst involvement, thus adding to resources limitations. All recent methodologies developed recently for uncertainty quantification, utilize

propagation of uncertainties with cost-effective approaches such as tolerance limit statistics, limiting number of code runs in range of couple of hundreds.

1.6 Scope of Research and Outline of the Dissertation

This research is focused on developing an integrated methodology for uncertainty analysis of thermal-hydraulics computational codes such as Relap5, TRAC and recently consolidated TRACE code. The objective is to use the best features of the available methods and add new features to address their shortcomings. Code structure in this research is limited to physical models with corresponding parameters implemented in TH codes to simulate TH accident scenarios. These are representative of phenomena observed in transient behavior of abnormal nuclear power plants operation. Numerical structure including numerical resolution, convergence methods and styles are not addressed in this research as part of the code structure. These issues are part of the methodology for uncertainty assessment and have been addressed in two steps i) qualification, verification, and validation of modeling in all steps ii) code output updating for implicit consideration of the missing/screened sources of uncertainties as discussed in [Pourgol-Mohamad et al. 2006a, 2006b, 2006c)

Major uncertainty analysis methodologies developed for TH uncertainty analysis were discussed in this chapter. Chapter 2 describes phases and steps the proposed methodology (IMTHUA) in general terms. It leaves detail discussion on the steps to next chapters. Chapter 3 discusses a modified PIRT developed to help identify, ranking and screening based on TH importance as well as uncertainty importance. Chapter 4 discusses structural model uncertainty in context of TH system codes. Depending on the type of model and presence of single or multiple models, models

options, and alternatives, and data and information availability, treatment will be different. The chapter provides solution for parameter uncertainty quantification including maximum entropy, and Bayesian updating. TH code inputdeck options are also discussed. Code structure (form) uncertainty is discussed with solution for different configurations.

Chapter 5 describes the methodology for propagation of uncertainty through code calculations. Sampling technique and statistical inference for calculation of sample size are all discussed in this chapter. Sample size is calculated depending on number of outputs, one-sided or two-sided inference and consideration of transition of results from input phase to output phase. A modified version of Wilks tolerance limit is used for number of code calculation.

Chapter 6 explains the basis for the output updating for the results from input phase. It discusses a mathematical foundation of the approach, and the implementation in the context of TH code calculation and based on experimental data.

Chapter 7 demonstrates the methodology on two applications of Marviken test facility of blowdown transient and LOFT test facility LBLOCA. Based on restrictions on those facilities and non-similarities with actual size nuclear power plants, all aspects of the methodology cannot be demonstrated on these scenarios.

Finally Chapter 8 summarizes the methodology, provides some suggestion on future direction in this research topic. A series of appendices (A-D) and references are the last part of the document.

CHAPTER 2: IMTHUA METHODOLOGY FOR TH UNCERTAINTY ANALYSIS

2.1 Desirable Characteristics of TH Uncertainty Analysis

Comprehensive uncertainty analysis methodology in complex system models requires treatment of all, or at least important sources of uncertainty, considering all available information. The method should be general, applicable to wide range of scenarios, and efficient with respect to cost and resources. Availability of information and data plays an important role in quantifying uncertainty. Precise quantification of uncertainty given available evidence requires a formal and comprehensive analysis methodology. The methodology should consider uncertainties in input (broadly defined), models (individual sub-models including options and alternatives and interaction between them) and output adjustments based on integral performance information (OECD/NEA-CSNI 1996), independent of the data used from separate effects tests (OECD/NEA-CSNI 1994), and information used in assessing input variables.

As there are many TH phenomena that can contribute to uncertainties and with limitation in resources and knowledge it not possible to explicitly factor the impact of all such phenomena on output uncertainty. Implementation of a screening procedure however raises some serious questions about influence of sources of uncertainties not considered. It is understood that plant behavior is not equally influenced by all processes and phenomena that occur during a transient. It is also obvious that different sources of uncertainties such as the user effects, operation conditions, and

internal models do not have equal influence. CSAU (Technical Group 1989) and some of the other methodologies try to reduce the analysis effort to a manageable set of phenomena (e.g., from around 50 to 5-6). We note that if each of the screened out phenomena has about 2-5% contribution to the total output uncertainty, their cumulative effect is almost equal to that of the important ones. This is an issue that needs to be addressed in the methodology.

Uncertainty analysis is based on data and information. Credibility, form, and relevance of data, should be considered in the analysis. Inference about physical models from experiments, credibility assessment, and value of parameters and relevance of information require fairly sophisticated methodologies such as Bayesian methods. The methodology should also be applicable to a wide range of scenarios and applications, and not tightly linked to peculiarities of specific cases. Currently the broad applicability of available methodologies has not been demonstrated. Finally, method for the assessment and propagation of uncertainties must be efficient with reasonable demands on cost and available resources.

It is helpful to mention again that the existing uncertainty analysis methodologies are either input-driven or output-driven. Output-based methods (e.g., UMAE) cannot distinguish uncertainty contribution of the individual sources, require significant amount of experimental data and do not provide a methodic approach for generalization beyond the cases studied.

Input-based methods also introduce issues and limitations such as:

Initial Screening of Phenomena and Parameters

Intentionally Limiting the Scope (for example by not considering "user effects"). Qualification process as a required step is not enough for sources of uncertainty that are not considered. It is desirable to account for them quantitatively in the output uncertainty distribution.

Issue of Unknown Phenomena or Incomplete Spectrum of Alternative Models (For example, 30 phenomena identified by Westinghouse/EPRI vs. 17 identified in the PIRT of original CSAU. Refer to Table 5 for detail of comparison between PIRT results.)

An ideal methodology is a hybrid approach where an input-driven "white box" approach is augmented with output correction based on experimental results relevant to code output. Figure 10 illustrates schematically the idea.

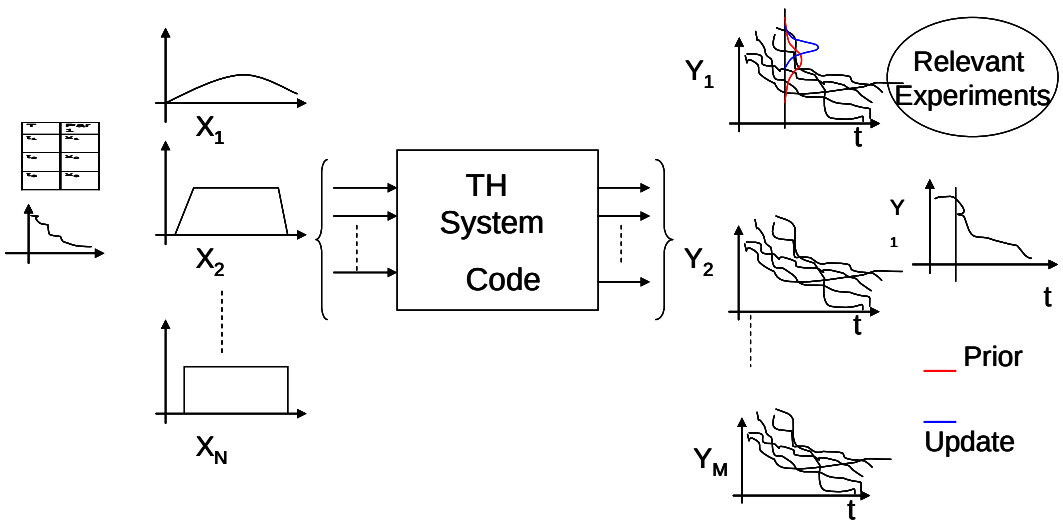

Figure 10: A Schematic Illustration of a Hybrid Input-Output Based Uncertainty Analysis Methodologies

2.2 Characteristics of IMTHUA

Figure 12 shows the steps of the proposed methodology (IMTHUA) for TH uncertainty analysis. Details of the steps will be provided in following sections and chapters. Unique characteristics of the proposed methodology are:

1. Modified PIRT; a modified form of PIRT process is proposed. The two-step method identifies and ranks phenomena not only based on their TH influence using AHP but also assess their uncertainty importance based on an expert judgment procedure.

2. Hybrid Input/Output Driven. A two-step process to quantify uncertainties has been proposed: The first step explicitly quantifies uncertainties associated with input data and information and also uncertainty about model structures. Second step updates output uncertainty with independent experimental data and validation information. This "output correction" step is intended to account for user effects, numerical approximations, and other unknown or not considered sources of uncertainties.

3. White box approach; A key objective of the proposed method is the quantification of uncertainty due to model form (as opposed to model parameters). This is done by a method for measuring the contribution of model structural uncertainty to output uncertainty in addition to parameter uncertainties. This is applied both at the sub-model level as well as the entire TH code as a whole. The IMTHUA structure of the code, treated in this research is shown in Figure 11.

4. Systematic method of input uncertainty quantification by the maximum entropy approach and expert judgment based on availability and type of data and information. Bayesian methods are used to update uncertainty distribution upon arrival of new evidence (fully or partially relevant data, expert onion, qualitative assessments).

5. Efficient uncertainty propagation through use of modified Wilks Tolerance Limit Criteria Sampling to reduce the number of Monte Carlo iterations for a given required accuracy.

6. Capable of being integrated into existing TH code for automatic propagation of uncertainties.

Accordingly the proposed methodology is a fully probabilistic approach for quantifying the uncertainties in the predictions of TH codes. Figure 12 provides an overview of the steps of the methodology. It includes treatment of sub-model uncertainties, considering alternative models and their interactions, and input parameters. TH modeling code structure is based on two-phase (totally 6 equations) with closure models and many other models such as components models. There are many correlations and models in the code which work together to simulate transients. The developed closure (constitutive) models and correlations for calculating coefficients in different situations are not 100% accurate. Behavior of TH code structure is dynamic where only some of the models and correlations are involved in calculation at any given time step, upon satisfying certain specific conditions. There are other sources of uncertainties such as user effects, nodalization uncertainties, scaling, numerical solutions which are considered and taken into account implicitly in output updating of distribution obtained from first phase. All uncertainties can be categorized as being input-related, or associated with code internal models and sub-models. Information on input parameters and code output performance data (based on tests) are incorporated through a two-stage Bayesian updating at input and output levels. These are briefly explained in the following sections.

2.2.1 Input Phase

Input uncertainty quantification phase is focused on identification of uncertainties in code input parameters, and those associated with the models and sub-models. As such is covers all those sources of uncertainty (model and parameter) that can be explicitly accounted for. These uncertainties are propagated through code calculations to arrive at a distribution of uncertainty of the output. Sources of uncertainty in "input" include model parameters, boundary/initial conditions, and also uncertainties in structure of sub-models considering interactions between them. A screening process, an inevitable step for this phase of methodology, identifies the most important aspects to consider in an effort to limit the size of the problem.

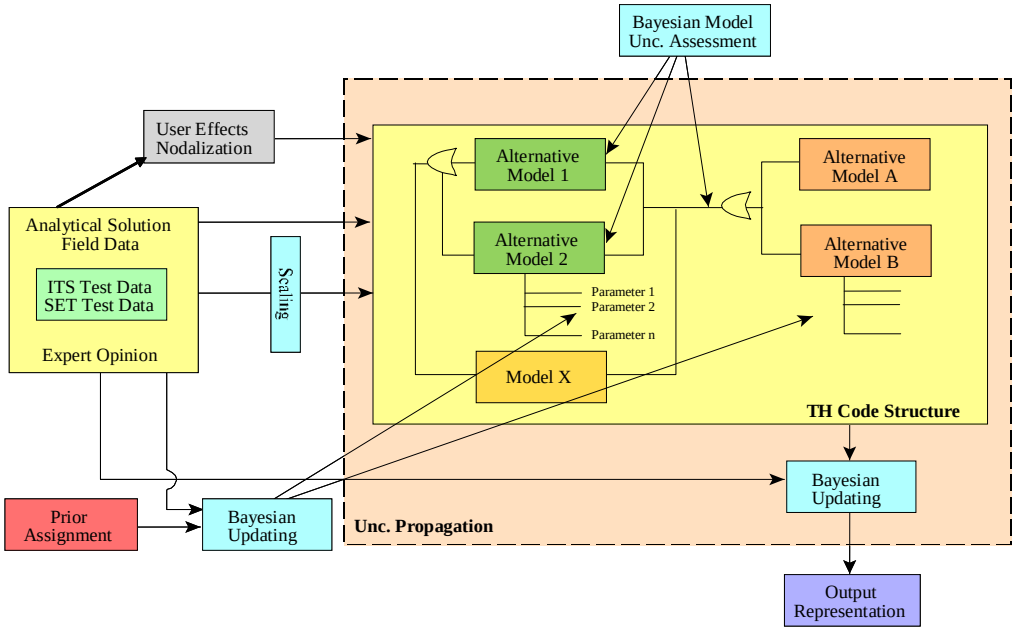

Figure 11: Code structure treated in IMTHUA Methodology for Uncertainty quantification

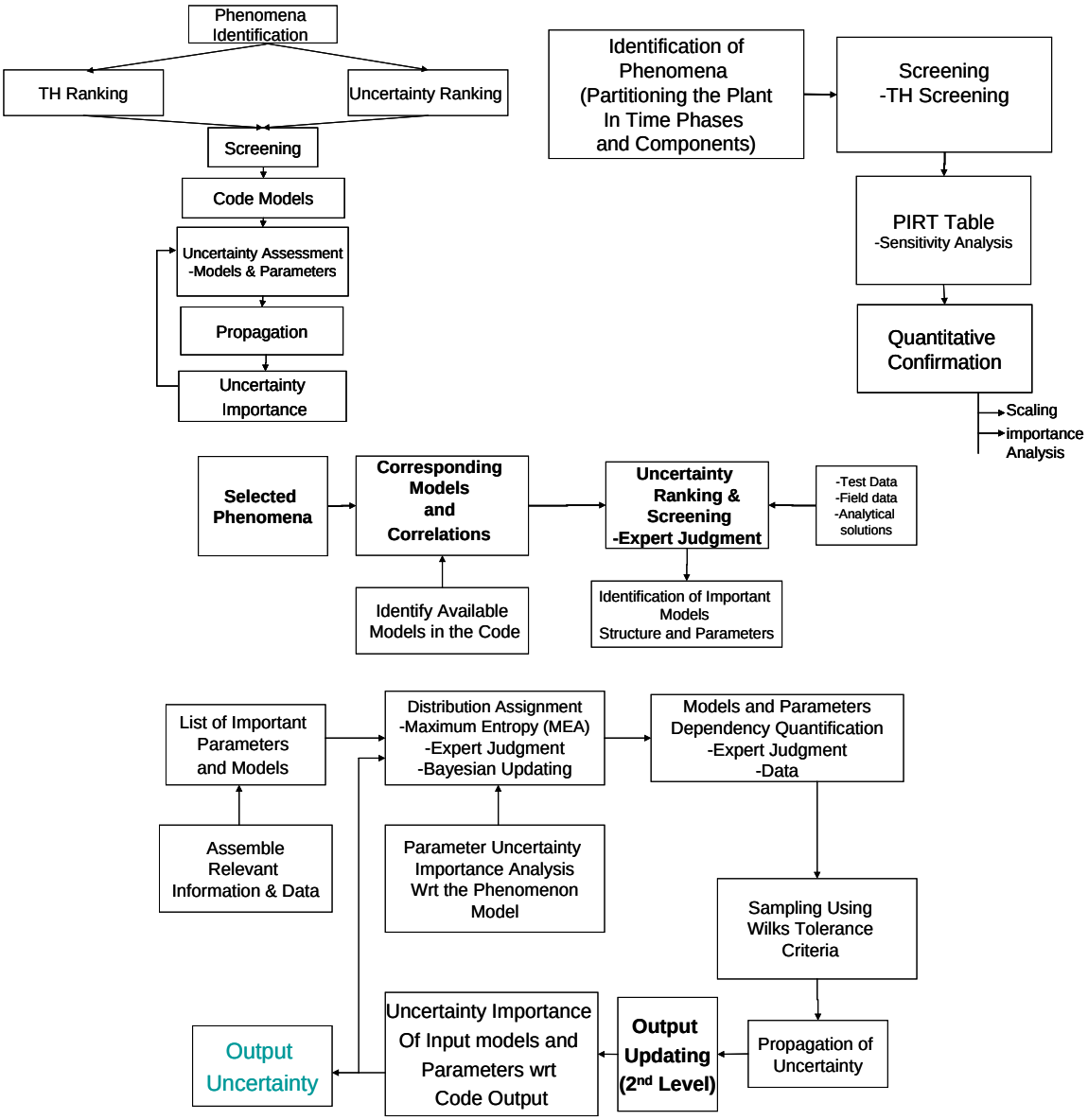

Figure 12: IMTHUAMethodology's Steps Flow Chart

2.3.2 Output Phase

The second, output phase, of the uncertainty assessment methodology is intended to account for the impact of other sources of uncertainties not considered in the input phase. Figure 12 describes steps involved in this phase of the methodology. This phase allows updating output uncertainties upon availability of new information about

models or output. This phase utilizes a Bayesian statistical method (Droguett and Mosleh 2001) for output distribution correction based on fully or partially available. Droguett and Mosleh (2001) proposed a methodology based on paired relation between experimental and code data. Under ideal paired data situation, each experimental data $\{x_1, x_2, \ldots, x_N\}$ has its counterpart in model predicted data set $\{x'_1, x'_2, \ldots, x'_M\}$ with N=M. However, often the available TH experimental data can not be paired with code predictions in a one-to-one mapping. The non-paired situation $x_i \neq x'_i$ and/or $N \neq M$, situation requires a special treatment of the data. Detailed description of this phase of methodology is provided in (Rust et al. 2005).

In case of TH computer codes, applicable experimental data come from scaled-down facility such as SET designed for the assessment of specific model or correlation relevant to each phenomenon or component, and ITF designed for the assessment of the behavior of a reactor system. SET data usually is used for input-based uncertainty quantification while ITF data are suitable for output uncertainty correction in next phase. Figure 13 demonstrates output updating phase using available information.

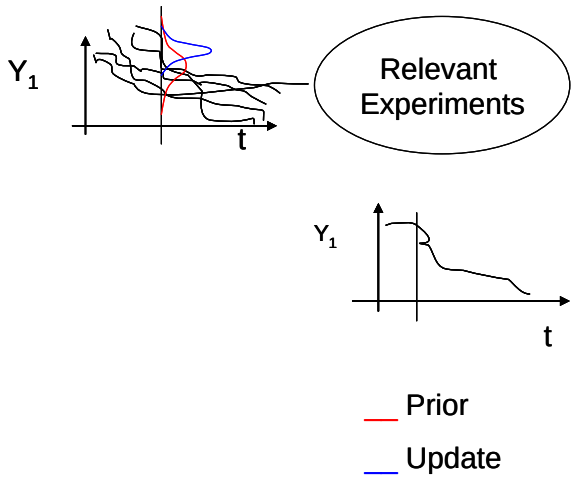

Figure 13: Schematic Demonstration of Output Updating

Chapter 3: MODIFIED PHENOMENA IDENTIFICATION AND RANKING TABLE (PIRT) FOR UNCERTAINTY ANALYSIS

3.1 PIRT Objectives

With many physical phenomena involved, TH analyses deals with many sources of uncertainty. While ideally all sources of uncertainties should be considered in the analysis explicitly, this is neither practical nor necessary to evaluate all processes and components in detail. PIRT is a helpful decision making tool to identify and rank important phenomena in the nuclear power plants scenarios. Figure 14 highlights the idea behind the PIRT process. PIRT can be used to support several important decision-making processes. PIRT development becomes difficult if multiple reactor types or accident scenarios are considered simultaneously (Wilson and Boyack 1998). Therefore PIRT is developed for a specific plant design and scenario. Both the occurrence of phenomena and processes and the importance of phenomena and processes are plant and scenario-specific. The ranking process is designed to direct the examination of importance to those processes having the most significant effect on the figure of merit.

Traditional PIRT considers the effects of an input phenomenon on the magnitude of the output. It is a necessary step but does not carefully examine the knowledge and information about the phenomena. The knowledge on various phenomena results on the models and correlation developed. Credibility of models is directly related on our understanding of the reality of the phenomena and the portion captured in the

analysis. Wilson et al. (1997) presents a discussion on the philosophical basis of notions such as reality, modeling, models, and their relation.

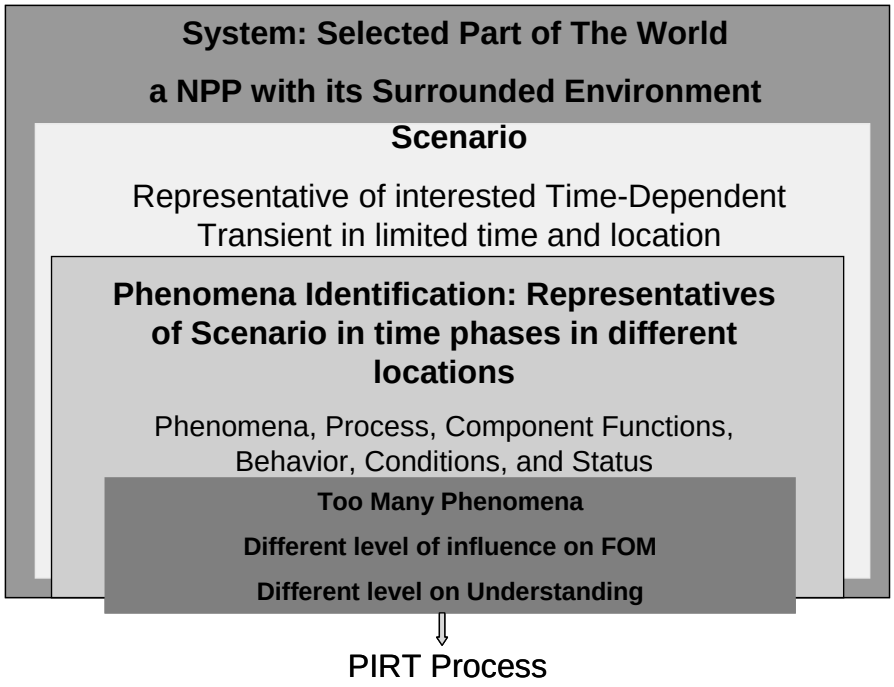

Figure 14: Philosophy of PIRT Process

3. 2 PIRT Process

Wilson and Boyack (1998) explain in detail the steps of the PIRT process. The steps in a typical PIRT (illustrated in Fig. 1 of the reference), are summarized as follows:

1. Define objectives of the process (PIRT process is conditioned on the objectives).

2. Identify plant design and the scenario type.

3. Define parameters of interest or figure of merit as phenomena have different impacts on different parameters.

4. Partition transient scenario into convenient time phases and plant design into subsystems and components.

5. Identify plausible phenomena by phase and component

6. Develop a ranking for identified components and phenomena by expert judgment and discussions or by using pair-wise AHP methodology.

7. Perform sensitivity analysis to confirm the results from the previous steps.

8. Define screening criteria if only important phenomena remain for the next step analysis (e.g., TH uncertainty analysis).

Some of the steps are controversial and will be discussed in this dissertation. As part of the research leading to the development of the method proposed in this dissertation, extensive literature review was conducted to evaluate the merits and limitation of the PIRT method with the objective of incorporating the best features into a new more comprehensive method.

3.2.1 Phenomena Definition

Phenomena are defined differently in various applications. As a matter of definition, the term "phenomena" as used in this research and consistent with other PIRT processes, should be taken to mean "phenomena, process, component functions, behavior, conditions, and status". All of the following examples are identified as phenomena even though only the first one is truly physical phenomena: flashing, break mass flow, decay heat, steam generator pressurizer level, accumulator temperature, initial core power, and primary-to secondary heat transfer.

There is no consensus on the list of phenomena considered in TH studies. Early PIRT processes considered mostly actual phenomena as in original CSAU (USNRC Technical Group 1989). Phenomena in AP600 PIRT (Wilson et al. 1997) are more detailed in which actual phenomena, as well as process, component functions,

behavior, conditions, and status were considered. AREVA (Martin and O'Dell 2005) and Westinghouse/EPRI PIRT (Bajorek et al. 1998) consider initial condition and their impact on figure of merit. A recent PIRT study for a NPP with high burn-up (Boyack et al. 2001) approached the process by identifying the phenomena in four categories of plant transient analysis, integral tests transient fuel rod analysis, and separate effect tests category. Types of phenomena are different in each category.

3.2.2 Identification of Phenomena

In the identification procedure, the scenario is examined in its operational time periods. For each period, each component is examined to identify the various processes and phenomena involved. There are different ways to divide the scenario period to different phases. There is consensus to divide LBLOCA to the three operational phases of blowdown, refill, and reflood. It is different in case of SBLOCA and other operational transients. Short descriptions of each phase with identification of phenomena are given in following sections. The idea is identifying the phenomena occurring in important components for each phase. Figure 15 illustrates importance of phenomena by their TH and uncertainty importance. It is obvious that screening is dependent on regulation, type of analysis, and resources available.

Table 5 shows a comparison table of some of the recently completed PIRTs. They are all for LBLOCA in similar 4 loop PWR NPP. Marked phenomena are common in the studies. It clearly shows how different are the tables for similar transient scenario. This is a serious issue in PIRT process. Development of comprehensive phenomena matrix including all phenomena, process, component functions, behavior, conditions (including initial and boundary), and status helps for PIRT developers to reach a

consensus list of phenomena for similar scenarios in same NPP designs. OECD-NEA (1994) had initiated developing such matrices but it is limited to actual phenomena. A total of 67 phenomena were identified. Completion of phenomena matrix, as a handbook for expert, will improve consistency of PIRTs done by different expert groups.

Table 5: LBLOCA PIRT Comparison of 3 Studies Of AREVA, Original CSAU, And Westinghouse/EPRI; Gray Area Are Common Phenomena Identified In The PIRT Studies

AREVA	Original CSAU	Westinghouse/EPRI
Dominant PIRT Parameters	**Break Flow**	**Plant Initial Conditions**
1.Break Flow	1. Mass Flow	1. RCS Average Fluid Temperature
2.Entrainment	**Stored Energy an Fuel Response**	2. RCS Pressure
3.Axial Power Distribution	1. Gap Conductance	3. Accumulator Fluid Temperature
4.Interfacial Heat Transfer	2. Peaking Factor	4. Accumulator Pressure
5.Core Multi-Dimnesional Flow	3. Fuel Conductivity	5. Accumulator Volume
6.ECCS Bypass	4. Fuel/ Fluid HT	6. Safety Injection Temperature
7.Steam Binding	5. Clad Conductivity	7.Accumulator Line Resistance
8.Spacer Effects	6. Fuel and Clad Heat Cap	**Plant Initial Core Power Distribution**
9.Cold Leg Condensation	7. Pellet Power Distribution	1.Nominal Hot Assembly Peaking Factor
10.Void Distribution	**ECCS Bypass**	2.Nominal Hot Assembly Average Relative Power
11. Accumulator Nitrogen Discharge	1. ECC Flow Deversion	3. Average relative power, lower third of core
12.Heat Transfer	**Steam Binding**	4. Average relative power, middle third of core
13.Upper Tie Plate CCFL	1. Liquid Mass Flow	5. Average relative power, outer edge of core
Treated Plant Parameters	2. Evaporation	**Thermal-Hydraulics Physical Models**
1.Core Power	3. Entrainment	1.Critical Flow Modeling (CD)
2.Pressurizer Pressure	4. De-entrainment	2. Broken Loop Resistance
3.Pressurizer Level	**Pump 2-Phase Flow**	3. Blowdown and reflood heat transfer
4.Accumulator Volume	1. Mass Flow	4. Minimum Film Boiling Temperature
5.Accumulator Pressure	2. Pressure	5. Condensation Modeling
6.Containment/Accumulator Temperature	3. Core Power	6. Break Type
7.Containment Volume	4. Disolved Nitrogen	7. ECCS Bypass
8.Initial Flow Rate	5. Non-Condensible Gas Partial Pressure	8. Entrainment and Steam Binding
9.Initial Operating Temperature		9. Effect of Nitrogen Injection
10.Offsite Power Availability		**(d) Hot Rod physical Models**
11.Deisel Start		1. Local Hot Spot Peaking Factor
		2. Fuel Conductivity
		3. Gap Heat Transfer Coefficient
		4. Fuel Conductivity after Burst
		5. Fuel Density after Burst (Fuel Relocation)
		6. Cladding Reaction Rate
		7. Rod Internal Pressure
		8. Burst Temperature
		9. Burst Strain

3.2.3 Ranking and Screening Process

"Primary evaluation criteria (or criterion) are normally based in regulatory safety requirements such as those related to restrictions in peak clad temperature (PCT)" (Wilson et al. 1998). Ranking and screening depends on analysis objective, regulatory requirements, availability of resources. Some of studies consider only high-ranked phenomena, but others consider medium and high phenomena. It is different in two-

step PIRT as every phenomenon possesses two ranks. Figure 15 illustrates two-dimensional importance. High-high combination is a criterion for decision making, while medium and high combinations should be other alternatives. It was decided that the low, medium, and high rank scheme should be adopted based upon past experience with the PIRT process for both TH and uncertainty ranking process.

High = the phenomenon or process has a dominant impact on the primary evaluation criterion,

Medium = the phenomenon or process has moderate influence on the primary evaluation criterion.

Low = the phenomenon or process has small effect on the primary evaluation criterion.

3.3 Two-Step PIRT Process

A methodology of characterizing important phenomena, called "Modified PIRT" is used in this research. This methodology provides a robust process of PIRT for more precise quantification of uncertainty. It is a two-step process for identifying and ranking based on TH importance as well as uncertainty importance. We will rank and screen phenomena based on both TH and uncertainty importance. Experience with TH phenomena shows that phenomena with TH and uncertainty importance contribute more significantly to output uncertainty than those based on TH importance alone, or just uncertainty importance. This is not totally the general and there are exceptions. Analytical Hierarchical Process (AHP) has been used for as a formal approach for TH identification and ranking. AHP is a powerful tool for ranking of alternatives and attributes of a decision, especially when limited experts

are available. Formal uncertainty importance technique is used to estimate the degree of credibility of the TH model(s) used to represent the important phenomena. This part uses subjective justification by evaluating available information and data from experiments, and code predictions. The idea is shown in Figure 15.

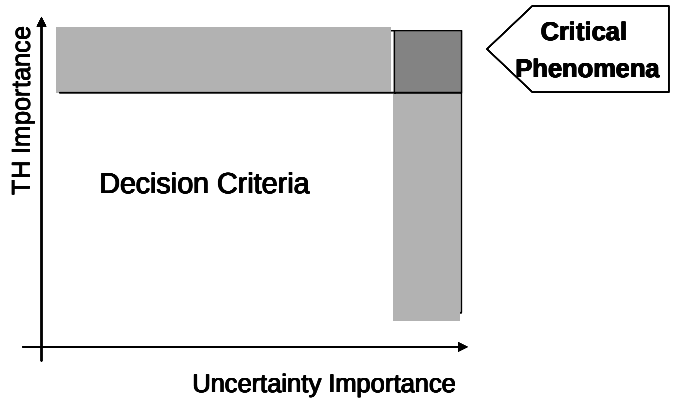

Figure 15: TH Importance vs. Uncertainty Importance in Chosen Criteria

Table 6 shows some phenomena with their TH and uncertainty importance. By uncertainty importance, we mean level of contribution of the phenomena to the uncertainty in the code prediction (for a given figure of merit). For example, decay heat power was considered high in its TH importance due to its impact on PCT itself. The phenomenon is well-known and correlations are well developed to predict it. Therefore, low uncertainty was assigned to it to demonstrate high confidence of the phenomena model used in TH codes. TH importance has impact on output's mean value while uncertainty importance affects the variation. There are different qualitative and quantitative approaches to assigning ranks to phenomena. Ranking of high, medium, and low was used in some studies while others use ranking on scale of 1 to 9, where 9 means highest importance and 1 is the lowest.

Table 6: Some Phenomena with Their TH And Uncertainty Rank

TH \ Uncertainty	High	Medium	Low
High	Spacer Grid Rewetting and Droplet Breakup	Rewet CCFL	Decay Heat Power
Medium	Time of Burst?	Rod-to-Spacer Grid Local Heat Transfer	Cladding Phase Change
Low	Rod-to-Rod Mechanical Interactions	Cladding Oxidation (ID&OD)	Fuel Relocation

3.3.1 TH Ranking-AHP Method

Analysts have a high capability to determine the relative importance of two items, when the number of items does not exceed four-five. As the number of items in a group increases beyond 4 or five, the ranking capability decreases at an increasing rate. Accordingly, AHP methodology has been developed to organize large ranking problems into subsets that capitalize human abilities to work with (Saaty 2001). AHP is a systematic, logical approach developed by T.L. Saaty (Saaty 2001) to reduce complex issues into manageable pieces. The decision maker can sort through the variables and determine to what degree a particular variable will influence the final decision. With more than 67 (OECD/NEA-CSNI 1994) actual phenomena and many others processes, status, and conditions considered as phenomena identified in LOCA scenarios in NPPs, AHP approach with such capability help justify LOFT LBLOCA PIRT. AHP is very useful for LOFT LBLOCA PIRT for limitation to access enough TH phenomena experts.

The AHP methodology is used for ranking of phenomena based on their TH importance. Phenomena are compared in a pair-wise manner to find their relative

importance on the output or any other figure of merit. Examples are tabulated in the Table 8. The UMD-AHP (AHP-UMD 1998) software is used for computation of TH ranks for every component and system considered. List of all of them are shown in Appendix B with explanation for justification on assigning the pair-wise ranks.

3.4 TH PIRT by AHP Method

With more than 67 {5] phenomena identified in LOCA scenarios in NPPs, AHP ranking methodology can help in the PIRT-type ranking. AHP is a systematic, logical approach developed by Saaty (1985) to reduce complex issues into manageable pieces. The decision maker can sort through the variables and determine to what degree a particular variable will influence the final decision. Figure 16 demonstrates utilization of AHP method for ranking of TH phenomena and models.

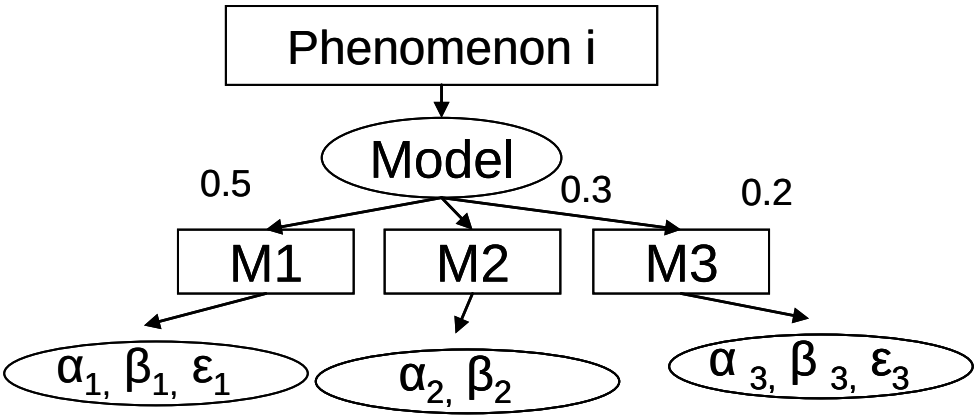

Figure 16: AHP Demonstration in Process of TH Ranking

3.5 Uncertainty Ranking-Expert Justification

Formal uncertainty importance technique is used to estimate the degree of credibility of the TH model(s) used to represent the important phenomena. This part uses subjective justification by evaluating available information and data from

experiments, and code predictions. High rank signifies sufficient knowledge about phenomena which leads to development of precise model(s) and correlation (s) and low rank indicate poor knowledge.

3.6 PIRT Confirmation and Screening Process

Table 7 shows experimental data used for qualification of PIRT results and confirmation on the list of phenomena selected based on the criteria. These data are used for validation of results obtained for ranking of the phenomena and confirmation of results from level 0 PIRT.

Table 7: Table of Data for PIRT Validation and Confirmation

Test Facility	**1**	**2**	**3**	**4**	**5**	**6**
LOFT	L2-3	L2-5	LP-LB-1	L3-1	L3-7	
Marviken	22	24	20			
ISP	2,5,8,9,11	13,17,12 27,38				
UPTF						
Flecht-Seaset						
TPTF						

3.6.1 Scaling

Most of the data on nuclear power industry are from those facilities because of regulatory and safety limitations (Benerjee 1997). There are some techniques called scaling for scaling up the data to evaluate the experimental facility in its full size with real nuclear core. Scaling analysis for each facility yields a separate set of non-dimensional scaling groups e.g., -Groups (Wulff 1996). Scaling Criteria are the requirement that for similitude of two systems corresponding groups have pair-wise the same numerical values, and that scaled constitutive relations are the same for both systems (law of corresponding states). In contrast to the scaled time and space-dependent variables, scaling groups are constant, formed from fixed geometrical and controlled operating parameters, such as initial conditions and thermo-physical properties at initial conditions.

There is one and only one group for each transfer process or phenomenon taking place in the system. Partial similitude is achieved when the scaling groups of dominant phenomena are matched. Equations for scaling are mass, energy and momentum equation of conservative and thermal and caloric Equations of states. The governing equations are normalized such that the normalized variables and their derivatives with respect to normalized time and space coordinates are of order unity and the magnitude of each term of the normalized conservation equation is measured by its normalizing, constant coefficient. The governing equations are then scaled by division the driving through the coefficient of the driving term. This renders the driving term of order unity and yields (from an equation of (m) terms) fewer, i.e., (m-1) non-dimensional -Groups or scaling groups, which measure the magnitude of

their respective terms, and therewith the importance of the associated transfer processes, relative to the driving term. = 1 for the driving (reference) term (Benerjee 1997).

Scaling of the overall system can be carried-out by starting with the models for the system-enclosing control volume and continuing by modeling the components (Top-Down), or alternatively, by starting from the component models and the assembling the system model (Bottom-Up).

The results from scaling can be used for quantitative confirmation of PIRT by

1. The downward vertical scan of the numerical -values in the reactor column reveals the decreasing order of their magnitudes, with the largest values being associated with H, and the smallest values with L.
2. The horizontal scan of the numerical -values in the row of a process shows for which test facility the numerical -values approximate best the -values of the reactor.
3. The difference between the -value of the test facility for a phenomenon and the corresponding -values of the reactor is a measure distortion that must be expected from the test facility.

Chapter 4: TH STRUCTURAL MODEL UNCERTAINTY

4.1 Structure of TH Codes

Structure of TH codes is not different from modeling in other computational codes except they developed base on regulatory needs and available experimental data and other information in nuclear industry. They were developed to simulate big portion of the structure of nuclear power plant in abnormal operation for studying the macroscopic behavior only. They are unable to calculate details due to number of nodes limitation. Limitation in computational power of computers (improved over time along with the codes performance) and resources consideration are the factors for the code structure characteristics. A general discussion on model uncertainty is necessary before describing on TH code structure and methods for the treatment.

4.1.1 Structure of TH Codes and Complexities

TH codes such as RELAP5 are capable of modeling a wide range of systems from simple configurations such as single pipes, to small-scale experimental facilities, to as complex as a full scale nuclear reactor plant. RELAP5 has models for thermal hydraulics phenomena including non-condensable gas transport, control systems, heat transfer to and from solid surfaces, and nuclear reactor kinetics. (see USNRC (1988) for detail discussion of phenomena and modeling in nuclear facilities.) The models are built up from volumes connected together with junctions associated with attached heat structures. The most difficult part of the solution is to solve the thermal-hydraulic behavior of the fluid coupled to the fuel/structural heat transfer through the HTCs. This area is more complex because there are more coupled field equations

associated with the fluid (more independent variables), more phenomena to be considered, and because the HTCs are very dependent on the fluid properties and velocities. The structural complexity of the TH code is in part due to:

i. Knowledge-driven Complexity

Lack of control on structure of the code by user as well as developer (Massoud 2005)

Lack of appropriate data and information about models, sub-models, and actual variables such as HTC

ii. Inherent Complexity of Physical Phenomena

As many as few thousands models and correlations may be involved in the computations

Dynamics behavior of the code, i.e., different portions of the code models are involved in the calculations at different points in time depending on fulfillment of specific conditions

Presence of many horizontal and vertical regime phases in the code calculation, and fuzzy borders between them.

Limitations in precision of solution of field equations for specific configurations due to large average nodes. For instance in the case of choked flow phenomena, use of relatively big nodes masking some microscopic scale phenomena limits precision of field equations. The TH code calls for choked flow model for velocity calculation if the momentum equation calculation result is not satisfactory. This is the reason that TH codes are coupled with CFD codes).

Figure 17 shows this complexity in its dynamic behavior. It emerges in spectrum of possible LOCAs, and other types of transients. Each scenario has its sequence of events resulting in observation of different set of phenomena. Modeling of these phenomena involves different sets of models and correlations which is dependent on time, and on progress of the transient. Assume, we have N models and correlation in the code. Each model provides a description of the y_i. Assume also that each model consists of N_S alternative model, where each model $M_i = (S_i, \ _i)$ consists of an alternative structure S_i based on alternate hypotheses which are plausible given existing information, and the associated parameter vector $\ _i$. Each model in the set provides a different description of the unknown quantity y_i. Structure of TH code calculating behavior during transient relies on these models and correlations. When certain conditions are satisfies, some models and correlations get involve in the computation and some stay out, in specific time step. Since structure of computational model in the TH code is dynamic and presence of models and correlations in the specific time depends on governing conditions which is also dynamic, then uncertainty analysis of code becomes difficult regarding uncertainty about portion of transient where a given model involves in the calculation. This dynamic behavior adds more to complexity of uncertainty analysis.

Uncertainty grows in time step advancement of this dynamics configuration. It means that uncertainty in code output, e.g., clad temperature for given rod accumulates with progress of transient and changing arrangement of models and correlations in the calculation. These models and correlations have different levels of accuracy and credibility, affecting the results in different rank. The ideal way to

quantify uncertainty in the code"s figure of merit in temporal quantities as core temperature, vessel pressure in time step to time step propagating the uncertainties by calculating indicator of uncertainties e.g., standard deviation or coefficient of variance. It means that these statistics are evaluated for their changes in each time step. As it looks very interesting, it comes difficult in complex simulation of complex NPP transient cases. The practical alternative is utilization of the Monte Carlo type propagation, which has found many interests in TH codes calculations.

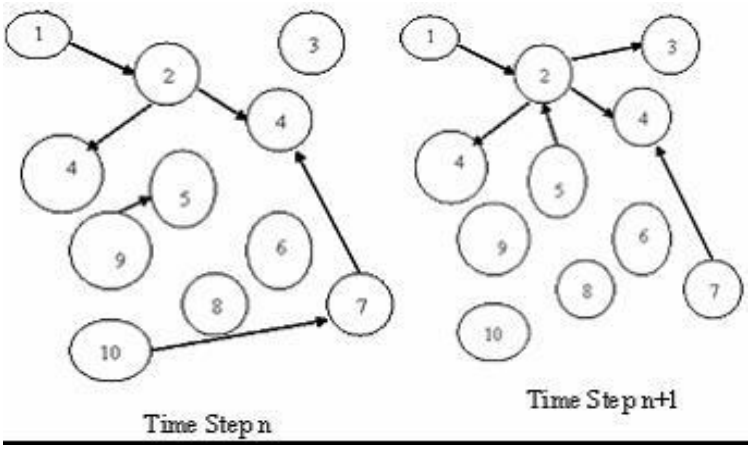

Figure 17: Dynamic Behavior of TH System Code

4.1.1 Code User and Inputdeck

The so-called User Effects in preparation of the inputdeck for specific application has been recognized as an important issue in the quantitative evaluation of the code uncertainties. User has a potentially big influence on inputdeck by the many options he/she has in manipulating the settings of the code. Some of these are

-System Nodalization

This includes user authority to choose number of nodes, selection of appropriate component model. Important areas for user influence in input are (Technical Program Group 1989):

Input Parameters related to specific system characteristics

Input parameters needed for specific system components

Specification of initial and boundary conditions

Specification of state and transport property data

Selection of parameters determining time step size

-Code Options

In spite of many recommendations in code manual for inputdeck preparation, there are various possibilities for the user to influence the code calculation by the options available in the inputdeck both in preparation and execution. Since in many cases directly measured data are not available, or at least not complete, the user is left to it"s engineering judgment to specify completion of the inputdeck. Some of these options are (Aksan et al. 1994):

Choice between alternative engineering models e.g., critical flow models

Multipliers

The Efficiency of separators

Two-phase flow characteristics of main coolant pumps

Pressure loss coefficient for pipes, pipe connections, valves, branches etc.

There are other options for the user to influence the calculation by changing the code source in code structure, numerical scheme and limitation in interpretation of experimental results. The case studies for evaluation of user effects, especially ISP assessments, show dominant effect on the predicted system behavior in the end results. Some cases on user effect are report in Aksan et al. (1994) including user affects on number of nodes, selection of component models, and estimation on value of a parameter by different users. Some suggestions are made in the report as remedy for qualification of users. They include user training and discipline, improved user guidelines, and code improvement.

While these efforts are essential for user and inputdeck preparation quality, they do not eliminate errors and uncertainties added to the calculation with user effects. Conditions are highly variant dealing with choices and options in preparation of the inputdeck. Degrees of uncertainties of the options are also different. Figure 18 shows these effects in code calculation of different users. A problem with same data results in wide range of output results.

Input options and alternatives treatment is designed to be part of PIRT decision-making. Any option related to models and correlations of important phenomena should be evaluated for their effect in the figure of merit and designed to be part of explicit uncertainty propagation.

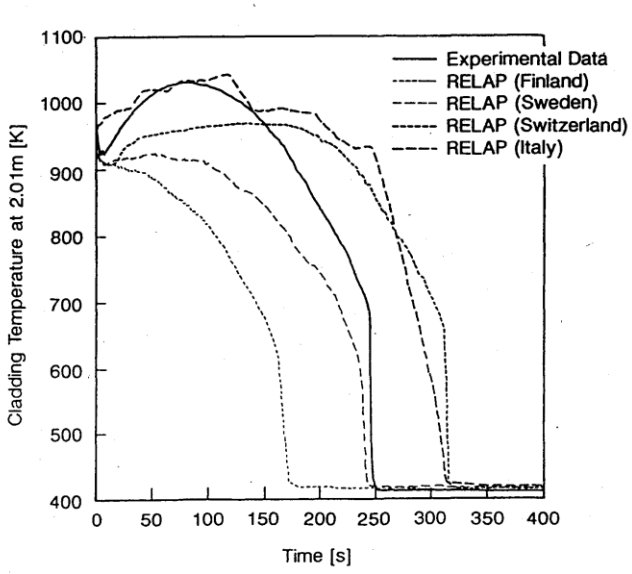

Figure 18: User Effects Study; Effects of Different Users on Code Calculation (Aksan et al. 1994)

We may classify the credibility of user options as following:

Universally Recommended

In this case the option is recommended highly in that specific condition. There should be strong evidence, which confirm the hypothesis. If this is the result of elicitation, its uncertainty should be considered as insignificant on the calculation results.

Recommended

Universally recommended options and alternatives are not always available. There are cases where consensus for specific option does not exist. This may happen as part of a pre-processing (such as PIRT) to identify and classify them regarding their level of uncertainty. If uncertainty is significant for a specific option, it should be considered in process of uncertainty quantification. If the effect is insignificant, it may be left out of in the explicit assessment of uncertainty. Table 8 shows available

code options for Relap5/MOD3.3 related to volumes, junctions, initial and boundary conditions.

Table 8: Available Code Options in the Relap5/MOD3.3 Code

Volume-Related Options
Thermal Front Tracking Model
Level Model
Water Packing Scheme
Vertical Stratification Model
Interphase Friction Model
Normal Pipe Interphase Friction Model
Rod Bundle Interphase Friction Model
Wall Friction Calculation
Phasic Non-Equilibrium Or Equilibrium
Junction-Related Options
Energy Correction
Countercurrent Flow Limiting (CCFL) Model
Horizontal Stratification Vapor Pullthrough/Liquid Entrainment Model
Choking (Critical Flow) Model
Operative Area Change
Phasic Velocity Assumption
Momentum Flow Dating of the Output Uncertainty Process.
Initial Condition Options
Volume Fluid State Initialization
Junction Flow Initialization
Heat Structure Initialization
Control Variable Initialization
Trip Initialization
Boundary Condition Options
Fluid Pressure; PRZR, SG Safety Valves, And Power-Operated Relief Valves (PORVs), Turbine
Fluid Temperature; Safety Injection, Makeup, And Main And Auxiliary Feedwater Systems
Fluid Flow; Safety Injection (HP And LP Injection), Makeup, Main And Auxiliary Feedwater Systems, And For The Main Coolant System Recirculation
Heat Source; Core Power And Pressurizer Heaters
Adiabatic Surface; Exterior Of Insulated Piping
Fluid State Boundary Conditions; Time-Dependent Volume
Fluid Flow Boundary Conditions; Time-Dependent Junction

4.2 A Simple Example of EES as Prototype for TH Codes

Before discussing complex structure of TH codes further, simple prototype problem is solved in EES software (Klein 2006). The case involves solving a simple form of energy and momentum equations in a single pipe configuration as shown in Figure in Appendix C. This program calculates the velocity and temperature along the cross section for a fully developed steady pipe flow in a cylindrical tube with a constant heat flux. The objective is integration across the pipe of the equations in the Appendix C. In the EES software, we have control over modeling for conservation equations. EES has temperature and pressure dependent properties and a numerical solution for the simulated configuration which makes it similar to TH codes such as RELAP5. The details and coding for the problem and its schematic view are given in Appendix C. The results are shown in Figure 19.

The problem of uncertainty quantification is similar to TH system codes. We are interested in calculating the bands bounding the calculated output results. The main difference is dynamic scenario and interdependency of the coefficients and variables in TH code calculation. The process is different when comparing with a simple algebraic equation with independent parameters. The latter results in a straightforward uncertainty assessment with a simple Monte Carlo or method of moments type propagation.

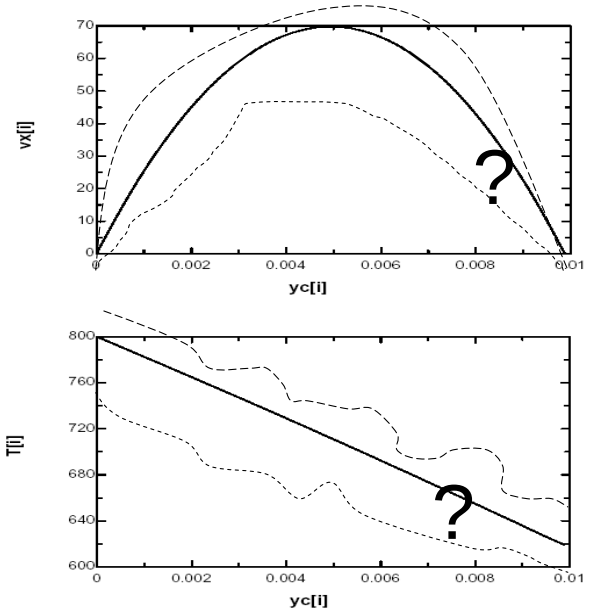

Figure 19: Results of EES Simulation

4.3 Safety Calculation Approaches

We assume the modeling procedure starts from a known initial state. All the physical quantities in the model we classify as input, output, and latent data (Guba and Makai 2003). There are different approaches to modeling the relation between inputs and outputs. It may be as a "black box" modeling with no knowledge of the structure of the code or a "white box" modeling with this knowledge. A description of these types of modeling will be given in following sections.

4.3.1 Black Box Modeling

We have a model describing the system and it enables us to calculate physical parameters (e.g. clad temperature, void content) characterizing the system at an arbitrary instant, t. The simplest way to connect inputs to output through the system code is black box modeling. It treats the system as a "black-box", so it doesn't

explicitly use knowledge of the internal structure. Black box analysis is usually described as focusing on functional requirements. We may be uncertain about the value or state of various inputs. These inputs include initial and boundary conditions in the code input and parameters and coefficients in the code structure. The value or status of output(s) would then be uncertain due to input uncertainties, as well as other sources of uncertainties besides the known inputs. A Monte Carlo based propagation of uncertainty through black box computation results in output range as seen in Figure 20. Simplicity of the methodology makes it popular for fast uncertainty quantification. In complex TH system codes with many variables involved in the calculation, it is difficult to quantify uncertainties due to all input variables. Also as stated before in most the TH codes, input-based quantification of uncertainty in output is not sufficient and comprehensive due to imperfect code structure.

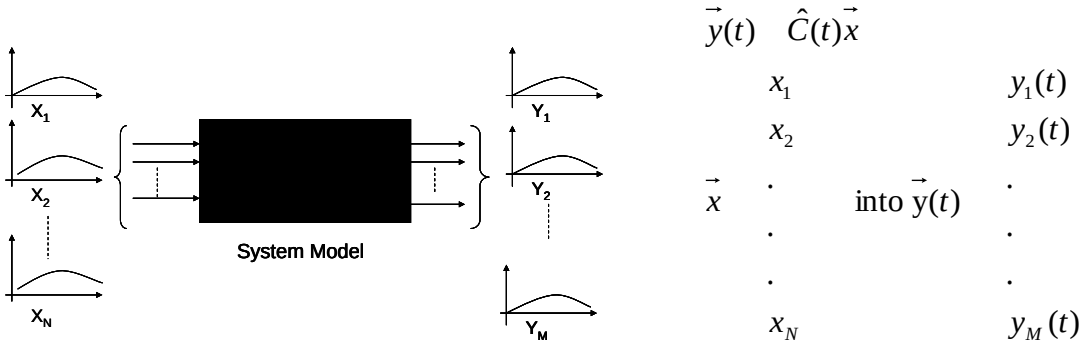

Figure 20: Black Box Uncertainty Assessment

4.3.2 White Box Modeling

Structural or white-box uncertainty assessment allows one to peek inside the "box", focusing specifically on using internal knowledge of the code to guide the utilization of data and knowledge. A typical white box for TH code structure developed for IMTHUA is shown in Figure 11.

4.4 Other Methodologies for Code Structure Uncertainty Treatment

There are typically, hundreds of interacting modes and correlations in the TH code when simulating given scenario. Thousand of variables (including input variables, code coefficient, latent and interim parameters) are varied in every time step if their corresponding model is involved in the computation. An ideal solution should be the quantification of uncertainties in every variable in each time step and the monitoring of these uncertainties propagation advanced to the next time step. This is not possible because:

1. In general, other than flow properties (such as pressure, temperature, flow rate, and mass,) measurement of convoluted items such as interfacial mass transfer is impossible.

2. RELAP5 calculates all these values. However, they may not directly available as intermediate output. (In this research Relap5 code was modified by to include some of interfacial heat transfer coefficient in output printout. But the list of needed variables is in order of hundreds and requires significant resources to consider all.

3. Complexity of structure makes it difficult to fully understanding all factors and parameters influencing the output.

Other approaches for treating structural uncertainties of TH codes are briefly reviewed in the following.

4.4.1 GRS Approach

Quantifications of subjective probabilities for model uncertainties are based on the experience and expert elicitation. Subjective probabilities are assigned to sub-models

(inside the code), if these sub-models are generally involved in the application. Specific sub-models (e.g. for high pressure situations) are considered, if experience shows that these models are appropriate for the underlying application. The subjective probability generally assigned to a specific model is smaller than the subjective probability for a model of general validity. Alternative models are treated by the assignment of confidence weights, reflecting the degree of belief about the accuracy level of each model). For example 30%, 70% are assigned to alternative models "Wilson drift model" and "flooding based drift-flux model" respectively. Correction multipliers with limited model parameters quantifications are used for treatment of uncertainty calculated from comparison of experiment and calculations (Kloos 2006).

4.4.2 CSAU Methodology

They are a number of cases of model uncertainty in TH codes assessed by CSAU. One-Dimensional models, time and space averaging (use of relatively big nodes dominating some microscopic scale phenomena, input level of uncertainty) were treated in the original CSAU. Processes were designed in the methodology in a systematic way (PIRT) to identify sources of uncertainty at conceptual level. Uncertainty is aimed to consider all sources of information qualitatively as well as quantitatively. Applicability of the TH code for a specific safety study of a particular scenario, and other qualified steps are part of model uncertainty treatment for LOCA uncertainty quantification.

4.4.3 UMAE Methodology

Some levels of qualifications are considered for implicit code structure model uncertainty. These include user and nodalization and test data qualifications. TH Code is treated as black box in this methodology and only code output for figure of merit is compared with results from experiments in qualified scaled down test facilities. The "accuracy based" calculations are then extrapolated to calculate uncertainties for full scale plant application. Accuracy calculation stands for code level structural model uncertainty. UMAE method generates overall code uncertainty value based on various uncertainty sources including code structure sub-model uncertainties (D'Auria 1998).

4.4.4 ASTRUM (W-House) Methodology

Westinghouse's previously approved best-estimate large-break loss-of-coolant-accident (LBLOCA) methodology (known as CQD, and described in WCAP-12945-P-A (Nissley 98)) was modified to use statistical tolerance limit instead of original response surface method, with some other minor differences in other steps. Both methodologies are patterned after the Code Scaling, Applicability, and Uncertainty (CSAU). The new Westinghouse methodology called Automated Statistical Treatment of Uncertainty Method (ASTRUM) is for handling of uncertainty in best estimate LBLOCA calculation. The main differences between the ASTRUM (Nissley 2003) and the CQD methodology is the calculation of the final PCT uncertainty distribution by a combination of response surface equations and Monte Carlo sampling. In ASTRUM, the 95th percentile PCT is established at 95-percent confidence using non-parametric order statistics. Qualifications in the methodology are almost the same as the original CSAU methodology. To the extend possible the

code structure uncertainties are treated the same with some sort of data-informed engineering judgment. Conservative biases resulting from phenomena that are conservatively predicted by WCOBRA/TRAC are ignored in both approaches (Nissley 2003).

4.5 IMTHUA Methodology Overview for Input, and Code Structure

All sources of uncertainties should be ideally considered in the analysis explicitly, but this is not practical considering lack of knowledge and/or limitation in resources. It is clear impossibility of considering all sources of uncertainties in process of thermal-hydraulics system codes uncertainty analysis. Limitation in sources of data (test and field both) is a significant barrier on nuclear facility dynamic (transient) behavior. This causes difficulties in quantification of structural uncertainties of the code. Possible sources of data and their application are given in Table 9 with applicability limitation of each data item.

Table 9: Nuclear/TH Data and Application

Nuclear Industry Data and Information	
Analytical Solutions	Validation and Verification
Field data (Nuclear Power Plant Operation)	Initial Conditions
Scale-Down Test Facilities	
Integrated Effect Tests Facilities (IET)	On overall behavior of facilities
Separate Effects Test Facilities (SET)	About Phenomena and local effects

The IMTHUA methodology for uncertainty treatment is a fully probabilistic and based on the Bayesian approach. It means that any piece of information about code calculation in inputs, code structure calculations, and the output is utilized in an

effective way. Information about code consists of past evidence regarding the descriptive/predictive performance of the model and can be classified as information from the model and about the model (Droguett E.L., 1999). With the problem stated in this way, Bayes Theorem is the preferred choice as a framework for utilizing the available information, IM, to express the state of knowledge about X. Therefore, according to the general Bayesian framework, the posterior state of the knowledge about interested quantity is obtained from updating calculation of prior distribution of past information with likelihood function of new data. A successful treatment of model uncertainty results in an expression of uncertainty that includes the true value at some stated level of confidence.

There are varieties of sources of uncertainties in code structure. These include: uncertainties in inputdeck, code models, model or sub-model applicability, and presence of alternative models. Quantification of these uncertainties are addressed explicitly with the techniques discussed in (Pourgol-Mohamad et al. 2006a) or implicitly by output updating through Bayesian framework developed in this research (Pourgol-Mohamad et al 2006b). The technique is applicable for code output as well as code models and sub-models inside. Qualification steps should be taken to make sure that input deck is qualified, and code and calculation are precise enough by utilizing V&V techniques.

4.5.1 Treatment of Input Parameter Uncertainty; Maximum Entropy Approach

Maximum entropy (rooted in information theory) is a general methodology for developing probability distributions on the basis of partial information. The principle states that one should not make more assumptions than the minimum needed. The

principle behind maximum entropy approach is that unreasonable to express probabilities which present more information than is initially given (Bari et al. 1989). The maximum entropy approach has found increasing applications in uncertainty characterization of complex system in the presence of sparse data and evidence about the system parameter. Uncertainty distributions developed through the ME approach are then used as the prior distribution when additional evidence and data become available.

The process of assessing ME distributions followed in this research is explained through the following example. Assume that we are interested in assigning a prior distribution of T (the temperature of downcomer in the reactor core, or clad temperature.) Assume also that we have a single estimate of this parameter, e.g., a mean value, and also have some information about the shape of distribution. Following are the cases considered in this research for shape assignment.

Case 1: Total Ignorance/Uniform Distribution

In case of complete ignorance, uniform distribution with minimum and/or maximum approaching infinity (or take maximum possible values) can be used. If the analyst expresses total ignorance about a particular distribution except that it must be bigger than X_{min} and smaller than X_{max} , then uniform distribution is still best estimate for distribution.

Case 2: Exponential Distribution

If we know a single value about the unknown, then enforcing maximum entropy leads us to the exponential distribution.

$$f(x) \quad e^{\ x}$$

$\bar{x}$ given for variable

$$\frac{1}{x} = \qquad (1)$$

For cases with 2 parameters (expect uniform) situation is different and a given single value does not lead to unique distribution. In this case the form of distribution or other types of information should be given about the distribution in addition to the above information. Following cases are for normal and lognormal distribution. Similar formulation may be derived for other forms of distribution such as Weibull and Beta.

Case 3: Normal Distribution

With a single value such as mean or mode of the distribution and with assumption of distribution shape being normal, we can calculate the distribution parameters by using Lagrange multipliers method.

$$f(x) \quad N(\ , \ ^2) \quad \frac{1}{\sqrt{2}} e^{\frac{1}{2}(\frac{x}{}\text{—})^2}$$

$$H(f(x)) \quad k \quad f(x)Ln(f(x))dx \qquad (2)$$

$$H(N(\ , \ ^2) \quad K \quad 0.5 \quad [\ln(2 \quad ^2) \quad (x \quad)^2 / \quad ^2](2 \quad ^2)^{0.5} \quad e^{(x \quad)^2/(2 \quad ^2)}dx$$

$$1/2(\text{Ln}(2 \quad ^2) \quad 1$$

where μ, σ are parameters of the knowledge-based prior distribution to be specified by maximizing the entropy equation given below

$$\frac{F}{} \quad \frac{F}{} \quad 0 \text{ (3)}$$

It is clear that there is no normal distribution of maximal entropy subject to the constraint of known mean. Knowing mean and variance will lead to a normal distribution with known parameter

Case 4: Lognormal Distribution

Assume again we know lognormal distribution is the right form:

$$f(x) \quad \frac{1}{\sqrt{2}\ T} e^{\left(\frac{1}{2^{\ 2}}(\ln T \quad)^2\right)} \text{ (4)}$$

Again μ, σ are the parameters that need to be specified by maximizing the entropy equation given below:

$$H \qquad K \quad f(T)\log f(T)dx \text{ (5)}$$

Using Lagrange multipliers assuming mean is given we have

$$F \quad H \qquad \bar{x} \text{ (6)}$$

with

$$\frac{F}{} \quad \frac{F}{} \quad 0 \text{ (7)}$$

Then we will have, (Bari et al 1989)

$$\frac{1}{2} \quad \ln \bar{x} \text{ (8)}$$

1

Figure 21 shows an example of input parameters quantification using maximum entropy approach for Marviken test facility blowdown experiment uncertainty analysis. Refer to (Pourgol-Mohamad 2006a) for detail of analysis.

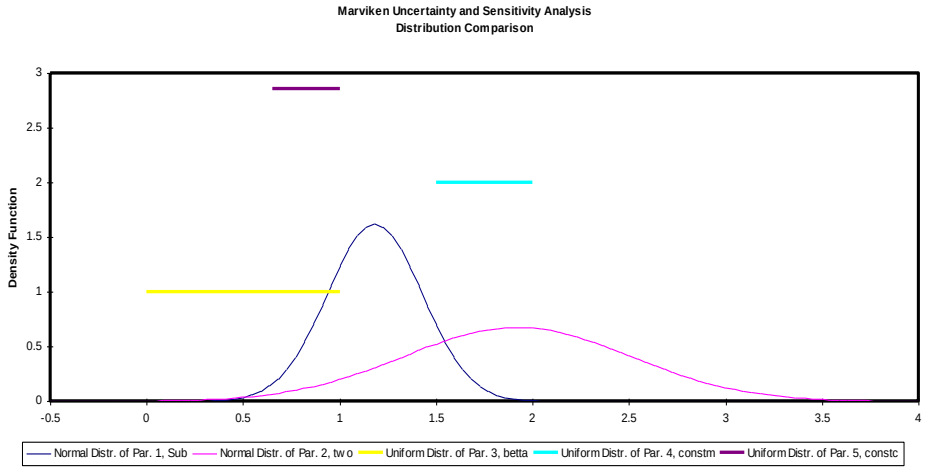

Figure 21: Parameter Distribution Estimation with Maximum Entropy Approach

4.5.2 Bayesian Updating with New Evidence

Bayesian methodology is used to account for any evidence about input variables including input parameters and model forms. The Bayesian method will be applied first to all input parameters and phenomena model (sub-model or code module). The latter could be based on evidences obtained from experiments (test data) including Separate Effect Tests (SETs) and Integral Test facilities (ITFs) on the estimated performance of actual plant. All evidences and data about key plant responses should be used to update our belief about predicted response. Analysis can be repeated upon receiving any new piece of information.

The process developed by Droguett and Mosleh (1999) is explained through the following example. Assume our prior knowledge about one given indicator input

parameter in LOCA analysis (e.g., choked flow discharge coefficient) is a parametric PDF, π_0(T), developed by maximum entropy approach as discussed in previous section.

Performing experiments, gathering field data or from expert opinion, we get a new evidence for this specific parameter. Relevance of this piece of evidence is another subject of evaluation and will be discussed in next section. Assume that this evidence will be a single value of T through a model. Other cases include evidence in form of distribution including homogenous and non-homogenous which will not be discussed here.

Let us assume that a model M provides an estimate T_1 about the quantity T, and that the available quantitative information on Model D, consists of past evidence regarding performance of the model. According to Droguett and Mosleh (1999), the updated belief about distribution of T can be presented by Bayes' theorem as follows:

$$(T|T_1,D) \quad \frac{L(T_1,D|T)\ \ _0(T)}{_T L(T_1,D|T)\ \ _0(T)dT} \quad \textbf{(9)}$$

where $L(T_1, D|T)$ is the likelihood of the evidence T_1 given that the true value of the unknown quantity is T can be decomposed as

$$L(T_1,D|T) \quad L(T_1|D,T)L(D|T) \quad \textbf{(10)}$$

Under the assumption that past performance data do not depend on T (the true value of interest in the current application of the model), we have L(D|T) =L(D), therefore

$$(T|T_1,D) \quad \frac{L(T_1|D,T)\ \ _0(T)}{_T L(T_1|D,T)\ \ _0(T)dT} \quad \textbf{(11)}$$

According to the methodology we now assume a parametric form for the likelihood function such that

$$L(T_1|D,T) \quad L(T_1|D,T) \quad (\_|T)d\_ \quad \textbf{(12)}$$

where

$$(\_|D) \quad \frac{L(D|\_) \ _0(\_)}{_T L(D|\_) \ _0(\_)d\_} \quad \textbf{(13)}$$

Additive or Multiplicative Error models [9] can be applied for developing the likelihood function.. The estimate from the model is considered as a random variable, T_1, which is the sum of the true but unknown value, T, and a random error term E as equation (14).

$$T_1=T+E \quad \textbf{(14)}$$

The error can be biased or non-biased. If we take mean value of both sides of above equation, we get:

$$\bar{T}_1 \quad T \quad b \quad \textbf{(15)}$$

If the error is un-biased then b will be zero. Different models have been discussed for error model [7] but by using additive error model, normal distribution is a reasonable choice for distribution of E. Errors in experiments and measurement tend to be normal distribution. Then the likelihood function $L(T_1|T)$ is a normal distribution with mean obtained from :

$$L(T_1|T,b, \ ) \quad \frac{1}{\sqrt{2}} e \ \frac{1}{2}(\frac{T_1 \quad (T \quad b)}{})^2 \quad \textbf{(16)}$$

where σ is standard deviation. The b and σ are unknown to us and can be estimated based on evidence. For is instance if the evidence is E (Droguett 1999):

$$(\_|T) \quad (b, \ |E) \quad \frac{L(E|b, \ ) \ _0(b, \ )}{_b L(E|b, \ ) \ _0(b, \ )dbd} \quad \textbf{(17)}$$

where,

$$L(E|b, \quad) \quad \frac{1}{\sqrt{2}} e^{\frac{1}{2}(\frac{E \quad b}{\quad})^2} \quad \textbf{(18)}$$

if we had more than one evidence in form of T_1, T_2, … , T_N then problem can be modified in form of $L(E1, E2, \ldots, EN|b, \quad)$ where the likelihood function is constructed considering each evidence. Given the model, estimates of each realization are independent as:

$$L(E_1, E_2, \ldots, E_N \mid b, \quad) \quad \prod_{i \ 1}^{N} L(E_i \mid b, \quad) \quad \textbf{(19)}$$

and this can be constituted in (17).

And $_0(b, \quad)$ can be justified based on our belief about b and σ. For example, limited shape of $_0(b, \quad)$ can be justified by a uniform distribution with

$$\begin{matrix} b_1 & b & b_2 \\ 0 & & _1 \end{matrix} \quad \textbf{(20)}$$

Then,

$$(b, \quad |E) \quad \frac{\frac{1}{\sqrt{2}} e^{\frac{1}{2}\frac{(T_1 \quad (T \quad b)^2}{\quad^2}}}{\int_b \frac{1}{\sqrt{2}} e^{\frac{1}{2}\frac{(T_1 \quad (T \quad b)^2}{\quad^2}} dbd} \quad \textbf{(21)}$$

then $L(T_1|D, T)$ can be calculated by substituting (19) in (12). With Calculating $L(T_1|D, T)$ and considering prior knowledge about T as π_0(T), we can calculate updated distribution of $(T|T_1, D)$ based on information.

Process is difficult and in most cases impossible to solve analytically. In this research an MCMC based numerical solution using WINBUGS14 (Lawson 2003, Bugs Project 2006) was developed for these purposes. There are different cases of

updating depends on status of problem. Problem can be single model or multi model. Data can be treated as homogeneous or non-homogeneous based on the problem, assumptions and expert opinion. This is discussed in Chapter 6.

4.6 Model Structure Quantification

Code structure uncertainties are a crucial source for uncertainty quantification. Code structure refers among other things the set of models and correlation for simulation of physical phenomena, system components for fluid and structural simulation. There are cases in the TH code where more than one sub-models are applicable. One example is availability of 3 different correlations for calculation of choked flow [CF]. They are developed by different experts for same purposes. In his case the code provides the user with option to choose one of them for code computation. Depending on whether we have single or multiple (alternative) models, a different treatment is possible to account for model uncertainty. The option is discussed in the following subsections.

4.6.1 Model Uncertainty Treatment for Single Model

There are different methods to deal with uncertainty of single models in complex structure of the code. Depending on objective for analysis, type of data and information, model arrangement with other sub-models, analysis type may be chosen from following methods.

a. Correction Factor

Statistical correction factor is a traditional way to data-informed uncertainty quantification. It is essentially based on comparison of data and model predictions.

The form is often additive or multiplicative. Multipliers are more commonly used in TH code uncertainty analysis for model correction, while additives are used for bias correction. An example of correction multiplier is correcting the choked flow model through Marviken test facility data. The Henry-Fauske model is implemented in the TH code for calculation of critical flow, if it is activated for calculation. A factor R_{in} is defined for quantification of discrepancies between code calculation and test data.

$$R_{in} = \frac{\text{Measured Flow Rate}}{\text{Predicted Flow Rate}}$$

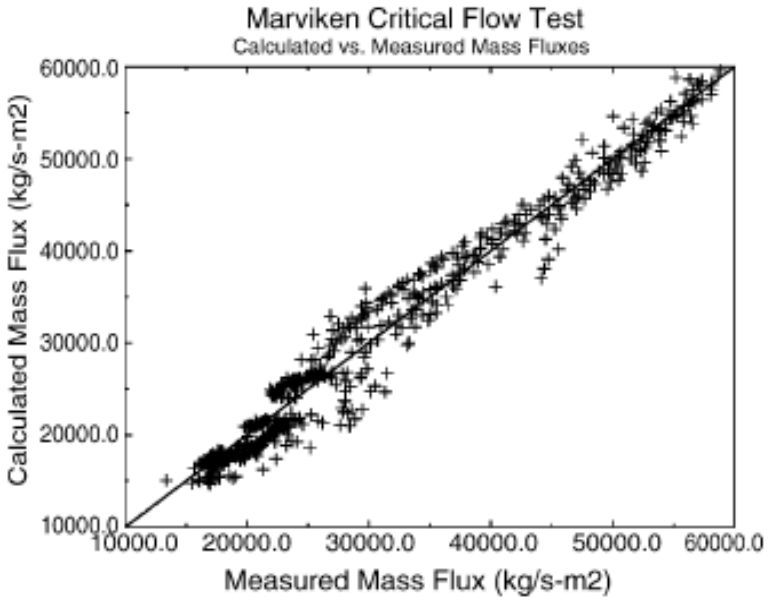

Figure 22: Scatter plot for code calculation (RELAP5 Code Development Team 2003)

This data (Figure 22) is used to estimate the multipliers for subcooled and two-phase choking models implemented in TRAC-PF1 code and also available in Relap5/mod3 as shown in Table 10.

Table 10: Multiplier Factors for Choked Flow models

Subcooled Choking Flow Multiplier	$R_{in} \quad 0.696\exp[0.649(\frac{L}{D})^{0.168}$
Two-phase Choking Flow Multiplier	$R_{in} \quad 0.778\exp[0.679(\frac{L}{D})^{0.25}$

In some cases there is no code parameter to characterize specific identified phenomena. An example is the ECC Bypass in the original CSAU uncertainty quantification. Separate bound in output ranging for compensation of its effect was considered in calculation of uncertainties in original CSAU.

b. Bias Consideration

In some cases Comparison of code calculation with available data from plant and test in different scales shows bias in models performance. The film de-entrainment model for ECC bypass and upper plenum de-entrainment calculation are examples of conservative biases at full scale in TRAC code calculation (Nissley et al. 2003). Bias can be defined as the average of the measured quantity divided by the same code calculated quantity. Young et al. (1998) discussed (based on finding of Dederer (Relap5 2003)) that the TRAC natural choking model had an average bias of 1.2 where the bias is the average of the measured test flow rate divided by the code calculated flow rate, for several different tests, test configurations, and test diameters. A bias of 1.2 means that on average, the TRAC-PD2 model over-predicts the measured critical flow by 20 percent. The bias may be caused by scaling and/or intrinsic bias in the model. The biases should be evaluated one-by-one in models and correlations

4.6.2 Alternative Model Uncertainty

There are several situations where the user and the code (internally) have options to choose from alternative models. Depending on the data and information available, and the conditions, there are varieties of treatments. As discussed in detail below, weighting and combining the available models, or switching between them, are among the options. Expert judgment plays an important role in this process.

Case 1: Automatic Code Switching (Upon Satisfaction of Some Conditions)

Model switching as shown in Figure 23 is one option in suing alternative models in the code. Model switch can be made when certain pre-specified conditions are present at any time.

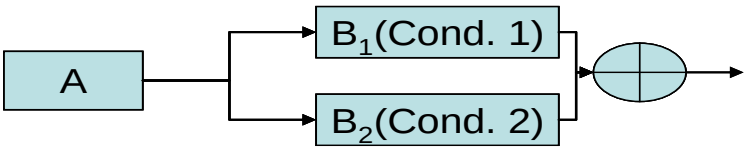

Figure 23: Model Switch Based on Condition (Time, Thermodynamics Condition or Expert Justification)

An example is the flow phase change in an ongoing transient causing effects on conditions for the choked flow phenomena. It will change conditions from 1-Phase Choked flow to 2-Phase choked flow model by the changing in flow conditions. It is illustrated for the calculation of mass flow of Marviken blowdown scenario in Figure 24. This approach may encounter problems in continuous behavior prediction of phenomena, as seen in Figure 53.

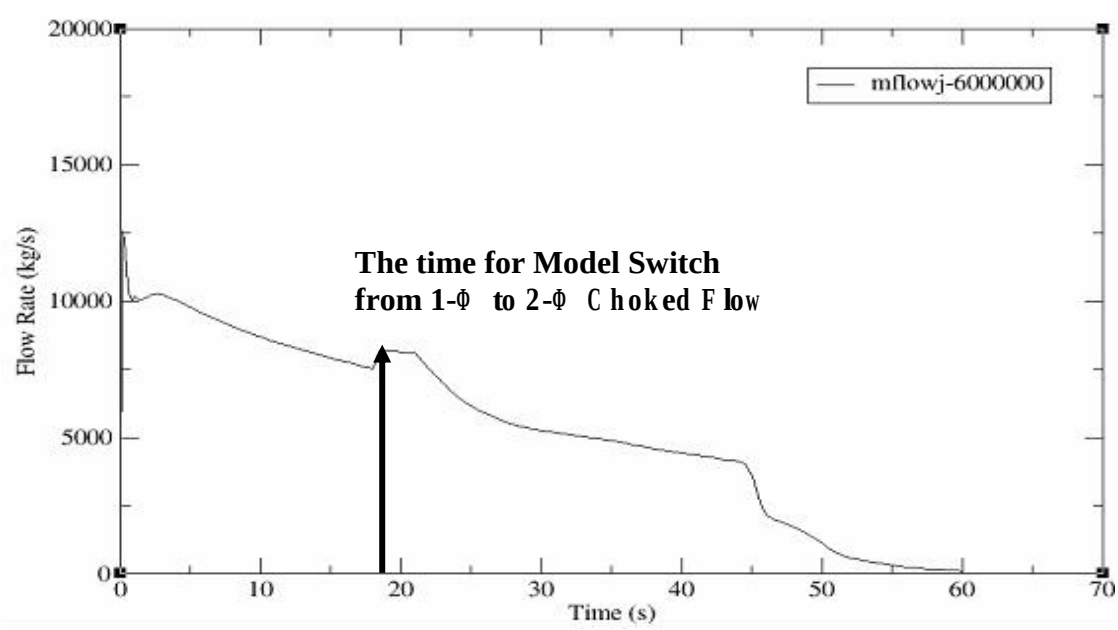

Figure 24: Model Switch from 1 Phase Choked Flow to 2 Phase Choked Flow

Case 2: Run the Code as Recommended

There are some recommendations in the code for execution of specific problems. An example is the user choice for operative area change of alternatives abrupt area change vs. smooth area change, or partially area change based on user justification. Figure 25 shows schematically such situation.

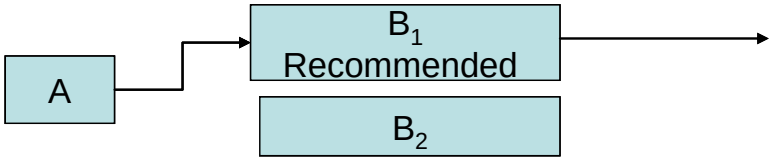

Figure 25: Run Code on Recommended Path

Two different data sets with different structures is the prerequisite for this type of treatment.

Case 3: Change of Code Models by User in Same Run

In some cases data supports switch in time t from model 1 to Model 2, it should be part of the calculation for more precise simulation of transient in a single run.

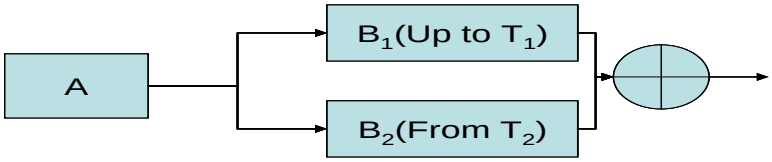

Figure 26: Model Change in a Single Run by User

The situation is shown schematically in Figure 26. T_1 is the time change in conditions or change of model for better results. This capability has been implemented by the author in Relap5 code to switch from Henry-Fauske model to the original one (Ransom-Trap model) and vise versa. It produces better results as shown in Figure 27. The code was run 3 times. First with Ransom-Trap choked flow model and then with Henry Fauske model. In the third case, the model in switched from Ransom-Trap to Henry-Fauske model in the calculation at the t=20 seconds. This is the time which separates the phases of the transient of better prediction for each model.

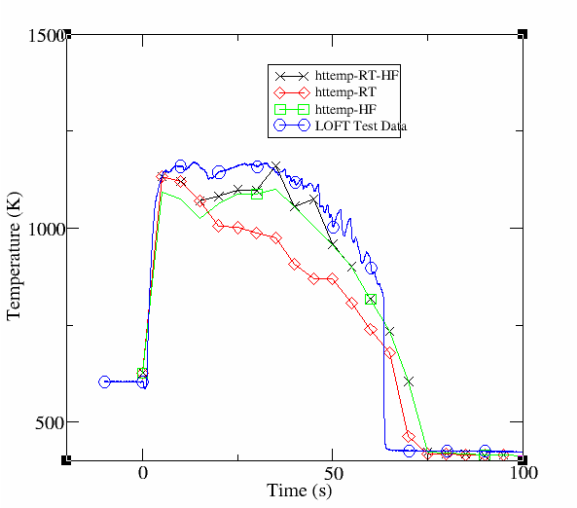

Figure 27: Effect of Model Switch by Code or User

Case 4: Model Mixing

Same underlining data, but different model structures, is the requirement for model mixing as shown pictorially in Figure 28. An example is CCFL model of Wallis, Kutateladze and Bankoff correlation available in Relap5 code. A general countercurrent flow limitation (CCFL) model is used that allows the user to select the Wallis form, the Kutateladze form, or a mixture of the Wallis and Kutateladze forms. This general form was proposed by Bankoff and is used in the TRAC-PF1 code as well as RELAP5 code. It depends on geometry of interest. A variable β specifies the level of mixing. When β = 0 the code uses Wallis Correlation, and for β = 1 Kutateladze Correlation is used. For of 0<β<1, Bankoff Model which is a weighting of Wallis and Kutateladze Correlation will be used. Recommendation is for the Wallis (or Kutateladze) form to be used small (or large) diameters. Other approaches (Relap5 Code Development Team 2004) appear to be more restrictive by defaulting to the Wallis form at small diameters and the Kutateladze form at large diameters. It is on the user to select type of correlation based on conditions.

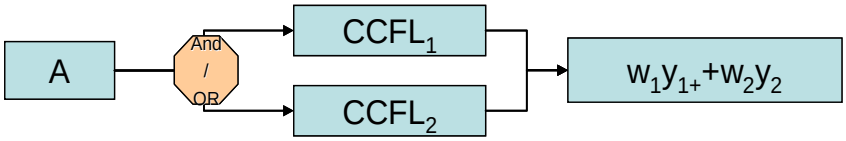

Figure 28: Model Mixing

Figure 29 shows three different code executions of Relap5 for LOCA calculation of Calvert Cliff's nuclear power plants with CCFL models of Wallis, Kutateladze and Bankoff correlations. The absence of experimental data for making decision on correlation selection, expert justification will be crucial.

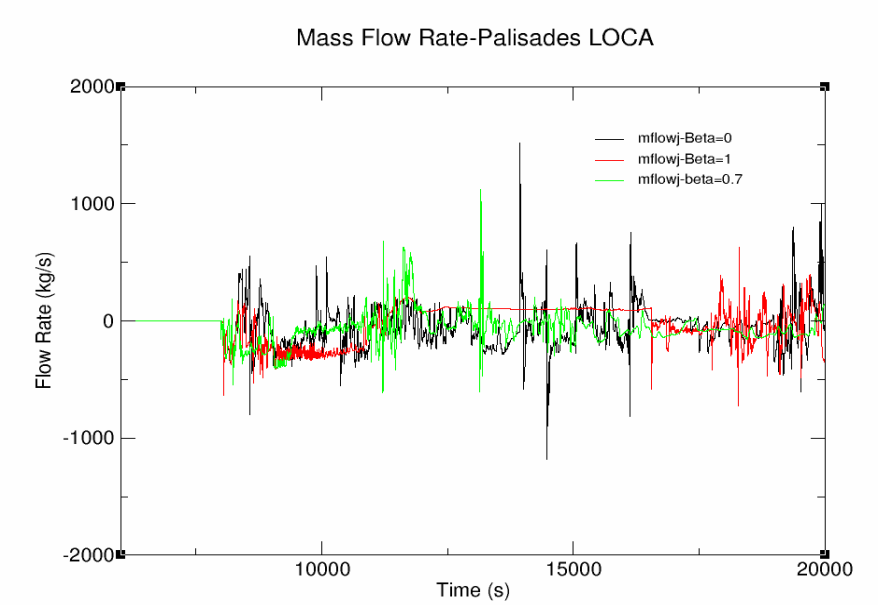

Figure 29: Model Mixing; a) Wallis CCFL Model b) Kutateladze CCFL Model c) Bankoff Mix CCFL Model Beta=0.7

Case 5: Model Maximization/Minimization

In this approach maximum value produced by one of the two alternative correlations will be used in calculations An example is Superheated Interfacial Heat Transfer Coefficients (h_{il}, h_{ig}) Analytically Derived Correlation by Plesset and Zwick vs. Deduced correlation by Lee and Ryley from the observed data.

4.7. Uncertainty Treatment for Code Structure

4.7.1 Model Updating with Performance Data

When performance data (in form of code calculated values and experimental results) on a single sub-model, is available, the non-paired method (see next Chapter) of analysis for output updating may be used for uncertainty quantification for code sub-models. The method depends on experimental data availability about sub-model output. The methodology and procedure are the same as what will be discussed in

next section for output updating. It is illustrated in the following example for choked flow model with data from Marviken test facility.

The critical flow test with the aim of obtaining critical flow data is chosen to demonstrate the methodology. Since the Marviken test facility is not a full size nuclear power plant some aspects of proposed methodology are not applicable to this special problem. Refer to Studsvik Energiteknik (1979a and 1979b) on details about test facility and tests data. Experiments are considered reference points for this application. Effects of possible experimental errors are not considered. However, maximum errors calculated on experiments were based on the manufacturer's specifications. These were discussed with some statistical quantities such as error limits and their confidence, and also probable error. See Studsvik Energiteknik (1979c) for details on experimental errors.

For this step of analysis a total of 100 points (number of code runs) and 3 experimental data points are available. A uniform prior distribution is assumed for the results from input uncertainty propagation and a normal for test data distribution as shown in Figure 30. Non-paired updating method as discussed above was then applied and results for one data point (t=30s) are shown in Figure 31.

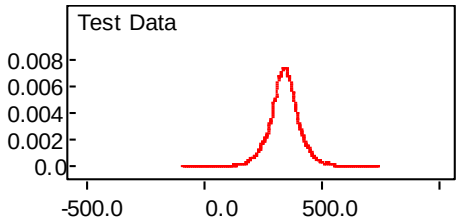

Figure 30: Experimental Data Distribution

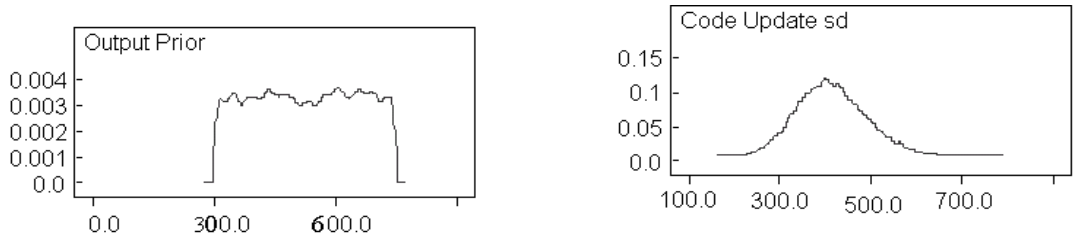

Figure 31: Output Updating in Time 30s after Transient Initiation

4.7.2 Model Updating with Partially Relevant Data

Data from experiments should be evaluated for their degree of relevance to the conditions of the scenario. The data may be evaluated as completely relevant and used directly for updating purpose or assessed as partially relevant. A Bayesian weighting process is developed by (Droguett 1999) for considering partially relevant information. Criteria for assigning the weights in case of TH experiments are deduced from assessment of similarity degree of test data to the calculation. Data is in form of set of model estimate from code calculation and corresponding experimental data such that D= $\{D_1, D_2, \ldots, D_N\}$

A relevance factor φ can be assigned to the data based on the above mentioned criteria. The φ factor is an indicator of data applicability and relevance. Some attributes of scenario facility and experimental facilities for applicability assessment, are:

Distortion from Scaling (e.g., π group values)

Location and Size of Break,

Rate of Power,

Scaling Ratio of the Facility,

Involved Safety Systems,

Nuclear Core Configuration

These attributes should be compared pair wise (Figure 32) for applicability and relevance assessment and evaluation.

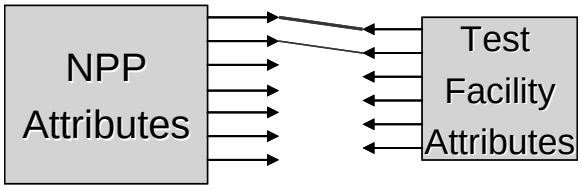

Figure 32: Binary Matching and Comparing Attributes

The value of φ factor is between 0 (absolutely not applicable) and 1 (absolutely applicable) (see Table 11). This factor will be utilized in a Bayesian process proposed by (Droguett and Mosleh 2001) as shown below:

$$(T \mid IM, D) \quad \frac{[L(IM, D \mid T)] \ . \ (T)}{\int_T [L(IM, D \mid T)] \ . \ (T) dT} \quad \textbf{(22)}$$

The correction in the Bayesian formula in the likelihood adjusts for the effect of the data relevance. Assume that the form of the likelihood is normal distribution. If $\varphi = 0$ (Absolutely not Applicable Data), the likelihood term equates to 1 and posterior is same as the prior. This means that the data does not change the prior distribution from first phase. If $\varphi = 1$, the we have the likelihood in full strength (no adjustment in shape) and the data will update the result completely. If the φ factor is in range (0,1) then it will defuse the likelihood resulting in smaller effect of the data on the posterior.

Likelihood adjustment method is another alternative to use φ factor for updating of the output distribution. As mentioned, φ factor is based on source data assessment. According to this methodology a shape is assumed for Likelihood (e.g., Normal) and

objective is assess the distribution parameters (e.g.,) form data and information implementation as:

$$[L(IM,D|T)] \quad L(IM,D|T) \quad [L(IM,D| \ , \ )] \quad \textbf{(23)}$$

Table 11: Applicability Weights for φ factor

Applicability Weight	
Value (φ)	**Statement**
0.00	**Absolutely not Applicable**
0.20	**Strongly not Applicable**
0.40	**Moderately not Applicable**
0.50	**Slightly Applicable**
0.60	**Moderately Applicable**
0.80	**Strongly Applicable**
1.00	**Absolutely Applicable**

An expert group should quantify the φ for each test facility and test itself based on similarities and differences between it and nuclear power plant and the transient scenario. This φ will be used on unitization of the data for parameter, model and output uncertainty distribution.

Chapter 5: UNCERTAINTY PROPAGATION

5.1 TH Code Uncertainty Propagation

Sub-model and input parameter uncertainties need to be propagated through code computations. The dynamic behavior of the TH codes executed in each time step, transfers accumulated errors and uncertainties to next time step. Depends on NPP type, scenario specification, and the software used, propagation of uncertainty will end in different results. Type of sources of uncertainty and information available will also affect the results significantly. Positive and negative effects of uncertainties sources on the output compensate the net value. There are different methods for propagation of uncertainty including Monte Carlo sampling (Helton at el 2000), fast probability integration (Haskin 1996), response surface (Prosek 2000), sensitivity based (Chang 2004 and Ronen 1988), and accuracy based propagation (D"Auria 2006 , Han 2004). In the Monte Carlo class of there are different approaches to obtain samples from sources of uncertainties including simple sampling, Latin Hypercube (Iman at el 1984, Helton at el 2002) and Helton at el 2000), and importance based sampling (Helton at el 2000). Based on merits of each methodology, and depending on the type of the problem, a propagation method is selected. Thermal-hydraulics computational code has its specific requirements mostly drawn from regulatory (Orechwa 2004) and other limitations due to the complexity and resource requirements. Response surface method was used in early methodologies for uncertainty analysis of thermal-hydraulics computation codes (Boyack 1990, Wulff 1990 and Lelloche 1990). Response surface method becomes ineffective as the number of uncertain parameters increases requiring larger number of code executions

(Glaeser 2001). As systems and their models become more complex and costly to run, the use of tolerance limit characterization is gaining popularity. Often in complex computer-based models in which calculation of output values require significant amount of time and effort, are cases in which traditional Monte Carlo simulation is not practical. There are a number of more effective Monte Carlo based uncertainty propagation methods especially those utilizing order statistics, non-parametric tolerance limit, and Bootstrap approach.

After extensive literature review, on merit and limitation of different methodologies, order statistics based tolerance limit method is selected for the core of uncertainty propagation in the IMTHUA method. Table 12 shows different types of statistics used for quantification of uncertainties and inferences about the results (Pal and Makai 2004, Pal and Makai 2005). Depending on type of input and output (such as continuous or discrete, single or multiple output,) and the propagation framework is selected. Dependency among the models and parameters (Iman 1982) is very important and should be considered in the assignment of uncertainty distributions and sampling for input entities.

Table 12: Different Order Statistics

Continuous
Discrete
Single
Joint
Parametric

Non-Parametric

Following sections will discuss foundation for the order statistic based tolerance limit inference.

5.2 Relevant Statistical Concepts and Methods

A tolerance interval is a random interval (L, U) that contains with probability (or confidence) at least a fraction γ of the population under study. The probability and fraction and γ are analyst"s selected criteria depending on the confidence desired. The pioneering work in this area is attributed to Wilks (Wilks 1941 and Wilks 1942) and later to Wald (Wald 1943, 1964a, 1964b). Wilks" Tolerance Limit is an efficient and simple sampling method to reduce sample size from few thousands to around 100 or so. Number of sample size does not depend on number of uncertain parameters in the model.

There are two kinds of tolerance limits:

Non-parametric tolerance limits where nothing is known about distribution of the random variable except that it is continuous

Parametric tolerance limits where the distribution function representing the random variable of interest is known and only some distribution parameters involved are unknown.

The problem in both cases is to calculate a tolerance range (L, U) for a random variable X represented by the observed sample, $x_{1,\ldots}$,x_m, and the corresponding size of the sample.

Consider γ *tolerance limits* L and U for *probability level* of a limited sample S_1 of size N, the probability that at least γ proportion of the X"s in another indefinitely large sample S_2 will lie between L and U is obtained from (Pal, Makai 2004):

$$p(\int_L^U f(x)dx \quad) \qquad \textbf{(24)}$$

where, f(x) is the probability density function of the random variable X.

Let us consider a complex system represented by a model (e.g., a risk model). Such a model may describe relationship between the output variables (e.g., probability of failure or performance value of a system) as a function of some input (random) variables (e.g., geometry, material properties, etc.). Assume several parametric variables involve in the model. Further assume that the observed randomness of output variables is the result of the randomness of input variables. If we carry out N runs with random input, then we obtain a sample N output values $\{y_1, \ldots, y_N\}$ for y = f(x). In using equation (24) for this problem note that probability bears the name confidence level. To be on the conservative side, one should also specify probability content γ in addition to the confidence level as large as possible. It should be emphasized that γ is not a probability, although is a non-negative real number of less than 1 (Pal, Makai 2005). Having fixed and γ; it becomes possible to determine the number of runs (samples of output) N required to remain consistent with the selected and γ values.

Let $y_1 \ldots y_N$ be N independent output values of y. Suppose that nothing is known about the density function g(y) except that it is continuous. Arrange the values of $y_1, \ldots, y_N$ in an increasing order and denote them by y(k), hence

$$y(1) \quad \min_{1 \le k \le N} y_k, \qquad y(N) \quad \max_{1 \le k \le N} y_k \quad \textbf{(25)}$$

and by definition y(0) = -∞ ; while y(N+1) = +∞ . It can be shown that for confidence level [6] is obtained from

$$\beta \quad \sum_{j=0}^{k-r-1} \binom{N}{j} \gamma^j (1-\gamma)^{N-1} \qquad \textbf{(26)}$$

$$0 \le r < k \le N, \text{and } L = y(r), U = y(s)$$

From equation (30) sample sizes N can be estimated. For application of this approach consider two cases of the tolerance limits: one-sided and two-sided:

Statistical aspects relevant to safety analysis of complex TH systems codes are generally addressed in some articles in 1940s (Wilks 1941 and 1942, Walds 1943, 1964a and 1964b), and more specific to the topic, recently (Conover 1999, Guba and Makai 2003 and 2004, Wallis et al 2004 and 2005).

Output T of TH code is presumed being random variable with unknown distribution. Lets the results of running the code N times be ordered in increasing temperature as a set of values T_1, T_2, T_3,… ,T_N, i.e., $T_1 < T_3 <$ … $< T_N$ as shown in Figure 33 . Usually there is a safety or operational limit for T. These limits are usually set by regulatory for assurance of acceptable risk to public (Pal and Makai 2004). We define a fix acceptance and a fix rejection interval to variable T. Let the acceptance interval be $H_a = [L_T, U_T]$, and $H_r = (-\infty, L_T) \cup (U_T, +\infty)$ the rejection interval. If the limit is only on one side then the acceptance range be given as $(-\infty, U_T]$. With unknown distribution of T, we are looking for a quantile

$$P\{T \quad H_a\} \qquad \int_{T} dG(T) \qquad \textbf{(27)}$$

where G(T) is the unknown CDF of output variable T. T_γ is to be derived from measured value thus, itself is a random variable.

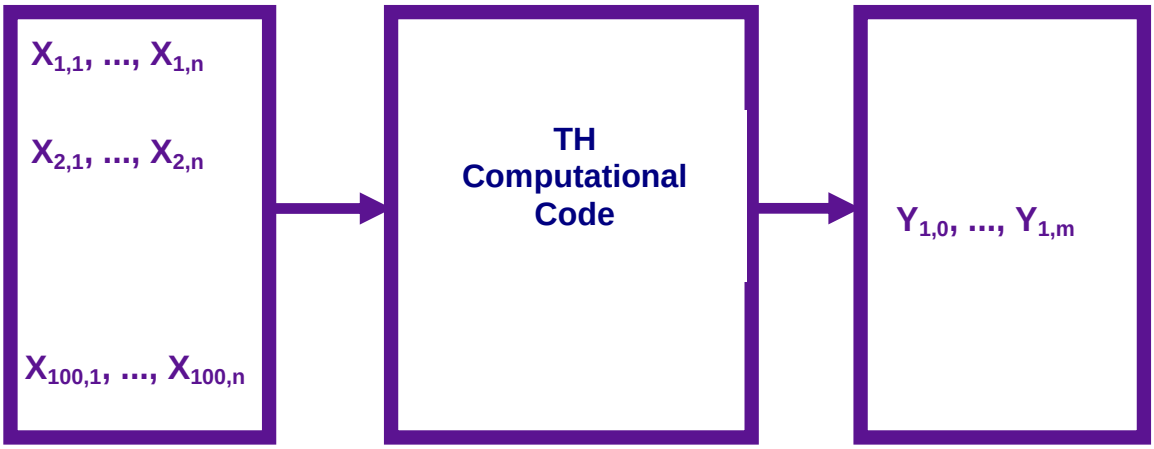

Figure 33: Sampling and Propagation of Uncertainties in Order Statistics Based Frameworks for Single Output

5.2.1 Tolerance Interval Method

The statement for tolerance limit can be described as follows. On the basis of a sample $S_N = \{T_1, \ldots, T_N\}$ can we state that a fraction larger than γ of the distribution G(T) lays with probability β in an interval $[L_T, U_T]$?

Random interval $(-\infty, T_N]$ covers a portion larger than γ of the unknown distribution function G(T) with probability β when $\beta = P(T_s > T_\gamma)$. It can be shown that (Pal and Makai 2003):

$$\sum_{j=0}^{s-1} \binom{N}{j} (1-\gamma)^{N-j} \quad \textbf{(28)}$$

where s = N, i.e., the largest element of the sample is chosen as upper limit of the random interval, one can obtain the well-known formula

$$1-\gamma^{N} \quad \textbf{(29)}$$

In case of two-sided quantiles, we arrive at the following formulation for β (Wallis 2003)

$$1-\gamma^{N}-N(1-\gamma)\gamma^{N-1} \quad \textbf{(30)}$$

β is the probability that the largest value T_N of the sample is greater than the γ quantile of the unknown distribution of output variable T. In other words, β is the probability that the interval $(-\infty,T_N]$ covers a larger than γ portion of the unknown distribution G(T) of the output variable T. This leads to 59 observations of N with probability of 0.95 to keep T_N upper $T_{0.95.}$ Details and proofs are provided in Pal and Makai (2004).

As a result, N=59 runs is sufficient statistics to calculate one-sided 95% of the output single variable T with 95% confident. The required runs for 95%|95% will be resulted in 93 samples number.

There are other statistics for cases of 2-sided, non-single output variables which are addressed in the literature [Wallis 2004, Wallis 2006] and will be discussed later. As Guba et al (2003) formulate statistics based on coverage concept of previous Wilks and Wald work, Wallis and Nutt (2005) introduces bracketing method to consider for dependency between outputs in the case of multi-outputs (e.g., PCT, MLO, CWO) which is required by USNRC (USNRC 1989)

There is a challenge in the 95%|95% methodologies addressed by [Pal 2005]. In some rare cases, there is a possibility for T_N to exceed the upper limit U_T. They suggested a methodology based on sign test. They test probability of $p = P\{T \leq U_T\}$ as sign test to make sure that it is big enough. Case of known distribution for random variables is also addressed in Pal and Makai (2003). Several tests were performed to validate Wilks' tolerance limit before utilizing it this research which discussed at end of the chapter.

5.3 Wilks Tolerance Limit Samples for One-Sides and Two-Sided

5.3.1 One Sided Tolerance Limit

This is the more common case, for example when measuring a model output value such a temperature or sheer stress at a point on the surface of a structure. We are interested in assuring that a small sample of, for example, estimated temperatures, obtained from the model, and the corresponding upper sample tolerance limit T_U according to equation (30), contains with probability (say 95%) at least the fraction γ of the temperatures in a fictitious sample containing infinite estimates of such temperatures. Table 13 shows values for sample size N based on values of β and γ. For example, if $= 0.95; \gamma = 0.90;$ then $N = 45$ samples taken from the model (e.g., by standard Monte Carlo sampling) assures that the highest temperature T_H in this sample represent the 95% confidence upper limit below which 90% of the all possible temperatures lie.

Table 13: Minimum sample Size (One-Sided)

β → γ ↓	**0.90**	**0.95**	**0.99**
0.90	22	45	239
0.95	29	59	299
0.99	44	90	459

5.3.2 Two Sided Tolerance Limit

We now consider the two-sided case, which is less common in nuclear power calculation (Less concern on lower bound). Table 14 shows the Wilks' sample size. With γ and both equal to 95%, we will get N=93 samples. For example, in the 93 samples taken from the model (e.g., by standard Monte Carlo sampling) we can say that limits (T_L, T_H) from this sample represent the 95% confidence interval within which 95% of the all possible temperatures lie.

Table 14: Minimum sample Size (Two-Sided)

β → γ ↓	**0.50**	**0.90**	**0.95**	**0.99**
0.50	3	17	34	163
0.80	5	29	59	299
0.90	7	38	77	388
0.95	8	46	93	473
0.99	11	64	130	663

5.4 Output Number Effect

Now we assume the output to comprise of m variables. Let these variables be $y_1, \ldots, y_n$ as shown in Figure 34. If they are statistically completely independent, we can apply the results of previous sections, otherwise we need new considerations.

5.4.1 Multi-Output

If there are more than one output variables (as expected in relation with regulatory requirements for joint inferences on all PCT, MLO and CWO conditions will be different for the size of samples. It is shown schematically in Figure 34. Wallis (2004) has provided a mathematical basis for number of samples, while Pal and Makai (2004) have tabulated the number of samples based on confidence level, probability coverage, and number of outputs (Table 15).

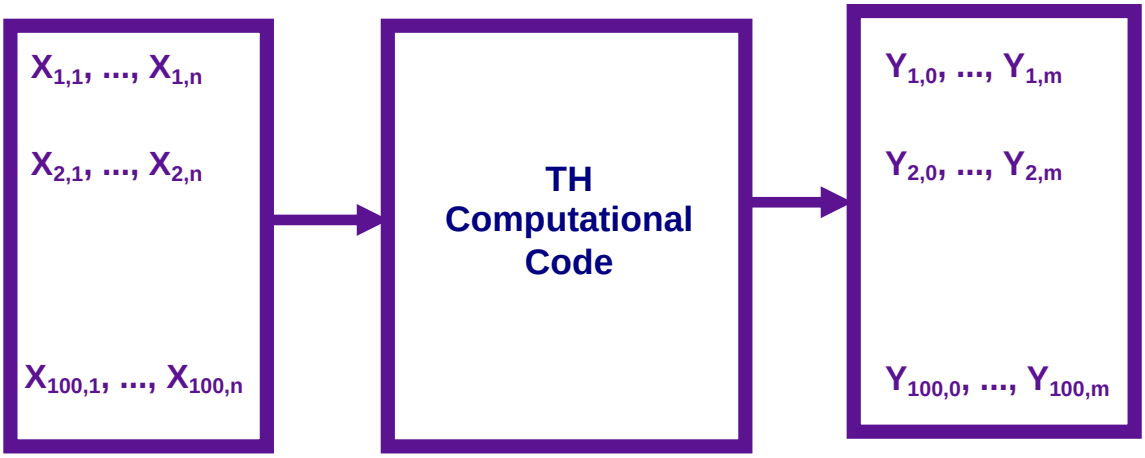

Figure 34: Sampling and Propagation of Uncertainties in Order Statistics Based Frameworks for Multi-Output

Table 15: Number of runs needed to determine the two-sided tolerance region for n = 1, 2, 3 output variables for listed values [Pal and Makai 2004]

	0.95	**0.96**	**0.97**	**0.98**	**0.99**	**n**
0.95	93	117	156	235	473	1
	153	191	256	385	773	2
	207	260	348	523	1049	3
0.96	98	123	165	249	499	1
	159	200	267	402	806	2
	215	269	360	542	1086	3
0.97	105	132	176	266	533	1
	167	210	281	422	848	2
	224	281	376	565	1134	3
0.98	114	143	192	289	581	1
	179	224	300	451	905	2
	237	297	397	598	1199	3
0.99	130	163	218	329	661	1
	197	248	331	499	1001	2
	258	324	433	651	1307	3

5.5 Why a Modified Tolerance Limit Sampling?

As discussed before, results of first phase uncertainty distribution will be transferred to second phase for output updating. Tolerance limit statistics gives a confidence level on the level of coverage depending on sample size, number of output and one-sided or two-sided type of statistics. This information should be transferred to second phase. An example of 93 random sample was generated to test preservation of the information using two method discussed in the previous chapter. A normal distribution is fitted to this data is shown in Figure 35 and the statistics presented in Table 16.

Table 16: Statistics for Normal Distribution by Utilizing MCMC

node	M	SD	MC error	2.50%	median	97.50%
Normal	6.072	1.177	0.009958	3.766	6.067	8.354

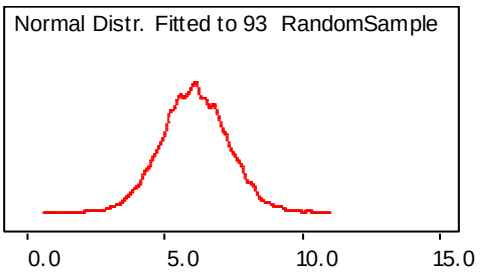

Figure 35: Normal Distribution Fitted to 93 Random Samples

It is clear that coverage between minimum and maximum on the samples (7.958352-4.04043=3.917922) is larger than 95% coverage obtained by the fitted distribution as (8.354-3.766=4.588).

Table 17: 93 Random Samples

4.04043	4.494523	5.032903	5.420264	5.895744	6.334116	6.572366	6.968523	7.653392	7.917863
4.12494	4.53715	5.035933	5.439503	5.92239	6.34038	6.588923	7.082209	7.672888	7.948444
4.132404	4.57311	5.100876	5.468008	5.926086	6.344126	6.595213	7.113972	7.718356	7.958352
4.187836	4.6191	5.146549	5.477714	6.014812	6.344203	6.696165	7.185268	7.750647	
4.28269	4.622185	5.21513	5.490791	6.144281	6.3559	6.774479	7.368802	7.790866	
4.287855	4.669372	5.232057	5.509861	6.184593	6.415802	6.793106	7.370046	7.823204	
4.30817	4.769765	5.284906	5.557236	6.240229	6.424928	6.854972	7.451792	7.838922	
4.371444	4.834017	5.38261	5.589783	6.242436	6.515551	6.923087	7.475193	7.876668	
4.411731	4.959731	5.400106	5.77895	6.282623	6.540274	6.934501	7.517394	7.883566	
4.445004	4.972261	5.419599	5.809594	6.31974	6.556814	6.938715	7.565532	7.907973	

Another approach is to use smallest and biggest value in the ordered sample as shown in equation (31), in order to preserve the information from order statistics based tolerance limit.

$$\frac{x_{0.95}}{x_{0.05}} \quad \begin{matrix} 1.96 \\ 1.96 \end{matrix} \qquad \textbf{(31)}$$

It results =5.999391 and =0.99946 for the distribution. The problem in this approach is that we only use information on extreme values and throw away information from other data points, resulting in weakly fitted distribution. A modified

Wilks sampling method is proposed with higher samples but accurate in conserving the information in first phase transferring to output-updating phase.

5.5.1 Boot Strap Based Sampling

Joucla at el (2006) proposed a bootstrap based methodology to propagate uncertainties in TH code calculations. The basic idea of bootstrap is re-sampling with replacement, leading to the randomization of the initial sample. It was concluded that with the increase of computational power allowing running several hundreds of calculations, bootstrap method give more precise results compared to Wilks formula. The reason is the increase in the number of samples taken (a total of 590 samples gives more than 99% confidence on 95% coverage in two-sided Wilks tolerance limit). It was justified in number of Bootstrap samples should be al least 100 but Efron at el (1993) justified that number of bootstrap samples should be increased until the standard deviation error is acceptable. Considering the idea of bootstrap sampling and order statistics, total of 300 runs are considered as following:

3 Times Wilks Sampling 100, 100, 100

Bootstrap 100 200 300 … … …

It is concluded that results with both approach results in better accuracy if we increase the sample size.

5.6 Dependency Effects

If all uncertain variables are independent, then their propagation is mathematically easier. However, when uncertainties are dependent, things become much more

delicate. Data-informed dependency calculation is most common way to calculate dependency in domain of TH code calculation (Iman at el 2003).

The steps are as follows:

$$\text{Expected \% of Effect Variable } X_J \text{ on Output Y Uncertainty} = \frac{Var(E[Y \mid X_J])}{Var(Y)} \quad 100\% \quad \textbf{(32)}$$

This results in change of uncertainty range for the output Y, if we exclude parameter X_j from the list of uncertain parameters.

Step 1. The variance of the output Y from the model is estimated from *n* computer runs using randomly selected values of the input variables. In particular, let **X** represent an $n \times$ m (in the example m=4) matrix of sample input characteristics to be utilized with the computer model

$$X \quad \begin{matrix} X_{11}\ X_{12} \ldots . X_{1N} \\ X_{21}\ X_{22} \ldots . X_{2N} \\ \ldots . \\ X_{N1}\ X_{N2} \ldots . X_{NN} \end{matrix} \qquad \textbf{(33)}$$

Step 2. Let $\mathbf{X}_M$ represents a vector of means of the input variables:

$$X_M \quad [\bar{X}_1 \ \bar{X}_2 \ldots \ \bar{X}_{N\ 1}\ \bar{X}_N] \quad \textbf{(34)}$$

Step 3. Generate a new matrix of inputs $\mathbf{X_1}^*$ by replacing the last three entries in each row of **X** with their corresponding means from the vector **X**M given in Equation 10.

The new matrix appears as follows:

$$X^*_1 \quad \begin{matrix} X_{11}\ \bar{X}_{12} \ldots . \bar{X}_{1N} \\ X_{21}\ \bar{X}_{22} \ldots . \bar{X}_{2N} \\ \ldots . \\ X_{N1}\ \bar{X}_{N2} \ldots . \bar{X}_{NN} \end{matrix} \qquad \textbf{(35)}$$

Step 4. Run the computer model using the matrix $\mathbf{X_1}$* and calculate V(Y). Denote this variance as $V(E[Y|X_1])$.

Step 5. Repeat steps 3 and 4 for X_2 where the 1st, 3rd … and N th columns of **X** are replaced by their respective means in the vector $\mathbf{X}_M$. Denote the resulting variance estimate as $V(E[Y|X_2])$.

Step 6. Repeat steps 3 and 4 for X_3 where the 1st, 2nd … and N_{th} columns of **X** are replaced by their respective means in the vector **X**M. Denote the resulting variance estimate as $V(E[Y|X_3])$.

Step 7. Repeat steps 3 and 4 for other X_N where the 1st, 2nd and 3rd …..columns of **X** are replaced by their respective means in the vector $\mathbf{X}_M$. Denote the resulting variance estimate as $V(E[Y|X_N])$.

Step 8. Substitute the variance estimates in Steps 4 to 7 into Equation 8 with the estimate of V(Y) from Step 1 to estimate the expected percentage reductions for X_1 to X_N.

5.7 Sensitivity Analysis

Several sensitivity analysis techniques are available from the simplest of scatter plots to more sophisticated sensitivity analysis techniques. Pearson product moment correlation coefficient is the usual linear correlation coefficient computed on the (x_{ij}, y_i), i= 1, … , N. The product moment part of the name comes from the way in which it is calculated, i.e., by summing up the products of the deviations of the scores from the mean. The correlation $r_{x_j y}$ between the input variable X_j and the output Y is defined by

$$r_{x_j y} \quad \frac{\sum_{i\ 1}^{N} (x_{ij} \quad \overline{x_j})(y_i \quad \overline{y})}{[\sum_{i\ 1}^{N} (x_{ij} \quad \overline{x_j}]^{1/2}[\sum_{i\ 1}^{N} (y_i \quad \overline{y})^2]^{1/2}}$$

Where **(36)**

$$\overline{y} \quad \sum_{1i}^{N} \frac{y_i}{N}, \qquad \overline{\mathrm{x}_{\mathrm{j}}} \quad \sum_{1i}^{N} \frac{x_{ij}}{N}$$

The coefficient $r_{x_j y}$ provides a measure of the relationship between X_j and Y. (Saltelli 2001). The approach is used in the IMTHUA methodology when binary information on dependency between two parameters is available. The results are used for calculation of the samples for parameters.

5.8 Tolerance Limit Validation Tests

Several tests were performed designed for validation of the order statistics propagation approach in this research e methodology and are discussed below.

5.8.1 Test 1-Sum and Products of random variables

(a.) The simple test is to obtain the sum of five normally distributions random variables with. The parameters of the five distributions are (5, 2), (7, 2.5), (9, 1.5), (11, 3) and (14.5, 5.5). Consequently, the parameters of the sum are (46.5, 7.194).

In Wilks' simulation, 93 samples were randomly selected, while in straightforward Monte Carlo simulation 10000 samples were performed randomly. The result is shown in Figure 36.a

(b.) The same procedure was used for five lognormal variables, to calculate the following equation:

$$p \quad \frac{x_1 x_2 x_3}{x_4 x_5} \quad \textbf{(37)}$$

It is clear that "p" also follows a lognormal distribution. The results are shown Figure 36.b.

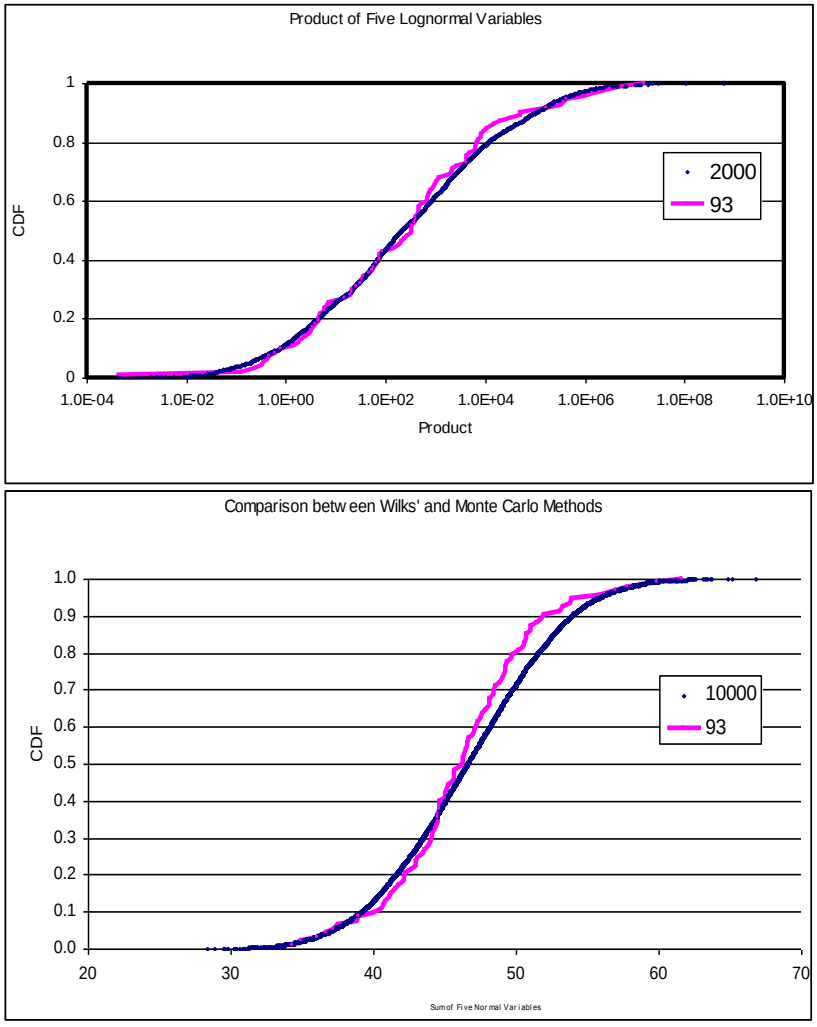

Figure 36: a. Normal Test b. Lognormal Test

5.7.2 Test 2- Large Scale Comparison of Simple Monte Carlo with Wilks' Formula

In this validation test, the scenario of PTS-case4 (a 2.828-inch surge line LOCA) in Oconee-1 NPP was selected. The temperature, pressure and heat transfer coefficient

profiles followed the Normal distributions against the nominal profiles given by RELAP5. Flaw size, C_Dist (the distance from the flaw inner tip to the interface between base and clad of reactor vessel) and aspect ratio were set to be random variables with the distributions shown in Table 18. Three Wilks runs with 100 samples each and two Monte Carlo runs with 1000 and 2000 samples were performed. The UMD PFM code (A code developed for calculation of probabilistic fracture mechanics in pressurizer vessel) (Fei Li 2000) was used for the calculations. Results are shown in the Figure 37.

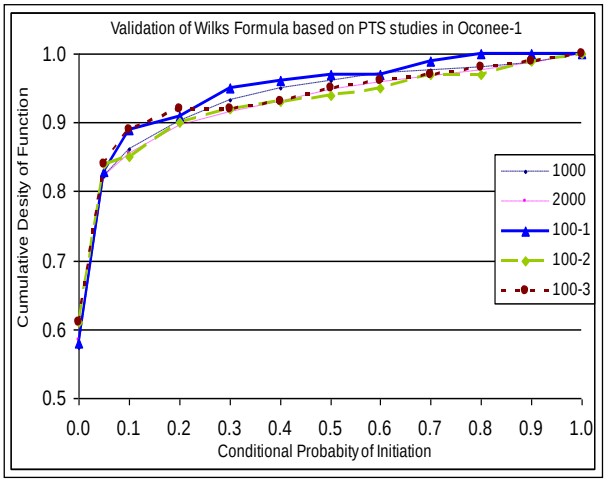

Figure 37: Results for test-2; Probabilistic Fracture Calculation for PTS study of Oconee-1 NPP

Table 18: Table Input parameters specifications

Flaw Characterizations	Distributions	Lower and Upper Ranges
Flaw Size	Uniform	[0, 1.5] inch
C_Dist	Uniform	[0, 3] inch
Aspect Ratio	Discrete	2, 6, 10
Temp, Pres, Heat Coe.	Normal	Oconee Case c4_0

5.8.3 Test 3-Comparison of Tolerance Limits Calculation to PTS Sensitivity Based Methodology

Results of PTS uncertainty quantification for Oconee-1 NPP, was compared by repeating it using Wilks Tolerance limit criteria (Chang at el 2004). The same uncertain parameters (total of 11) were used in both with the same range of variation (Chang at el 2004). 100 unique combinations were created to achieve 95% of probability content with 95% confidence. Results are comparable with the result of uncertainty ranges calculated in the Oconee-1 PTS project (Chang et al 2004).

Table 19: The list of influential parameters with their characteristics

Parameters	Characteristics	PDF	Unit	Range of Variations	
				Lower Bound	Upper Bound
Parametric (Boundary Condition) Uncertainty	Break Size	Piecewise Uniform	inch	1.5	8.0
	Break Location	Discrete		Hot Leg	Cold Leg
	Decay Heat	Uniform	MW	HZP	Nominal
	Season	Discrete			
	HPI Flow Rates	Normal		85%	115%
	CFTs Pressure	Normal	psi	Nominal – 75	Nominal + 75
RELAP5 Code Model Uncertainty	RVVVs State	Normal		0	1
	Component Heat Transfer Rate	Discrete		70%	130%
	Flow Resistance	Discrete		Nominal	100% More
	Break Flow Rate (Break Area)	Normal		55%	145%

Table 20: Parameters for Distributions of the Variable in Table 20

				Range of Variations	
				Lower Bound	Upper Bound
Parametric (Boundary Condition) Uncertainty	Break Size			1.5	8.0
	Break Location			Hot Leg	Cold Leg
	Decay Heat			HZP	Nominal
	Season				
	HPI Flow Rates	1	0.040	85%, $8.85*10^{-5}$	115%, 0.9999
	CFTs Pressure	0	19.5	Nominal – 75, $6.0*10^{-5}$	Nominal + 75, 0.99994
RELAP5 Code Model Uncertainty	RVVVs State	0.5	0.247	0 A*0.95706+0.02147	1
	Component Heat Transfer Rate				
	Flow Resistance			Nominal	100% More
	Break Flow Rate (Break Area)	1	0.222	55% A*0.95734+0.02133	145%

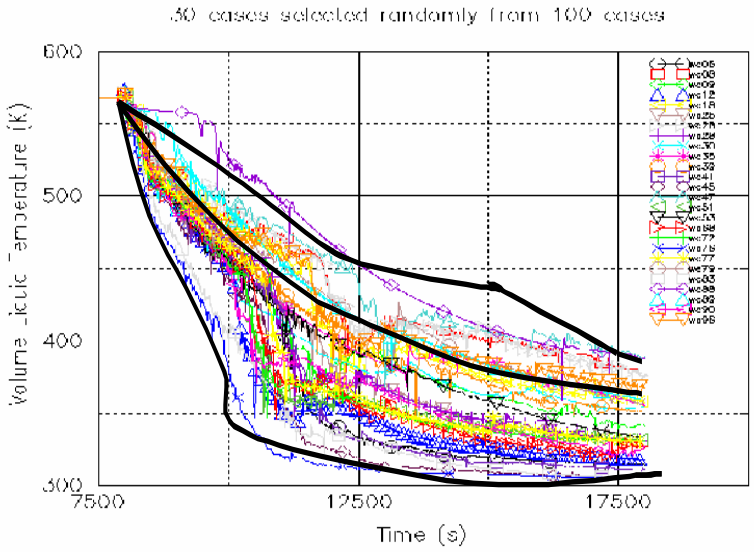

Figure 38: Comparison of uncertainty calculation with Wilks tolerance limits and PTS

Uncertainty Analysis for Oconee-1 NPP

CHAPTER 6: OUTPUT UPDATING

6.1 Output Phase Uncertainty Updating

As was discussed in previous chapters on deficiencies of existing "input-based" and "output-based" uncertainty analysis methods, output-based methods can not distinguish uncertainty contribution of the individual uncertainty sources, require significant amount of experimental data, and do not provide a conceptual and methodic base for generalization beyond the cases studied. On the other hand input-based methods may not be sufficient in capturing structural uncertainty, and initial screening of phenomena and parameters, intentionally limiting the scope (e.g., not considering "user effects"), and the issue of unknown phenomena or incomplete spectrum of alternative models and sub-models considered . As part of the research leading to the development of the method proposed in this dissertation, extensive literature review was conducted to evaluate the merits and limitations of the proposed methods with the objective of incorporating the best features into a new more comprehensive method.

The above mentioned limitations in both approaches have pointed to the desirability a hybrid approach where an input-driven "white box" approach is augmented with output correction and uncertainty assessment based on experimental results relevant to code output. As discussed in detail earlier in relation to specifications of the methodology, the proposed methodology is a two-step process to quantify uncertainties. In this chapter output based updating is discussed, together with the type of data needed, mathematical basis of the proposed method, and an application. This phase of methodology allows updating output variable uncertainties upon

availability of new information about models or output. We start with the mathematics of the Bayesian procedure, and show an application to LOFT ITF on the LB-1 transient scenario. Complete Application of IMTHUA methodology on LOFT LBLOCA will be discussed in next chapter 7.

6.2 Mathematical Basis for Output Uncertainty Updating

Several procedures with varying degrees of complexity, theoretical foundation and applicability domains for the assessment of output uncertainty updating have been proposed in the literature (Drugget et al 1999). Figure 39 illustrates the output updating for TH code calculations.

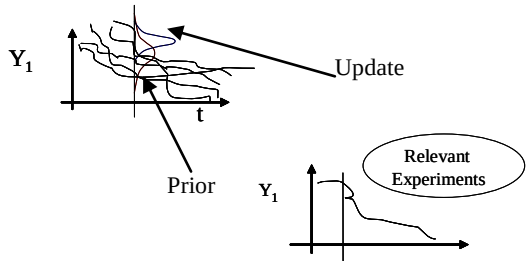

Figure 39: schematic demonstration of output updating

In case of TH computer codes for nuclear power plant accident analysis, applicable experimental data come from scaled-down facilities such as SETs. These facilities are designed for the assessment of specific model or correlation corresponding to various phenomena or system components. ITF are designed for the assessment of the behaviour of a reactor system. There are very limited field data due to regulatory restrictions on performing tests on operating nuclear power plants. SET data usually is used for input-based uncertainty quantification while ITF data are for output uncertainty correction.

Droguett and Mosleh (2001) developed a Bayesian methodology for output updating with comparing paired calculation and experimental data. The method produces an updated distribution of the output considering such information on model performance. In case of continuous output parameters, the method requires discretizing experimental and/or calculation data. Under ideal paired data situation (Droguett and Mosleh 2001), each experimental data $\{Y_1, Y_2, \ldots, Y_N\}$ has its counterpart in model predicted data set $\{Y''_1, Y''_2, \ldots, Y''_M\}$ with N=M. It results in an explicit form for error distribution as:

$$
\begin{aligned}
& E_i \quad Yi \quad Y_i' \\
& Y_{n\ 1}^{M} \quad Y_{n\ 1}^{M} \quad \overline{E} \quad z.S_E \\
& \overline{E} \quad \frac{1}{n} \sum_{j\ 1}^{n} E_j \\
& S_E^2 \quad \frac{1}{n\ \ 1} \sum_{j\ 1}^{n} (E_j \quad \overline{E})^2
\end{aligned}
\qquad \textbf{(38)}
$$

The output is updated using the error distribution. Error can be defined as additive (as above) or multiplicative. Bayesian method is utilized to obtain the posterior distribution for the output.

Figure 40 is an example of typical data for experiment and calculation of TH codes. It is unlikely that we have sufficient data and information to allow the generation of paired model predictions as required in the (Droguett-Mosleh 1999). Main reasons are:

1. In many cases, pairing is not possible due to difference in actual initial and boundary conditions of the test, and those assumed in code calculations, or generated through parametric uncertainty propagation.
2. Differences in predicting of timing of onset of specific events and phenomena compared with test results (as shown in Figure 40.)

With above-mentioned difficulties in applying paired data methodology, a non-paired methodology has been suggested in the literature (Dust at el 2004). The idea was expanded for correction.

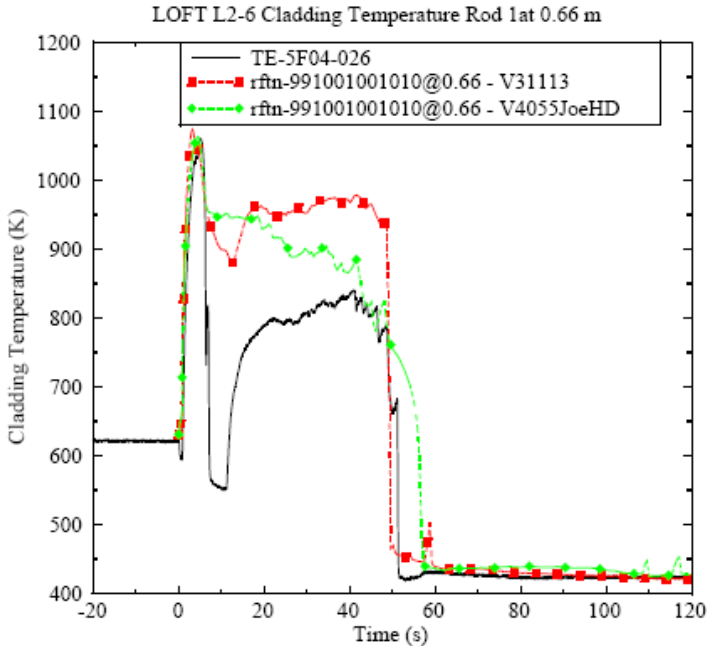

Figure 40: A Typical TH Code Calculations and Test Data

Consider a set of non-paired data, $Y_i \neq Y'_i$ and/or $N \neq M$. The data used should be different than those used in the input assessment. The procedure is as follows:

Specify parametric distribution forms for model predictions and for distribution of the test data. Apply all previous subjective knowledge to build prior distribution for

output. This is done by estimating prior distribution for parameters associated with the output variable.

Assume that μ_M, and σ_M are parameters of the normal distribution of code calculation output variable Y_M. We also use μ_D, and σ_D as the parameters of the normal distribution of test data Y_D. Other forms of distributions may be assessed for the data but analytical formulation may not be possible. In those situations, a numerical solutions (e.g., utilizing MCMC type approaches) may be used.

We recall from applied statistics [11] that if Y_D, Y_M have bivariate normal distribution then conditional distribution of $Y_M|Y_D$ will be normal:

$$f(Y_M Y_D) \sim N(\quad_{M|D},\quad_{M|D}) \quad \textbf{(39)}$$

The conditional mean and variance of Y_M, given that Y_D is:

$$\mu_{M|D} \quad \mu_M \quad \frac{M}{D}(Y_D \quad _D)$$

$$_{M|D} \quad _M\sqrt{1 \quad ^2} \quad \textbf{(40)}$$

$$Corr(Y_D, Y_M)$$

For bivariate normal distribution, the conditional PDF for one of the variables, given a known value for the other variable, is normally distributed.

We call Y_{new}^M, the updated variable of the output. Since the data are non-paired, ρ is an unestimable parameter. We will set it equal to 1 to maximize the correlation between Y_D and Y_M, desirable specification for the update process. Given $\rho=1$, the conditional distribution of Y_{new}^M is the degenerate distribution. It puts all probability on one point ($\sigma_{M|D}=0$) of one-to-one mapping between the code data, before and after updating as shown in Table 21.

Table 21: Statistics for Output Updating

$Y_{new}^{M} \quad \overline{Y_D} \quad \frac{S_D}{S_M}(Y_{new}^{M} \quad \overline{Y_M})$	
$S_M^2 \quad \frac{1}{m \quad 1}\sum_{j\ 1}^{m}(Y_j^M \quad \overline{Y}^M)^2$	$S_D^2 \quad \frac{1}{n \quad 1}\sum_{j\ 1}^{n}(Y_j^D \quad \overline{Y}^D)^2$
$\overline{Y}^D \quad \frac{1}{n}\sum_{j\ 1}^{n} Y_j^D$	$\overline{Y}^M \quad \frac{1}{m}\sum_{j\ 1}^{m} Y_j^M$

Development of a Bayesian solution requires that we first specify parametric forms for the distributions of code calculation and test data, specify a parametric form for their joint distribution, specify assumed values for unestimable parameters associated with this joint distribution, and specify a joint prior distribution for the estimable parameters. Finally, the simulated posterior distribution is employed to calculate an adjusted model prediction, Y^{D}_{new} based on a new model prediction, generated by the TH code.

We apply available data in a Bayesian method using Markov Chain Monte Carlo (MCMC) framework to get distribution for code calculation and experimental data. MCMC, as a computation-intensive calculation tool, has seen an enormous upsurge in application in different fields over the last few years. It has revolutionized practical Bayesian statistics by making the numerical calculations to get posterior distribution easier. The detailed foundation of MCMC was discussed in (Neal 1993 and Congdon 2003). The integration operation plays a fundamental role in Bayesian statistics. Given a sample y from a distribution with likelihood L(y|x) and a prior density for $x \quad R$ given by p(x), Bays" theorem relates the posterior $(x \mid y)$ to the prior via the formula:

$$(x \mid y) \quad L(y \mid x)\, p(x)$$

where the constant proportionality is given by **(41)**

$$\text{L9y} \mid \text{x)p(x)d(x)}$$

where x may be single or multivariate. Thus the ability to integrate often complex and high dimensional functions is extremely important in Bayesian statistics. MCMC method provides a convenient alternative to evaluate these integrations where we sample directly from the posterior directly, and obtain sample estimate of the quantities of interest, thereby performing the integration implicitly.

WINGUGS14 (Winbugs 2006) code is utilized to implement the Bayesian solution proposed in this research. Bayesian inference Using Gibbs Sampling (BUGS), as basis and programming language for WINGUGS, is a program that carries out Bayesian inference on statistical problems using MCMC methods (Neal 1993). It is intended for complex models for which there is no exact analytic solution or for which even standard approximation techniques have difficulties. WINBUGS assumes a Bayesian probability model, in which all unknown parameters are treated as random variables. The model consists of a defined joint distribution over all unobserved (parameters and missing data) and observed quantities (data); then it is necessary to condition on the data in order to obtain a posterior distribution for the parameters and unobserved data. Empirical summary statistics can be obtained from samples of the posterior and are used to draw inferences for the quantities of interest. Correct new predictions of the model assuming bivariate normal distribution is obtained with maximizing of correlation between code prediction and corrected value as representative of test data. A detailed discussion about WINBUGS may be found from its official website (Winbugs 2006).

There are various situations in relating code predictions and data from experiments. The proposed methodology was tested in different cases of small and large data sets with test and code data scattered in same area and with some outlier test data. Paired method results are also compared with non-paired method for small and large data set.

6.3 Inference with Partially Relevant Data

Data from experiments should be evaluated for their degree of relevance to the conditions of the scenario. The data may be evaluated as completely relevant and used directly for updating purpose or assessed as partially relevant. A Bayesian weighting process is developed by (Droguett 1999) for considering partially relevant information. Criteria for assigning the weights in case of TH experiments are deduced from assessment of similarity degree of test data to the calculation. Data is in form of set of model estimate from code calculation and corresponding experimental data such that $D = \{D_1, D_2, \ldots, D_N\}$

A relevance factor φ can be assigned to the data based on the above mentioned criteria. The φ factor is an indicator of data applicability and relevance. Some attributes of scenario facility and experimental facilities for applicability assessment, are:

Distortion from Scaling (e.g., π group values)

Location and Size of Break,

Rate of Power,

Scaling Ratio of the Facility,

Involved Safety Systems,

Nuclear Core Configuration

These attributes should be compared pair wise (Figure 32) for applicability and relevance assessment and evaluation..

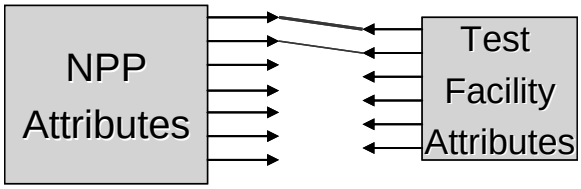

Figure 41: Binary Matching and Comparing Attributes

The value of φ factor is between 0 (absolutely not applicable) and 1 (absolutely applicable) (see Table 22). This factor will be utilized in a Bayesian process proposed by Droguett and Mosleh as shown below:

$$(T \mid IM, D) \quad \frac{[L(IM, D \mid T)] \ . \ (T)}{\int_T [L(IM, D \mid T)] \ . \ (T) dT} \quad \textbf{(42)}$$

Likelihood adjustment method is another alternative to use φ factor for updating of the output distribution. As mentioned, φ factor is based on source data assessment. According to this methodology a shape is assumed for Likelihood (e.g., Normal) and objective is assess the distribution parameters (e.g.,) form data and information implementation as:

$$[L(IM,D|T)] \quad L(IM,D|T) \quad [L(IM,D| \ , \ )] \quad \textbf{(43)}$$

Table 22: Applicability Weights for φ factor

Applicability Weight	
Value (φ)	**Statement**
0.00	**Absolutely not Applicable**
0.20	**Strongly not Applicable**
0.40	**Moderately not Applicable**
0.50	**Slightly Applicable**
0.60	**Moderately Applicable**
0.80	**Strongly Applicable**
1.00	**Absolutely Applicable**

An expert group should quantify the φ for each test facility and test itself based on similarities and differences between it and nuclear power plant and the transient scenario. This φ will be used on unitization of the data for parameter, model and output uncertainty distribution.

6.3.1 Scaling

Most of the data in nuclear power industry are from scale down facilities. There are certain techniques (called scaling) to scale up the data to evaluate facility in its full size, with real nuclear core. Scaling analysis for each facility yields a separate set of non-dimensional scaling groups e.g., -Groups (Wulff 1996). Scaling discussed in Chapter 3 in quantitative confirmation of PIRT results can also be used for evaluation of relevance of data for obtaining the weights for Bayesian updating. -Groups numbers is used for this purpose. These numbers are indication of how big is the distortion of the data in transition to full size. Data from facilities with less distortion are more relevant to our analysis.

6.4 Example on LOFT LBLOCA Case

Methodology is demonstrated using model data and data for the LOFT (Loss-of-Fluid Test) test facility. Details of the LOFT test facility systems are described in Reference (OECD 1984). A detailed description of the tests including measured initial conditions, timing sequence of the scenario is given in (Wang and Shumway 2004). A full application of IMTHUA methodology for LOFT LB-1 LBLOCA is given in Chapter 7.

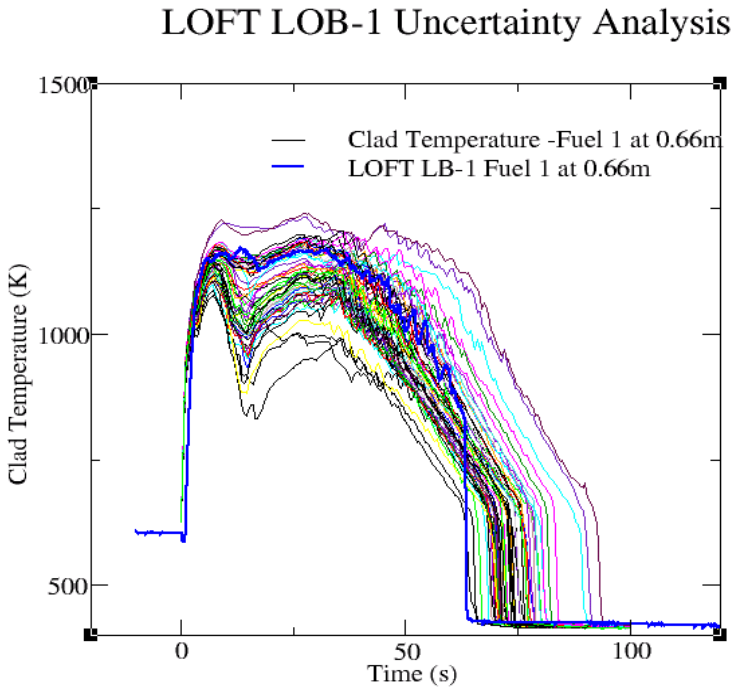

Figure 42: Uncertainty scatter over the time for LOFT Clad Temperature

Input phase uncertainty propagation was already shown in Figure 42. As discussed in detail in (Droguett 1999), code structure uncertainties were explicitly propagated to obtain uncertainty scatters for the hottest fuel rod at 0.66m height of the active core. Figure 42 shows uncertainty scatters for clad temperature and Figure 43 is the scatter

plot for peak clad temperature (PCT). This is the result of 59 code runs by propagation sources of uncertainties considered in the first phase explicitly.

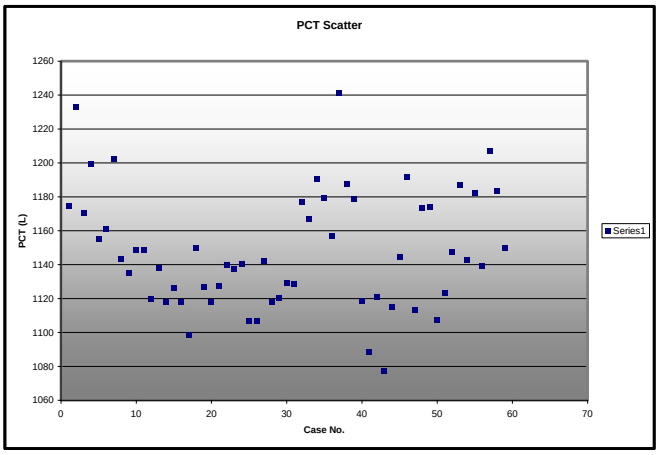

Figure 43: Scatter Plot for Peak Clad Temperature

Figure 44 shows scatter plots for data obtained from RELAP5 calculation and test data for PCT. For demonstration of the methodology, only 3 data points are selected out of more than 20 tests. As it was discussed above, tests data with either full or partial relevancy may be used in the process. The selected 3 data points are very close to the LB-1 test conditions considering criteria in the list of LOFT test data discussed. Other less relevant test data may be evaluated for their information to update output distribution through an extension of the current methodology.

Figure 45 shows the results of fitting normal distributions to code data and test data 1. Two methods were developed for transition from input phase to output phase;

1. A distribution shape is assumed for the data (e.g., normal or lognormal distribution) which best fits the data. For a given distribution, we estimate parameters from the data. Coverage area of the distribution from tolerance interval is assigned to distribution quantiles, depending on coverage (e.g., the smallest to

2.5% and the largest to 97.5%, see Figure 44). The parameters of distributions are obtained from these quantiles. As expected, the test data distribution is wider due to smaller number of data point.

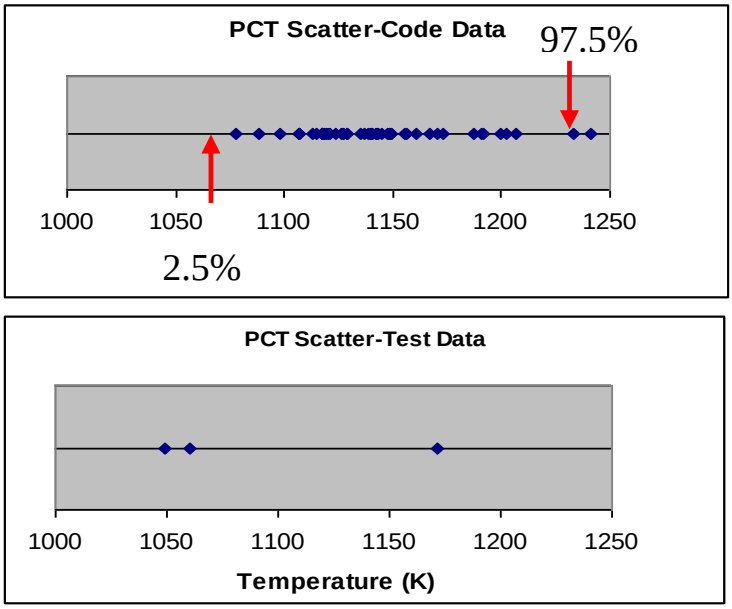

Figure 44: a) Calculation Data for PCT b) Completely Relevant Test Data for PCT

2. A distribution shape is assumed for the data. Some prior distributions (Normal or uniform) are assumed for the parameters of the distribution. Update distribution of parameters are found utilizing MCMC Bayesian process:

$$(\quad , \quad) \quad \frac{L(T_1,T_2,\ldots,T_N) \quad _0(\quad , \quad)}{L(T_1,T_2,\ldots,T_N) \quad _0(\quad , \quad)} \quad \textbf{(44)}$$

,

Where are parameters of assumed distribution, N is number of code runs; L is likelihood function of data and π_0 is prior distribution of the parameters. With known distribution for distribution parameters, we can calculate

$$f(T) \qquad f(T \mid ,) \; (,) d \; d \quad \textbf{(45)}$$

or by substitution of a statistics of such as mean or mode, we arrive at a simple relation for output distribution as:

$$f(T) \quad f(T \mid \bar{}, \bar{}) \quad \textbf{(46)}$$

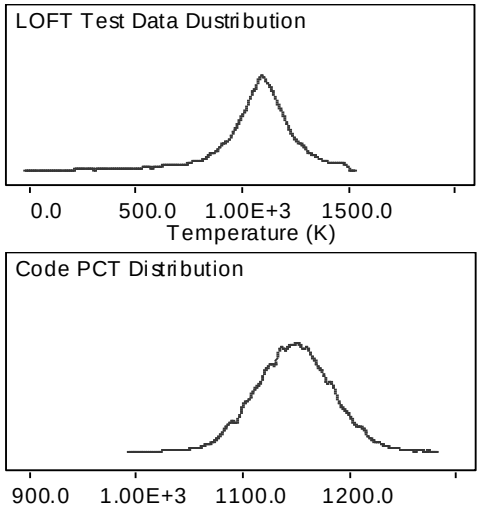

Figure 45: a) Code Data Distribution b) Test Data Distribution

Final results are shown in Figure 46 including scatter of the code results after updating with test data, the normal distribution fitted to the data, and statistics for PCT output and the parameters of fitted distribution. As expected, the procedure has shifted the code data distribution slightly toward test data. It also has caused widening of the distribution.

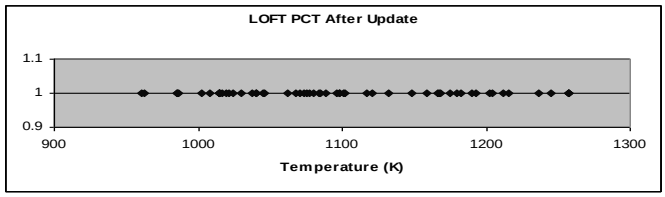

Node	Mean	SD	MC Error	2.50%	Median	97.50%
Code	1099	95.95	0.946	911.4	1099	1288
Code μ	1098	12.51	0.131	1073	1098	1122
Code σ	95.43	9.027	0.1073	79.57	94.75	115

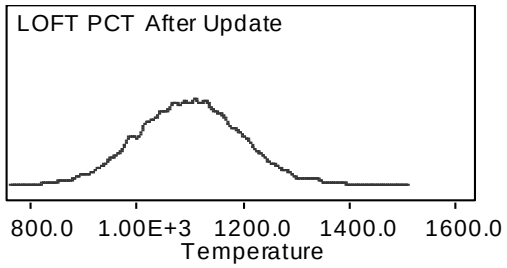

Figure 46: Update Distribution for Output A) PCT Scatter Plot B) PCT Distribution Statistics C) PCT Distribution

6.5 Uncertainty Importance Analysis

As it was discussed in description of methodology, and shown in methodology flow chart [Chapter 2], uncertainty importance aims at ranking sources of uncertainty for their level of contribution to output. Bhattacharyya and Ahmed (1982) and Bier (1983) have presented a measure as percentage change in the top-event variance caused by a given percentage change in the variance of the basic event parameter which is similar to IMTHUA importance measure. Iman and Hora (1990) have developed a measure by using the Taylor series expansion that yields the total contribution to the variance or the frequency change of the top-event that can be assigned to the corresponding quantities of each basic event. Park and Bari (1985) suggest a relative uncertainty importance measure, by using maximum entropy approach by which the information content of the uncertainty distributions considered

are compared. A theoretically complete formulation of an uncertainty importance measure is given in reference (Bari et al1994). This step calculates percentage of each source contribution in the output uncertainty band.

In this research we have proposed a different uncertainty importance assessment that is more effective given the computational complexities of the TH codes. Because of relatively high cost for TH code computation and conditions in TH code uncertainty results from previous phases, this uncertainty measure is efficient. The measure is defined in xσ change in the given parameter over the change in the FOM from such change. Here x is number of σ"s (2, 4, or 6.) 2σ importance measure is ΔPCT resulting from running the code for +1σ and -1σ change in the parameter nominal value. An average of 2, 4, or 6σ importance measure can also be used for the analysis but it should be applied uniformly for all contributors. The example for this uncertainty importance is given in Chapter 7 with the LOFT application.

	X_1	X_2	X_3	X_4	.....	X_N
+1σ	Out(X_1+1σ)	Out(X_2+1 σ)		.....		Out(X_N+1 σ)
+2σ	Out(X_1+2 σ)	Out(X_2+2 σ)		.....		Out(X_N+2 σ)
+3σ						
	.					
	.					
-1σ						
-2σ						
-3σ	Out(X_1-3 σ)	Out(X_2-3 σ)		…		Out(X_N-3 σ)

Importance Measure= $\frac{out_{x_1}}{\quad}$

Figure 47: Uncertainty Importance Measure for IMTHUA

CHAPTER 7: APPLICATIONS

7.1 Application of the methodology on the Marviken CFT test Facility

7.1.1 The Facility Description

Marviken test facility was originally built as a boiling water reactor but never charged with nuclear fuel. It was modified to conduct a series of safety experiments. (Studsvik Energiteknik 1979a). The critical flow test with aim of obtaining critical flow data is chosen to demonstrate the TH Code uncertainty methodology during its development. Figure 48 and Table 23 provide the basic specifications of the test facility and the tests. In the tests the vessel was filled with degassed water up to a certain level which varied between the tests (16.7m above vessel bottom). Full description of the facility and experiments, test measurement and test accuracy are given in (Studsvik Energiteknik, 1979a, 1979b, and 1979c). A pre-test warm-up period produced a temperature profile along the vessel height. After a stabilizing period of several hours, the test was initiated by failing the discs in the rupture disc assembly. Measurements were recorded in the vessel, discharge pipe, and the test nozzle, while the vessel fluid was discharged through the test nozzle into the containment and further through the exhaust pipes to the ambient atmosphere. The test was terminated when the ball valve begun to close or when pure steam entered the discharge pipe.

Since the Marviken test facility is not a full size nuclear power plant, some aspects of proposed methodology are not applicable to this special problem. Experiments are

considered as reference points for the application. Effects of possible experimental errors are not considered. However, maximum errors calculated on experiments were based on the manufacturer"s specifications. These are all calculated with some statistical quantities such as error limits and their confidence, and also probable error. (See Studsvik Energiteknik, (1979c) for details on experimental errors.)

Table 23: Marviken Test Facility Specifications

L/D (D=500 mm)	**0.33**
Inside Parameter	**5.22 m**
Height	**24.55 m**
The net available internal volume	**420 m3**
Initial water level in the vessel (above Discharge pipe inlet)	**16.7 m**
The pressure vessel with a net volume	**425 m3**
a maximum design pressure	**5.75 MPa**
a maximum design temperature	**545 ºK**

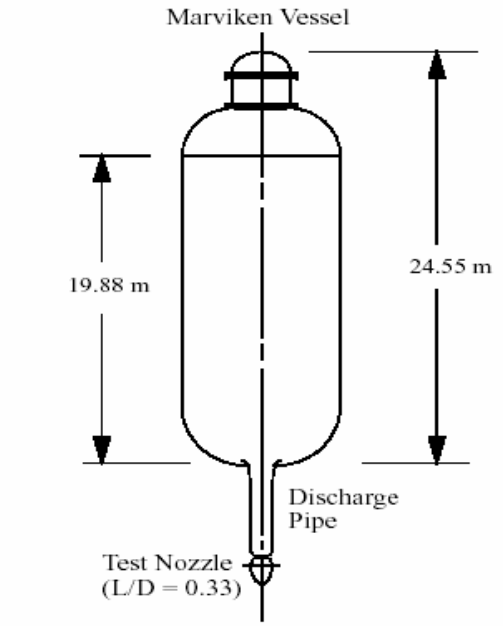

Figure 48: The Marviken Test Facility

Figure 49 demonstrates nodalization of the facility for preparation of inputdeck for calculation both steady state and transient. Qualification of nodalization as a

necessary step in IMTHUA was done by comparison of the inputdeck with available qualified nodalizations and inputdeck (NRC Database 2006).

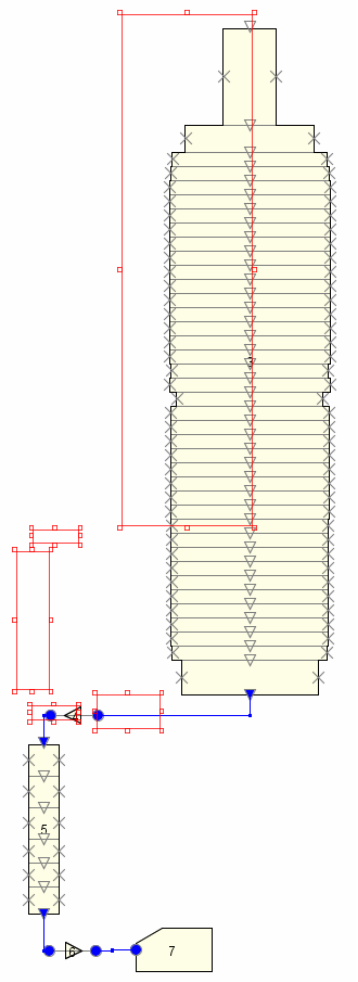

Figure 49: Nodalization of the Marviken Facility

7.1.2 Input Phase

Following steps summarize application of first phase of the uncertainty assessment methodology applied to this facility. Only a limited numbers of phenomena were observed due simplicity of the scenario as a single blowdown phase. The test facility as a SET was designed to study blowdown effects as choked flow phenomena in different configurations. The following are the steps necessary for input phase

uncertainty quantification for the scenario. Relap5 code was used for computation and propagation of uncertainties for the figure of merit which was considered break mass flow.

Step 1: Phenomena Identification and Ranking

A PIRT table was developed for the scenario to identify and rank phenomena. Phenomena identification and ranking for scenario was obtained by screening PIRT table developed for small break LOCA by Idaho National Laboratory INL (Wilson at el 98) for blowdown phase and phenomena in PWRs identified by the Committee on the Safety of Nuclear Installations of OECD/NEA. Some advice and expert consultation was obtained to qualify importance ranks in the table (di Marzo 2004). Table 24 shows the resulting PIRT table. Scenario was treated as a single phase blowdown. TH importance and uncertainty importance are shown in separate columns.

Table 24: PIRT for Marviken CFT test 24 (PIRT Revision 0)

Component	Phenomena	TH Rank	Uncertainty Rank
Tank	**Mass Flow**	**H**	**L**
	Evaporation Due to Depressurization	**H**	**M**
	Level Swell	**M**	**M**
	Stored Energy Release	**H**	**M**
Break	**Choked Mass Flow**	**H**	**M**
	Energy Release	**H**	**L**

	Flow Resistance	**M**	**M**

H: High L: Complete Knowledge
M: Medium M: Partial Knowledge
L: Low H: Unknown

Based on combined TH and uncertainty importance for each phenomenon, selected criteria, some code calculations, and sensitivity analysis, the table was reduced to Table 25.

Table 25: PIRT revision 1

Component	**Phenomena**
Vessel	Mass Flow
Break	Choked Mass Flow
	Evaporation Due to Depressurization
	Flow Resistance

Step2: Identification of models and correlations

Correlations and models corresponding to the identified phenomena are as follows:

Henry-Fauske Correlation for Subcooled, 2-

Evaporation model

Friction coefficient

Some other initial condition are also identified and considered as part of important parameters in propagation of uncertainty. These include initial pressure and liquid level of the vessel which affect mass flow of the break.

Step3: Uncertainty Importance

Eleven parameters and correction factors were selected and their influence on output evaluated. Only 3 parameters and 2 correction factors were found to have significant effect on the output. Figure 50 shows the results of sensitivity of output to variation in each of the selected variables. This led to selection of only 5 important parameters.

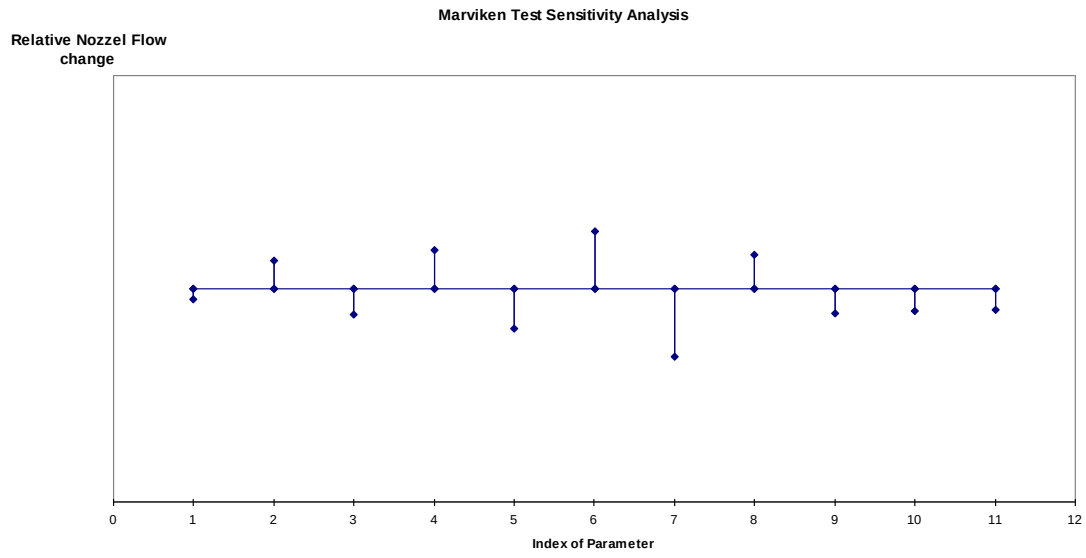

Figure 50: Uncertainty importance for parameters and correction factors

Step 4: Quantification of Uncertainty of the Input Variables

Figure 51 shows the uncertainty distributions for the five selected parameter and correction factors. Normal and uniform subjective distributions were assigned to correction factors and parameters, respectively. This was based on expert opinion.

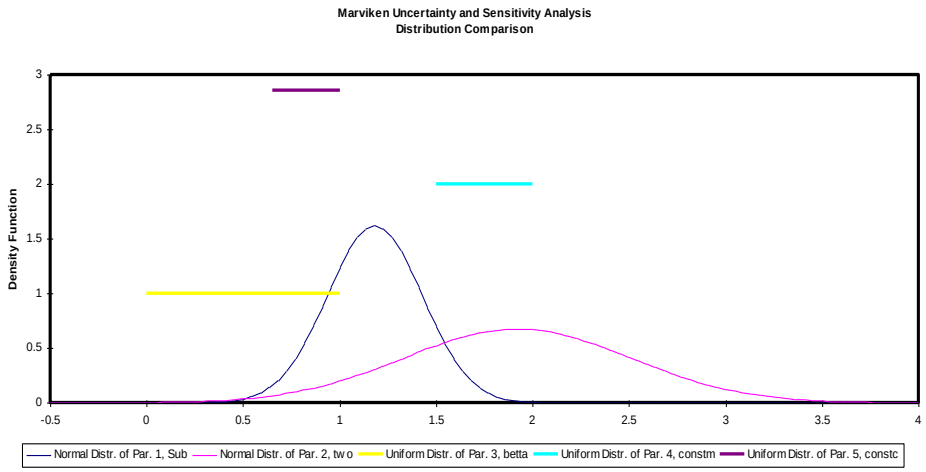

Figure 51: Uncertainty Distribution for Parameters and Correction Factors

Step5: Propagation of Input Uncertainty

With probability content, $\gamma = 95\%$, and confidence level, $\beta = 95\%$, sample size of 93 is calculated for a two-sided tolerance interval. It should be noted that many safety calculations need only one-sided uncertainty bound quantification.(for example clad temperature should not exceed specified safety margin). This reduces the size of sampling from 93 to 57 samples. Considering two-sided tolerance interval for this application, random values were sampled 100 times from each input variables and used to modify the input deck and source code (RELAP5/MOD3.2). Figure 53 provides the results of propagation of uncertainty. They are compared with data from experiment (dotted bold curve).

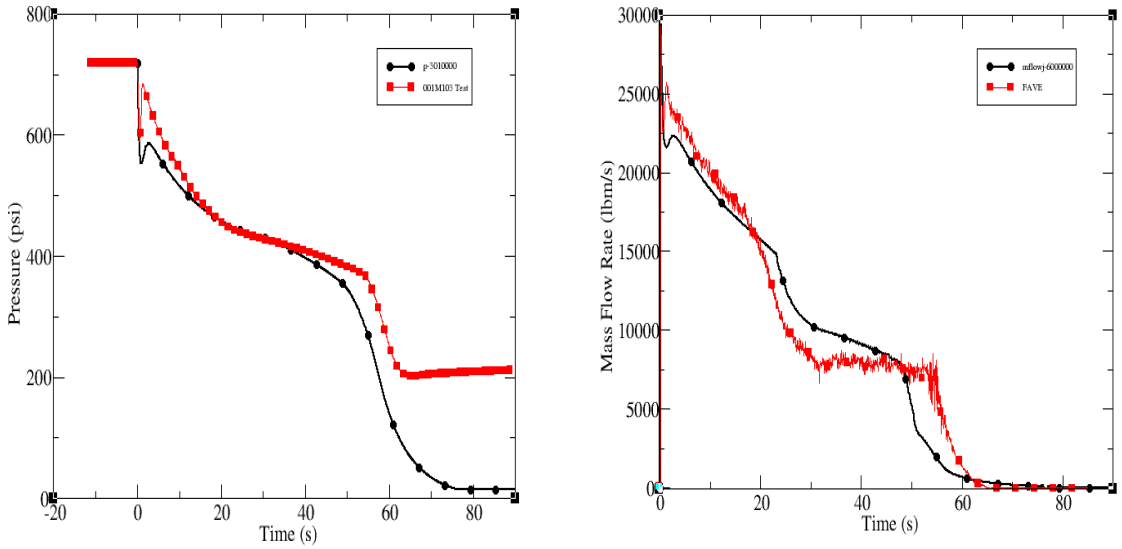

Figure 52: a) Pressure Trend in Top of Vessel b) Mass Flow Rate at Nozzle Outlet

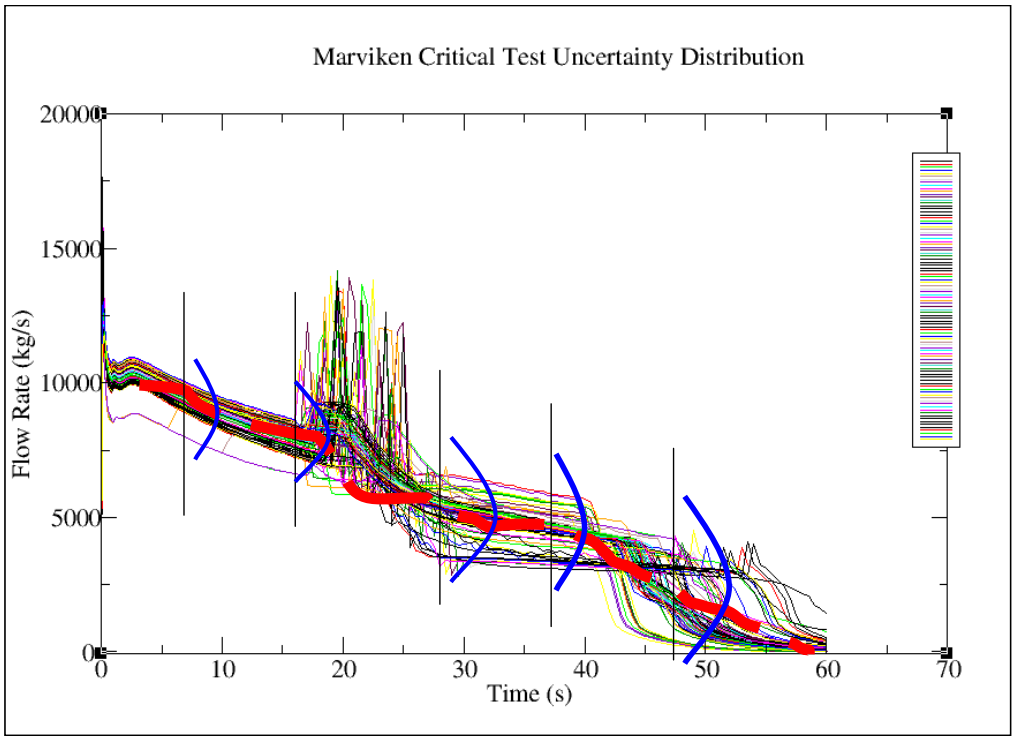

Figure 53: Uncertainty Distribution for Output and Comparison with Experiment

7.1.3 Output Updating

For this step of analysis, a total 100 point (number of code runs) and 3 experimental data points are available. A uniform prior distribution is assumed for the results from input uncertainty propagation. Non-paired updating method as discussed in Chapter 6 was then applied and results for one data point (t=30s) is shown in Figure 54.

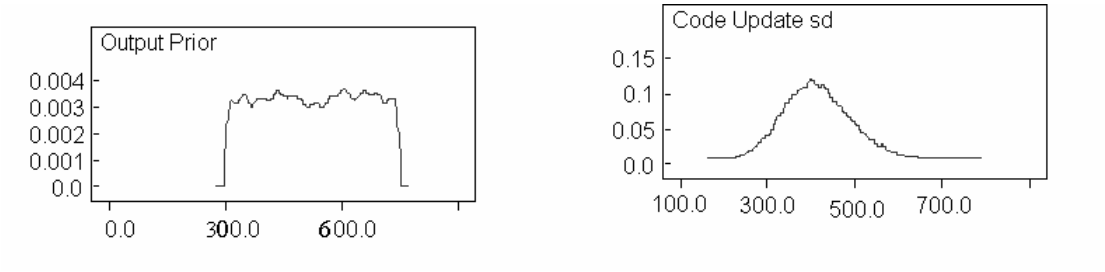

Figure 54: Output Updating in Time 30s after Transient Initiation

7.2 Loft Application

The LOFT facility is a 50-MWt pressurized water reactor with instrumentation to measure and provide data on the thermal-hydraulic conditions throughout the system. The unique feature of the facility is its UO2 powered core. The facility is scaled to represent a 1/60-scale model of a typical 1000-MWe commercial four-loop PWR. Three PWR primary-coolant loops are simulated by a single intact loop in LOFT scaled to have the same volume-to-power ratio. A broken loop in LOFT simulates the fourth PWR primary-coolant loop where a break may be postulated to occur. Detail description of the facility is discussed in Ref. Studsvik Energiteknik (1979a) and other LOFT facility documents (Reeder 1979, Studsvik Energiteknik 1979b, 1979c and Lubbesmeyer 1991, Brittain 1990).

The TH code uncertainty methodology is tested on selected Large Break LOCA 200% cold leg break, LB-1 test. The test with highest core power of 49 MWt with

disconnected flywheel is of highest interest, because of its realistic results and relevance to actual nuclear power plants LBLOCA simulation. LB-1 test boundary/initial conditions are used for all calculation. PCT is selected as the figure of merit, but not necessarily applied to a fixed point in the core, rather it is used for all possible locations that may exceed specified temperature.

7.2.1 The Facility Description

A schematic view of LOFT test facility is shown in Figure 55 and specification are given in Table 26. The general philosophy in scaling coolant volumes and flow areas in LOFT was to use the ratio of the LOFT core [50 MWt] to a LPWR core [3000 MWt]. For some components, this factor is not applied; however, it is used as extensively as practical. In general, components used in LOFT are similar in design to those of a PWR. Because of scaling and component design, the LOFT is expected to closely model a PWR LOCA (OECD 1984). Then facility is designed and scaled to represent a 1/60-scale model of a typical 1000-MWe commercial four-loop PWR. Three PWR primary-coolant loops are simulated by a single intact loop in LOFT scaled to have the same volume-to-power ratio. A broken loop in LOFT simulates the fourth PWR primary-coolant loop where a break may be postulated to occur. The facility includes most of components in a typical 4-loop nuclear power plant consisting of five major systems of: 1) Primary Coolant System, 2) The Reactor System with 1.68m nuclear core, 3) Blowdown Suppression System, 4) Emergency Core Cooling System, and 5) Secondary Coolant System.

With recognition of the differences in commercial PWR designs and inherent distortions in reduced scale systems, the design objective for the LOFT facility was to

produce the significant thermal-hydraulics phenomena that would occur in commercial PWR systems in the same sequence and with approximately the same frames and magnitudes. (Wang at el 2004)

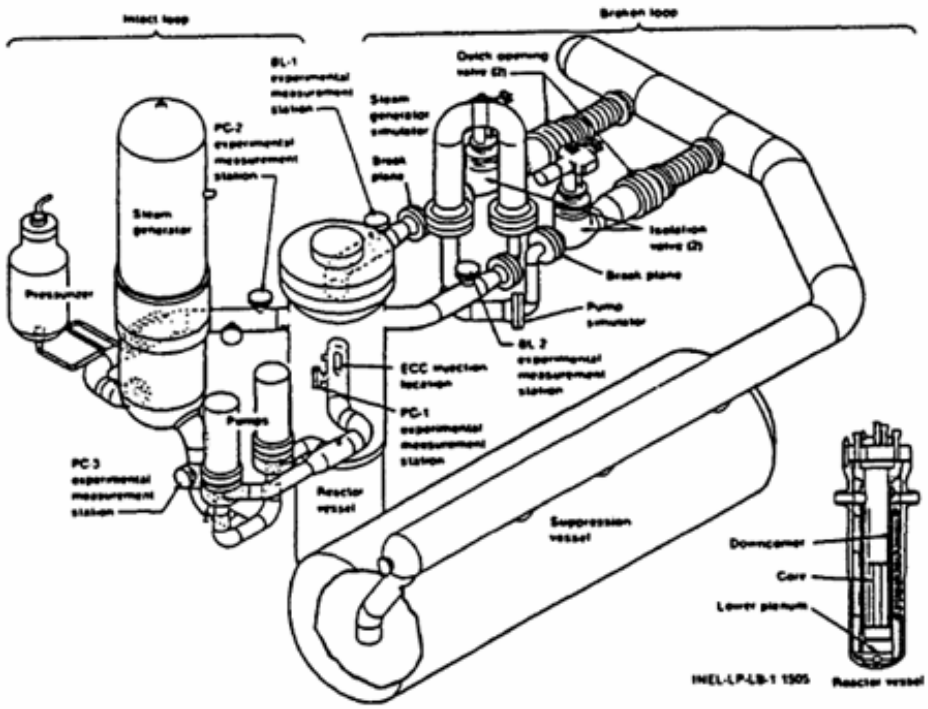

Figure 55: The LOFT Test Facility (Wang et al 2004)

Table 26: LOFT Test Facility Specifications (Wang et al 2004)

Item	*LOFT*
Fuel rod number	1300
Length (m)	1.68
Inlet flow area (m3)	0.16
Coolant volume (m3)	0.295
Maximum linear heat generation rate (kW/m	39.4
Coolant temperature rise (K)	32.2
Power (MW)	36.7
Peaking factor	2.34
Power/coolant volume (MW/m3)	124.4
Core volume/system volume	0.038
Mass flux (Kg/s-m2)	1248.8
Core mass flow/system volume (Kg/s-m3)	25.6

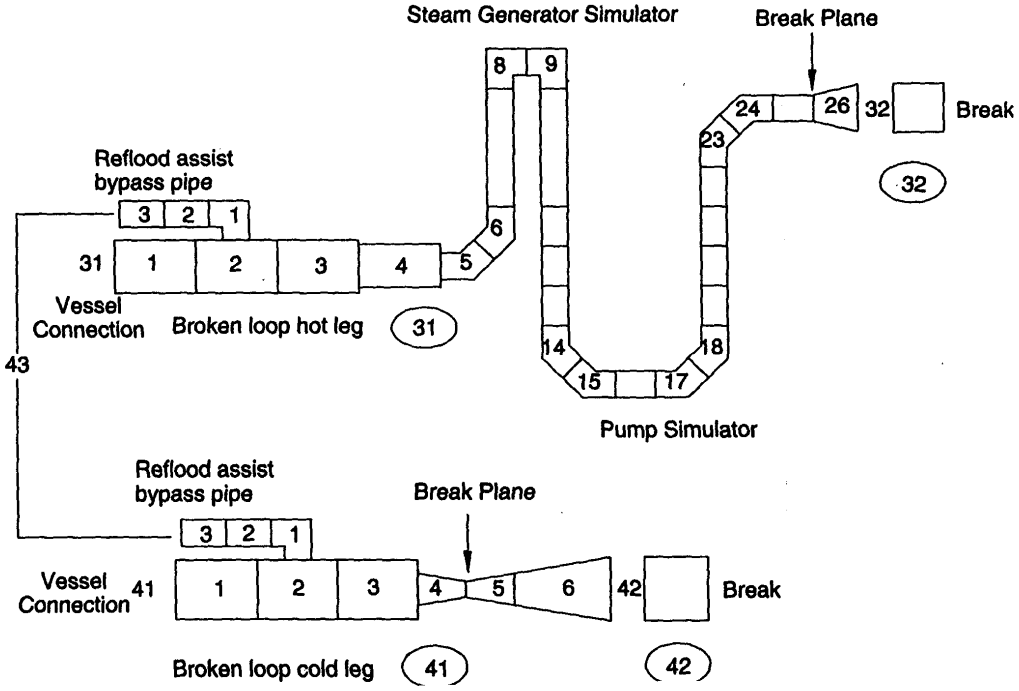

Figure 56: LOFT Facility Nodalization; Primary Loop (Courtesy of NRC Databank 2005)

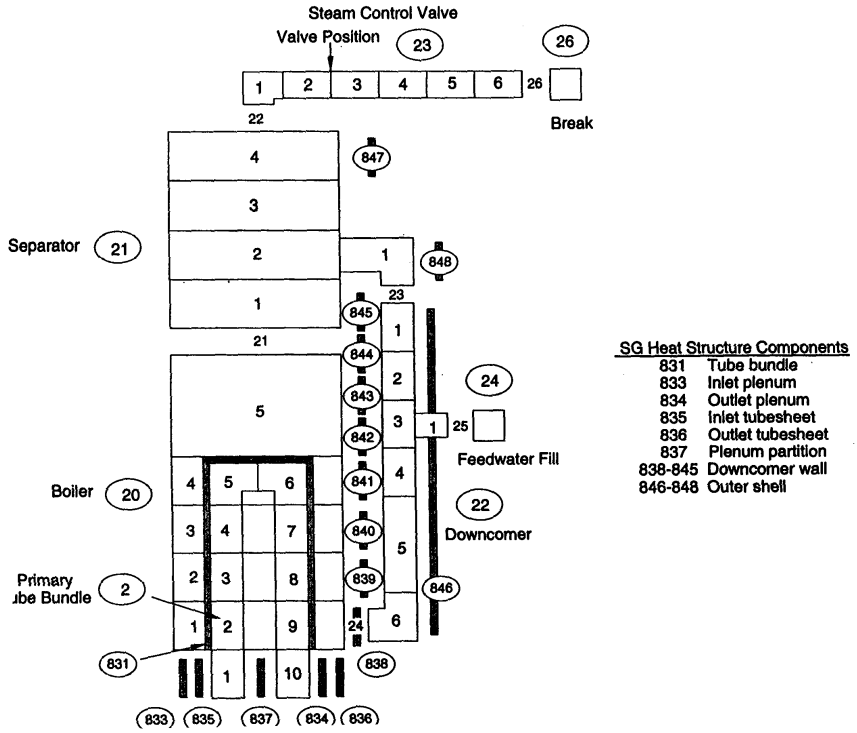

Figure 57: LOFT Facility Nodalization; the Steam Generator (Courtesy of NRC Databank 2005)

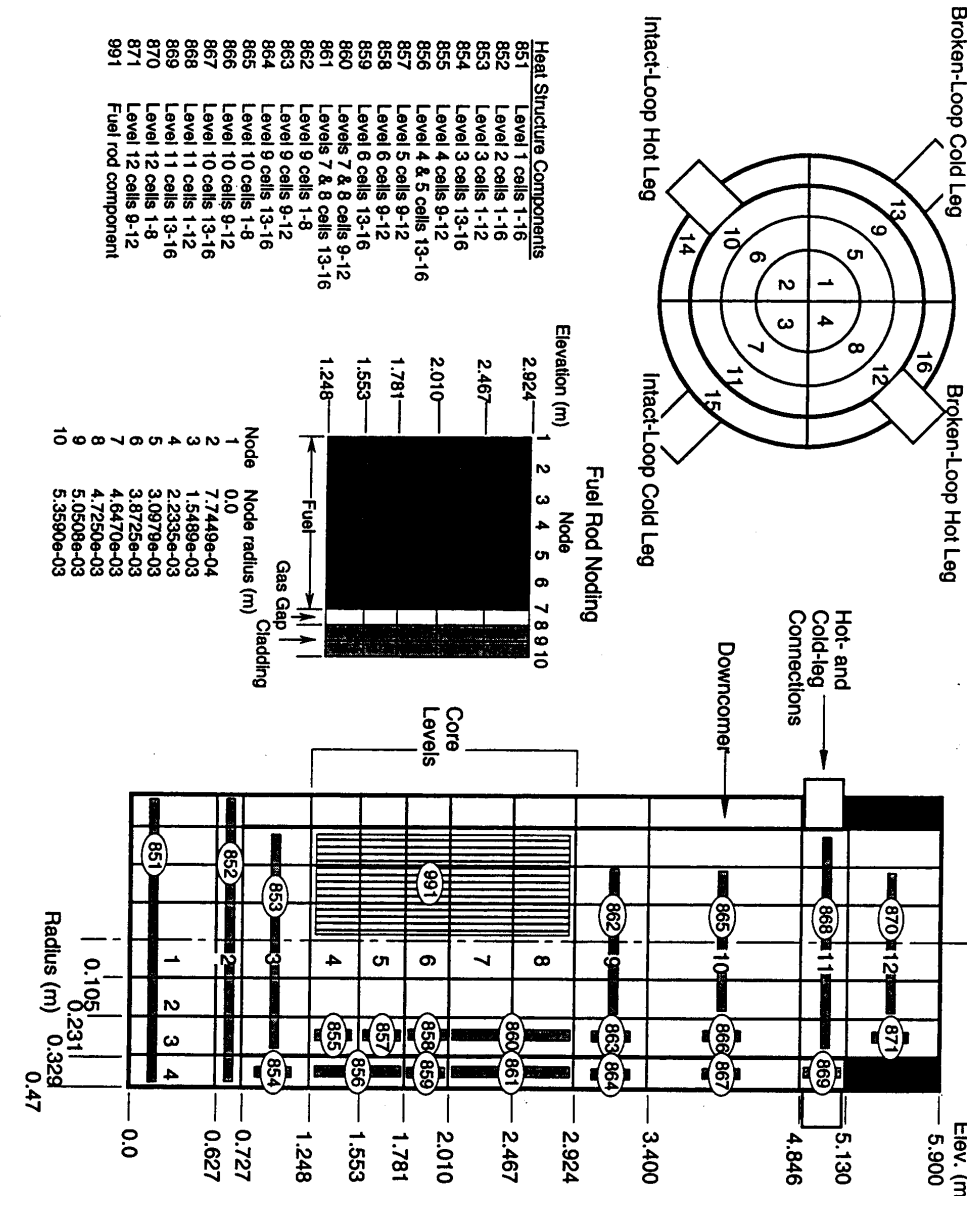

Figure 58: LOFT Facility Nodalization; The core (Courtesy of NRC Databank 2005)

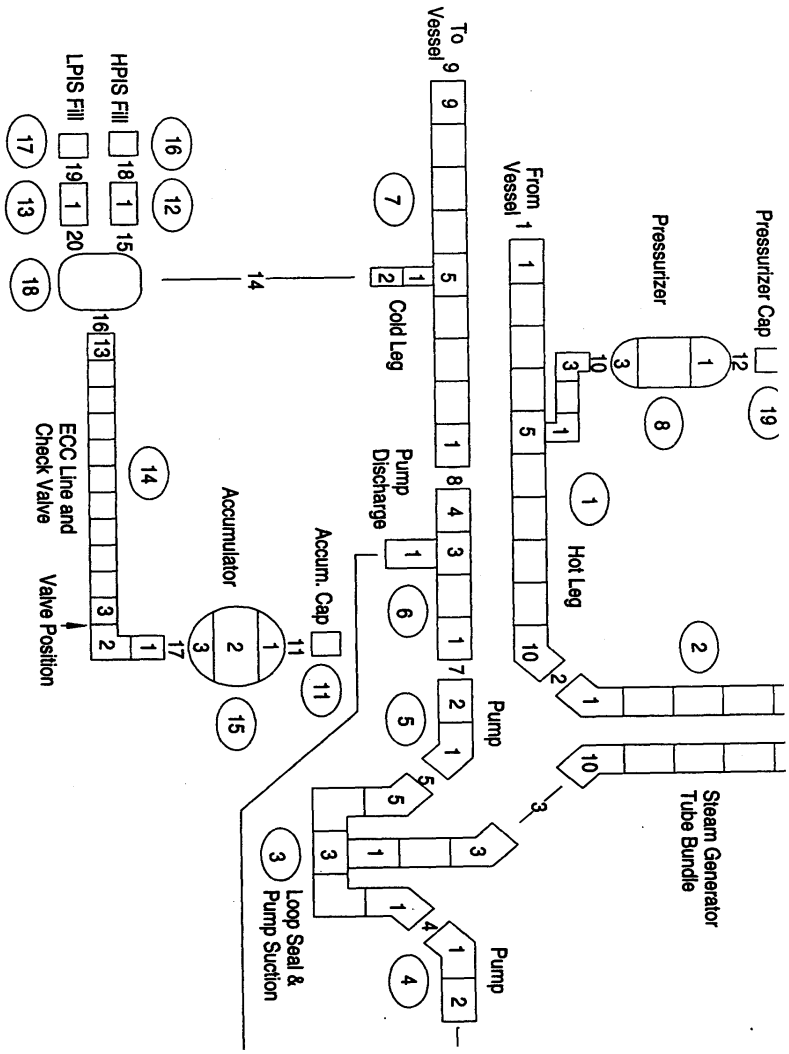

Figure 59: LOFT Facility Nodalization; Primary Loop (Courtesy of NRC Databank 2005)

7.2.2 Scenario Description

LOFT LOCA Test LB-1 is a 200% cold leg break test. Table 27 gives the measured initial conditions for the test. A detailed description of the test is given in (Lubbesmeyer 1991 and Brittain 1990). The transient sequence of events for Test LB-1 is shown in Table 28. Reactor power was tripped on a low pressure in the experiment. However, the pressure set point for tripping the reactor power for this test was higher than the other tests (49.3 MW) and IMTHUA a higher loop flow. The

high pressure injection was assumed inactivated for this test. The intact loop pumps were disconnected from the fly wheel at the time of pump trip.

Computational analysis and experimental data indicate that a PWR-LBLOCA involves three phases or periods, based on trends of changes in the liquid inventories of the vessel, the core, and the lower plenum. The three periods are: Blowdown, Refill and Reflood. The PIRT results from a Westinghouse 4 loop PWR NPPs PIRT results (Boyack 199) and results from (Shaw 1989) and list of 67 phenomena identified by (OECD 1994) were used as starting point for developing PIRT for the scenario.

Table 27: Loft Measured Initial Conditions for Test Lb-1

Parameter	***LB-1***
Reactor Power (MW)	***49.3***
Low Pressure Scram Set Point (MPa)	***14.5***
Intact-loop Mass Flow (kg/s-m2)	***305.8***
Hot-leg Pressure (MPa)	***14.77***
Hot-leg Temperature ($_K$)	***586.1***
Cold-leg Temperature (K)	***556.6***
Pump Speed (rad/s)	***209***
Pressurizer Steam Volume (m^3)	***0.38***
Pressurizer Liquid Volume (m)	***0.55***
Steam-generator Pressure (MPa)	***5.53***
Steam-generator Mass Flow (kg/s)	***25.4***
Accumulator Pressure (MPa)	***4.21***
Accumulator Temperature (K)	***305***
Accumulator Initial Level (m)	***2.31***
Accumulator Level at End of Discharge (m)	***1.75***
Accumulator Liquid Level Change (m)	***0.56***
Accumulator Liquid Volume Discharged (m^3)	***0.76***
Accumulator Initial Gas Volume (m^3)	***0.65***
Accumulator Initial Gas/Liquid Fraction	***0.85***

Sequence of events in the LOFT is shown in Table 28 based both measurement from experiments and calculations. It shows the deviation of code results from test values as well as sources of measurement errors.

Table 28: Loft Test LB-1 Sequence of Event Timing

LOFT Test LB-1 Sequence of Event Timing		
Event	***Measured***	***Code Results***
Break initiated (s)	***0***	***0***
Reactor scrammed (s)	***0.13***	***0.13***
Primary-coolant pumps tripped (s)	***0.63***	***0.63***
Pressurizer emptied (s)	***Instrument failure***	***15.5***
Accumulator A injection initiated (s)	***17.4***	***14***
Reflood Tripped On (s)	***NA***	***0***
HPIS injection initiated (s)	***NA***	***NA***
LPIS injection initiated (s)	***24.8***	***24.8***
Maximum cladding temperature (°K)	***1170***	***1050***

7.2.3 Input Phase

The following provides a step by step discussion of the application of methodology for LBLOCA LOFT test facility.

7.2.3.1 Modified PIRT

PIRT for LBLOCA-LOFT is built for the purpose of uncertainty analysis of the transient scenario calculation by the TH code, RELAP5/MOD3.3. In general the PCT occurs in the blow down phase. There are two quantities that dominate the PCT: the linear heating rate and the reflood rate. The linear heating rate determines, more than anything else, the stored and decay heat. The reflood rate determines how long it will take the ECC to get to the upper part of the core and thus, how long decay heat is raising the peak temperature of the fuel. All the other variables are less important because compensating factors make them less important than they seem. If we calculate the heat transfer coefficient so it is too low, the fuel will be hotter than expected and, when the mode of heat transfer changes later in the transient, the heat transfer will generally be higher (Reeder 1979, Studsvik Energiteknik 1979b, 1979c

and Lubbesmeyer 1991, Brittain 1990). First PCT occurs in blowdown phase caused by:

Initial stored energy transfer

Degraded fuel rod-to-coolant heat transfer

Critical flow at the break

Heating of the fuel rods due to degraded heat transfer

Degraded performance of the reactor coolant pump due to coolant flashes

Degradation of steam generator heat transfer because of low primary system temperatures than secondary system temperatures

Second (refill) and third (reflood) peaks occurs due to temperature increase because of decay heat and poor fuel-to-coolant heat transfer (Shaw at el 1989).

7.2.3.2 Blowdown Phase

The phase begins with the break initiation and ends when the accumulator injection initiates in the intact loops, a period of approximately 16 seconds. The summary of LOFT LBLOCA phenomenology is given below for this phase. The detail can be found in Reeder (1979), Studsvik Energiteknik (1979b, 1979c) and Lubbesmeyer (1991), Brittain (1990) as well.

Scenario starts with opening the blowdown valve in broken loop hot and cold legs which initiate the flow from the break. It causes the primary system pressure to fall. and saturated conditions being reached in the upper plenum at 0.04s. The void fraction upstream of the break planes starts to rise.

The reactor scrammed automatically when the intact loop hot leg pressure dropped to 14.5 MPa at 0.1 seconds.

Primary coolant pumps were tripped manually and decoupled from their flywheels within one second, affecting a rapid coastdown.

Due to the excessive pressure drops over the steam generator and the pump, the pump-side break flow is considerably less than the vessel-side break flow during blowdown

By 1s, flow reversal has started in the bottom of the core, creating a flow stagnation zone in the lower portions of the core.

The core voiding reduces its liquid mass to approximately one fourth of the original content by 1s and voiding in the lower plenum expels about 12% of its liquid mass by this time.

With the exception of the mid-section of the high power rods, the fuel rod temperatures remain at pre-break values through the first second, while the stored heat is being removed by the fluid.

During the next 1s of the transient, voiding appears in the intact loop hot leg and the hotter portion of the core transitions to a vapor-only state. By 2s the flow stagnation zone has extended into the upper level of the lower plenum.

By 2s the vessel side break has transitioned to two-phase flow. The increased flow void fraction reduces the discharge flows and decreases the rate of depressurization.

During the 2s the liquid content of the core continues to decrease further, leading to a high void fraction at the core exit. Similar behavior is seen in the upper part of the lower plenum.

The voiding in the core initiates boiling and departure from nucleate boiling (DNB) on the fuel rods. This leads to a rapid rise of clad temperature as the stored heat redistributes itself in the fuel rods and the decay heat adds to it.

By 2s, increasing voids in the hotter parts of the U-tubes in steam generators lead to an increasing hydrostatic pressure over the steam generators in the intact loops. This is due to the imbalance caused by low density vapor in the rise side and high density mixture in the downside and the return lines of the steam generators.

Accumulator injection into the broken cold leg starts at about 2 s due to the rapid pressure decrease in this loop.

The increasing hydrostatic head in steam generators increases the liquid flow through the intact loops" pumps and cold legs, leading to a liquid surge at the core inlet from 2 to 6s. This results in a temporary rewet of the average and high power rods at about 3 to 5s.

The intact loop pumps activate at about 3 to 5s and flows in the cold legs fall sharply.

By 5 s, voiding has appeared throughout the broken loop, the pressurizer, and all of the intact loops.

Liquid from the pressurizer and its stand- pipe flow down and split in two directions. A major portion of this liquid flows back to the upper plenum and contributes to a second rewet of the fuel rods.

Reduced upward steam flow from the core allows the liquid held up in the guide tubes to drain back into the upper plenum. This drainage, combined with the returning pressurizer liquid, lead to a new peak in the upper plenum liquid inventory at about 7 to 8s.

The increased liquid mass in the upper plenum penetrates into the core and causes a second rewet of the rods at about 7 to 8s. The top-down rewet of the fuel rods leads to quenching that lasts through the end of the blowdown.

The pressurizer emptied at about 15.0 s after the opening of the break valves. At this moment, pressure in the pressurizer has decreased to a value of 7.6 MPa.

Reduction of pressure to about 600 Psi initiates accumulator injection into the intact.

PCT of more than 1260K has been measured during the phase.

Table 29 shows the complete list of identified phenomena during the phase. As it was discussed earlier, the LBLOCA PIRT already developed for AP600 (Wilson at el 1998) and Westinghouse nuclear NPPs (Boyack at el 2003) results, formed the basis for important phenomena identification in each phase for every component.

Table 29: Phenomena Identification Table for Blowdown Phase

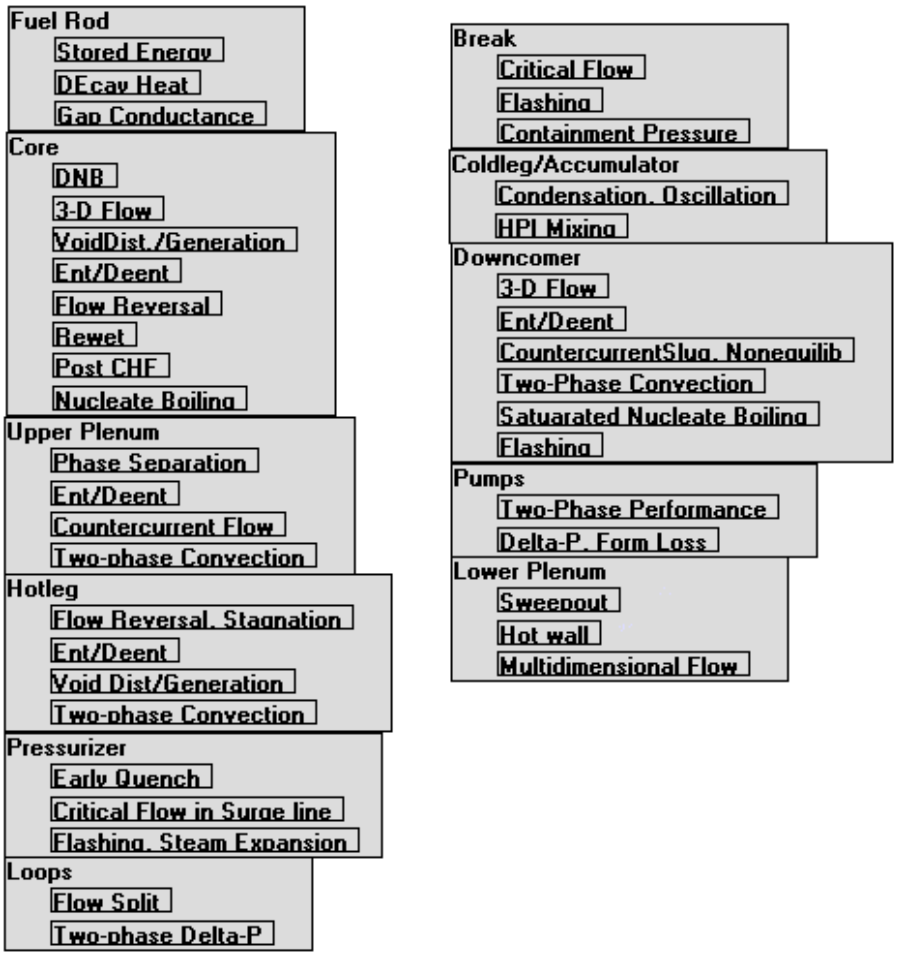

7.2.3.3 Refill Phase

The phase begins with the accumulator injection and ends when the mixture level in the lower plenum reaches the core inlet, a period of approximately 20s.

Accumulator injection in the intact loops starts at about 12s and the pumped LPIS flows begin at about 17.4s, when pressure falls below set point.

Between 22 and 36s the system pressure reduces to a constant level, in equilibrium with the containment pressure and the vessel-side break flow

becomes negligible. Discharge through the pump-side break continues due to the ECC liquid injection into the broken loop.

By 23s the liquid mass fraction in lower plenum is at a minimum and the core is completely voided. Heat transfer from the rods to vapor is only through natural convection.

Clad temperatures rise due to decay heat and insufficient cooling.

As the ECC flow increases, some liquid begins to accumulate in the upper parts of the downcorner. The release of this liquid, at about 23s, contributes to the refill of the lower plenum.

Decreased steam flow in the downcomer allows the ECC flows to penetrate the downcomer and increase the lower plenum liquid inventory.

Heat transfer from the metallic structure to liquid in the lower plenum increase steam generation, leading to surge of two phase mixture into the core and the downcomer.

By 33 to 36s after break, the lower plenum liquid level reaches the core inlet and core Liquid mass begins to rise. This ends the refill period.

The Accumulator empties at almost 40s after the initiation of the break.

Table 30 shows complete list of identified phenomena during this phase. As it was discussed earlier, previous LBLOCA PIRT results are used to identify the phenomena in each phase for every component.

Table 30: Phenomena Identification Table for Refill Phase

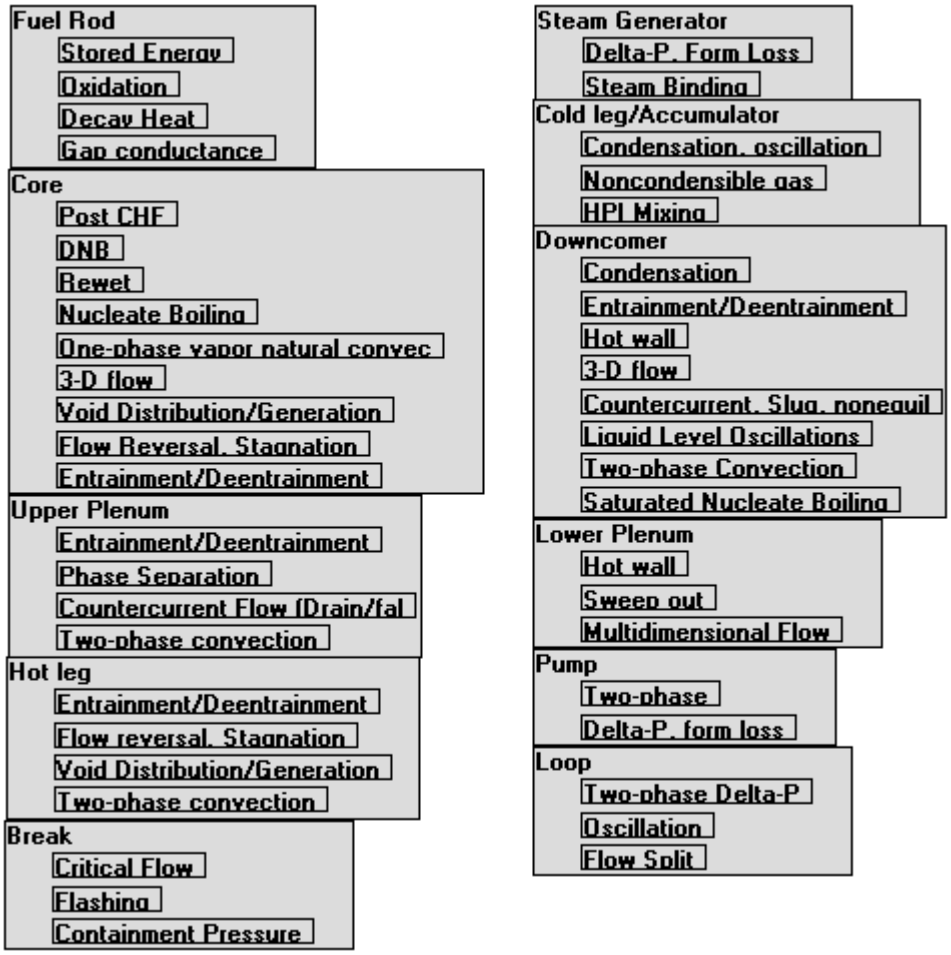

7.2.3.4 Reflood Phase

The phase begins when the liquid mass in the core starts to increase and ends when the whole core is quenched and submerged again, a period lasting 20 to 80s.

At the start of reflood, a liquid-rich two phase level begins to rise from the lower plenum into the core and the rising mixture level at the core bottom initiates quenching of the heated rods.

The decay heat in the fuel continues to heat up the fuel rods and cladding at the higher elevations, due to insufficient cooling.

By 38 to 46s, the quenching level reaches about 1/6 of the core height, while early quenching appears also at the top elevations. The quench front propagation is preceded by intensive boiling and liquid entrainment, and steam flow out of the core carries the entrained liquid into the upper plenum and steam generators.

De-entrained liquid on the upper head structure produces a draining liquid flow back into the core. This creates another quench front that moves down on the rods and leads to the early quenching at the top elevations.

The core liquid mass increases with large amplitude oscillations due to boiling and manometric fluctuations between the core and the downcorner. Termination of the accumulator injection at about 51s causes the highest peak in these oscillations at about 56s.

Liquid droplets, carried into the steam generator, evaporate due to the reversed heat transfer and create a local pressure rise above the core from 55 to 67s. This pressure creates a temporary resistance against the rising liquid level in the core (steam binding effect).

The quench front moves faster on rod segments with low heat flux and more slowly on high power rods. The front propagation is influenced by the gap and cladding heat conductance.

The pumped ECC flows are increasing at the end of accumulator injection and the flows attain a constant level from about 80s through the end of refill. This leads to an increasing trend in the core liquid mass.

The reactor vessel liquid content increases steadily while the core is cooled by pool boiling. This trend continues through the end of reflood.

The hottest parts of the fuel rods (at mid- height) are quenched at 75 to 9s in the calculations, while measured data on shorter rods show quenching at mid height at about 48 to 52s. Complete quenching of the high power rods (and the whole core) is accomplished at about 140s.

The reactor vessel liquid content increases steadily while the core is cooled by pool.

Table 31 shows complete list of identified phenomena during this phase. Again, previous LBLOCA PIRT results are used to identify the phenomena in each phase for every component.

Table 31: Identification of phenomena table for reflood phase

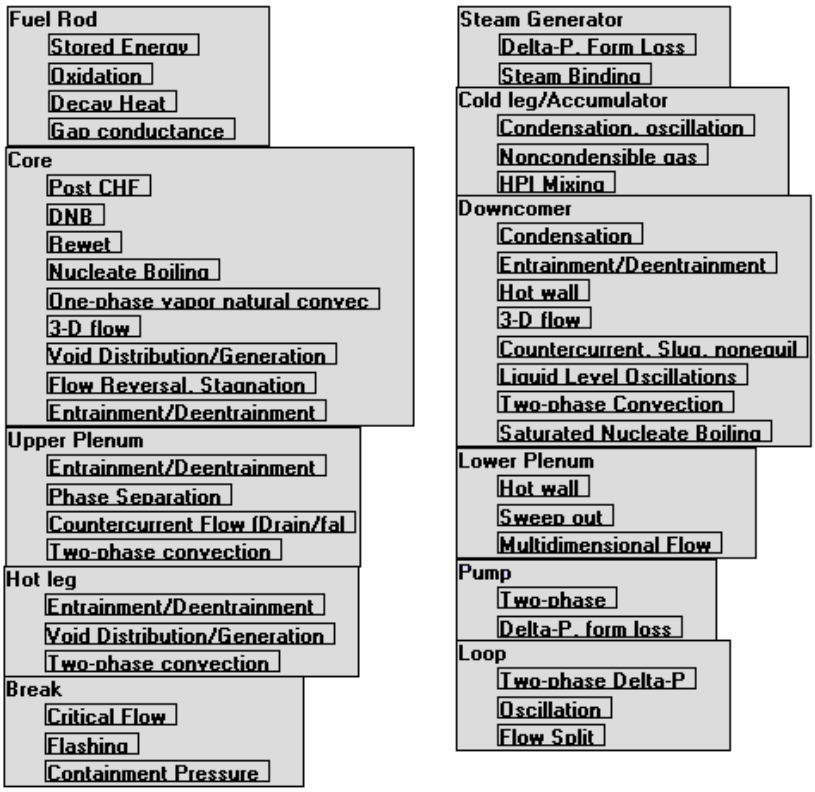

7.2.3.5 Modified PIRT Results

CHOICE (2006) and UMD AHP software were used for TH importance based Phenomena ranking. Based on identified phenomena in previous sections, theses software were utilized to rank them with expert based pairwise comparison of various phenomena for given component. Details of the AHP calculations are given in Appendix A. Ranks are on the scale of 0.0 to 1.0, with 0.0 as lowest rank and 1 as the highest. They were converted to qualitative format, low-medium-high, for consistency with other available PIRT reports. The results are shown in Table 32 and Table 33.

Table 32: AHP-Based Rankings of LOFT LBLOCA Phenomena of High Importance with Expert-Based Uncertainty Importance

Component	Phenomena	Rank for Phase			ncertainty Importanc
		Blowdown	Refill	Reflood	
Fuel Rod	Stored Energy	H	H	H	Low
	Decay Heat	M	M	H	Low
	Oxidation	L	M	H	Medium
	Gap Conductance	L	L	H	Medium
Core	Post-CHF heat Transfer	H	H	M	High
	Rewet	H	H	M	Medium
	Reflood Heat Transfer plus quench	L	M	H	High
	3-D flow	M	M	H	Medium
	Void generation/distribution	M	M	H	Low
	Entrainment/Deentrainment	M	M	L	Medium
	Nucleate Boiling	M	L	L	Medium
	Flow Reversal, Stagnation	L	L	L	Medium
	DNB	M	L	L	Low
	One-phase vapor natural convection	L	M	M	Low
	Radiation Heat transfer	L	L	L	Medium
Upper Plenum	Entrainment/deentrainment	M	M	H	Medium
	Phase Separation	H	L	L	Low
	Countercurrent Flow	L	M	M	Medium
	Two-Phase Convection	M	L	L	Medium
Hot Leg	Entrainment/deentrainment	L	M	H	Medium
	Flow Reversal, Stagnation	M	*	*	Medium
	Void Distribution, Generation	M	M	M	Medium
	Two-phase Convection	L	M	L	Medium

Table 33: AHP-Based Rankings of LOFT LBLOCA Phenomena of High Importance with Expert-Based Uncertainty Importance

Pressurizer	Early Quench	7	*	*	Medium
	Critical Flow in Surge Line	M	*	*	Medium
	Flashing, Steam Expansion	M	*	*	Low
Steam Generator	Steam Binder	*	M	H	High
	Delta-p, Form loss	*	M	L	Medium
Pump	2-phase performance	H	M	M	Low
	Delta-P, form losses	L	M	H	High
Cold Leg /Accumulator	Condensation, Oscillation	H	H	M	Medium
	Noncondensible gases	*	L	H	Low
	HPI Mixing	L	M	L	Medium
Downcomer	Entrainment/deentrainment	M	H	L	Medium
	Condensation	*	H	L	High
	Hot wall	*	L	H	High
	Liquid level Oscillation	*	*	M	Low
	3-D Flow	M	H	L	Medium
	Countercurrent, Slug, Nonequilibrium flow	L	L	L	Medium
	Two-phase convection	M	L	L	Medium
	Saturated nucleate boiling	L	L	L	High
	Flashing	L	*	*	Low
Lower Plenum	Sweep out	M	H	L	High
	Hot wall	L	M	H	High
	Multidimensional flow	M	M	M	High
Break	Critical flow	H	H	L	medium
	Flashing	L	L	L	Low
	Containment Pressure	L	L	H	Low
Loops	2-phase Delta-P	H	M	M	Medium
	Flow Split	H	M	L	High
	Oscillations	M	H	H	Medium

A screening criterion of Medium-High, High-High, and High-Medium is selected and with sensitivity analysis (described in Appendix A) for confirmation of assigned weights. The results are shown in Table 34. Refer to Appendix C for sensitivity assessment of uncertain parameters.

Table 34: PIRT Results after Quantitative Confirmation

Critical Flow
Rewet
Entrainment/Deentrainment
Post-CHF Heat Transfer
Core 3-D Flow
Pump Two-Phase Flow
Non-Condensable Gases
Steam Binding
Conductive/ Convective Heat Transfer

As it was discussed before, phenomena by broad definition are not exclusive sources of uncertainties. Initial conditions have significant effect on end results. Table 35 shows list of these parameters identified for the LOFT LBLOCA scenario.

Table 35: LOFT Facility Important Operation Parameters

Initial Core Power
Pressurizer Pressure
Pressurizer Level
Accumulator Pressure
Accumulator Volume
Safety Injection Temperature
Containment Volume
Initial Flow Rate
Initial Operating Temperature
RCS Pressure
RCS Average Fluid Temperature

7.2.3.6 Code Models and Parameters

Table 36 shows all identified models, correlations, and parameters corresponding to selected phenomena. The quantifiable parameters related to these models and correlations are listed in the table.

Table 36: Correlations and Models for corresponding selected Phenomena and initial Conditions

-Choked Flow **1-Phase model multiplier** **2-Phase Model Multiplier**
-Post CHF Heat Transfer **Gap Conductance Model** Fuel Conductance Input Table in Inputdeck

-Pressurizer Level **Level Controller Card in the Inputdeck** -Measurement Error 1.04 +/- 4 cm
-Core Power **Power table** -Measurement error 49.3 Mwt+/-1.3 MW_t **Fuel and Cladding Thermal Conductivity**
-Entrainment **Hydraulics Diameters (Hot Leg, Downcomer, …)**
-Peaking Factor **Radial** **Axial**
-Accumulator **Pressure**
- Steam Binding **Core Hydraulics Diameter** **Entrainment in S.G. Inlet Plena** **Entrainment in Hot Legs** **Entrainment in Upper Plenum**
-Pump Two-Phase Flow **Mass Flow** **Pressure** **Pump Head** **Pump Torque**

The list may be further screened to a shorter list of parameters more relevant and, more influential on PCT uncertainty. It depends on the resources and the decision making criteria.

7.2.3.6 Input and Model Structure Quantification

Inputdeck options should be checked for their level of influence on the figure of merit. Important options should be considered in uncertainty quantification process. Inputdeck options are part of post-PIRT process to find models and correlations related to important phenomena. If there are some options in the inputdeck that are not related to important phenomena and are influential on the output uncertainty computation, they should be analyzed for implementation of the models in numerical structure.

1. LOFT LBLOCA application is limited by type of phenomena happening for this special transient. CCFL phenomenon is an example. It is concluded (di Marzo 2005) that it will not occur in the transient. There is no other example of mixing of models identified.

2. LOFT test facility was a scale down facility. It was not possible to use scale down facilities to analyze scale up distortion for PIRT results confirmation and data relevance assessment. Limited aspects of methodology are demonstrated in this application.

7.2.3.8 Quantification of Uncertainties in Inputs and Dependency Consideration

Identified sources of uncertainties in code models and correlations are quantified by assigning probability distribution as discussed in Chapter 4. There are various sources of information which are used for the quantification of uncertainties. Data from different separate effects tests listed in Chapter 3 as well as data from LOFT test facility itself are used for more precise quantification of parameter uncertainties. As

discussed on Chapter 5, combination of maximum entropy plus expert justification is used for quantification of input uncertainties. Table 37 shows initial conditions for different parameters calculated and measured for LP-LB-1 test. This is an important source for quantification of initial conditions selected for the uncertainty analysis part of the PIRT process discussed before.

Table 37: Initial Conditions for LP-LB-1 Test (Nalezny 1983)

Parameter	**Specified Value**	**Measured Value**
Primary Coolant System		
Core ΔT (°K)	31-33.2	29.5 ± 1.4
Hot Leg Pressure (MPa)	14.95±0.10	14.77±0.06
Cold Leg Temperature (°K)	555 ± 1.1	556.6±1
Mass Flow rate (Kg/s)	As required to establish primary system initial Conditions	308±2.6
Boron Concentration (ppm)	As required to establish primary system initial Conditions	513 ±15
Primary Coolant Pump Injection (Both Pumps) (L/s)	0.127±0.016	0.122±0.003
Reactor Vessel		
Power Level (MW)	50.0-1.0	49.3±1.2
Maximum Linear Heat (kW/m)	-----	51.7±3.6
Control Rod Position	As required to establish primary system initial Conditions	1.455±0.0002
Pressurizer		
Liquid Volume (m^3)	----	0.55±0.02
Steam Volume (m^3)	----	0.38±0.02
Water Temperature (°K)	----	615±1.7
Pressure (KPa)	14.95 ±0.10	14.84 ±0.11
Liquid Level (m)	1.15 ±0.10	1.04 ±0.04
Broken Loop		
Cold Leg Temperature (°K)	≈555	552±6
Hot Leg Temperature (°K)	≈540	534±11
Suppression Tank		
Liquid Level (m)	1.27±0.13	1.31±0.06
Gas Volume (m^3)	----	54.9±2.1
Water Temperature (°K)	----	359.3±3
Pressure (gas space) (kPa)	----	114±3
Recirculation (L/s)	Full Pump Capacity	Verified
Boron Concentration (ppm)	----	3506±15

Emergency Core Cooling System(°K)		
Borated Water Storage Tank Temperature	----	301±7
Accumulator Liquid level (m)	2.362±0.025	2.32±0.02
Accumulator Standpipe Position (Above Inside Bottom of tank)	2.11±0.025	2.11±0.025
Accumulator Pressure (MPa)	4.22±0.17	4.21±0.06
Accumulator Liquid Temperature (°K)	307±3	305±6

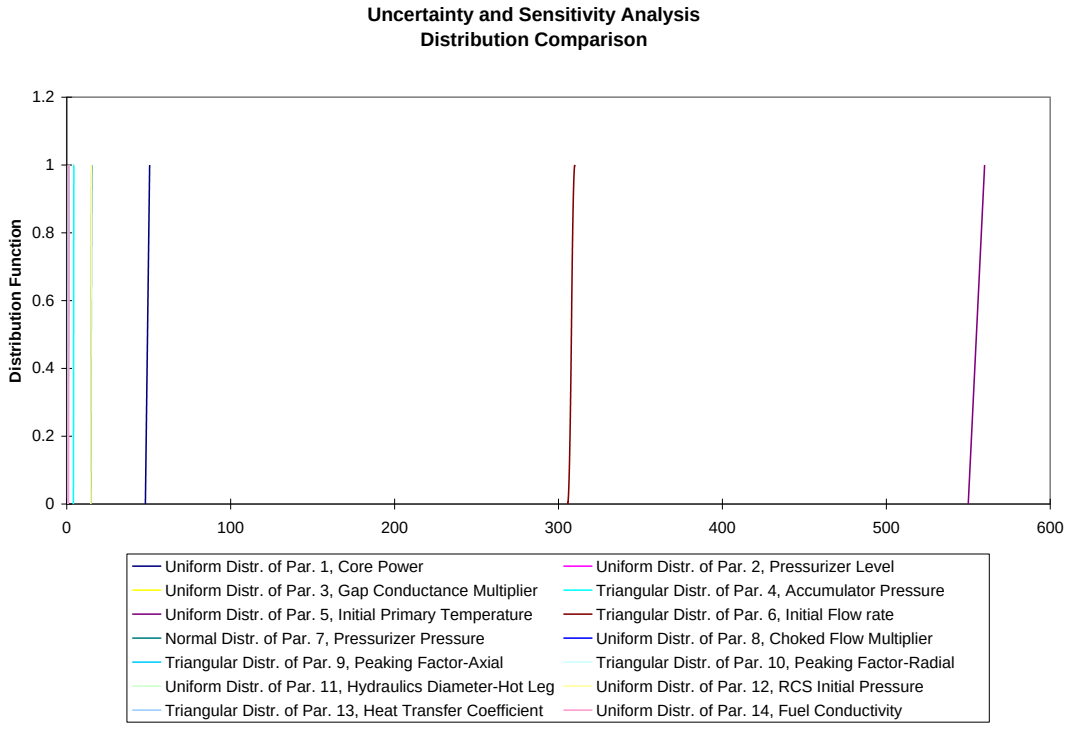

Figure 60: Uncertain Parameter Probabilistic Cumulative Distributions

Code model structures applicable to LOFT LBLOCA uncertainty analysis are:

1. Switching in code model demonstrated choked flow model. Code source modified for switching the model manually, by time or by a thermodynamic condition.
2. Maximization/ Minimization of the models demonstrated by Superheated Interfacial Heat Transfer Coefficients (h_{il}, h_{ig})

Analytically Derived Correlation by Plesset and Zwick vs. Deduced correlation by Lee and Ryley.

3. Run models as recommended -There are several models as "recommended" for the LOFT LBLOCA situations. These are kept as strong evidences and code was run with this recommendations.
4. There is no applicable model for mixing on LOFT application. A CCFL phenomenon is judged as not to occur in LOFT LBLOCA

7.2.4.3 Dependency

Figure 61 shows dependency assignment between gap conductance and RCP temperature. Figure 62 shows dependency between pressurizer level and pressure. Pearson dependency is used for calculation of samples with consideration of dependency as shown in Appendix E. The dependencies considered, are for demonstration. In case other dependency between other parameters is found to exist they also need to be considered.

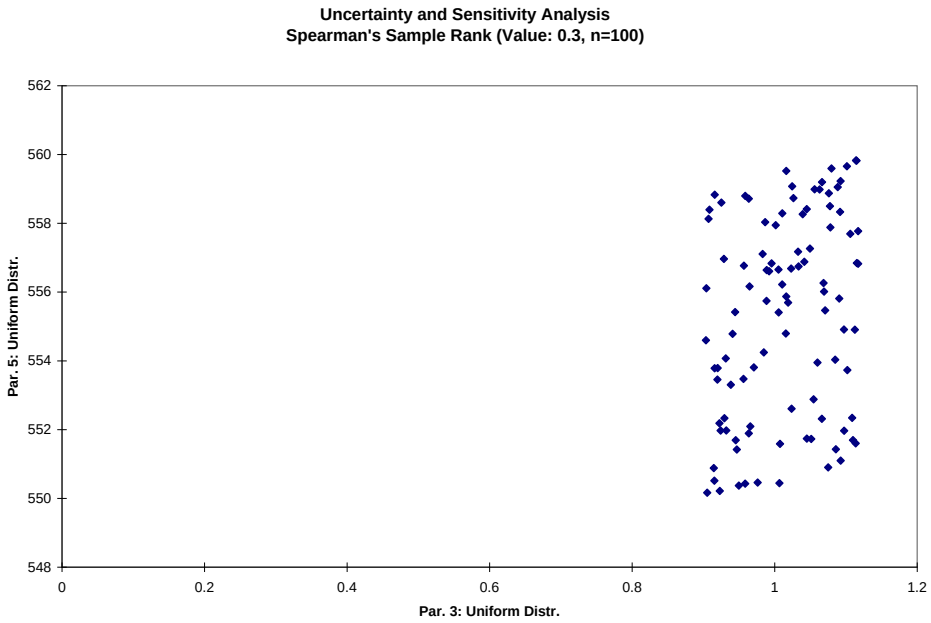

Figure 61: Dependency between Gap Conductance and RCP Temperature

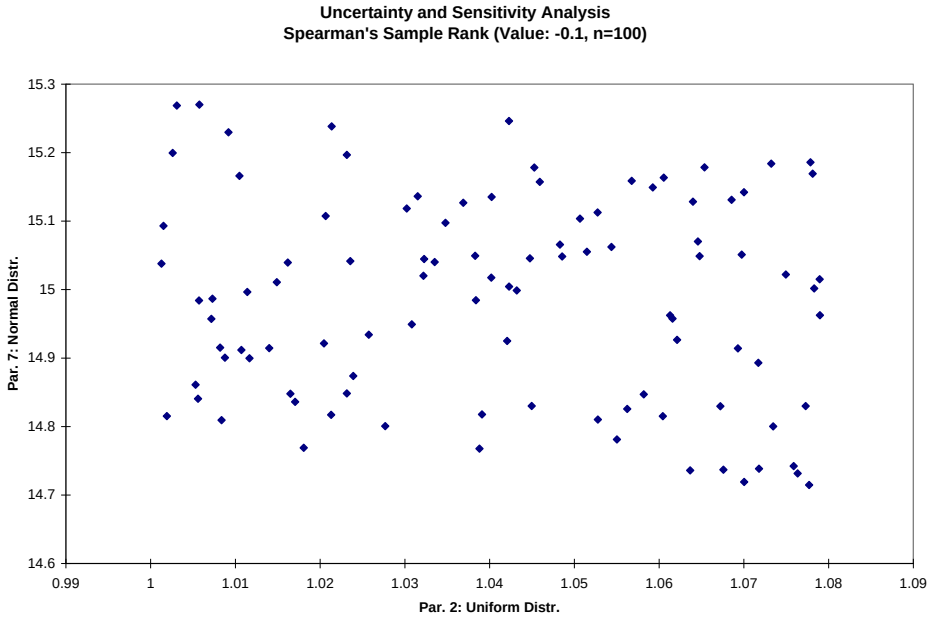

Figure 62: Dependency between Pressurizer Level and Pressure

Results from 186 RELAP5 code runs are shown on Figure 64, Figure 66, and Figure 68. Figure 64 shows all 186 runs together. Figure 66 and Figure 68 shows two separate 93 runs for arriving to 95|95 inference about output.

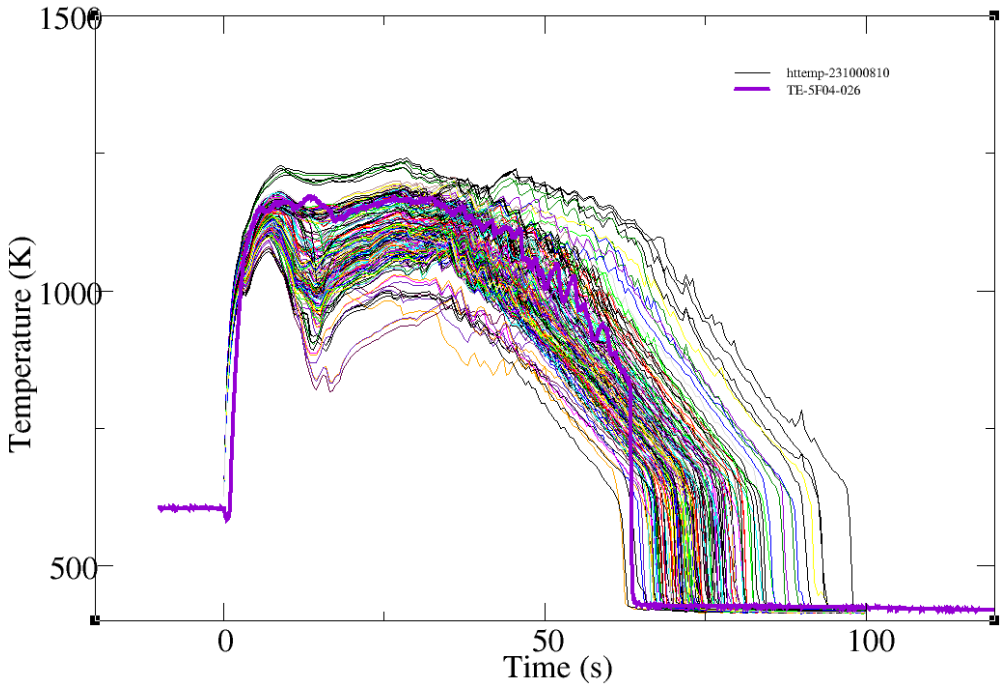

Figure 63: Code Run Results-Total of 186 with Experimental Results

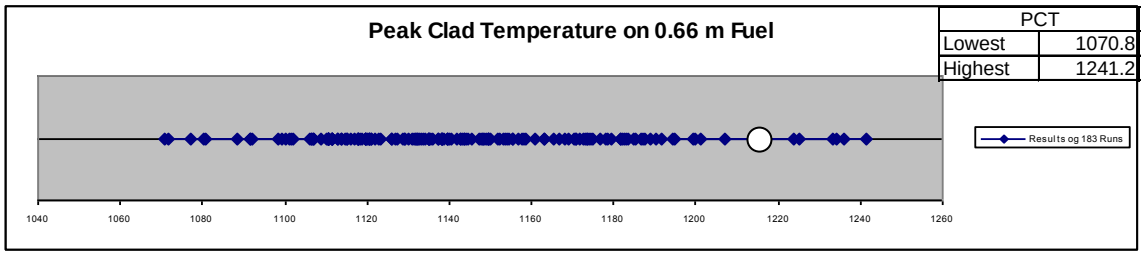

Figure 64: Peak Clad Temperature Scatter for 186 Code Runs with Highest PCT from Experiment

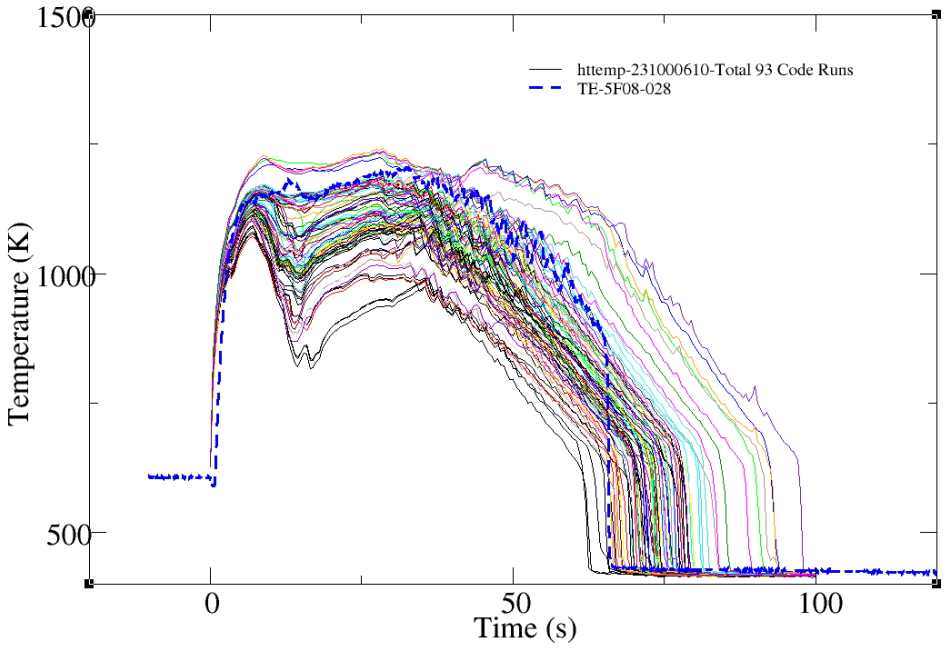

Figure 65: Uncertainty Propagation Results 1- Clad Temperature on Rod 0.66m

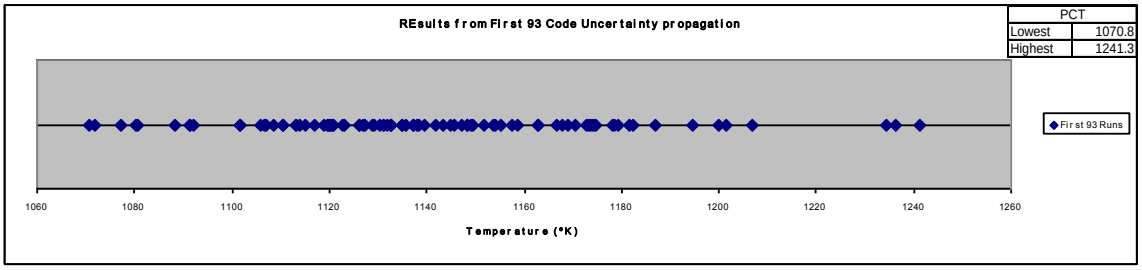

Figure 66: Peak Clad Temperature Scatter for First 93 Code Runs

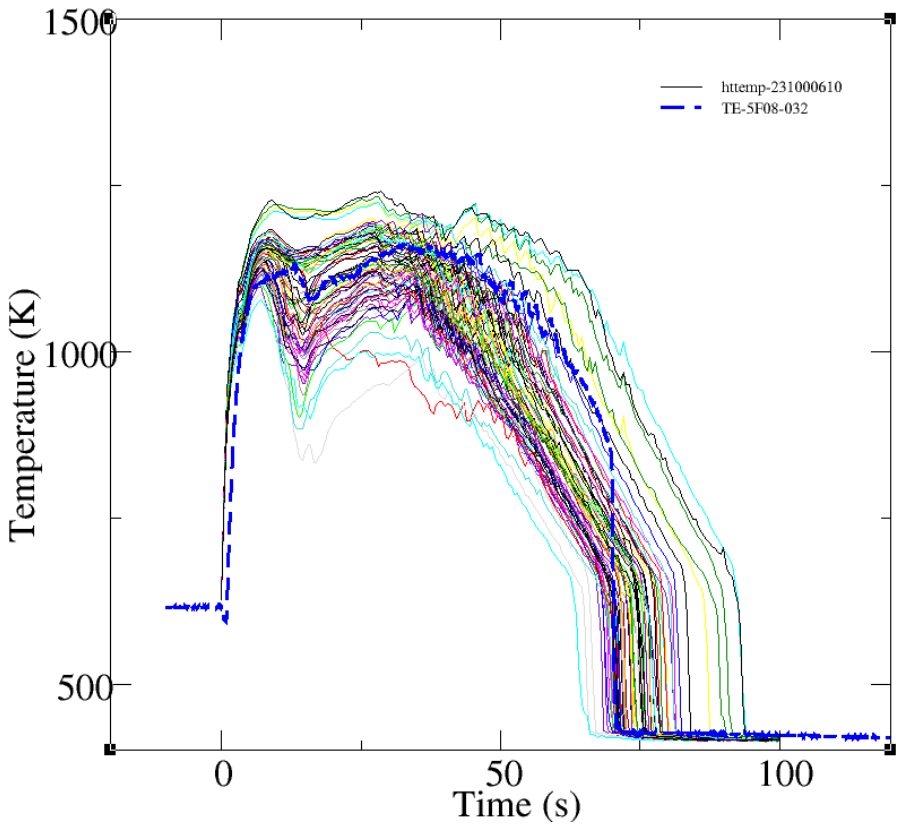

Figure 67: Uncertainty Propagation Results 2- Clad Temperature on Rod 0.66m

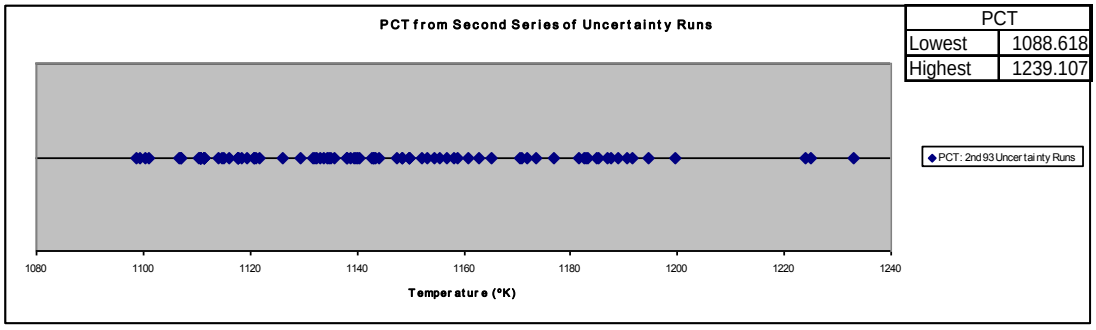

Figure 68: Peak Clad Temperature Scatter for Second 93 Code Runs

The lowest and highest values and ΔPCT in each set of run as well as total Run series are given in Table 38. It shows difference in coverage bound from one set of run to other.

Table 38: Lowest and Highest PCT Temperature in 1st, 2nd and Total Uncertainty Propagation

PCT	1st Runs	2nd Runs	Total
Lowest	1070.8	1098.618	1070.8
Highest	1241.2	1233.107	1241.2
ΔPCT	170.4	134.4884	170.4

The results show a 20°K difference in ΔPCT band for 2 uncertainty set of uncertainty runs. As discussed in Chapter 6, we choose more conservative one to preserve information in transit from first phase to second one. Second run demonstrate bigger band for the PCT.

7.2.5 Output Updating

Data from code calculation and LOFT experiments are given in Figure 69 a) and Figure 72 b) respectively. The calculation data is from 1st run. There are

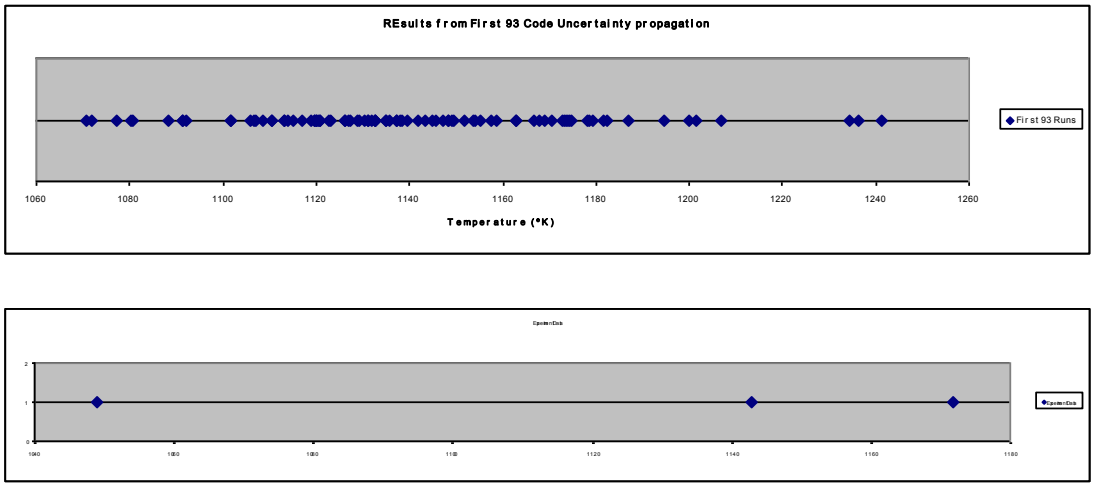

Figure 69: PCT Data from a) The Code Computation b) LOFT Tests

This data are used in the framework discussed on chapter 6 for calculation of parametric distributions. Normal distribution is fitted to for each set of data.

7.2.5.1 Parametric Results

Figure 70 shows result from fitting parametric normal distributions to code and experimental data. The statistics for the PTC as well as its mean and standard deviation parameters are shown in the tables beneath each distribution.

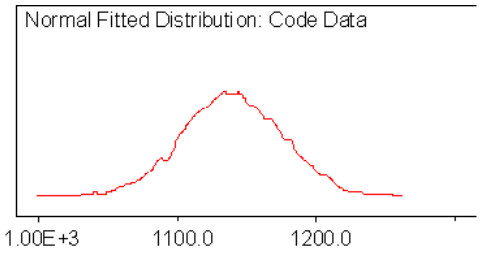

Node	Mean	SD_DEV	MC Error	2.50%	Median	97.50%
CODE	1140	35	0.4226	1071	1140	1208
MEAN	1140	0.14	0.002047	1140	1140	1140
SD_DEV	35	0.2232	0.006848	34.56	34.99	35.44

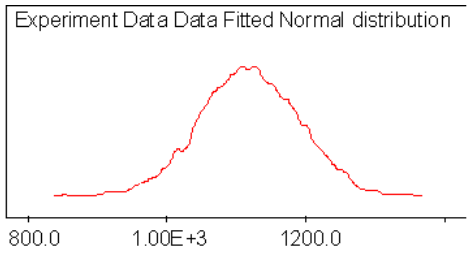

Node	Mean	SD_DEV	MC Error	2.50%	Median	97.50%
CODE	1120	70.02	0.846	981.6	1119	1256
MEAN	1120	0.1184	0.001731	1120	1120	1120
SD_DEV	70	0.1181	0.003549	69.77	70	70.24

Figure 70: Results for Normal Distribution; a) Code Data with Statistics b) Experimental Data with Statistics

The results for update PCT are given in Figure 71.

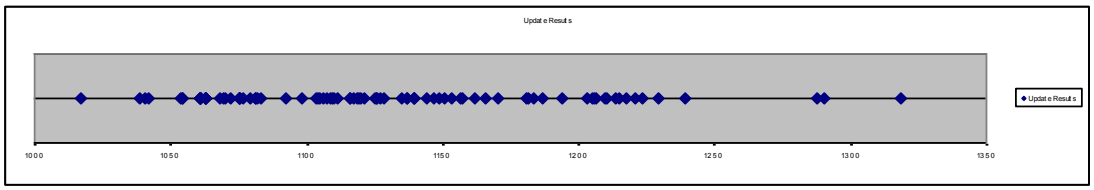

Figure 71: The Results of Update PCT

The normal distribution fitted for updating PCT distribution is given in Figure 73. The statistics are also provided for comparison with results from input phase results.

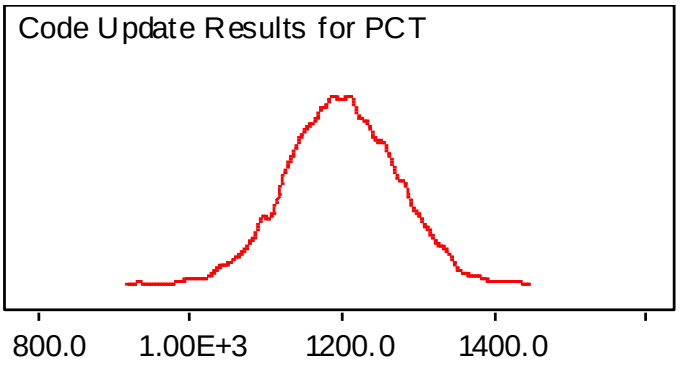

Node	Mean	SD_DEV	MC Error	2.50%	Median	97.50%
CODE	1203	70.04	0.8462	1061	1199	1336
MEAN	1203	0.09904	0.001448	1200	1200	1200
SD_DEV	70.03	0.1383	0.004049	69.75	70.02	70.3

Figure 72: The results for Update Code Distribution

Updated results show shifting toward experimental results. Depending on relation between code and test data, different outputs are possible. There is an underestimation in the calculation of LOFT LBLOCA with the RELAP5 code. The updating corrects this problem and updates the results to more realistic results. Those conditions are discussed in Chapter 6.

7.2.6 Uncertainty Importance

The results for pressurizer level parameter uncertainty importance analysis for LOFT LBLOCA calculation is shown in Figure 73 and Table 39. Figure 73 is uncertainty range for the parameter and Table 39 is the calculations based on changes for pressurizer level to study level of changes in PCT.

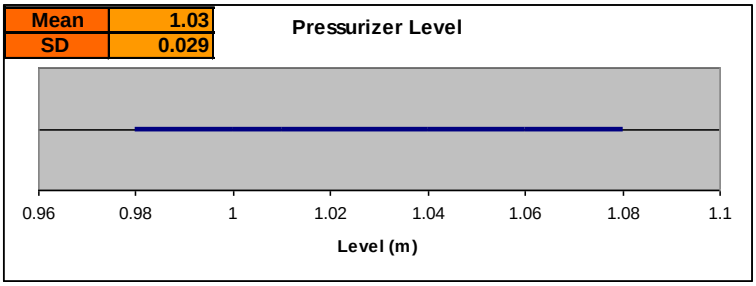

Figure 73: Uncertainty Range for Pressurizer Level in LOFT Test Facility with μ= 1.03 m and σ= 0.029 m .

Pressurizer level was perturbed 6 times in standard deviation steps and the results in change of PCT were recorded. With total uncertainty range for PCT from uncertainty quantification, uncertainty is calculated for pressurizer level parameter.

Table 39: Results of Uncertainty Importance for Pressurizer Level: a) Changes in Pressurizer Level b) Calculation of Importance Measure

Node	Mean	SD
Code	1148	35.4

Change in Uncertain Parameter	ΔPCT
Pressurizer Level + 1 Sigma	-0.2925
Pressurizer Level + 2 Sigma	-0.978
Pressurizer Level + 3 Sigma	-3.3408
Pressurizer level + 1- Sigma	1.087
Pressurizer Level + 2- Sigma	3.2445
Pressurizer Level + 3- Sigma	4.1013

2-Sigma Importance	0.022444
4-Sigma Importance	0.05964
6-Sigma Importance	0.070076
Pressurizer Uncertainty Importance Measure	0.05072

Importance of pressurizer level is calculated in 2, 4, 6 sigma and shown in the Table 39. The average value is calculated for uncertainty importance of the parameter. Each single value can also be used as the importance measure but it should be consistent for all parameters. The values for importance are relative (importance measure value for a parameter is compared with the importance of other components).

CHAPTER 8: CONCLUSIONS AND RECOMMENDATIONS

8.1 Summary and Conclusions

This research discusses an integrated thermal-hydraulics uncertainty analysis methodology for "best estimate" thermal hydraulics codes such as RELAP5. The main thrust of the methodology is to utilize all available types of data and information in an effective way to identify important sources of uncertainty and to assess the magnitude of their impact on the uncertainty of the TH code output measures. The proposed methodology is a fully quantitative and uses the Bayesian approach for quantifying the uncertainties in the predictions of TH codes**.** The methodology uses the data and information for a more informed and evidence based ranking and selection of TH phenomena through a proposed modified PIRT method. The modification considers importance of TH phenomena as well as their uncertainty importance. In identifying and assessing uncertainties, the proposed methodology treats the TH code as a white box, thus *explicitly* treating internal sub-model uncertainties, and propagation of such model uncertainties through the code structure as well as various input parameters. A systematic framework of maximum entropy-Bayesian method is designed to utilize all data and information for quantification of parameter uncertainties distributions. Bayesian techniques are used to incorporate available data (experimental, expert opinion and limited field data) to estimate the parameter uncertainties. The code output is further corrected through the use of a Bayesian framework with available experimental data at the integrated test facilities.

In assessing corresponding uncertainties, possible sources of information include results of code validation experiments and expert judgments (e.g., on credibility and validity of models) are used for more comprehensive uncertainty analysis. For this purpose a Bayesian framework for TH code model uncertainty is developed. It utilizes the data directly related to code output as figure of merit (mostly from ITF data) to account *implicitly* for missed/screened out sources of uncertainties. Representations of uncertainty bound with physical meaning (history trace) rather than a statistical representation are among the issues tackled in this research. The proposed methodology uses an efficient Monte Carlo sampling technique for the propagation of uncertainty. Because of the computational intensity of the Monte Carlo simulations, especially when applied to complex TH calculations, modified Wilks' sampling criteria of tolerance limits is used to significantly reduce the number of Monte Carlo type iterations required, depending on the accuracy requested.

Methodology has been demonstrated on LOFT facility for 200% cold leg LBLOCA transient scenario.

8.2 Recommendations for Future

Following are several recommendations for continuation of the research. Uncertainty analysis on TH codes requires reasonable amount of resources for getting accurate results. A team of TH experts with statisticians and TH code professional should work together to perform a TH uncertainty analysis for a given scenario.

8.2.1 Automating the uncertainty treatment in TH Code

The idea of internal assessment of uncertainty has been proposed and implemented by D'Auria (2001). CIUA is a special case for UMAI methodology. Similar process can be proposed for IMTHUA. The option can be developed so that user easily obtains estimates of the uncertainty in calculated code outputs. The option should be specifically implemented so that a user may perform an uncertainty analysis on any problem in an understandable, systematic manner.

8.2.2 Application of the methodology on a full scale model of nuclear power plant

Limited demonstration of methodology on LOFT and Marviken test facilities does not show all aspects of methodology. Full demonstration of methodology can be shown in a NPP transient such as LBLOCA and so on. Broader list of phenomena are involved in the transient and higher variety of code models and options are encountered in the calculation. Scaling issue can be discussed in such example too.

8.2.3 Mixing Aleatory and Epistemic Uncertainty

Issue of mixing aleatory and epistemic uncertainties has been posed in several technical meeting in problems where both kinds of uncertainties contribute to the total uncertainty especially to PRA type of risk calculation. The distinction is useful because epistemic uncertainties are in principle and practically reducible by obtaining more or better information. Therefore if we know what portion of the uncertainty in the model outputs is due to epistemic sources of uncertainty, then we know that in principle this uncertainty is removable or at least reducible, whereas that part due to aleatory uncertainties is irreducible.

8.2.4 Comparison of results of IMTHUA with other available methodologies (GRS, CSAU and ASTRUM)

Comparison of results for uncertainty analysis of LOFT LBLOCA with other available methodologies such as GRS, CSAU, and ASTRUM will demonstrate strengths and weaknesses of the available methodologies. Step by step comparison results in understanding the utilization of data and information for purpose of uncertainty analysis. As discussed before, this is not possible by only looking at the end results to compare credibility and accuracy of TH uncertainty analysis methodologies. The strength of various methodologies can not be answered only by checking end results.

8.2.5 Temporal Uncertainty Consideration

Uncertainty of physical phenomena has magnitude as well as temporal dimensions. As it was observed in LOFT application, sequence of events is shifted in the scenario by change in some uncertain players. This is treated in UMAE methodology in special situation, which is not applicable to IMTHUA methodology. For comprehensive analysis of uncertainty, this issue should be addressed.

8.2.6 Comparison of result with and without considering structural uncertainties

The comparison provides some insight on relative contribution of parameter and code structure uncertainties to the output distribution. This can be done by assessing the uncertainties twice once with and once without structural uncertainty.

8.2.7 Representation on uncertainty in time dimension

It is important to interpret and represent the output uncertainty results correctly for time variant output parameters. It can be discussed in statistical and physical meanings.

APPENDIX A: TABLES FOR AHP CALCULATIONS FOR COMPONENTS IN DIFFERENT PHASES

Following are the Tables for AHP process and the justifications for the ranks. Justifications are based on literature review and especially trying to understand relation on ranks for a traditional Westinghouse (Shaw 1988)). A group of TH experts may justify more accurate pairwise ranks for the phenomena. The UMD-AHP software developed in University of Maryland was used for calculation of the ranks of phenomena for every component in the transient phases.

Blowdown phase

Table A-1: Fuel Rod

Fuel Rod	Stored Energy	Decay Heat	Gap Conductance
Stored Energy	1.000	9.000	5.000
Decay Heat	0.111	1.000	0.200
Gap Conductance	0.200	5.000	1.000

2-3 Stored Energy released during the first minute of a LBLOCA might be equal to, or greater than (by a factor of 2 to 4) the energy generated by the decay heat during the same period.
2-4 Gap conductance is only one of the factors limiting the transfer of stored energy to the cladding and is less important than other factors such as fuel rod thermal properties characterizing stored energy
3-3 Decay heat is less important in early blowdown comparing gap conductance which determines the delivery of stored energy

Table A-2: Core

Core	DNB	POST CHF	REWET	NUCLEATE BOILING	3-D Flow	VOID DIST.	ENT/DEENT	Flow Reversal
DNB	1.000	3.000	1.000	3.000	5.000	1.000	5.000	3.000
POST CHF	0.333	1.000	0.200	5.000	5.000	1.000	5.000	3.000
REWET	1.000	5.000	1.000	7.000	7.000	1.000	5.000	3.000
NUCLEATE	0.333	0.200	0.143	1.000	7.000	3.000	5.000	3.000

BOILING								
3-D Flow	0.200	0.200	0.143	0.143	1.000	0.333	0.333	0.333
VOID DIST.	1.000	1.000	1.000	0.333	3.000	1.000	7.000	0.333
ENT/DEENT	0.200	0.200	0.200	0.200	3.000	0.143	1.000	0.333
Flow Reversal	0.333	0.333	0.333	0.333	3.000	3.000	3.000	1.000

2-3 DNB is end of high heat transfer period. Its timing affects the amount of stored energy removed early blowdown , hence, the PCT. POST-CHF has less effect on the PCT
2-4 LOFT test L2-5 and L2-3 showed DNB and rewet have significant, but comparable effect on PCT
2-5 These two phenomena are closely related. A delay in DNB will allow more energy to be removed, thus limiting PCT. DNB is more important because it ends high heat transfer rates
2-6 Time-to-DNB is important factor determining PCT. One Analysis showed that 3-D effects resulted in a PCT of only 15K less than 1-D models. [1]
2-7 Judged to be equally important; DNB affects energy removal; void generation affects energy production and heat transfer rates.
2-8 Removal of the stored energy, i.e., the time-to-DNB, Is considered a strong factor affecting PCT; entrainment effects are small since the core empties within a few seconds. Minimal entrainment occurs during the rewet.
2-9 The flow reversal and stagnation in the core contributes to the achievement of CHF conditions, but the amount of energy present during this period is influenced by DNB.
3-4 Rewet removes huge amount of the initial stored energy then more important
3-5 The amount of heat removed during the post-CHF period Is greater than during nucleate boiling due to the time spent in each period.
3-6 Post-CHF is considered to be more important because core flows are basically 1-D during Blowdown.
3-7 This phenomena are highly coupled and, thus, consisted to be equally important.
3-8 Entrainment will exist especially during the bottom rewet; however, its effect is small relative to post-CHF heat transfer
3-9 Tests[2] show that the high power rods remained relatively unaffected by reverse core flow magnitude and duration.
4-5 In LOFT experiments L2-2 and L2-3, DNB occurred at 1.3 and 1.7 s, respectively; thus, little time was spent in nucleate boiling. Rewet had pronounced effect of lowering cladding temperatures.
4-6 Rewet has significant effect but 3-D effects are not significant during blowdown.
4-7 These elements were judged to have an equivalent effect since void generation affects both production and the ability to rewet, and rewet has strong effect on PCT
4-8 Fall back from the upper plenum is possible if storage occurs there; however, rewet is considered to be of high-importance.
4-9 variation in reverse core flow can effect time to DNB in low power regions of the core, but early rewet is more important.
5-6 The time the core is in nucleate boiling is relatively short with early DNB, Core flows are 1-D during blowdown then 3-D effects is not significant.

5-7 Nucleate boiling contributes to the void generation.
5-8 Nucleate boiling is important because of the high heat transfer rates and the voiding role in determining moderator density. Entrainment, which occurs at the quench front (first rewet) due to intense vapor generation, is considered such less important during blowdown.
5-9 Both elements are very important. Nucleate boiling removes energy rapidly, thus it is considered to be slightly more important
6-7 Voiding is more important because of its role in power reduction and heat transfer. Blowdown is basically 1-D in character.
6-8 Neither element is considered very important during blowdown, but some precursory cooling may occur due to entrainment during the quench. Blowdown is 1-D in character.
6-9 Flow stagnation Is more important since it leads to CHF conditions. Blowdown is 1-D in character.
7-8 Void distribution strongly affects Local heat transfer rates and power reduction, whereas minimal effect has been attributed to blowdown entrainment in the core.
7-9 Flow stagnation in the core leads to voided conditions and CHF end, hence, is judged to be more important. Voiding is important because of moderator density.
8-9 As above, flow stagnation results in CHF conditions, whereas the only entrainment in the core during blowdown is at the quench front (if a rewet occurs) and probably contributes little in the form of pre-cursory cooling.

Table A-3: Hot Leg

Hot Leg	Flow Reversal, Stagnation	Ent/Deent	2-Phase Convection	Void Dist, Void Generation
Flow Reversal, Stagnation	1.000	3.000	2.000	4.000
Ent/Deent	0.333	1.000	0.333	1.000
2-Phase Convection	0.500	3.000	1.000	3.000
Void Dist, Void Generation	0.250	1.000	0.333	1.000

2-3 Flow reversal Is considered more important because of potential for rewetting the core.
2-4 The effect of flow reversals on PCT has been shown; the effect of blowdown two-phase convection in the hot leg has not been shown to have high significance.
2-5 Flow reversals have occurred In experiments and the effects have been shown to be significant.
3-4 Structural heat transfer is judged more important during blowdown; entrainment/deentrainment is of more concern Later In the transient.
3-5 Neither element is judged to be very significant during blowdown, although the hot legs will be highly voided during blowdown.
4-5 Structural heat transfer is judged to be the slightly more important element; however, definitive test data does not exist to support that hypothesis.

Table A-4: Downcomer

Downcomer-Blowdown	Entrainment/deentrainment	Countercurrent, slug, nonequilibrium flow	2-phase convection	Saturated Nucleate Boiling	3-D Effects	Flashing
Entrainment/ deentrainment	1.000	7.000	1.000	5.000	1.000	7.000
Countercurrent, slug, nonequilibrium flow	0.143	1.000	0.333	1.000	0.333	5.000
2-phase convection	1.000	3.000	1.000	5.000	1.000	7.000
Saturated Nucleate Boiling	0.200	1.000	0.200	1.000	0.200	5.000
3-D Effects	1.000	3.000	1.000	5.000	1.000	7.000
Flashing	0.143	0.200	0.143	0.200	0.143	1.000

2-3	The inventory carried up the downcomer and out the break is more important than non-equilibrium during blowdown.
2-4	Entrainment obviously effects system Inventory, while two-phase convection removes superheat. Downcomer material temperatures in Semi-scale Teat S-07-1 show the removal of wall heat.[2]
2-5	The data shows the occurrence of both elements, but the entrainment is considered to have the more important effect with regard to PCT.
2-6	The multi-dimensional flow patterns in the downcomer influence the carryout; thus, these two elements are strongly coupled and considered equally important.
2-7	Referred to Semiscale test, both elements obviously occur; however, the rote of entrainment on system inventory is more important than downcomer flashing.
3-4	There was no true countercurrent flow during blowdown in Semiscale (all the downcomer flow was reversed). Some of the stored heat will be removed by 2-phase convection, but date does not exist to quantify the importance.
3-5	These elements are judged to be equally important, but both are more refill phenomena than blowdown phenomena.
3-6	The vessel-side break flow exceeds the combined intact loop cold leg flows, indicating nearly all the intact loop flows circle the downcomer and exit the break. Countercurrent flow is not established well until the refill phase.
3-7	Neither element is considered very important during blowdown. If countercurrent flow occurs, however, the effect could be significant in quenching the core.
4-5	The period of saturated nucleate boiling will be very limited; therefore, two-phase convection is judged to be more important.
4-6	These elements were judged equally important in this analysis due to lack of enough data.

4-7 Semiscale data shows removal of some of the wall superheat during blowdown, but the effects of flashing have not been quantified.
5-6 The transmission of inventory around the downcomer and out the break is judged to be more important than downcomer nucleate boiling due to hot waits.
5-7 Semiscale data shows removal of some of the wall superheat during blowdown, but the effects of flashing have not been quantified.
6-7 Flashing will occur, but the. initial displacement of coolant is judged to be much more important.

Table A-5: Pressurizer

Pressurizer	Early Quench	Flashing, Steam Expansion	Critical Flow in Surge Line
Early Quench	1.000	1.000	1.000
Flashing, Steam Expansion	1.000	1.000	1.000
Critical Flow in Surge Line	1.000	1.000	1.000

2-3 Flashing contributes to the pressurizer pressure Lag but, as above, the relative importances are inconclusive.
2-4 Flow through the surge line can Influence the inventory supply to the core (hence early quench). The early quench was attributed to pressurizer dumping into the core. LOFT had occasional negative flow in the hot legs but early quench was attributed to pump coastdown.
3-4 Flow through the surge line can influence the inventory supply to the core (hence early quench). LOFT had occasional negative flow in the hot legs, but early quench was attributed to pump coastdown. The relative importance is inconclusive. Flashing also contributes to the pressurizer pressure leg.

Table A-6: Pump

Pump	Two-phase	Delta-P, Form loss
Two-phase	1.000	5.000
Delta-P, Form loss	0.200	1.000

2-3 Since the pumps normally are coasting down during blowdown, the form loss pressure drop is not as important as the two-phase degradation, which causes a sharp reduction in cold leg flow rates. Another study has shown, however, that the form loss under certain conditions can cause elimination of the early quench.

Table A-7: Cold leg/Accumulator

Cold Leg, Accumulator	Condensation, Oscillation	HPI Mixing
Condensation, Oscillation	1.000	7.000
HPI Mixing	0.143	1.000

2-3 HPI flow rates are very Low and were operational only for a short period at the end of blowdown. The potential for some condensation of steam flowing into the steam generators exists, but neither would have significant impact on system response.

Table A-8: Upper Plenum

Upper Plenum	Phase Separation	Ent/Deent	2-f Convection	Countercurrent Flow (Drain/Fallback)
Phase Separation	1.000	3.000	1.000	9.000
Ent/Deent	0.333	1.000	0.333	1.000
2-phase Convection	1.000	3.000	1.000	9.000
Countercurrent Flow (Drain/Fallback)	0.111	1.000	0.111	1.000

2-3 Experimental data shows evidence of liquid separation, but the effect of these elements can not be determined experimentally. Calculations have shown that most upper plenum flow will impinge on the internals.
2-4 Closely related phenomena and evaluated in same significance
2-5 It is assumed that the two-phase convection is more Important. Data is only available on reflood phase on these phenomena
3-4 Experimental data show occurrence of fall back then phase separation is considered high importance with high uncertainty
3-5 Judged to be equally important.
4-5 Convective heat transfer is judged to be more important during blowdown than the limited observed amount of fallback.

Table A-9: Break

Break	Critical Flow	Flashing	Containment Pressure
Critical Flow	1.000	7.000	7.000
Flashing	0.143	1.000	5.000
Containment Pressure	0.143	0.200	1.000

2-3	The LOFT LBLOCA experiments show a significant critical flow modeling influence on PCT. Flashing at the break plane causes a reduction in break flow, but is considered less-important than the critical flow calculation.
2-4	Since system pressure at the end of blowdown approximately 4 MPa, the flow still choked and containment pressure will have an Insignificant effect on blowdown
3-4	As above, flashing has an effect on critical flow during blowdown, whereas containment pressure does not.

Table A-9: Loop

Loop	Flow Split	2 Phase Delta-P
Flow Split	1.000	1.000
2 Phase Delta-P	1.000	1.000

2-3	These phenomena are closely coupled and therefore, are considered equally important

Table A-10: Lower Plenum

Lower Plenum	Sweep out	Hot wall	Multidimensional Flow
Sweep out	1.000	5.000	3.000
Hot wall	0.200	1.000	0.500
Multidimensional Flow	0.333	2.000	1.000

2-3	Partial sweep out of the tower plenum obviously occurs, but hot wall effects.
2-4	As mentioned above, partial sweep out of the lower plenum will occur, but no data exists to support or reject the judgment that multi-dimensional effects in the Lower plenum are insignificant.
3-4	Hot wall effects are not judged to be of major significance during blowdown. 3-D flow may occur, but also Is not during blowdown.

Refill Phase

Table A-11: Fuel Rod

Fuel Rod-Refill	Stored Energy	Oxidation	Decay Heat	Gap Conductance
Stored Energy	1.000	5.000	3.000	3.000
Oxidation	0.200	1.000	0.500	0.500
Decay Heat	0.333	2.000	1.000	1.000
Gap Conductance	0.333	2.000	1.000	1.000

2-3	Experiments and some code calculations indicate that cladding temperatures are not high enough to result in significant oxidation. Cladding temperatures are dominated by transfer of stored energy to the cladding surface
2-4	The fuel stored energy contribution is in higher importance than the decay heat contribution during refill.
2-5	Total stored energy determines the potential peak fuel cladding temperatures and the gap conductance determines the ability to conduct the stored energy to the clad. Some experiments show that the gap conductance does not strongly influence the stored energy.
3-4	Semiscale and LOFT data show that cladding temperatures do not get high enough to cause significant energy generation from metal-water reaction
3-5	Gap conductance Is more important than oxidation because data shows that cladding temperatures do not get high enough to cause significant oxidation, hence, conduction of stored energy across the gap is a larger effect.
4-5	Gap conductance and decay heat are rated of equal importance since Late In refill (after stored energy has mostly been removed), the fuel and cladding temperature will be determined by the decay energy generation rate and the ability to conduct this energy to and from the cladding.

Table A-12: Core

Core-Refill	DNB	POST CHF	REWET	NUCLEATE BOILING	3-D Flow	VOID DIST.	ENT/DEENT	Flow Reversal	One-phase vapor natural Convection
DNB	1.000	0.143	1.000	1.000	0.200	0.200	0.143	9.000	0.200
POST CHF	7.000	1.000	7.000	7.000	5.000	2.000	4.000	9.000	3.000
REWET	1.000	0.143	1.000	5.000	0.333	0.500	0.500	9.000	0.333
NUCLEATE BOILING	1.000	0.143	0.200	1.000	0.143	0.125	0.500	9.000	0.111

3-D Flow	5.000	0.200	3.000	7.000	1.000	0.200	1.000	9.000	0.200
VOID DIST.	5.000	0.500	2.000	8.000	5.000	1.000	5.000	9.000	1.000
ENT/DEENT	7.000	0.250	2.000	2.000	1.000	0.200	1.000	9.000	0.200
Flow Reversal	0.111	0.111	0.111	0.111	0.111	0.111	0.111	1.000	0.111
One-phase vapor natural Convection	5.000	0.333	3.000	9.000	5.000	1.000	5.000	9.000	1.000

2-3 For the most part, DNB occurs during blowdown and post-DNB regimes dominate the refill period. Even if RNO occurs during the refill, subsequent DNB occurs at a time when much stored energy has been removed and Lower PCT results relative to the first peak.
2-4 Rewet after DNB (if it occurs) removes a considerable amount of stored energy. DNB is generally a blowdown phenomenon but successive rewets-DNBs can occur.
2-5 Same as 2-4
2-6 Data from Semiscale, CCTF, and SCTF show 3-D effects during refill those are due to radial power distribution, grid spacers, etc., whereas DNB is basically a blowdown phenomenon.
2-7 CCTF and SCIF data show the influence of void distribution on the post-CHF heat transfer, whereas DNB is a blowdown phenomenon.
2-8 DM8 is a blowdown phenomenon, whereas entrainment and deentrainment have the propensity to cool per regions of the core during refill.
2-9 During refill, Semiscale data show there are no core flow re-reversals, so If the rods have DNB, the PCT is not strongly influenced by the small core flow and the heatup is close to adiabatic. LOFT data show under certain conditions that re-reversal of core flow due to pump control can cause quenches to occur.
2-10 DNB is basically a blowdown phenomenon. During periods of the refill, the core can be exposed to stagnant vapor and the basic heat transfer mechanism is natural convection.
3-4 Rewets airing refill depend heavily on pump control and core flow direction. Rewet may or may not occur. If they do, they are then considered part of the post-CHF regime, which in general has en effect on PCT.
3-5 More than half of the stored energy has been removed from the fuel rod. Nucleate boiling during the refill will remove considerable amo4.rlts of stored energy, but the rods may not get back Into nucleate bolting--hence the larger range and generally Larger importance of post-CHF in general.
3-6 Multi-dimensional effects are present, but core averages can be used in the post-CHF regime to get acceptable Interpretation of the cladding temperature response. CCTF data does not show substantial radial void gradients.
3-7 Post-CHF regimes depend on the void generation and axial void profile; thus, these two elements are coupled strongly.
3-8 Post CHF ranks higher because there is little opportunity for entrainment/deentrainment during refill, as the core sees mostly a high void fraction, two-phase mixture end can likely have superheated steam.
3-9 Post CHF ranks higher because the core flow is very small or near zero anyway.
3-10 Single phase natural convection may be part of the post-CHF regime during refill. If the core flow gets very low, natural circulation may be a dominant heat transfer mode.
4-5 Rewet during refill depends heavily on pump control. If rewet occurs, it is considered part of post-CHF heat transfer and nucleate boiling is considered part of blowdown heat transfer.

4-6 Rewet has significant effect but 3-D effects are not significant during blowdown.
4-7 These elements were judged to have an equivalent effect since void generation affects both production and the ability to rewet, and rewet has strong effect on PCT
4-8 Fall back from the upper plenum is possible if storage occurs there; however, rewet is considered to be of high-importance.
4-9 variation in reverse core flow can effect time to DNB in low power regions of the core, but early rewet is more important.
4-10 Rewet, if it occurs, can have a pronounced effect on the cladding temperature. The range is large because natural circulation to steam can be a dominant heat transfer regime if the core contains superheated steam.
5-6 During refill, large scale tests (CCTF) do not show strong multi-dimensional effects. Rewets, If they occur will have larger impact on cladding temperature than multi-dimensional fluid behaviors.
5-7 Same as No. 5-6 and based on CCTF data.
5-8 Rewet ranks higher since there is very Little fluid (high void fraction) in the core during refill.
5-9 In LOFT1 pump effects induced some rewetting near the core inlet. This had a far more pronounced effect on cladding temperature than core stagnation since the flow was near stagnation anyhow.
5-10 Rewet, if it occurs, can have a pronounced effect on the cladding temperature. The range is large because natural circulation to steam can be a dominant heat transfer regime if the core contains superheated steam.
6-7 Void fraction axial distribution will dominate the rod heat transfer, and three-dimensional effects are minimal.
6-8 Neither of these effects has shown to be dominant, although fall back from the upper head draining can influence the top of the core.
6-9 Flow reversal has not been observed in experimental date. The core is nearly stagnant. Three-dimensional effects are not dominant per CCTF data, but are of more significance than flow reversal.
6-10 Because of the pressure of superheat in the Semiscale experiments and results of CCTF experiments, natural circulation to steam is more important.
7-8 Post CHF heat transfer is dependent on void fraction, and the core is steam filled or has a high void fraction fluid during refill. Upper head draining can influence the void fraction in the upper core.
7-9 Semiscale data show the core is steam filled and can produce superheated steam. Natural circulation is thus more significant than flow stagnation, reversal.
7-10 Both natural circulation and axial void distribution can influence heat transfer during refill. They are ranked equal since data shows that either or both can be prevalent during refill.
8-9 As above, flow stagnation results in CHF conditions, whereas the only entrainment in the core during blowdown is at the quench front (if a rewet occurs) and probably contributes little in the form of pre-cursory cooling.
8-10 The core contains mostly superheated vapor, or at least, very high void fluid based on Semiscale results. If there are any entrained droplets, the rods do not see much of them because the cladding temperature is high.
9-10 Semiscale Mod-i data show the core is steam filled and can produce superheated steam. Natural circulation Is thus more significant than flow reversal, stagnation.

Table A-13: Upper Plenum

Upper plenum	Entrainment/deentrainment	Countercurrent flow (drain/fallback)	Two-phase Convection	Phase Separation
Entrainment/deentrainment	1.000	0.333	5.000	3.000
Countercurrent flow (drain/fallback)	3.000	1.000	3.000	3.000
Two-phase Convection	0.200	0.333	1.000	1.000
Phase Separation	0.333	0.333	1.000	1.000

2-3	Upper head drain/fall back is shown In Semiscale Mod-3 data to have the effect of turning over the cladding temperatures in the upper part of the core.
2-4	Some deentrainment of No. 20 mixture caused by steam mixing with upper head fluid drain could occur. Since all the structures are hot air and the two-phase mixture Is at saturation, these could be structural/fluid heat transfer but not dominant.
2-5	Deentrainment of upper head fall back/drain fluid is possible. Phase separation should not dominate because mostly steam is coming out of the core.
3-4	Semiscale data shows effect of fall back on cladding temperature. Fall back causes turnover in the blowdown peak.
3-5	Since mostly steam is coming from the core, there is very little phase separation, and fall back from upper head draining will be more influential.
4-5	Do not know of any data that shows dominance of one over the other. Neither felt to be dominant for refill.

Table A-13: Hot Leg

Hot leg-Refill	Ent/Deent	Flow Reversal, Stagnation	Void Distribution, Void Generation	Two-Phase Convection
Ent/Deent	1.000	1.000	1.000	1.000
Flow Reversal, Stagnation	1.000	1.000	0.333	0.333
Void Distribution, Void Generation	1.000	3.000	1.000	0.333
Two-Phase Convection	1.000	3.000	3.000	1.000

2-3	Neither phenomenon is felt to be dominant during refill. Hot Leg flow Is generally positive during this time period.
2-4	Neither phenomenon is felt to be dominant during refill. Hot Leg flow Is generally positive during this time period.
2-5	Neither phenomenon is felt to be dominant during refill. Hot Leg flow Is generally positive during this time period.

3-4 Hot leg flow is generally positive during refill. The flow regime and void generation could contribute to steam voiding Later in the transient.
3-5 Convection ii slightly more important since any liquid trapped in the hot Leg could be vaporized by wall heat transfer.
4-5 Wall heat transfer may contribute to void generation.

Table A-14: Steam Generator

Steam Generator	Delta-P, Form loss	Steam Binding
Delta-P, Form loss	1.000	1.000
Steam Binding	1.000	1.000

2-3 Mostly vapor is flowing in the steam generator(s) during refill. There is not a large contribution of steam binding.

Table A-15: Pump

Pump	Two-phase	Delta-P, Form loss
Two-phase	1.000	2.000
Delta-P, Form loss	0.200	1.000

2-3 The Loop pump will be in a coastdown mode for the majority of the refill period arid the degradation characteristics wilt influence the core flow and cladding temperatures.

Table A-16: Cold leg, Accumulator

Cold leg, Accumulator-Refill	Condensation, Oscillation	Noncondensible gas	HPI mixing
Condensation, Oscillation	1.000	7.000	7.000
Noncondensible gas	0.143	1.000	0.111
HPI mixing	0.143	9.000	1.000

2-3 Noncondensible gas generally wilt discharge from the accumulator after refill. Condensation effects were shown in Semiscale to have a significant effect on ECC penetration.
2-4 HPI is a small flow compared to accumulator flow. Accumulator Liquid thus has a much larger condensation effect.
3-4 Noncondensible gas will come out of the accumulator late in refill. There could be some effects due to HPI mixing/condensation, although it is overshadowed by accumulator injection.

Table A-17: Break

Break	Critical Flow	Flashing	Containment Pressure
Critical Flow	1.000	3.000	3.000
Flashing	0.333	1.000	0.333
Containment Pressure	0.333	3.000	1.000

2-3 During refill, integral systems tests show that a saturated two-phase mixture is discharged at the break. Thus, the upstream break conditions determine the mass discharge rate and flooding at the throat is not a dominant effect, since there are no rapid pressure changes.
2-4 Integral systems tests show that system pressure remains above the containment pressure until late in the refill. Therefore, critical flow Is ranked slightly higher since the break will be choked for the majority of refill.
3-4 The break will unchoke late in refill and the containment pressure leaving the system will factor into the determination of the mass rate. By this time, however, mostly steam will be discharging and flashing will not be a dominant effect.

Table A-18: Loop

Loop-Refill	Two phase Delta-P	Oscillation	Flow Split
Two phase Delta-P	1.000	1.000	1.000
Oscillation	1.000	1.000	1.000
Flow Split	1.000	1.000	1.000

2-3 Two phase pressure drop in the Loops determines the rate at which mass can leave the system. Oscillations doe to cold Leg condensation will affect the overall loop pressure drop. They are ranked equal since neither has a dominant impact on refill phase.
2-4 Condensation dynamics create flow splits and plugs in the cold legs that Influence the two-phase pressure drops, but neither are dominant refill mechanisms.

3-4	Condensation dynamics create flow splits and plugs in the cold Legs that influence the two-phase pressure drops, but neither are dominant refill mechanisms.

Table A-19: Downcomer

Downcomer-Refill	Condensation	Ent/Deent	Hot wall	3-D Effect	Countercurrent, Slug, nonequilibrium flow	liquid level Oscillations	Two-phase Convection	Saturated nucleate boiling
Condensation	1.000	3.000	3.000	3.000	1.000	3.000	3.000	5.000
Ent/Deent	0.333	1.000	0.333	1.000	1.000	3.000	3.000	5.000
Hot wall	0.333	3.000	1.000	0.333	1.000	3.000	3.000	1.000
3-D Effect	0.333	1.000	3.000	1.000	1.000	3.000	3.000	5.000
Countercurrent, Slug, nonequilibrium flow	1.000	1.000	1.000	1.000	1.000	5.000	5.000	7.000
liquid level Oscillations	0.333	0.333	0.333	0.333	0.200	1.000	1.000	3.000
Two-phase Convection	0.333	0.333	0.333	0.333	0.200	1.000	1.000	3.000
Saturated nucleate boiling	0.200	0.200	1.000	0.200	0.143	0.333	0.333	1.000

2-3	Condensation of core generated steam in the downcomer inlet annulus drives downcomer steam upflows. This causes flooding and Likely some entrainment of fluid from the lower plenum. Condensation driven flows arc considered a more dominant mechanism.
2-4	Condensation in the upper annulus drives downcomer behavior. Hot wail effects contribute to overall effects and are more influential In small systems. Thus, condensation is ranked higher.
2-5	Three-dimensional effects are very prevalent during refill. Condensation effects in essence cause three-dimensional effects. Condensation Is therefore rated higher.
2-6	These phenomena are closely coupled and are thus rated the same. Condensation causes countercurrent flow, periodic dumping, etc.
2-7	Condensation Is more important since the downcomer Level does not form until refill of the lower plenum is complete late in the refill period.
2-8	Wall heat transfer is very important In small systems in that it contributes to vapor generation. In large systems, this is a lesser effect as demonstrated by LOFT tests.
2-9	Well heat transfer is very important In small systems in that it contributes to vapor generation. In large systems, this is a Lesser effect as demonstrated by LOFT tests.
3-4	In small scale systems, hot wall effects contribute to ECC penetration/delay, inducing entrainment.
3-5	LOFT data show the presence of multi-dimensional effects. ECC Liquid can go down one side of the downcomer and steam entrained Liquid to the other side.
3-6	These two processes are closely coupled, since countercurrent flow will cause entrainment ralrnent, slugging, and perhaps nonequilibrium in the downcomer. Thus, they are rated approximately the same.
3-7	The downcomer liquid level oscillations do not become a dominant factor until reflood starts,

although the inventory is an important consideration during refill. Entrairanent/Deentraiment can influence the Inventory and are Thus rated slightly higher.
3-8 Wall heat transfer is important in small scale systems since steam generated on the walls contributes to downcomer steam flows and can Induce entrainment. In large systems, the entrainment due to wall generated steam is less; therefore, entrainment is rated higher.
3-9 Wall heat transfer is important in small scale systems since steam generated on the walls contributes to downcomer steam flows and can induce entrainment. In large systems, the entrainment due to wall generated steam is less. Therefore, entrainment Is rated higher.
4-5 Multi-dimensional effects are more Important in large systems than is the hot wall effect, as evidenced by LOFT data.
4-6 The hot wall effect can contribute to countercurrent flow and nonequilibrium flows. This is a dominant effect is small systems. They are rated equal because of Interdependence.
4-7 Hot wall is rated higher because there is no significant level formation until late in refill.
4-8 Two-phase convection heat transfer contributes to hot wall effects by potentially superheating steam flowing in the downcomer. However, the hot wall is more influenced by steam generated by boiling on the downcomer walls after the walls have dried out and then wetted again.
4-9 These two effects are closely coupled and thus are ranked equal.
5-6 These effects are closely coupled and are thus ranked equal.
5-7 Three dimensional effects are more important since a level does not form in the downcomer until late in the reflood.
5-$_8$ In Large systemmu1ti-dimensionat flow effects are more influential then wall heat transfer effects.
5-9 In Large system, multi-dimensional flow effects are more Influential than wall heat transfer effects.
6-7 Condensation-driven flows end periodic slugging are dominant effects Influencing ECC penetration. The Level does not form until late in refill.
6-8 Wall heat transfer will contribute to nonequilibrium via the potential for superheating steam in the downcomer. This effect is Less important than condensation-driven countercurrent flow and slugging.
6-9 Nucleate boiling will contribute to net vapor generation in the downcomer. However, condensation dominated processes inducing countercurrent flow and slugging appear to be more important.
7-8 These effects are rated equal because neither is dominant during the majority of refill.
7-9 Late In refill (lower plenum nearly full), a level can build up in the downcomer. If the downcomer walls are hot, boiling and vapor generation can occur, causing the level to oscillate. This can induce core vapor generation and resultant pressure oscillations on the whole system.
8-9 For Large systems, it is unlikely that downcomer wall heat transfer has a dominant effect on refill, and thus they are ranked equally.

Table A-20: Lower Plenum

Lower Plenum	Sweep out	Hot wall	Multidimensional Flow
Sweep out	1.000	1.000	0.333
Hot wall	1.000	1.000	5.000
Multidimensional Flow	3.000	0.200	1.000

2-3 In the Semiscale geometry, level swell due to hot walls end depressurization resulted in sweep out of Lower plenum fluid by reverse core flow driven by ECC condensation. Thus, the voiding is dependent on both hot watt and reverse core flow and they are rated equal.
2-4 Sweep out of lower plenum fluid by reverse core flow is a multi-dimensional process and the sweep out depends on the lower p1 anus length to diameter ratio. Lower plenum depth is considered to be more important than multi-dimensional flows.
3-4 Semiscale tests showed that level swell due to hot wall and depressurization effects caused the tower plenum Level to rise into the downcomer where the velocity was high enough to entrain liquid out of the system. Multi-dimensional flows in the Lower plenum were not noted to be a significant effect.

Reflood phase

Table A-21: Fuel Rod

Fuel Rod-Refill	Stored Energy	Oxidation	Decay Heat	Gap Conductance
Stored Energy	1.000	0.200	0.250	0.250
Oxidation	5.000	1.000	0.500	2.000
Decay Heat	4.000	2.000	1.000	1.000
Gap Conductance	4.000	0.500	1.000	1.000

2-3 By the time reflood starts, part of the stored energy has been removed from the fuel rod and the remainder has caused cladding temperature heatup. Stored energy is therefore no Longer a Large source of energy. If the cladding temperatures get high enough, oxidation can constitute an energy source and has other implications as far as hydrogen generation and cladding degradation.
2-4 Fuel decay heat Is the dominant source of energy generation since most fuel stored energy has been removed or has contributed to fuel cladding heatup.
2-5 Gap conductance is more important because the stored energy has already been removed or has contributed to cladding heat up. The gap heat transfer properties are a factor determining the rate at which energy can be removed from the fuel. If there Is a Low gap conductance it is possible to quench the cladding without quenching the fuel.
3-4 Decay heat is more important because most integral systems test data Indicate that cladding temperature does not get high enough during reflood to cause significant oxidation. FLECHT data show that the temperature rise during initial reflood Is a strong function of the flooding rate and the Linear heat rate at the start of reflood and under some conditions, the peak temperature could be

sufficient to cause oxidation.
3-5 Oxidation is rated more Important because FLECUT data show that, for certain combinations of power and reflood rate, cladding temperatures can get high enough to result in significant oxidation and hence an energy source. Gap conductance may limit the rate at which energy generated is transferred to the surface and will affect the fuel temperature profile. However, during reflood, most of the stored energy has been removed and the gap should have a second order effect.
4-5 Decay heat and gap conductance are fated approximately equal because the gap conductance will limit the rate at which decay heat Is transferred to the cladding

Table A-22: Core

Core-Reflood	Post CHF	DNB	Rewet	Reflood heat transfer plus quench	nucleate boiling	3-D flow	Void dist, void generation	Ent/Deent	Flow Reversal, Stagnation	Radiation heat transfer
Post CHF	1.000	7.000	5.000	0.200	5.000	0.333	0.333	1.000	9.000	3.000
DNB	0.143	1.000	1.000	0.111	0.200	0.143	0.200	0.143	9.000	0.111
Rewet	0.200	1.000	1.000	0.111	0.111	0.111	0.111	0.111	1.000	0.111
Reflood heat transfer plus quench	5.000	9.000	9.000	1.000	9.000	1.000	1.000	3.000	9.000	7.000
nucleate boiling	0.200	5.000	9.000	0.111	1.000	5.000	0.200	0.200	9.000	0.500
3-D flow	3.000	7.000	9.000	1.000	0.200	1.000	1.000	0.200	9.000	2.000
Void dist, void generation	3.000	5.000	9.000	1.000	5.000	1.000	1.000	1.000	9.000	7.000
Ent/Deent	1.000	7.000	9.000	0.333	5.000	5.000	1.000	1.000	9.000	5.000
Flow Reversal, Stagnation	0.111	0.111	1.000	0.111	0.111	0.111	0.111	0.111	1.000	0.333
Radiation heat transfer	0.333	9.000	9.000	0.143	2.000	0.500	0.143	0.200	3.000	1.000

2-3 The post-CHF regime Is the dominant heat transfer regime during reflood whereas DNB is a blowdown phenomenon.
2-4 Rewet is interpreted as a blowdown phenomenon, not to be confused with quench. Post-CHE heat transfer is a dominant heat transfer mode during reflood.
2-5 Reflood heat transfer Is a general description of alt the heat transfer occurring during this time interval; post-CHF heat transfer is a subset. Quench terminates the high cladding temperature period during reflood, and as such is a principal phenomenon during the reflood phase.

2-6 Post-CHF heat transfer provides the energy removal from the cladding prior to quench, and It is during this period that the peak cladding temperature will occur. Therefore, it has a greater significance than nucleate boiling, which occurs after quench, and after the peak cladding temperature has occurred.
2-7 Three dimensional effects occur during reflood because of radial (and axial) power gradients, gravity and inertial forces being the same order of magnitude, and the Length to diameter ratio of the core (approximately unity). All of these effects can promote cross flows that affect the local heat transfer characteristics through entrainment, local quality, etc. CCTF and SCTF data tend to indicate fairly uniform radial void profiles across the core although there are noticeable differences in the quench front profiles due to radial power distribution.
2-8 Void distribution and void generation have a fundamental effect on the heat transfer from the cladding surface. The presence or lack of liquid at any Location In the core will govern the ability to remove energy from the cladding surface and control not only the peak cladding temperature, but also the propagation of the quench front.
2-9 Entrainment/deentrainment phenomena can have a significant effect on post-CHF heat transfer, so the two phenomena are ranked of equal importance. Post-CHF is considered potentially slightly more important because of the possibility that significant entrainment/deentrainment might not occur for a given transient.
2-10 The potential for flow reversal and stagnation during the reflood phase is small, and the effect on post-CMF heat transfer or peak cladding temperature is expected to be small. Flow reversal Is principally a blowdown phenomenon.
2-11 Radiation heat transfer can affect the cladding temperature response through interactions between radiating surfaces such as the fuel rod cladding and other fuel rods or structural surfaces, and between the fuel rod cladding and the steam or entrained droplets. Radiation can also affect the steam superheat through communication between the steam and the entrained liquid. It Is not as big en effect as post-CHF heat transfer, but it is significant.
3-4 DNB and rewet are primarily blowdown phenomena. However, LOFT data for Test L2-3 show that multiple dryout and rewets can occur during reflood due to top-down quenches caused by fallback of water from the upper plenum.
3-5 Reflood heat transfer arid quench are the most important mechanisms during reflood whereas DNB is primarily a blowdown phenomenon.
3-6 Nucleate boiling occurs during the final quench of the fuel cladding while DNB is a blowdown phenomenon.
3-7 Three dimensional effects are present during ref bed because of radial (end axial) power gradients, gravity and Inertial forces being the same order of magnitude, and the Length to diameter ratio of the core (approximately unity). All o these effects can promote cross flows that cause radial variations in the quench front, entrainment, etc. CCTF and SCTF data tend to indicate fairly uniform radial void profiles across the core although there are noticeable differences in the quench front profiles due to radial power distribution.
3-8 The core heat transfer is a direct function of the Local void fraction during reflood.
3-9 Entrainment/deentrainment can result in Increased flooding rates and hence enhance reflood heat transfer and quench front propagation. CCTF and SCTF data show that Entrainment/deentrainment in the core cools the upper bundle region end also decreases steam binding potential in the loops.
3-10 Complete flow reversals do not occur during reflood although manometric oscillations are prevalent.
3-11 Radiation beet transfer in the region above the quench front helps to coot the cladding end also removes superheat from the steam (steam to droplet radiation). FLECHT data reduction techniques account for the radiation component of heat transfer as do most reflood correlations used in analysis techniques.
4-5 Rewet is mainly a blowdown phenomenon and will have little effect during reflood. Therefore, ref

load heat transfer and quench are considered significantly more important.
4-6 Rewet is mainly a blowdown phenomenon and will have little effect during reflood. Therefore, nucleate boiling is considered significantly more important.
4-7 Rewet is mainly a blowdown phenomenon and will have little effect during reflood. Therefore, 3-D flow Is considered significantly more important.
4-8 Rewet is mainly a blowdown phenomenon and will have Little effect during reflood. Therefore, void distribution and void generation are considered significantly more Important.
4-9 Rewet is mainly a blowdown phenomenon end will have little effect during reflood. Therefore, entrainment/deentrainment is considered significantly more important.
4-10 Both of these phenomena are principally blowdown phase phenomena, end neither is expected to have a significant impact on the system response during the reflood phase. Therefore, both are ranked equally.
4-11 Rewet is. mainly a blowdown phenomenon and will have little effect during reflood. Radiation affects PCT, and although it is not the principal phenomenon, it is significantly more Important than rewet.
5-6 Nucleate boiling will occur below the quench front. It is a significant heat transfer mechanism, but It does not impact the peak clad temperature as such as the occurrence of the quench Itself. Therefore, reflood heat transfer and quench is significantly more important.
5-7 3-D flow and reflood heat transfer plus quench are both expected to be significant phenomena during the reflood phase. Because of its more direct Impact on the peak cladding temperature, reflood heat transfer plus is considered somewhat more important, but the rank for both is considered to be nearly equal.
5-8 Heat transfer Is strongly dependent on the Local void fraction. Because of this strong coupling, these two phenomena were ranked equal in importance.
5-9 Reflood heats transfer and quench represents the overall heat transfer during reflood and has a direct impact on the determination of the peak cladding temperature. While entrainment/deentrainment can have a significant impact on the heat transfer, It is not quite so directly related to the PCT. In addition, there is a possibility that it may not affect a given transient, so it is ranked somewhat Lower in importance than reflood heat transfer.
5-10 Flow reversal and stagnation are considered blowdown phase phenomena and are not expected to be significant during reflood. On the other hand, reflood heat transfer and quench are very significant during this time interval
5-11 Reflood heat transfer plus quench is the predominant phenomenon governing the determination of PCT in the core during reflood. Radiation heat transfer has a noticeable, but significantly smaller, effect on the PCT, so It is ranked significantly lower.
6-7 The multidimensional flow patterns can influence the heat transfer in the upper portions of the core during reflood. This can influence the PCT, whereas nucleate boiling occurs below the quench front end has no direct impact on PCT.
6-8 Void generation and distribution above the quench front can have a significant effect on the reflood heat transfer. Voids generated by nucleate boiling below the quench front can impact the reflood heat transfer as well.
6-9 11 Ent/Deent can significantly impact the heat transfer process above the quench front, and can have a significant effect on PCT. Nucleate boiling occurs below the quench front and does not directly impact the PCT.
6-10 Flow reversal and stagnation are principally blowdown phenomena and little impact on reflood.
6-11 Neither nucleate boiling nor radiation heat transfer has major influence on PCT, but radiation heat transfer has been shown to have noticeable effect on the heat transfer in the upper parts of the core during reflood.

7-8 Both of phenomena have a significant impact on the PCT. They are related in that the 3-D flow affects the transport and distribution of voids in the upper portions of the core.
7-9 same as above.
7-10 Flow reversal is essentially blowdown phenomena, and little effect on PCT in reflood phase but 3-D flow having a more effect on PCT.
7-11 Both expected to influence PCT with 3-D having a more effect.
8-9 Both of these phenomena can be significant factors in affecting PCT and judged having same ranks.
8-10 Flow reversal and stagnation is basically Blowdown phenomena having little effect on reflood phase. Void distribution is expected to be a significant factor in determining the heat removal rate from the cladding
8-11 Both affecting PCT but the overall effects of the void distribution are more far reaching than those of radiation
9-10 Flow reversal is essentially blowdown phenomena and little effect on PCT in reflood phase. Ent/Deent is expected to be a significant factor in determining the heat removal rate from the cladding
9-11 Ent/Deent will affect the overall heat transfer in the upper parts of the core by affecting the amount of liquid present to cool the cladding.
10-11 Flow reversal is essentially blowdown phenomena and little effect on PCT in reflood phase. Radiation heat transfer is a small but noticeable affect to the total heat transfer from the cladding under highly voided conditions.

Table A-23: Upper plenum

Upper Plenum	Phase Separation	Ent/Deent	Two phase Convection	Countercurrent Flow (Drain/Fallback)
Phase Separation	1.000	0.200	0.333	0.333
Ent/Deent	5.000	1.000	3.000	1.000
Two phase Convection	3.000	0.333	1.000	1.000
Countercurrent Flow (Drain/Fallback)	3.000	1.000	1.000	1.000

2-3 Entrained liquid from the core can be carried to the upper plenum and de-entrained on the structural members there. This liquid can then form a pool in the upper plenum and provide water to drain back into the upper portions of the core and cool the fuel rods.
2-4 With respect to core inventory, wall heat transfer and phase separation are important but wall generated vapor is expected to have a more pronounced effect on core inventory than phase separation.
2-5 Heat transfer can cause some vapor generation in the upper plenum region that can influence the mass inventory. However the mass inventory is more influenced by Ent/Deent phenomenon.
3-4 Phase separation will occur in the upper plenum as a result of the flow area increase and the Deent. By structural components. This liquid will drain as a rate determined by countercurrent flow conditions at the tie plates. Drain/fallback is therefore rated slightly more important

3-5 These phenomena are closely related and thus are ranked equal.
4-5 These phenomena rated equal because it is difficult to distinguish importance but both are important for the phase.

Table A-24: Hot leg

Hot leg-Reflood	Ent/Deent	Void Distribution, Void generation	Two-phase convection
Ent/Deent	1.000	3.000	3.000
Void Distribution, Void generation	0.333	1.000	2.000
Two-phase convection	0.333	0.500	1.000

2-3 Ent/Deent will influence the void distribution in the hot leg. The hot leg as a sink/source of entrained liquid from the core is more important than the hot leg void profile.
2-4 Wall heat transfer is a second order effect during reflood. Fluid mechanics aspects are more dominant and influence the steam binding.
3-4 Wall heat transfer will influence the void generation distribution. Other elements such as entrainment also influence the void profile.

Table A-25: Steam Generator

Steam Generator	Delta-P, Form loss	Steam Binding
Delta-P, Form loss	1.000	0.200
Steam Binding	5.000	1.000

2-3 The increased volume that must be removed from the system due to vapor generated in the steam generator has a more impact on PCT than the form loss.

Table A-26: Cold leg, Accumulator

Cold leg, Accumulator-Refill	Condensation, Oscillation	Noncondensible gas	HPI mixing
Condensation, Oscillation	1.000	0.500	0.333
Noncondensible gas	2.000	1.000	6.000
HPI mixing	3.000	0.167	1.000

2-3 Noncondensible gas will come out of the accumulator some time during the initial stages of reflood. The gas will pressurize the system and can cause an increase in the reflood rate. This is considered to be more important than oscillations
2-4 HPI is a small flow compared to the accumulator and is expected to be overshadowed by accumulator flow induced condensation.
3-4 Accumulator gas injection can have an effect on system pressure and reflooding rate and can actually initiate reflooding of the core

Table A-27: Downcomer

Downcomer-Reflood	Condensation	Ent/Deent	Hot wall	3-D Effect	Countercurrent, Slug, nonequilibrium flow	liquid level Oscillations	Two-phase Convection	Saturated nucleate boiling
Condensation	1.000	1.000	0.500	1.000	1.000	0.200	1.000	1.000
Ent/Deent	1.000	1.000	0.500	1.000	1.000	0.200	1.000	1.000
Hot wall	2.000	2.000	1.000	2.000	2.000	0.167	2.000	2.000
3-D Effect	1.000	1.000	0.500	1.000	1.000	0.167	1.000	1.000
Countercurrent, Slug, nonequilibrium flow	1.000	1.000	0.500	1.000	1.000	0.200	1.000	1.000
liquid level Oscillations	5.000	5.000	6.000	6.000	5.000	1.000	5.000	5.000
Two-phase Convection	1.000	1.000	0.500	1.000	1.000	0.200	1.000	1.000
Saturated nucleate boiling	1.000	1.000	0.500	1.000	1.000	0.200	1.000	1.000

2-3 By the time reflood starts, most of the stored energy in the walls will be removed so the potential for entrainment should be decreased.
2-4 Condensation effects will be confined mostly to the cold leg, whereas hot wall effects can induce entrainment and downcomer head degradation.
2-5 Three-dimensional effects are more confined to blowdown, and condensation effects should be confined mostly to the cold leg.
2-6 The downcomer is not likely to see significant effects due to any of these processes during reflood. Thus, they are rated equal.
2-7 Level oscillations in the downcomer are partially driven by condensation/evaporation in other parts

of the system. Therefore, level oscillations are ranked higher.
2-8 The downcomer in not likely to see significant effects due to any of these processes during reflood. These are rate equally.
2-9 The downcomer in not likely to see significant effects due to any of these processes during reflood. These are rate equally
3-4 Entrainment will be caused by hot wall effects so the hot wall is rated slightly more important.
3-5 Neither effect should be dominant in the downcomer during reflood and then rated equal.
3-6 Neither effect should be dominant in the downcomer during reflood and then rated equal.
3-7 Level oscillations are predominant during the initial stages of reflood as vapor is generated in the core, pressure buildup in the upper plenum occurs and the core level decreases while the downcomer level increases. Level oscillations then rated more important than entrainment.
3-8 Any entrainment will likely be due to heat transferred at the solid boundary by heat transfer to the two phase mixture in the downcomer. These effects are closely coupled and thus equal.
3-9 The effects are closely coupled and therefore are rated equal.
4-5 there is potential for hot wall effects if there is significant stored energy in the walls during reflood. Hot wall is thus ranked slightly higher than three-dimensional effects since the multi-dimensional behavior is more prevalent during blowdown.
4-6 no significant effects from both but the hot wall effect is ranked slightly higher
4-7 Level oscillations in the downcomer driven by phenomena in other parts of the system are more significant than the hot wall effect for large scale systems.
4-8 Wall heat transfer is the mechanism causing the hot wall effect so it is ranked higher.
4-9 Wall heat transfer is the mechanism causing the hot wall effect so it is ranked higher.
5-6 Level oscillations (i.e., hydraulic effects) dominant the cladding temperature performance and core performance early in the reflood.
5-7 These effects rated equal since neither is dominant during reflood of large systems.
5-8 Level oscillations driven by condensation/evaporation dynamics and the monometer arrangement of the core, lower plenum, and downcomer dominate the effects of wall heat transfer.
5-9 ???
6-7 Level oscillations driven by condensation/evaporation dynamics and the monometer arrangement of the core, lower plenum, and downcomer dominate the effects of wall heat transfer.
6-8 These effects are rated equal since neither is dominant during reflood of large systems.
6-9 These effects are rated equal since neither is dominant during reflood of large systems.
7-8 Level oscillations driven by condensation/evaporation dynamics and the monometer arrangement of the core, lower plenum, and downcomer dominate the effects of wall heat transfer.
7-9 Level oscillations driven by condensation/evaporation dynamics and the monometer arrangement of the core, lower plenum, and downcomer dominate the effects of wall heat transfer.
8-9 Both heat transfer modes will contribute to the hot wall effects.

Table A-28: Lower Plenum

Lower Plenum	Sweep out	Hot wall	Multidimensional Flow
Sweep out	1.000	0.500	1.000

Hot wall	2.000	1.000	0.500
Multidimensional Flow	1.000	2.000	1.000

2-3 During reflood, the lower plenum should be full and, there is little potential for violent sweep out like that occurring during refill. The lower plenum hot wall may have a more significant impact although neither has been shown to be a large effect.
2-4 Neither should be a big effect during reflood since the lower plenum will be full and act primarily as a connection between the core and downcomer.
3-4 Neither should be a big effect during reflood since the lower plenum will be full and act primarily as a connection between the core and downcomer.

Table A-29: Break

Break	Critical Flow	Flashing	Containment Pressure
Critical Flow	1.000	1.000	0.333
Flashing	1.000	1.000	0.200
Containment Pressure	3.000	5.000	1.000

2-3 same ranking since the break is unchoked for the most part during reflood
2-4 Containment pressure is ranked higher because the break is unchoked and the differential pressure is the driving force for the flow out of the system.
3-4 The pressure is low so there is no flashing. The system-containment pressure difference drives the flow out of the system.

Loop

Loop-Refill	Two phase Delta-P	Oscillation	Flow Split
Two phase Delta-P	1.000	0.500	9.000
Oscillation	2.000	1.000	7.000
Flow Split	0.111	0.143	1.000

2-3 Oscillations due to condensation dynamics in the cold leg and core steam generation are more important than loop pressure drop

2-4	Loop pressure drop are more dominant than flow split effects.
3-4	Flow splits are more important during blowdown; oscillations are more dominant during reflood.

APPENDIX B: SENSITIVITY ANALYSIS

The results for sensitivity analysis for identified important parameters are discussed in this section. The results are used for confirmation of modified PIRT results and for quantification of uncertainty ranges/distributions for those parameters. The parameters are perturbed to evaluate the influence of the figure of merit, PCT.

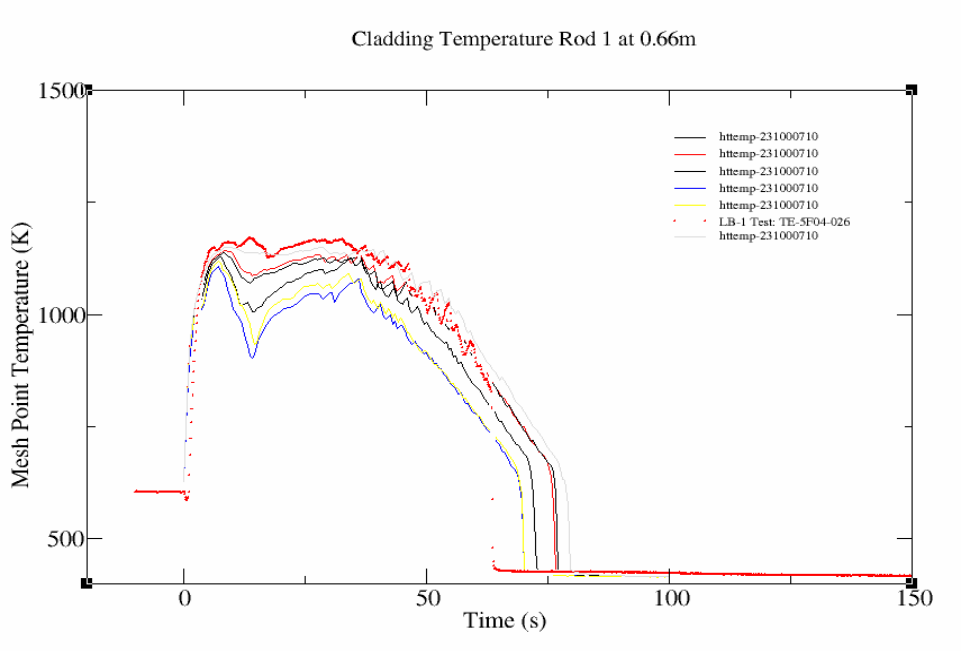

Figure B-1: Cladding Temperature

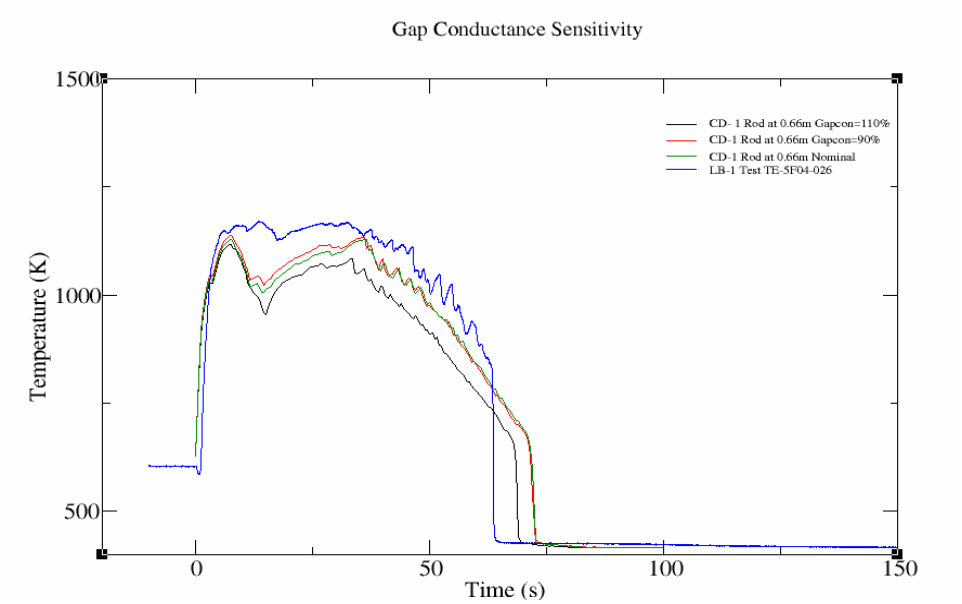

Figure B-2: Gap Conductance Sensitivity

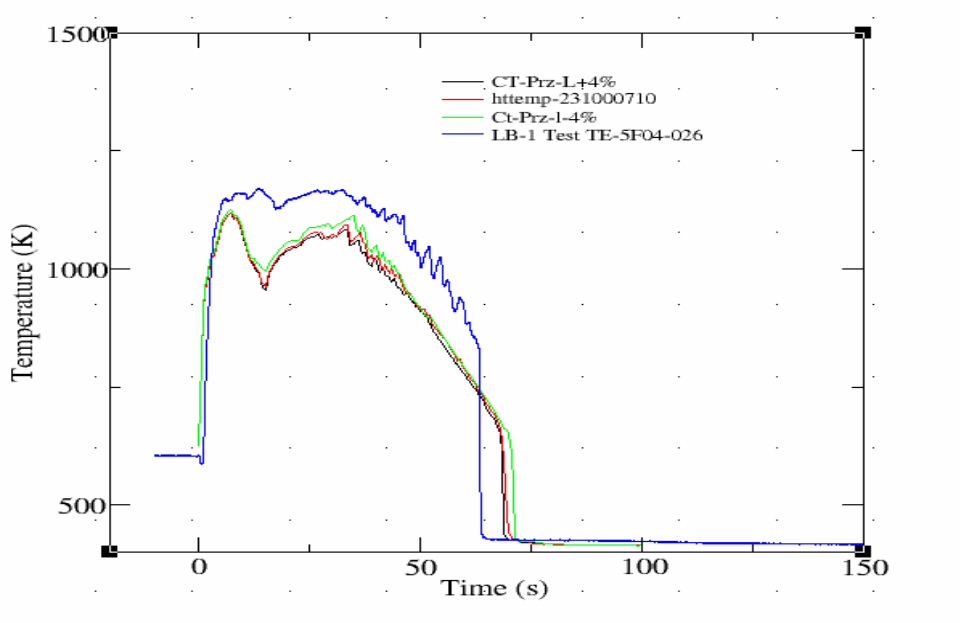

Figure B-3: Pressurizer Level Sensitivity

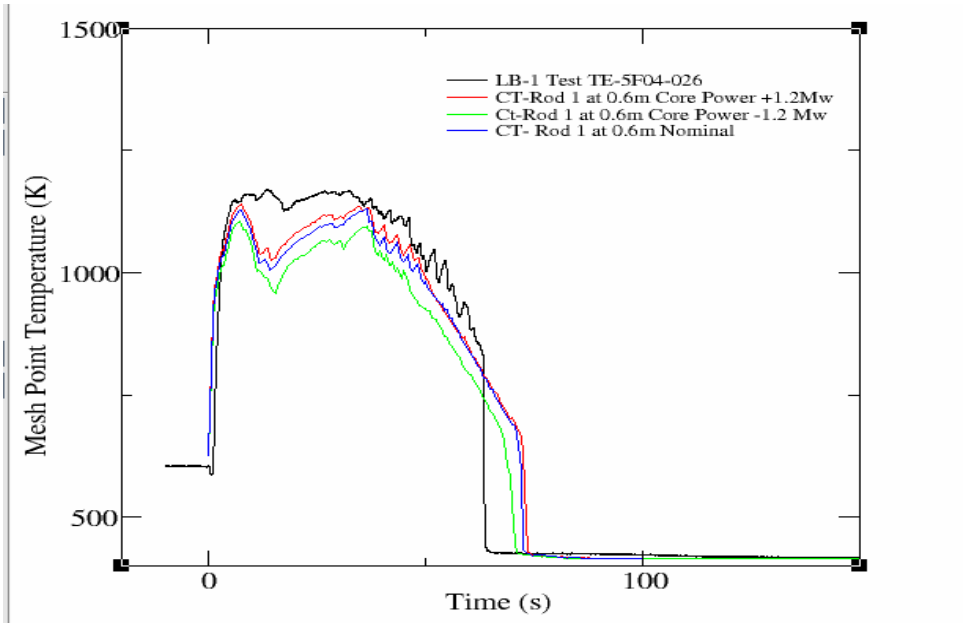

Figure B-4: Core Power Sensitivity

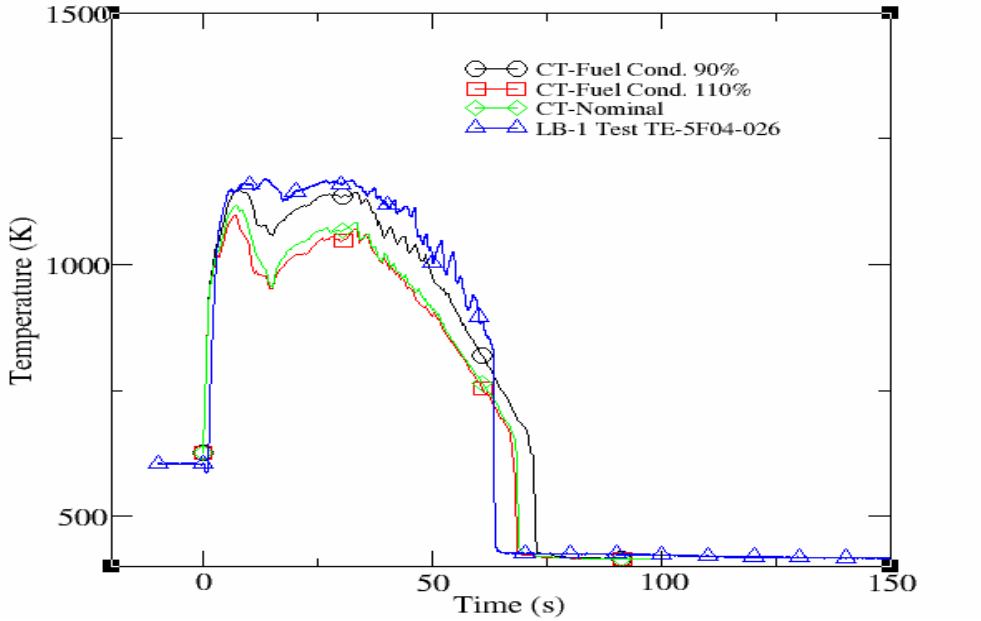

Figure B-5 Fuel Conductivity Sensitivity

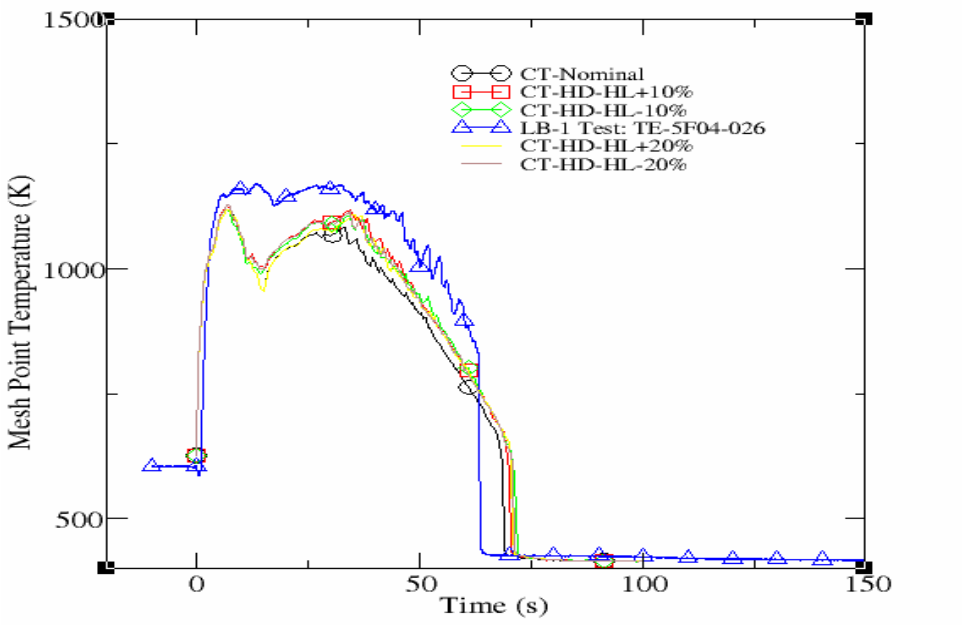

Figure B-6: Entrainment Sensitivity

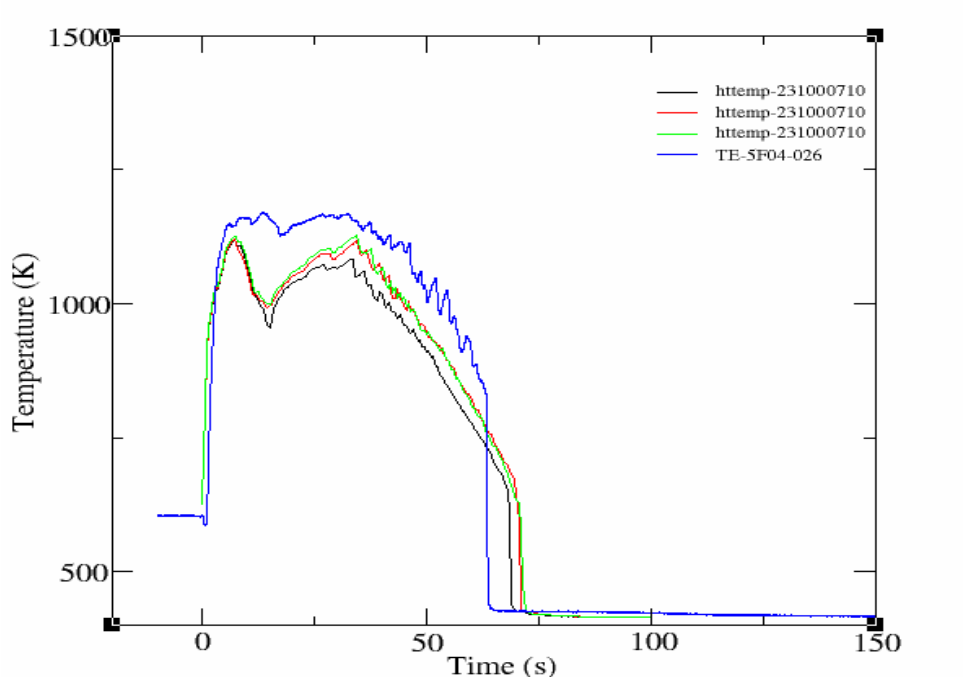

Figure B-7: Core Entrainment Sensitivity

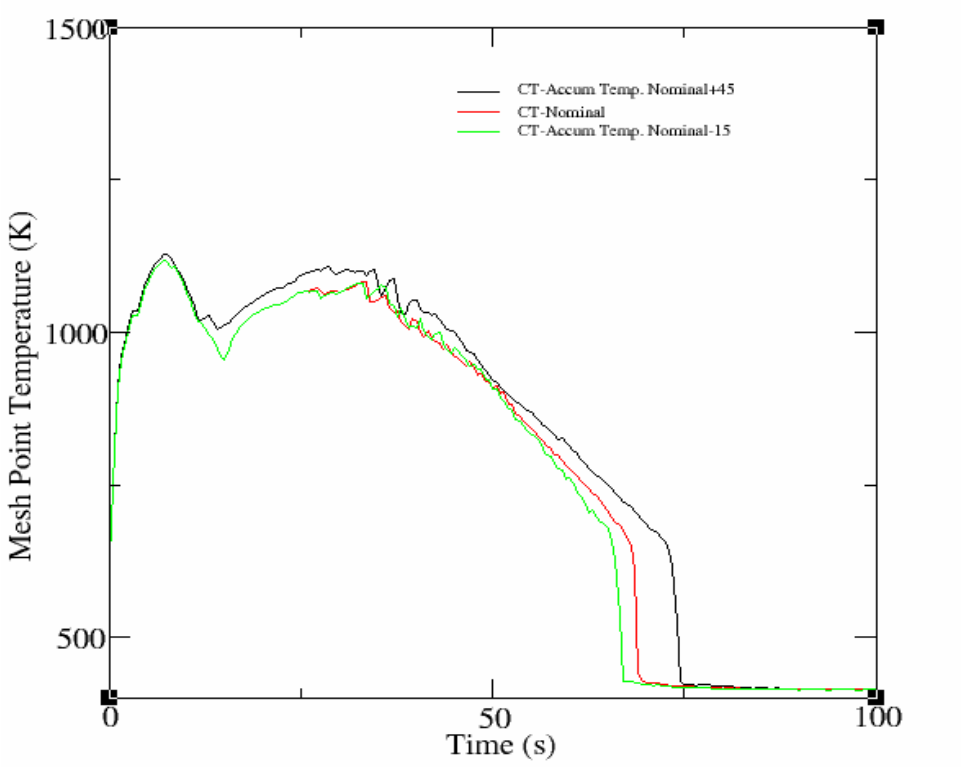

Figure B-8: Accumulator Temperature Sensitivity

APPENDIX C: DESCRIPTION AND PROGRAMMING OF THE SYSTEM SOLVED BY EES

This appendix describes the example solved by EES software. The problem is solving a simple form of energy and momentum equations in a single pipe configuration as shown in Figure c-1.

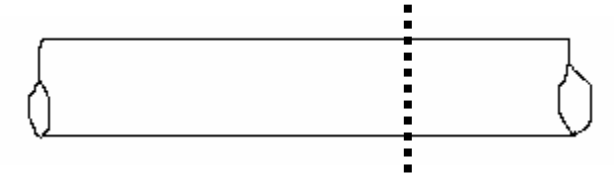

Figure c-1: Configuration of the system solved by EES

$$\text{Energy Equation}: \quad \frac{dP}{dx} \quad \frac{1}{r}\frac{d}{dr}\left(\quad \frac{dv_x}{dr}\right)$$

$$Momentum Equation: \quad .c_p . \; _x . \frac{dT}{dx} \quad \frac{1}{r}\frac{d}{dr}\left(\quad \frac{dT}{dr}\right) \quad \frac{d}{dx}\left(\quad \frac{dT}{dr}\right) \quad _x \frac{dP}{dx}$$

Following are assumptions applied to problem to solve it:

-Single Phase

-Fully Developed

-Steady State

-The program is set up to solve where the heat flux qpdot is constant through the wall, in which case $dT/dx = dT_{mean}/dx$

-It must be modified to solve a problem where the temperature of the wall is constant, in which case $dT/dx = (T_{wall} - T)/(T_{wall} - T_{mean})*dT_{mean}/dx$.

-The wall boundary condition for momentum is the no-slip velocity condition.

-Constant Pressure drop along pipe length

Following is the coding for solving the problem and results were plotted in figure 6.

The question comes with quantification of uncertainty with state of art knowledge

about all input parameters:

```
dely = 0.01 {m}
qpwall = 1000 {W/m^2}
Pres = 100000 {Pa}
MW = 28.96 {kg/kgmol}
Twall1 = 800 {K}
mdot = 0.2 {kg/s*m}
{dP/dx = -100 {Pa/m} }
{Set number of cells for discretization.}
     ncells = 40
 C Determine location of cell boundaries in radial direction, rb
     and determine location of cell centers in radial direction, rc.
               Also set up differences between cell centers for derivatives, drc}
Nodalization:
yb[0] = 0
yc[0] = yb[0]
DUPLICATE n=1,ncells
yb[n]=dely*(1- (ncells-n)/ncells)
yc[n]=0.5*(yb[n]+yb[n-1])
dyc[n] = yc[n] - yc[n-1]
END
C   Set conditions for cell at centerline and zero gradient at centerline of tube.
mu = viscosity(AIR,T=T[0])
lambda = conductivity(AIR,T=T[0])
rho = Pres*MW/(8314.5*T[0])
vx[0] = 0
T[0] = Twall1
mom[1] = rho*vx[1]*(yb[1] - yb[0])
qpwall = -lambda*(T[1] - T[0])/dyc[1]
DUPLICATE n=1,ncells-2
vx[n+1] = vx[n] + dyc[n+1]/mu *((vx[n] - vx[n-1])*mu/dyc[n] +
0.5*(dyc[n+1]+dyc[n])*dPdx)
mom[n+1] = rho*vx[n+1]*(yb[n+1] - yb[n])
T[n+1] = T[n] + dyc[n+1]/lambda *((T[n] - T[n-1])*lambda/dyc[n] +
0.5*(dyc[n+1]+dyc[n])*(vx[n]*dPdx))
END
C {Calculate boundary conditions at wall. Set Twall to a constant for current problem
since location along tube is not specified}
```

```
vx[ncells] = vx[ncells-1] + dyc[ncells]/mu *((vx[ncells-1] - vx[ncells-
2])*mu/dyc[ncells-1] + 0.5*(dyc[ncells]+dyc[ncells-1])*dPdx)
mom[ncells] = rho*vx[ncells]*(yb[ncells] - yb[ncells-1])
T[ncells] = T[ncells-1] - dyc[ncells]*qpwall/lambda
vx[ncells] = 0
C {Calculate mass flow and mean velocity in flow and heat transfer through walls.}
mdot = sum(mom[i],i=1,ncells)
vxmean = mdot/sum(rho*(yb[i]-yb[i-1]),i=1,ncells)
```

APPENDIX D: MEASURABLES AND QUANTITIES ABBREVIATION

Following are the measurable variables and the abbreviation used in LOFT calculation. These tables help on extracting data from LOFT test data and RELAP5 calculation.

Table D-1: Measurable Parameters in LOFT Test Facility

Abbreviation	Parameter
CV	Valve Position
DE	Fluid Density
FE	Fluid Velocity -Local Velocity -Average Velocity
FR	Mass Flow Rate -Average Mass Flow Rate
FT	Volumetric Flow
LD	Liquid Level
ME	Local Momentum
NE	Local Heat Generation Rate
PCP-F	Frequency for Primary Coolant Pump
PCP-P	Electrical Power for Primary Coolant Pump
PDE/PDT	Differential Pressure
PT /PE	Absolute Pressure
RE	Average Power
RPE	Pump Speed
RPT	Control Rod Position
SC	Fluid Subcooling Temperature
SP	Saturation Pressure
ST	Saturation Temperature
TC	Fuel Centerline Temperature
TE/TT	Coolant Temperature

Table D-2: Relap5 Code Abbreviation

acqtank	Accum Energy Trans to Gas (W)
acrhon	Accumulator NC Density (Kg/m^3)
acttank	Accumulator Wall Temp (K)
acvdm	Accumulator Gas Volume (m^3)
acvlig	Accumulator Liquid Volume (m^3)
Boron	Boron Density
count	Advancement Count
cputime	CPU Time (s)
Dt/dtcrnt	Time Step (s)
emass	Error Mass (kg) ?
floreg	Flow Regime
Htchf/htchfr	Critical Heat Flux (w/m^2)
hthtc	Heat Transfer Coefficient (W/m^2*^oK)
htrnr	Heat Flux (W/m^2)
httemp	Mesh Point Temperature (K)
htvat	Heat Structure Temperature (K)
mflowj	Flow rate (Kg/s)
p	Pressure (Pa)
pmphead	Pump Head (Pa)
pmptrq	Pump Torque (N*m)
pmpvel	Pump Velocity (m/s)
q	Volume Heat Source (W)
Quala/qualaj	Volume NC Mass Fraction
quale	Volume Equilibrium Quality
quals	Volume Static Quality
qwg	Volume Heat Source
Rho/ rhof/rhofj/rhog/rhogj	Density (Kg/m^3)
sattemp	Saturation Temperature (K)
sounde	Sonic Velocity (m/s)
tempf	Volume Liquid Temperature (K)
tempg	Volume Gas Temperature (K)
time	Time (s)
tmass	Mass (Kg)
uf/ufj	Liquid Internal Energy (J/Kg)
Ug/ugj	Gas Internal Energy (J/Kg)
vapgen	Vapor Generation Rate (Kg/m^3s)
Velf/velfj	Liquid Velocity (m/s)
Velg/velgj	Gas Velocity (m/s)
vlvarea	Valve Area ratio
vlvstem	Valve Stem ratio

voidf/voidfj	Liquid Void Fraction
chockef	

APPENDIX E: SAMPLING PROCESS FOR UNCERTAIN PARAMEETRS

Following are the description for the distribution of uncertain parameter. Details are discussed in Chapter 7. Shape of distribution and its parameters are given below. Second part is the samples of those parameter used for preparation of propagation inputdeck. Total of 300 samples are derived but only 186 samples are used for propagation (two set of 93 propagation runs). Pairwise dependency between parameters is considered in deriving the samples if such dependency is assigned.

DATUM: 2006/9/07

TIME: 21:26

TYPE OF DESIGN: SIMPLE RANDOM

NUMBER OF PARAMETERS = 14

NUMBER OF FULLY DEPENDENT PARAMETERS = 0

NUMBER OF FREE PARAMETERS = 14

SAMPLE SIZE = 300

INITIAL DSEED = 234567.0

==========

DISTRIBUTIONS OF THE PARAMETERS

==========

PARAMETER NO. 1 : U N I F O R M DISTRIBUTION

BETWEEN 4.8000E+01 AND 5.0600E+01

PARAMETER NO. 2 : U N I F O R M DISTRIBUTION

BETWEEN 1.0000E+00 AND 1.0800E+00

PARAMETER NO. 3 : U N I F O R M DISTRIBUTION

BETWEEN 9.0000E-01 AND 1.1200E+00

PARAMETER NO. 4 : T R I A N G U L A R DISTRIBUTION

BETWEEN 4.0500E+00 AND 4.4000E+00

WITH PEAK AT 4.2200E+00

PARAMETER NO. 5 : U N I F O R M DISTRIBUTION

BETWEEN 5.5000E+02 AND 5.6000E+02

PARAMETER NO. 6 : T R I A N G U L A R DISTRIBUTION

BETWEEN 3.0560E+02 AND 3.1000E+02

WITH PEAK AT 3.0800E+02

PARAMETER NO. 7 : N O R M A L DISTRIBUTION

WITH MY= 1.4950E+01, SIGMA= 2.0000E-01

TRUNCATED AT ITS

1.06E+01 %- AND 9.60E+01 %-QUANTILES

PARAMETER NO. 8 : U N I F O R M DISTRIBUTION

BETWEEN 7.0000E-01 AND 1.3000E+00

PARAMETER NO. 9 : T R I A N G U L A R DISTRIBUTION

BETWEEN 8.0000E-01 AND 1.2000E+00

WITH PEAK AT 1.0000E+00

PARAMETER NO. 10 : T R I A N G U L A R DISTRIBUTION

BETWEEN 8.0000E-01 AND 1.2000E+00

WITH PEAK AT 1.0000E+00

PARAMETER NO. 11 : U N I F O R M DISTRIBUTION

BETWEEN 9.0000E-01 AND 1.2000E+00

PARAMETER NO. 12 : U N I F O R M DISTRIBUTION

BETWEEN 1.4700E+01 AND 1.5050E+01

PARAMETER NO. 13 : T R I A N G U L A R DISTRIBUTION

BETWEEN 7.5000E-01 AND 1.5000E+00

WITH PEAK AT 1.0000E+00

PARAMETER NO. 14 : U N I F O R M DISTRIBUTION

BETWEEN 9.0000E-01 AND 1.1000E+00

==========

REQUIRED SAMPLE RANK CORRELATIONS BETWEEN FREE PARAMETERS

==========

PAR.1	PAR.2	SAMPLE RANK CORRELATION
2	7	-1.0000E-01
3	5	3.0000E-01

Table E-1: Samples from selected sources of uncertainty

	1	2	3	4	5	6	7	8	9	10	11	12	13	14
1	5.02E+01	1.03E+00	9.10E-01	4.16E+00	5.55E+02	3.08E+02	1.48E+01	8.67E-01	1.02E+00	8.47E-01	1.17E+00	1.50E+01	8.88E-01	9.71E-01
2	4.89E+01	1.02E+00	1.01E+00	4.27E+00	5.57E+02	3.10E+02	1.50E+01	7.97E-01	9.89E-01	1.05E+00	1.14E+00	1.48E+01	1.32E+00	1.05E+00
3	4.99E+01	1.01E+00	9.48E-01	4.23E+00	5.57E+02	3.08E+02	1.50E+01	1.24E+00	9.29E-01	1.13E+00	1.09E+00	1.48E+01	9.01E-01	1.08E+00
4	4.87E+01	1.03E+00	1.07E+00	4.26E+00	5.58E+02	3.07E+02	1.51E+01	1.13E+00	9.66E-01	9.09E-01	9.11E-01	1.47E+01	1.17E+00	9.25E-01
5	5.04E+01	1.04E+00	9.39E-01	4.21E+00	5.56E+02	3.08E+02	1.47E+01	1.06E+00	1.06E+00	1.02E+00	1.10E+00	1.50E+01	9.93E-01	9.14E-01
6	4.89E+01	1.01E+00	9.56E-01	4.21E+00	5.52E+02	3.08E+02	1.52E+01	7.24E-01	8.91E-01	1.01E+00	1.10E+00	1.49E+01	7.87E-01	1.07E+00
7	4.83E+01	1.01E+00	1.12E+00	4.26E+00	5.60E+02	3.09E+02	1.52E+01	1.29E+00	1.01E+00	9.16E-01	1.12E+00	1.48E+01	1.08E+00	1.04E+00
8	5.05E+01	1.07E+00	1.07E+00	4.37E+00	5.56E+02	3.09E+02	1.50E+01	8.36E-01	1.10E+00	9.79E-01	9.72E-01	1.50E+01	9.48E-01	1.03E+00
9	4.82E+01	1.05E+00	9.13E-01	4.26E+00	5.51E+02	3.08E+02	1.49E+01	1.28E+00	9.62E-01	9.53E-01	1.08E+00	1.49E+01	9.77E-01	9.43E-01
10	5.00E+01	1.01E+00	9.41E-01	4.19E+00	5.56E+02	3.08E+02	1.50E+01	9.03E-01	9.91E-01	1.01E+00	1.12E+00	1.48E+01	1.11E+00	9.20E-01
11	4.80E+01	1.03E+00	1.02E+00	4.21E+00	5.60E+02	3.07E+02	1.49E+01	1.12E+00	1.00E+00	9.82E-01	9.74E-01	1.48E+01	1.14E+00	1.01E+00
12	4.91E+01	1.06E+00	1.01E+00	4.25E+00	5.58E+02	3.08E+02	1.50E+01	7.89E-01	9.35E-01	1.07E+00	1.18E+00	1.50E+01	9.40E-01	9.75E-01
13	4.83E+01	1.07E+00	1.02E+00	4.30E+00	5.59E+02	3.08E+02	1.48E+01	9.63E-01	1.10E+00	9.30E-01	1.15E+00	1.48E+01	1.31E+00	1.04E+00
14	4.98E+01	1.00E+00	1.04E+00	4.16E+00	5.60E+02	3.07E+02	1.49E+01	9.30E-01	1.03E+00	1.01E+00	1.06E+00	1.50E+01	1.38E+00	9.92E-01
15	4.91E+01	1.05E+00	9.87E-01	4.28E+00	5.51E+02	3.08E+02	1.51E+01	8.08E-01	1.05E+00	8.69E-01	9.95E-01	1.48E+01	9.59E-01	9.62E-01
16	4.98E+01	1.03E+00	1.02E+00	4.28E+00	5.56E+02	3.06E+02	1.50E+01	1.24E+00	8.76E-01	9.97E-01	1.10E+00	1.49E+01	9.49E-01	9.77E-01
17	4.89E+01	1.07E+00	1.01E+00	4.16E+00	5.59E+02	3.06E+02	1.50E+01	7.30E-01	9.53E-01	9.95E-01	1.11E+00	1.50E+01	1.17E+00	9.65E-01
18	4.91E+01	1.01E+00	1.07E+00	4.13E+00	5.57E+02	3.08E+02	1.48E+01	9.80E-01	1.08E+00	1.01E+00	1.12E+00	1.49E+01	1.08E+00	9.53E-01
19	5.02E+01	1.06E+00	1.01E+00	4.16E+00	5.56E+02	3.07E+02	1.50E+01	9.95E-01	9.82E-01	1.00E+00	9.11E-01	1.50E+01	1.02E+00	1.06E+00
20	4.97E+01	1.00E+00	9.39E-01	4.14E+00	5.52E+02	3.09E+02	1.51E+01	1.27E+00	8.87E-01	9.21E-01	9.27E-01	1.50E+01	8.99E-01	1.00E+00
21	4.90E+01	1.03E+00	1.02E+00	4.26E+00	5.51E+02	3.08E+02	1.51E+01	9.07E-01	8.85E-01	9.57E-01	1.12E+00	1.49E+01	1.02E+00	9.43E-01
22	4.97E+01	1.06E+00	1.01E+00	4.28E+00	5.53E+02	3.08E+02	1.50E+01	1.25E+00	9.89E-01	1.07E+00	9.34E-01	1.50E+01	1.09E+00	1.06E+00
23	4.82E+01	1.07E+00	1.11E+00	4.13E+00	5.55E+02	3.08E+02	1.51E+01	8.01E-01	1.02E+00	1.03E+00	1.00E+00	1.49E+01	9.46E-01	9.64E-01
24	4.86E+01	1.07E+00	1.01E+00	4.34E+00	5.51E+02	3.07E+02	1.48E+01	1.09E+00	1.12E+00	1.13E+00	1.19E+00	1.47E+01	1.07E+00	9.89E-01
25	5.04E+01	1.07E+00	9.58E-01	4.29E+00	5.53E+02	3.09E+02	1.49E+01	9.13E-01	9.70E-01	1.08E+00	1.02E+00	1.48E+01	1.04E+00	1.01E+00
26	4.86E+01	1.01E+00	1.06E+00	4.12E+00	5.60E+02	3.08E+02	1.53E+01	8.81E-01	9.62E-01	9.87E-01	9.20E-01	1.50E+01	1.08E+00	1.04E+00
27	4.96E+01	1.06E+00	1.05E+00	4.19E+00	5.55E+02	3.08E+02	1.47E+01	8.93E-01	8.25E-01	8.77E-01	1.02E+00	1.47E+01	1.17E+00	1.08E+00
28	5.00E+01	1.03E+00	1.10E+00	4.20E+00	5.54E+02	3.07E+02	1.52E+01	1.21E+00	1.07E+00	1.13E+00	1.03E+00	1.49E+01	8.42E-01	9.87E-01
29	4.82E+01	1.05E+00	1.08E+00	4.30E+00	5.58E+02	3.09E+02	1.48E+01	1.06E+00	1.05E+00	1.18E+00	9.41E-01	1.47E+01	8.95E-01	1.01E+00
30	5.00E+01	1.06E+00	1.07E+00	4.20E+00	5.57E+02	3.08E+02	1.47E+01	1.29E+00	9.97E-01	1.02E+00	1.08E+00	1.50E+01	8.80E-01	1.04E+00
31	4.98E+01	1.01E+00	9.16E-01	4.15E+00	5.56E+02	3.07E+02	1.50E+01	9.12E-01	1.03E+00	8.89E-01	1.10E+00	1.49E+01	1.28E+00	9.41E-01
32	4.94E+01	1.06E+00	1.02E+00	4.29E+00	5.59E+02	3.07E+02	1.48E+01	8.85E-01	1.11E+00	1.00E+00	1.09E+00	1.48E+01	9.07E-01	9.48E-01
33	5.00E+01	1.04E+00	1.03E+00	4.26E+00	5.52E+02	3.08E+02	1.51E+01	1.28E+00	9.90E-01	9.42E-01	9.18E-01	1.47E+01	9.84E-01	9.13E-01
34	5.02E+01	1.06E+00	9.79E-01	4.20E+00	5.55E+02	3.07E+02	1.51E+01	9.27E-01	1.02E+00	9.17E-01	9.07E-01	1.49E+01	1.40E+00	9.86E-01
35	4.88E+01	1.06E+00	9.82E-01	4.21E+00	5.52E+02	3.09E+02	1.49E+01	8.06E-01	9.90E-01	1.02E+00	1.13E+00	1.48E+01	1.24E+00	1.05E+00
36	4.81E+01	1.06E+00	9.88E-01	4.17E+00	5.53E+02	3.08E+02	1.50E+01	1.26E+00	1.10E+00	1.02E+00	1.05E+00	1.49E+01	1.34E+00	9.81E-01
37	5.05E+01	1.01E+00	9.57E-01	4.36E+00	5.54E+02	3.09E+02	1.53E+01	1.19E+00	1.07E+00	1.11E+00	9.12E-01	1.47E+01	9.55E-01	9.45E-01
38	5.00E+01	1.07E+00	9.94E-01	4.18E+00	5.56E+02	3.08E+02	1.47E+01	8.45E-01	1.05E+00	1.03E+00	1.02E+00	1.49E+01	1.00E+00	1.08E+00
39	5.02E+01	1.04E+00	9.54E-01	4.25E+00	5.52E+02	3.09E+02	1.50E+01	7.77E-01	8.48E-01	1.09E+00	1.20E+00	1.49E+01	1.17E+00	1.04E+00
40	4.92E+01	1.05E+00	9.59E-01	4.21E+00	5.52E+02	3.09E+02	1.50E+01	1.18E+00	9.78E-01	1.10E+00	1.20E+00	1.50E+01	1.17E+00	9.81E-01
41	4.84E+01	1.04E+00	1.07E+00	4.25E+00	5.54E+02	3.06E+02	1.48E+01	1.25E+00	9.05E-01	8.88E-01	1.14E+00	1.49E+01	1.12E+00	9.65E-01
42	4.86E+01	1.01E+00	1.10E+00	4.22E+00	5.60E+02	3.08E+02	1.51E+01	7.55E-01	1.06E+00	1.15E+00	1.08E+00	1.48E+01	1.00E+00	1.08E+00
43	4.90E+01	1.07E+00	9.55E-01	4.11E+00	5.52E+02	3.06E+02	1.52E+01	9.02E-01	1.02E+00	9.61E-01	1.08E+00	1.50E+01	1.05E+00	1.10E+00
44	4.97E+01	1.01E+00	9.23E-01	4.21E+00	5.58E+02	3.09E+02	1.51E+01	1.11E+00	1.00E+00	9.99E-01	9.15E-01	1.49E+01	9.36E-01	9.37E-01
45	4.95E+01	1.01E+00	1.07E+00	4.30E+00	5.53E+02	3.09E+02	1.50E+01	8.55E-01	1.01E+00	1.00E+00	1.11E+00	1.47E+01	8.44E-01	9.56E-01
46	5.02E+01	1.07E+00	1.09E+00	4.29E+00	5.59E+02	3.06E+02	1.49E+01	7.79E-01	9.43E-01	9.99E-01	1.11E+00	1.47E+01	1.32E+00	9.78E-01
47	4.92E+01	1.04E+00	9.38E-01	4.22E+00	5.58E+02	3.08E+02	1.51E+01	1.27E+00	1.08E+00	9.83E-01	1.17E+00	1.49E+01	8.93E-01	1.00E+00
48	4.94E+01	1.07E+00	1.03E+00	4.16E+00	5.59E+02	3.08E+02	1.47E+01	7.48E-01	9.67E-01	8.47E-01	1.05E+00	1.47E+01	1.25E+00	9.39E-01
49	4.89E+01	1.08E+00	9.18E-01	4.20E+00	5.54E+02	3.08E+02	1.49E+01	1.14E+00	1.09E+00	9.91E-01	1.02E+00	1.49E+01	1.27E+00	9.41E-01
50	4.92E+01	1.03E+00	9.32E-01	4.17E+00	5.54E+02	3.08E+02	1.50E+01	1.30E+00	1.06E+00	9.50E-01	1.10E+00	1.49E+01	1.06E+00	9.94E-01
51	5.03E+01	1.05E+00	9.09E-01	4.22E+00	5.55E+02	3.08E+02	1.50E+01	7.07E-01	1.11E+00	1.01E+00	1.06E+00	1.50E+01	9.24E-01	1.04E+00
52	4.88E+01	1.00E+00	1.07E+00	4.36E+00	5.51E+02	3.08E+02	1.48E+01	1.23E+00	1.04E+00	9.93E-01	1.04E+00	1.48E+01	1.29E+00	1.08E+00
53	4.86E+01	1.01E+00	9.85E-01	4.17E+00	5.53E+02	3.07E+02	1.49E+01	9.68E-01	9.83E-01	1.04E+00	9.41E-01	1.48E+01	1.02E+00	1.08E+00
54	4.88E+01	1.01E+00	1.05E+00	4.26E+00	5.56E+02	3.10E+02	1.49E+01	1.18E+00	1.02E+00	1.07E+00	1.11E+00	1.48E+01	1.01E+00	1.08E+00
55	4.86E+01	1.08E+00	9.90E-01	4.23E+00	5.54E+02	3.09E+02	1.48E+01	7.75E-01	9.29E-01	9.29E-01	1.04E+00	1.50E+01	9.55E-01	1.06E+00
56	4.90E+01	1.06E+00	9.25E-01	4.24E+00	5.58E+02	3.09E+02	1.51E+01	9.88E-01	1.05E+00	1.10E+00	1.09E+00	1.48E+01	1.31E+00	9.86E-01
57	4.84E+01	1.01E+00	1.12E+00	4.26E+00	5.59E+02	3.07E+02	1.50E+01	9.78E-01	9.14E-01	1.06E+00	1.05E+00	1.51E+01	1.03E+00	9.33E-01
58	5.06E+01	1.02E+00	9.14E-01	4.20E+00	5.50E+02	3.08E+02	1.50E+01	9.59E-01	1.12E+00	1.08E+00	1.16E+00	1.50E+01	8.54E-01	1.03E+00
59	4.98E+01	1.07E+00	1.01E+00	4.30E+00	5.58E+02	3.09E+02	1.49E+01	1.01E+00	9.34E-01	9.93E-01	1.06E+00	1.49E+01	9.31E-01	1.01E+00
60	5.05E+01	1.05E+00	9.16E-01	4.38E+00	5.56E+02	3.08E+02	1.48E+01	1.20E+00	1.06E+00	1.16E+00	1.07E+00	1.48E+01	1.45E+00	9.10E-01
61	4.82E+01	1.07E+00	1.12E+00	4.27E+00	5.55E+02	3.08E+02	1.51E+01	9.42E-01	1.08E+00	1.10E+00	1.18E+00	1.48E+01	7.58E-01	9.89E-01
62	4.94E+01	1.02E+00	9.60E-01	4.24E+00	5.54E+02	3.07E+02	1.50E+01	8.89E-01	1.04E+00	1.04E+00	1.11E+00	1.50E+01	1.26E+00	1.09E+00
63	4.85E+01	1.05E+00	1.01E+00	4.08E+00	5.51E+02	3.07E+02	1.48E+01	9.87E-01	9.68E-01	1.09E+00	1.14E+00	1.48E+01	1.23E+00	9.88E-01
64	4.84E+01	1.05E+00	9.09E-01	4.13E+00	5.52E+02	3.08E+02	1.50E+01	7.57E-01	9.44E-01	9.89E-01	1.12E+00	1.48E+01	1.26E+00	9.84E-01
65	5.00E+01	1.01E+00	9.27E-01	4.39E+00	5.58E+02	3.08E+02	1.47E+01	7.44E-01	9.41E-01	9.85E-01	1.13E+00	1.50E+01	8.90E-01	1.03E+00
66	5.01E+01	1.02E+00	9.01E-01	4.18E+00	5.58E+02	3.10E+02	1.53E+01	8.61E-01	1.16E+00	1.06E+00	1.13E+00	1.48E+01	1.20E+00	1.03E+00
67	5.01E+01	1.03E+00	1.05E+00	4.29E+00	5.51E+02	3.09E+02	1.51E+01	1.14E+00	1.11E+00	9.14E-01	1.11E+00	1.50E+01	1.03E+00	1.06E+00
68	4.92E+01	1.07E+00	1.11E+00	4.27E+00	5.52E+02	3.09E+02	1.49E+01	8.73E-01	9.87E-01	1.07E+00	1.03E+00	1.48E+01	1.16E+00	9.49E-01
69	4.87E+01	1.02E+00	9.20E-01	4.19E+00	5.51E+02	3.09E+02	1.48E+01	8.03E-01	1.04E+00	1.07E+00	9.94E-01	1.50E+01	9.69E-01	9.46E-01
70	4.90E+01	1.01E+00	9.28E-01	4.18E+00	5.58E+02	3.08E+02	1.49E+01	7.90E-01	8.96E-01	1.05E+00	9.19E-01	1.50E+01	8.35E-01	1.06E+00
71	5.06E+01	1.02E+00	9.03E-01	4.29E+00	5.56E+02	3.08E+02	1.51E+01	7.01E-01	1.14E+00	8.87E-01	1.06E+00	1.47E+01	8.92E-01	1.07E+00
72	5.02E+01	1.05E+00	1.11E+00	4.23E+00	5.59E+02	3.08E+02	1.48E+01	1.03E+00	9.65E-01	1.11E+00	1.07E+00	1.50E+01	1.10E+00	9.67E-01
73	4.90E+01	1.01E+00	9.71E-01	4.22E+00	5.59E+02	3.08E+02	1.51E+01	9.79E-01	9.88E-01	1.02E+00	1.12E+00	1.50E+01	1.11E+00	9.66E-01
74	4.83E+01	1.01E+00	9.46E-01	4.23E+00	5.54E+02	3.08E+02	1.51E+01	1.25E+00	1.12E+00	9.68E-01	1.02E+00	1.47E+01	1.27E+00	9.37E-01
75	4.94E+01	1.06E+00	1.08E+00	4.19E+00	5.54E+02	3.06E+02	1.49E+01	8.71E-01	1.03E+00	8.85E-01	9.28E-01	1.50E+01	1.31E+00	9.33E-01

Table E-1: Samples from selected sources of uncertainty (cont.)

76	4.95E+01	1.02E+00	9.96E-01	4.16E+00	5.58E+02	3.09E+02	1.50E+01	8.09E-01	9.29E-01	1.05E+00	1.08E+00	1.48E+01	9.11E-01	9.58E-01
77	4.96E+01	1.01E+00	1.08E+00	4.13E+00	5.54E+02	3.09E+02	1.50E+01	1.22E+00	9.96E-01	1.12E+00	9.36E-01	1.50E+01	1.12E+00	9.31E-01
78	5.01E+01	1.07E+00	1.12E+00	4.22E+00	5.58E+02	3.06E+02	1.48E+01	1.08E+00	8.41E-01	9.29E-01	1.05E+00	1.48E+01	1.29E+00	1.02E+00
79	5.03E+01	1.07E+00	1.01E+00	4.12E+00	5.53E+02	3.07E+02	1.48E+01	8.76E-01	9.43E-01	1.10E+00	1.00E+00	1.48E+01	1.30E+00	9.51E-01
80	4.80E+01	1.04E+00	1.00E+00	4.18E+00	5.59E+02	3.08E+02	1.48E+01	1.22E+00	1.15E+00	9.45E-01	1.14E+00	1.48E+01	9.52E-01	9.20E-01
81	4.99E+01	1.01E+00	1.06E+00	4.24E+00	5.59E+02	3.09E+02	1.52E+01	1.24E+00	9.03E-01	9.87E-01	9.10E-01	1.48E+01	8.94E-01	1.09E+00
82	4.97E+01	1.04E+00	1.09E+00	4.14E+00	5.60E+02	3.09E+02	1.52E+01	8.76E-01	1.01E+00	1.00E+00	1.03E+00	1.47E+01	1.21E+00	1.04E+00
83	4.89E+01	1.05E+00	9.09E-01	4.21E+00	5.50E+02	3.06E+02	1.48E+01	9.83E-01	9.14E-01	1.05E+00	9.26E-01	1.50E+01	9.49E-01	1.06E+00
84	5.02E+01	1.04E+00	9.52E-01	4.26E+00	5.52E+02	3.08E+02	1.47E+01	1.21E+00	1.06E+00	1.12E+00	1.10E+00	1.50E+01	1.05E+00	1.00E+00
85	4.98E+01	1.04E+00	1.12E+00	4.15E+00	5.59E+02	3.07E+02	1.49E+01	1.19E+00	9.44E-01	9.77E-01	1.07E+00	1.47E+01	8.92E-01	9.59E-01
86	4.85E+01	1.01E+00	1.02E+00	4.26E+00	5.52E+02	3.08E+02	1.51E+01	9.49E-01	1.00E+00	1.02E+00	1.04E+00	1.47E+01	1.04E+00	9.60E-01
87	4.95E+01	1.01E+00	1.08E+00	4.23E+00	5.54E+02	3.10E+02	1.48E+01	8.43E-01	1.03E+00	1.09E+00	1.06E+00	1.47E+01	9.99E-01	1.07E+00
88	4.85E+01	1.00E+00	1.02E+00	4.23E+00	5.52E+02	3.08E+02	1.50E+01	9.12E-01	1.05E+00	1.12E+00	1.16E+00	1.50E+01	9.02E-01	9.33E-01
89	4.85E+01	1.00E+00	9.14E-01	4.24E+00	5.58E+02	3.09E+02	1.50E+01	7.65E-01	9.56E-01	1.02E+00	9.29E-01	1.47E+01	1.12E+00	9.73E-01
90	4.90E+01	1.01E+00	1.10E+00	4.08E+00	5.56E+02	3.08E+02	1.50E+01	8.08E-01	1.00E+00	9.11E-01	1.02E+00	1.47E+01	1.11E+00	1.02E+00
91	4.90E+01	1.08E+00	9.79E-01	4.14E+00	5.52E+02	3.08E+02	1.47E+01	1.07E+00	9.39E-01	1.05E+00	1.10E+00	1.50E+01	8.58E-01	9.89E-01
92	4.87E+01	1.02E+00	1.01E+00	4.14E+00	5.58E+02	3.07E+02	1.50E+01	9.83E-01	1.01E+00	1.01E+00	1.02E+00	1.47E+01	7.79E-01	9.63E-01
93	4.86E+01	1.01E+00	9.08E-01	4.22E+00	5.51E+02	3.08E+02	1.53E+01	9.19E-01	1.14E+00	1.03E+00	9.84E-01	1.47E+01	1.19E+00	1.05E+00
94	4.97E+01	1.00E+00	9.05E-01	4.20E+00	5.56E+02	3.08E+02	1.51E+01	1.20E+00	1.17E+00	8.61E-01	1.11E+00	1.48E+01	1.09E+00	1.10E+00
95	4.92E+01	1.06E+00	1.09E+00	4.26E+00	5.55E+02	3.09E+02	1.52E+01	8.90E-01	1.04E+00	9.14E-01	1.05E+00	1.48E+01	9.05E-01	1.01E+00
96	5.05E+01	1.06E+00	9.13E-01	4.31E+00	5.50E+02	3.09E+02	1.47E+01	8.28E-01	9.13E-01	9.47E-01	1.13E+00	1.50E+01	9.37E-01	1.04E+00
97	4.91E+01	1.06E+00	1.02E+00	4.28E+00	5.52E+02	3.08E+02	1.47E+01	8.41E-01	1.04E+00	9.40E-01	1.04E+00	1.48E+01	1.19E+00	9.54E-01
98	4.99E+01	1.08E+00	9.32E-01	4.31E+00	5.54E+02	3.09E+02	1.50E+01	1.08E+00	8.61E-01	1.11E+00	9.30E-01	1.50E+01	1.08E+00	9.95E-01
99	4.82E+01	1.03E+00	9.96E-01	4.11E+00	5.51E+02	3.08E+02	1.50E+01	1.29E+00	9.95E-01	8.95E-01	1.14E+00	1.48E+01	1.17E+00	9.58E-01
100	5.06E+01	1.08E+00	9.41E-01	4.24E+00	5.58E+02	3.06E+02	1.50E+01	9.40E-01	9.44E-01	9.85E-01	9.38E-01	1.50E+01	1.50E+00	1.09E+00
101	4.97E+01	1.04E+00	1.08E+00	4.14E+00	5.57E+02	3.07E+02	1.50E+01	8.46E-01	9.71E-01	9.70E-01	9.82E-01	1.48E+01	8.55E-01	1.09E+00
102	5.02E+01	1.04E+00	1.10E+00	4.14E+00	5.60E+02	3.08E+02	1.50E+01	1.04E+00	1.03E+00	1.15E+00	9.69E-01	1.48E+01	8.78E-01	9.43E-01
103	5.01E+01	1.06E+00	1.11E+00	4.26E+00	5.52E+02	3.08E+02	1.51E+01	8.26E-01	1.04E+00	9.77E-01	1.11E+00	1.49E+01	1.15E+00	9.61E-01
104	5.01E+01	1.02E+00	1.08E+00	4.32E+00	5.60E+02	3.08E+02	1.50E+01	1.15E+00	8.88E-01	9.61E-01	1.09E+00	1.48E+01	1.22E+00	1.00E+00
105	4.92E+01	1.03E+00	1.05E+00	4.35E+00	5.55E+02	3.07E+02	1.49E+01	9.91E-01	8.90E-01	9.19E-01	1.12E+00	1.47E+01	9.11E-01	1.07E+00
106	5.03E+01	1.02E+00	9.52E-01	4.17E+00	5.57E+02	3.09E+02	1.51E+01	1.05E+00	9.16E-01	1.05E+00	1.16E+00	1.50E+01	1.19E+00	1.01E+00
107	4.90E+01	1.05E+00	9.76E-01	4.30E+00	5.58E+02	3.09E+02	1.50E+01	1.05E+00	1.00E+00	9.40E-01	1.18E+00	1.49E+01	1.12E+00	1.01E+00
108	4.99E+01	1.05E+00	9.21E-01	4.22E+00	5.59E+02	3.07E+02	1.49E+01	1.18E+00	1.02E+00	1.01E+00	9.61E-01	1.47E+01	9.29E-01	9.88E-01
109	4.85E+01	1.00E+00	9.31E-01	4.21E+00	5.50E+02	3.07E+02	1.48E+01	9.96E-01	9.74E-01	1.04E+00	1.09E+00	1.48E+01	1.32E+00	1.09E+00
110	4.86E+01	1.04E+00	1.09E+00	4.22E+00	5.52E+02	3.07E+02	1.49E+01	7.65E-01	1.00E+00	9.59E-01	9.62E-01	1.50E+01	1.36E+00	1.07E+00
111	4.98E+01	1.08E+00	1.04E+00	4.23E+00	5.58E+02	3.09E+02	1.52E+01	1.18E+00	9.42E-01	8.82E-01	1.05E+00	1.50E+01	1.24E+00	1.06E+00
112	4.97E+01	1.03E+00	9.86E-01	4.26E+00	5.51E+02	3.09E+02	1.48E+01	7.07E-01	1.02E+00	1.13E+00	1.12E+00	1.49E+01	1.34E+00	9.85E-01
113	4.95E+01	1.00E+00	1.07E+00	4.30E+00	5.57E+02	3.08E+02	1.49E+01	7.60E-01	1.09E+00	8.76E-01	9.52E-01	1.48E+01	1.03E+00	9.80E-01
114	5.04E+01	1.06E+00	9.50E-01	4.34E+00	5.53E+02	3.06E+02	1.50E+01	1.04E+00	1.04E+00	9.45E-01	9.07E-01	1.47E+01	9.38E-01	1.01E+00
115	5.03E+01	1.02E+00	1.10E+00	4.38E+00	5.56E+02	3.06E+02	1.50E+01	9.41E-01	9.95E-01	9.52E-01	9.27E-01	1.48E+01	9.52E-01	1.09E+00
116	4.96E+01	1.07E+00	9.07E-01	4.38E+00	5.55E+02	3.08E+02	1.50E+01	1.00E+00	1.01E+00	9.91E-01	1.12E+00	1.49E+01	1.16E+00	1.00E+00
117	4.99E+01	1.06E+00	9.81E-01	4.13E+00	5.52E+02	3.08E+02	1.52E+01	9.23E-01	9.66E-01	1.05E+00	1.03E+00	1.48E+01	8.89E-01	9.63E-01
118	5.00E+01	1.06E+00	1.08E+00	4.24E+00	5.55E+02	3.08E+02	1.50E+01	8.29E-01	1.14E+00	1.10E+00	1.18E+00	1.48E+01	1.13E+00	9.84E-01
119	4.94E+01	1.04E+00	1.02E+00	4.34E+00	5.51E+02	3.08E+02	1.51E+01	8.22E-01	8.74E-01	1.09E+00	1.13E+00	1.48E+01	1.15E+00	9.40E-01
120	4.95E+01	1.03E+00	1.03E+00	4.30E+00	5.54E+02	3.09E+02	1.49E+01	1.08E+00	8.88E-01	1.05E+00	1.16E+00	1.48E+01	1.18E+00	9.63E-01
121	4.97E+01	1.02E+00	1.11E+00	4.10E+00	5.57E+02	3.09E+02	1.47E+01	1.22E+00	9.73E-01	9.26E-01	1.13E+00	1.48E+01	1.27E+00	9.57E-01
122	4.94E+01	1.03E+00	1.06E+00	4.30E+00	5.59E+02	3.08E+02	1.51E+01	1.26E+00	1.03E+00	1.14E+00	9.11E-01	1.49E+01	9.99E-01	9.20E-01
123	4.81E+01	1.01E+00	1.05E+00	4.26E+00	5.51E+02	3.07E+02	1.51E+01	8.13E-01	9.24E-01	1.08E+00	9.87E-01	1.50E+01	1.22E+00	9.13E-01
124	4.94E+01	1.02E+00	9.34E-01	4.22E+00	5.56E+02	3.07E+02	1.48E+01	1.28E+00	9.21E-01	1.11E+00	1.03E+00	1.47E+01	1.20E+00	9.97E-01
125	4.92E+01	1.07E+00	9.48E-01	4.35E+00	5.58E+02	3.07E+02	1.52E+01	1.23E+00	1.10E+00	8.89E-01	9.11E-01	1.47E+01	9.09E-01	1.02E+00
126	5.01E+01	1.01E+00	1.01E+00	4.29E+00	5.55E+02	3.09E+02	1.49E+01	1.20E+00	1.01E+00	8.92E-01	1.07E+00	1.49E+01	1.25E+00	9.17E-01
127	4.84E+01	1.06E+00	1.01E+00	4.09E+00	5.59E+02	3.08E+02	1.50E+01	7.47E-01	9.56E-01	1.02E+00	1.18E+00	1.48E+01	8.20E-01	9.32E-01
128	4.99E+01	1.03E+00	9.92E-01	4.37E+00	5.54E+02	3.08E+02	1.50E+01	1.14E+00	8.93E-01	1.10E+00	1.04E+00	1.50E+01	9.34E-01	9.30E-01
129	4.99E+01	1.04E+00	1.11E+00	4.20E+00	5.55E+02	3.09E+02	1.48E+01	1.03E+00	1.10E+00	9.98E-01	9.98E-01	1.49E+01	1.10E+00	9.08E-01
130	4.90E+01	1.05E+00	1.09E+00	4.23E+00	5.55E+02	3.09E+02	1.51E+01	1.13E+00	1.02E+00	9.69E-01	1.07E+00	1.49E+01	1.06E+00	1.01E+00
131	4.93E+01	1.03E+00	9.91E-01	4.37E+00	5.58E+02	3.08E+02	1.51E+01	1.24E+00	9.74E-01	1.17E+00	1.15E+00	1.49E+01	9.57E-01	1.03E+00
132	5.02E+01	1.07E+00	9.72E-01	4.16E+00	5.54E+02	3.09E+02	1.48E+01	1.16E+00	9.72E-01	8.40E-01	9.09E-01	1.48E+01	9.58E-01	9.04E-01
133	4.83E+01	1.03E+00	1.05E+00	4.25E+00	5.56E+02	3.08E+02	1.48E+01	1.19E+00	1.06E+00	9.48E-01	9.89E-01	1.50E+01	1.13E+00	1.04E+00
134	4.97E+01	1.07E+00	9.55E-01	4.25E+00	5.50E+02	3.08E+02	1.52E+01	8.99E-01	9.86E-01	1.05E+00	9.22E-01	1.48E+01	1.10E+00	1.00E+00
135	4.85E+01	1.03E+00	1.03E+00	4.27E+00	5.56E+02	3.08E+02	1.50E+01	1.21E+00	9.10E-01	9.61E-01	1.17E+00	1.49E+01	1.20E+00	1.04E+00
136	4.96E+01	1.03E+00	9.94E-01	4.14E+00	5.53E+02	3.07E+02	1.50E+01	1.30E+00	1.11E+00	9.03E-01	1.16E+00	1.50E+01	1.39E+00	1.03E+00
137	5.01E+01	1.05E+00	1.08E+00	4.22E+00	5.52E+02	3.08E+02	1.49E+01	9.61E-01	9.49E-01	1.08E+00	1.16E+00	1.48E+01	1.25E+00	9.16E-01
138	4.96E+01	1.05E+00	1.10E+00	4.26E+00	5.59E+02	3.08E+02	1.48E+01	1.26E+00	8.81E-01	9.01E-01	1.19E+00	1.50E+01	8.45E-01	9.37E-01
139	4.80E+01	1.07E+00	9.31E-01	4.19E+00	5.56E+02	3.07E+02	1.52E+01	1.08E+00	8.48E-01	1.13E+00	9.75E-01	1.48E+01	1.09E+00	1.10E+00
140	5.01E+01	1.06E+00	1.05E+00	4.32E+00	5.58E+02	3.09E+02	1.51E+01	8.73E-01	1.08E+00	1.02E+00	1.13E+00	1.50E+01	9.42E-01	1.05E+00
141	4.96E+01	1.03E+00	1.07E+00	4.34E+00	5.55E+02	3.08E+02	1.50E+01	9.71E-01	8.09E-01	8.62E-01	9.66E-01	1.48E+01	1.28E+00	9.19E-01
142	4.96E+01	1.04E+00	1.07E+00	4.25E+00	5.59E+02	3.08E+02	1.51E+01	7.15E-01	9.36E-01	1.01E+00	9.24E-01	1.50E+01	8.95E-01	1.03E+00
143	4.97E+01	1.07E+00	1.11E+00	4.21E+00	5.53E+02	3.08E+02	1.49E+01	8.44E-01	9.58E-01	1.00E+00	1.20E+00	1.47E+01	1.08E+00	9.36E-01
144	4.93E+01	1.08E+00	1.05E+00	4.23E+00	5.55E+02	3.08E+02	1.51E+01	1.10E+00	1.07E+00	9.86E-01	1.12E+00	1.48E+01	1.12E+00	1.05E+00
145	4.81E+01	1.07E+00	9.41E-01	4.17E+00	5.54E+02	3.06E+02	1.48E+01	9.04E-01	1.07E+00	8.14E-01	1.07E+00	1.47E+01	9.09E-01	9.11E-01
146	5.03E+01	1.06E+00	1.06E+00	4.24E+00	5.59E+02	3.07E+02	1.50E+01	1.23E+00	1.06E+00	1.14E+00	1.14E+00	1.49E+01	9.26E-01	9.86E-01
147	4.91E+01	1.03E+00	1.05E+00	4.31E+00	5.57E+02	3.07E+02	1.53E+01	1.26E+00	1.13E+00	9.42E-01	9.06E-01	1.49E+01	1.17E+00	9.13E-01
148	4.93E+01	1.04E+00	9.04E-01	4.20E+00	5.53E+02	3.07E+02	1.52E+01	8.65E-01	9.45E-01	1.02E+00	9.95E-01	1.49E+01	1.31E+00	1.05E+00
149	4.94E+01	1.03E+00	1.03E+00	4.34E+00	5.53E+02	3.08E+02	1.50E+01	7.24E-01	1.02E+00	9.65E-01	1.05E+00	1.49E+01	1.21E+00	1.01E+00
150	4.98E+01	1.05E+00	1.00E+00	4.21E+00	5.59E+02	3.07E+02	1.52E+01	8.52E-01	1.05E+00	8.27E-01	1.18E+00	1.50E+01	1.05E+00	9.50E-01

Table E-1: Samples from selected sources of uncertainty (cont.)

151	4.92E+01	1.02E+00	9.53E-01	4.22E+00	5.54E+02	3.08E+02	1.48E+01	1.00E+00	9.34E-01	1.06E+00	1.02E+00	1.50E+01
152	4.86E+01	1.05E+00	1.02E+00	4.26E+00	5.58E+02	3.08E+02	1.48E+01	1.23E+00	9.79E-01	9.02E-01	1.17E+00	1.49E+01
153	4.99E+01	1.00E+00	1.07E+00	4.16E+00	5.52E+02	3.06E+02	1.51E+01	1.23E+00	8.82E-01	8.76E-01	1.08E+00	1.50E+01
154	4.82E+01	1.07E+00	9.34E-01	4.30E+00	5.50E+02	3.09E+02	1.51E+01	1.26E+00	8.92E-01	9.52E-01	1.05E+00	1.50E+01
155	4.84E+01	1.05E+00	1.05E+00	4.24E+00	5.53E+02	3.09E+02	1.51E+01	1.27E+00	8.46E-01	9.88E-01	1.11E+00	1.47E+01
156	5.05E+01	1.03E+00	1.11E+00	4.27E+00	5.53E+02	3.08E+02	1.50E+01	7.77E-01	1.02E+00	8.89E-01	1.07E+00	1.49E+01
157	4.89E+01	1.01E+00	9.66E-01	4.30E+00	5.58E+02	3.07E+02	1.49E+01	8.91E-01	9.75E-01	1.13E+00	9.32E-01	1.49E+01
158	4.93E+01	1.04E+00	9.39E-01	4.31E+00	5.51E+02	3.08E+02	1.49E+01	1.04E+00	1.11E+00	9.09E-01	9.17E-01	1.47E+01
159	4.93E+01	1.02E+00	9.61E-01	4.16E+00	5.52E+02	3.08E+02	1.48E+01	1.17E+00	9.64E-01	9.69E-01	1.01E+00	1.48E+01
160	5.03E+01	1.06E+00	9.01E-01	4.18E+00	5.50E+02	3.08E+02	1.50E+01	9.31E-01	1.12E+00	1.13E+00	9.45E-01	1.50E+01
161	5.03E+01	1.01E+00	1.08E+00	4.19E+00	5.51E+02	3.08E+02	1.50E+01	9.53E-01	9.02E-01	1.00E+00	1.04E+00	1.48E+01
162	4.89E+01	1.04E+00	1.04E+00	4.10E+00	5.58E+02	3.08E+02	1.48E+01	8.44E-01	1.12E+00	1.05E+00	1.13E+00	1.47E+01
163	5.06E+01	1.03E+00	1.01E+00	4.21E+00	5.55E+02	3.06E+02	1.48E+01	7.75E-01	9.65E-01	1.02E+00	1.06E+00	1.47E+01
164	4.98E+01	1.06E+00	1.08E+00	4.13E+00	5.58E+02	3.09E+02	1.50E+01	1.20E+00	9.99E-01	8.66E-01	1.14E+00	1.50E+01
165	4.92E+01	1.05E+00	1.04E+00	4.22E+00	5.58E+02	3.08E+02	1.48E+01	9.96E-01	9.94E-01	1.06E+00	1.00E+00	1.47E+01
166	5.04E+01	1.02E+00	9.05E-01	4.13E+00	5.52E+02	3.07E+02	1.50E+01	1.08E+00	1.15E+00	9.60E-01	1.03E+00	1.50E+01
167	4.96E+01	1.05E+00	1.10E+00	4.22E+00	5.57E+02	3.08E+02	1.47E+01	1.23E+00	1.04E+00	8.79E-01	9.86E-01	1.48E+01
168	4.89E+01	1.00E+00	9.19E-01	4.16E+00	5.55E+02	3.07E+02	1.48E+01	9.31E-01	1.06E+00	9.85E-01	9.01E-01	1.47E+01
169	5.01E+01	1.01E+00	1.05E+00	4.23E+00	5.60E+02	3.07E+02	1.50E+01	8.41E-01	9.33E-01	8.99E-01	1.17E+00	1.48E+01
170	5.03E+01	1.00E+00	9.38E-01	4.29E+00	5.53E+02	3.08E+02	1.48E+01	7.07E-01	8.55E-01	9.64E-01	9.06E-01	1.50E+01
171	4.96E+01	1.01E+00	9.94E-01	4.20E+00	5.51E+02	3.06E+02	1.51E+01	7.20E-01	9.79E-01	8.52E-01	1.01E+00	1.48E+01
172	4.91E+01	1.07E+00	1.00E+00	4.22E+00	5.55E+02	3.09E+02	1.50E+01	9.63E-01	1.01E+00	9.59E-01	1.08E+00	1.50E+01
173	4.87E+01	1.00E+00	1.06E+00	4.25E+00	5.52E+02	3.07E+02	1.49E+01	8.85E-01	9.95E-01	1.01E+00	1.13E+00	1.49E+01
174	4.80E+01	1.06E+00	1.05E+00	4.35E+00	5.57E+02	3.08E+02	1.50E+01	1.01E+00	8.95E-01	9.71E-01	1.02E+00	1.50E+01
175	4.98E+01	1.01E+00	1.02E+00	4.18E+00	5.59E+02	3.08E+02	1.49E+01	1.00E+00	1.11E+00	1.16E+00	1.11E+00	1.50E+01
176	4.85E+01	1.02E+00	9.43E-01	4.12E+00	5.58E+02	3.07E+02	1.49E+01	8.53E-01	9.20E-01	1.03E+00	1.08E+00	1.48E+01
177	4.96E+01	1.01E+00	1.01E+00	4.26E+00	5.54E+02	3.08E+02	1.49E+01	7.46E-01	1.07E+00	9.08E-01	1.00E+00	1.48E+01
178	5.03E+01	1.01E+00	1.05E+00	4.11E+00	5.57E+02	3.09E+02	1.53E+01	1.19E+00	9.36E-01	8.50E-01	1.00E+00	1.47E+01
179	4.93E+01	1.02E+00	1.02E+00	4.17E+00	5.53E+02	3.06E+02	1.51E+01	7.99E-01	1.08E+00	8.17E-01	1.16E+00	1.50E+01
180	4.93E+01	1.01E+00	1.08E+00	4.12E+00	5.57E+02	3.09E+02	1.49E+01	9.59E-01	1.07E+00	1.06E+00	9.63E-01	1.49E+01
181	4.95E+01	1.01E+00	9.64E-01	4.24E+00	5.56E+02	3.08E+02	1.51E+01	8.48E-01	1.01E+00	1.09E+00	1.04E+00	1.49E+01
182	4.90E+01	1.03E+00	1.04E+00	4.27E+00	5.53E+02	3.09E+02	1.51E+01	9.09E-01	1.01E+00	9.59E-01	9.74E-01	1.48E+01
183	5.00E+01	1.06E+00	9.32E-01	4.26E+00	5.50E+02	3.08E+02	1.51E+01	1.13E+00	9.81E-01	9.57E-01	1.19E+00	1.49E+01
184	4.99E+01	1.02E+00	9.05E-01	4.20E+00	5.52E+02	3.07E+02	1.51E+01	7.96E-01	1.02E+00	1.01E+00	1.18E+00	1.47E+01
185	5.01E+01	1.02E+00	1.08E+00	4.30E+00	5.59E+02	3.06E+02	1.48E+01	9.35E-01	9.40E-01	9.88E-01	1.18E+00	1.48E+01
186	4.93E+01	1.04E+00	1.06E+00	4.20E+00	5.51E+02	3.09E+02	1.48E+01	1.14E+00	1.12E+00	8.83E-01	1.01E+00	1.49E+01
187	5.01E+01	1.07E+00	1.05E+00	4.16E+00	5.52E+02	3.07E+02	1.49E+01	1.00E+00	1.09E+00	9.63E-01	9.24E-01	1.48E+01
188	4.81E+01	1.02E+00	9.09E-01	4.22E+00	5.55E+02	3.07E+02	1.50E+01	7.48E-01	1.09E+00	9.34E-01	1.07E+00	1.48E+01
189	4.92E+01	1.05E+00	1.01E+00	4.21E+00	5.54E+02	3.08E+02	1.49E+01	9.45E-01	1.09E+00	1.15E+00	1.10E+00	1.49E+01
190	4.83E+01	1.02E+00	9.78E-01	4.37E+00	5.56E+02	3.08E+02	1.49E+01	1.26E+00	1.05E+00	9.22E-01	9.81E-01	1.50E+01
191	4.86E+01	1.02E+00	9.63E-01	4.33E+00	5.56E+02	3.08E+02	1.49E+01	7.32E-01	9.63E-01	1.02E+00	9.11E-01	1.48E+01
192	5.02E+01	1.06E+00	9.49E-01	4.20E+00	5.55E+02	3.08E+02	1.52E+01	7.17E-01	9.54E-01	9.62E-01	1.05E+00	1.48E+01
193	5.02E+01	1.03E+00	1.01E+00	4.23E+00	5.51E+02	3.08E+02	1.52E+01	9.92E-01	1.08E+00	9.87E-01	9.07E-01	1.47E+01
194	4.99E+01	1.02E+00	1.10E+00	4.16E+00	5.55E+02	3.07E+02	1.49E+01	1.20E+00	9.61E-01	9.64E-01	1.19E+00	1.48E+01
195	4.95E+01	1.04E+00	9.49E-01	4.26E+00	5.54E+02	3.08E+02	1.50E+01	1.11E+00	1.05E+00	9.14E-01	9.71E-01	1.49E+01
196	4.92E+01	1.06E+00	1.11E+00	4.28E+00	5.57E+02	3.08E+02	1.48E+01	7.29E-01	1.11E+00	1.01E+00	9.07E-01	1.50E+01
197	4.84E+01	1.03E+00	1.00E+00	4.29E+00	5.54E+02	3.08E+02	1.49E+01	8.59E-01	9.16E-01	9.74E-01	1.07E+00	1.47E+01
198	4.84E+01	1.03E+00	9.04E-01	4.27E+00	5.51E+02	3.09E+02	1.48E+01	9.41E-01	1.06E+00	8.35E-01	1.18E+00	1.48E+01
199	5.00E+01	1.03E+00	1.05E+00	4.24E+00	5.52E+02	3.08E+02	1.49E+01	8.56E-01	1.13E+00	1.04E+00	9.85E-01	1.48E+01
200	4.81E+01	1.07E+00	1.04E+00	4.27E+00	5.51E+02	3.09E+02	1.50E+01	7.22E-01	1.05E+00	1.08E+00	1.19E+00	1.49E+01
201	5.03E+01	1.02E+00	9.34E-01	4.30E+00	5.57E+02	3.07E+02	1.51E+01	1.18E+00	1.01E+00	1.02E+00	1.14E+00	1.49E+01
202	5.05E+01	1.03E+00	1.02E+00	4.22E+00	5.59E+02	3.08E+02	1.48E+01	9.20E-01	1.07E+00	1.10E+00	1.08E+00	1.50E+01
203	4.82E+01	1.01E+00	1.01E+00	4.32E+00	5.53E+02	3.07E+02	1.51E+01	7.04E-01	9.48E-01	9.87E-01	1.15E+00	1.48E+01
204	4.92E+01	1.01E+00	9.86E-01	4.23E+00	5.54E+02	3.09E+02	1.50E+01	1.06E+00	1.03E+00	1.00E+00	1.01E+00	1.48E+01
205	4.89E+01	1.06E+00	1.05E+00	4.25E+00	5.56E+02	3.09E+02	1.50E+01	7.36E-01	9.18E-01	9.56E-01	1.03E+00	1.47E+01
206	4.82E+01	1.07E+00	1.04E+00	4.07E+00	5.60E+02	3.08E+02	1.50E+01	8.44E-01	9.79E-01	1.04E+00	1.00E+00	1.48E+01
207	4.87E+01	1.06E+00	1.09E+00	4.15E+00	5.60E+02	3.08E+02	1.51E+01	1.10E+00	1.11E+00	1.03E+00	1.18E+00	1.50E+01
208	4.91E+01	1.01E+00	1.11E+00	4.17E+00	5.57E+02	3.08E+02	1.48E+01	8.99E-01	1.04E+00	1.04E+00	9.83E-01	1.49E+01
209	4.98E+01	1.05E+00	9.35E-01	4.11E+00	5.56E+02	3.06E+02	1.51E+01	1.12E+00	9.45E-01	8.26E-01	1.11E+00	1.47E+01
210	4.83E+01	1.06E+00	1.00E+00	4.16E+00	5.55E+02	3.09E+02	1.49E+01	1.15E+00	1.02E+00	9.69E-01	1.08E+00	1.48E+01
211	4.87E+01	1.02E+00	9.34E-01	4.18E+00	5.57E+02	3.07E+02	1.52E+01	1.26E+00	9.70E-01	9.64E-01	1.08E+00	1.47E+01
212	4.85E+01	1.05E+00	9.14E-01	4.15E+00	5.51E+02	3.07E+02	1.48E+01	1.09E+00	1.02E+00	1.06E+00	1.00E+00	1.49E+01
213	5.03E+01	1.03E+00	9.65E-01	4.26E+00	5.56E+02	3.06E+02	1.49E+01	1.09E+00	8.88E-01	1.14E+00	1.11E+00	1.49E+01
214	5.03E+01	1.07E+00	1.09E+00	4.10E+00	5.58E+02	3.07E+02	1.50E+01	7.80E-01	9.66E-01	1.02E+00	1.02E+00	1.50E+01
215	5.00E+01	1.07E+00	9.78E-01	4.19E+00	5.53E+02	3.09E+02	1.51E+01	1.05E+00	9.59E-01	8.82E-01	1.18E+00	1.48E+01
216	4.91E+01	1.02E+00	1.10E+00	4.25E+00	5.52E+02	3.08E+02	1.50E+01	9.71E-01	9.71E-01	1.17E+00	9.23E-01	1.50E+01
217	4.93E+01	1.07E+00	1.02E+00	4.23E+00	5.59E+02	3.09E+02	1.50E+01	7.04E-01	9.71E-01	1.01E+00	9.56E-01	1.50E+01
218	4.99E+01	1.03E+00	1.11E+00	4.21E+00	5.57E+02	3.07E+02	1.50E+01	7.18E-01	1.07E+00	9.32E-01	1.19E+00	1.48E+01
219	4.93E+01	1.02E+00	1.09E+00	4.23E+00	5.60E+02	3.07E+02	1.51E+01	7.55E-01	1.11E+00	8.91E-01	9.34E-01	1.50E+01
220	4.99E+01	1.05E+00	9.01E-01	4.30E+00	5.50E+02	3.07E+02	1.48E+01	1.20E+00	1.14E+00	8.93E-01	1.15E+00	1.48E+01
221	4.83E+01	1.08E+00	9.65E-01	4.35E+00	5.58E+02	3.08E+02	1.48E+01	8.49E-01	1.08E+00	1.01E+00	9.47E-01	1.49E+01
222	4.80E+01	1.06E+00	9.23E-01	4.31E+00	5.57E+02	3.08E+02	1.47E+01	1.05E+00	8.72E-01	9.95E-01	1.06E+00	1.50E+01
223	4.98E+01	1.04E+00	1.02E+00	4.19E+00	5.54E+02	3.07E+02	1.50E+01	1.19E+00	9.68E-01	1.13E+00	9.26E-01	1.47E+01
224	5.02E+01	1.00E+00	1.03E+00	4.32E+00	5.56E+02	3.08E+02	1.50E+01	1.25E+00	1.04E+00	8.84E-01	1.14E+00	1.48E+01
225	4.95E+01	1.01E+00	1.02E+00	4.15E+00	5.58E+02	3.08E+02	1.50E+01	1.06E+00	8.72E-01	9.67E-01	1.08E+00	1.47E+01

Table E-1: Samples from selected sources of uncertainty (cont.)

226	5.04E+01	1.05E+00	9.00E-01	4.11E+00	5.55E+02	3.09E+02	1.51E+01	1.04E+00	9.99E-01	9.83E-01	9.77E-01	1.50E+01
227	4.92E+01	1.01E+00	9.63E-01	4.23E+00	5.57E+02	3.09E+02	1.48E+01	1.00E+00	8.78E-01	9.38E-01	1.02E+00	1.48E+01
228	4.83E+01	1.04E+00	1.10E+00	4.26E+00	5.58E+02	3.08E+02	1.50E+01	8.20E-01	1.10E+00	1.05E+00	9.49E-01	1.50E+01
229	4.89E+01	1.07E+00	9.74E-01	4.16E+00	5.54E+02	3.07E+02	1.51E+01	1.13E+00	1.02E+00	9.19E-01	9.94E-01	1.49E+01
230	4.88E+01	1.04E+00	9.03E-01	4.24E+00	5.54E+02	3.07E+02	1.53E+01	9.63E-01	1.14E+00	1.07E+00	1.07E+00	1.50E+01
231	5.03E+01	1.05E+00	9.87E-01	4.29E+00	5.58E+02	3.09E+02	1.51E+01	7.00E-01	8.57E-01	9.97E-01	9.48E-01	1.50E+01
232	4.80E+01	1.01E+00	9.07E-01	4.15E+00	5.55E+02	3.10E+02	1.52E+01	1.30E+00	8.92E-01	1.07E+00	1.10E+00	1.49E+01
233	4.92E+01	1.02E+00	1.05E+00	4.18E+00	5.53E+02	3.07E+02	1.52E+01	7.30E-01	9.75E-01	8.94E-01	9.78E-01	1.47E+01
234	4.81E+01	1.06E+00	1.03E+00	4.13E+00	5.51E+02	3.08E+02	1.51E+01	9.57E-01	1.07E+00	1.10E+00	1.01E+00	1.50E+01
235	4.85E+01	1.06E+00	1.02E+00	4.09E+00	5.53E+02	3.09E+02	1.52E+01	7.58E-01	1.06E+00	1.01E+00	1.11E+00	1.48E+01
236	4.84E+01	1.02E+00	9.94E-01	4.12E+00	5.51E+02	3.09E+02	1.53E+01	8.17E-01	9.65E-01	9.02E-01	1.11E+00	1.49E+01
237	4.93E+01	1.01E+00	9.49E-01	4.18E+00	5.54E+02	3.07E+02	1.48E+01	1.01E+00	1.11E+00	1.12E+00	1.07E+00	1.48E+01
238	4.96E+01	1.06E+00	1.10E+00	4.27E+00	5.52E+02	3.07E+02	1.51E+01	9.87E-01	1.04E+00	1.09E+00	1.03E+00	1.48E+01
239	4.82E+01	1.02E+00	9.67E-01	4.28E+00	5.57E+02	3.08E+02	1.51E+01	8.74E-01	9.63E-01	1.02E+00	9.35E-01	1.49E+01
240	5.04E+01	1.02E+00	9.98E-01	4.11E+00	5.51E+02	3.09E+02	1.50E+01	8.38E-01	9.20E-01	8.86E-01	1.03E+00	1.48E+01
241	5.01E+01	1.01E+00	1.06E+00	4.24E+00	5.52E+02	3.06E+02	1.51E+01	8.01E-01	1.07E+00	1.15E+00	1.05E+00	1.48E+01
242	4.96E+01	1.04E+00	1.04E+00	4.08E+00	5.55E+02	3.07E+02	1.48E+01	1.01E+00	8.89E-01	1.10E+00	1.01E+00	1.49E+01
243	4.97E+01	1.05E+00	9.98E-01	4.10E+00	5.54E+02	3.07E+02	1.51E+01	1.02E+00	8.86E-01	1.01E+00	1.03E+00	1.48E+01
244	4.81E+01	1.04E+00	1.01E+00	4.07E+00	5.57E+02	3.08E+02	1.48E+01	7.70E-01	8.95E-01	9.63E-01	9.30E-01	1.49E+01
245	4.87E+01	1.07E+00	1.04E+00	4.25E+00	5.59E+02	3.08E+02	1.51E+01	1.28E+00	9.75E-01	1.02E+00	1.07E+00	1.48E+01
246	4.94E+01	1.06E+00	9.49E-01	4.22E+00	5.51E+02	3.08E+02	1.48E+01	9.62E-01	1.07E+00	1.06E+00	9.63E-01	1.49E+01
247	4.85E+01	1.01E+00	9.05E-01	4.23E+00	5.56E+02	3.08E+02	1.49E+01	9.45E-01	1.04E+00	8.50E-01	1.00E+00	1.50E+01
248	4.98E+01	1.05E+00	1.06E+00	4.23E+00	5.58E+02	3.07E+02	1.51E+01	9.45E-01	1.04E+00	1.06E+00	1.01E+00	1.47E+01
249	4.96E+01	1.03E+00	1.04E+00	4.21E+00	5.55E+02	3.08E+02	1.48E+01	9.73E-01	1.02E+00	1.06E+00	1.05E+00	1.48E+01
250	5.01E+01	1.03E+00	9.05E-01	4.15E+00	5.53E+02	3.09E+02	1.50E+01	9.60E-01	9.49E-01	1.02E+00	1.13E+00	1.48E+01
251	4.87E+01	1.02E+00	1.10E+00	4.20E+00	5.59E+02	3.07E+02	1.53E+01	1.15E+00	1.02E+00	1.04E+00	1.09E+00	1.50E+01
252	4.85E+01	1.06E+00	1.10E+00	4.19E+00	5.60E+02	3.09E+02	1.47E+01	1.29E+00	1.02E+00	1.01E+00	9.23E-01	1.50E+01
253	5.00E+01	1.01E+00	1.01E+00	4.19E+00	5.52E+02	3.08E+02	1.49E+01	1.20E+00	9.31E-01	9.35E-01	9.47E-01	1.50E+01
254	4.81E+01	1.02E+00	1.06E+00	4.30E+00	5.56E+02	3.06E+02	1.52E+01	7.39E-01	8.68E-01	1.04E+00	9.55E-01	1.50E+01
255	4.96E+01	1.03E+00	9.88E-01	4.25E+00	5.57E+02	3.08E+02	1.52E+01	7.56E-01	9.81E-01	9.64E-01	1.12E+00	1.49E+01
256	5.00E+01	1.06E+00	1.08E+00	4.12E+00	5.56E+02	3.09E+02	1.50E+01	9.05E-01	1.13E+00	1.06E+00	1.19E+00	1.47E+01
257	5.05E+01	1.03E+00	1.11E+00	4.25E+00	5.57E+02	3.08E+02	1.50E+01	1.14E+00	9.77E-01	9.46E-01	9.96E-01	1.50E+01
258	4.88E+01	1.07E+00	1.11E+00	4.12E+00	5.60E+02	3.09E+02	1.52E+01	1.29E+00	9.94E-01	9.61E-01	1.16E+00	1.50E+01
259	4.85E+01	1.01E+00	1.01E+00	4.21E+00	5.55E+02	3.09E+02	1.52E+01	1.30E+00	1.05E+00	1.15E+00	1.02E+00	1.48E+01
260	4.91E+01	1.03E+00	9.67E-01	4.25E+00	5.55E+02	3.09E+02	1.47E+01	8.49E-01	1.03E+00	8.93E-01	1.07E+00	1.48E+01
261	5.05E+01	1.07E+00	9.66E-01	4.19E+00	5.53E+02	3.08E+02	1.48E+01	1.23E+00	1.08E+00	8.89E-01	9.64E-01	1.50E+01
262	4.89E+01	1.01E+00	1.04E+00	4.16E+00	5.54E+02	3.08E+02	1.49E+01	1.09E+00	9.84E-01	1.02E+00	1.09E+00	1.50E+01
263	4.95E+01	1.05E+00	9.59E-01	4.15E+00	5.57E+02	3.08E+02	1.48E+01	7.53E-01	9.37E-01	9.28E-01	1.09E+00	1.50E+01
264	4.99E+01	1.06E+00	9.84E-01	4.27E+00	5.59E+02	3.08E+02	1.48E+01	1.24E+00	1.07E+00	1.01E+00	9.00E-01	1.47E+01
265	4.84E+01	1.06E+00	9.38E-01	4.28E+00	5.56E+02	3.08E+02	1.51E+01	9.67E-01	8.76E-01	9.21E-01	9.90E-01	1.48E+01
266	4.82E+01	1.07E+00	1.10E+00	4.28E+00	5.55E+02	3.07E+02	1.48E+01	1.29E+00	1.01E+00	1.02E+00	9.66E-01	1.48E+01
267	4.97E+01	1.03E+00	9.11E-01	4.38E+00	5.50E+02	3.07E+02	1.51E+01	9.41E-01	9.48E-01	1.02E+00	1.13E+00	1.49E+01
268	4.89E+01	1.04E+00	1.05E+00	4.33E+00	5.60E+02	3.08E+02	1.47E+01	8.69E-01	9.96E-01	8.98E-01	1.15E+00	1.49E+01
269	4.80E+01	1.06E+00	9.82E-01	4.28E+00	5.54E+02	3.06E+02	1.50E+01	9.45E-01	9.56E-01	1.01E+00	9.35E-01	1.50E+01
270	4.85E+01	1.00E+00	1.12E+00	4.24E+00	5.57E+02	3.08E+02	1.50E+01	1.19E+00	1.05E+00	9.54E-01	9.67E-01	1.50E+01
271	4.94E+01	1.04E+00	1.01E+00	4.14E+00	5.52E+02	3.08E+02	1.48E+01	1.29E+00	9.29E-01	8.23E-01	1.07E+00	1.50E+01
272	4.89E+01	1.01E+00	9.66E-01	4.31E+00	5.55E+02	3.06E+02	1.50E+01	8.49E-01	1.03E+00	9.34E-01	1.18E+00	1.49E+01
273	4.97E+01	1.07E+00	1.07E+00	4.20E+00	5.58E+02	3.08E+02	1.51E+01	8.62E-01	8.25E-01	1.15E+00	1.20E+00	1.48E+01
274	4.93E+01	1.06E+00	9.81E-01	4.18E+00	5.59E+02	3.09E+02	1.48E+01	8.29E-01	1.15E+00	1.07E+00	9.54E-01	1.49E+01
275	4.96E+01	1.05E+00	9.86E-01	4.14E+00	5.50E+02	3.09E+02	1.51E+01	1.07E+00	9.72E-01	9.80E-01	1.11E+00	1.48E+01
276	4.92E+01	1.02E+00	1.06E+00	4.25E+00	5.55E+02	3.07E+02	1.51E+01	1.05E+00	1.10E+00	9.32E-01	9.14E-01	1.50E+01
277	4.81E+01	1.08E+00	9.50E-01	4.24E+00	5.53E+02	3.08E+02	1.50E+01	8.97E-01	1.00E+00	8.78E-01	9.08E-01	1.49E+01
278	5.04E+01	1.01E+00	1.00E+00	4.12E+00	5.57E+02	3.09E+02	1.50E+01	1.24E+00	1.05E+00	1.01E+00	1.00E+00	1.48E+01
279	5.04E+01	1.02E+00	1.02E+00	4.20E+00	5.54E+02	3.07E+02	1.49E+01	8.07E-01	1.07E+00	1.03E+00	1.08E+00	1.49E+01
280	4.88E+01	1.01E+00	1.04E+00	4.33E+00	5.54E+02	3.09E+02	1.52E+01	7.65E-01	1.07E+00	8.93E-01	1.19E+00	1.50E+01
281	4.83E+01	1.03E+00	9.43E-01	4.17E+00	5.51E+02	3.06E+02	1.49E+01	9.68E-01	9.92E-01	1.02E+00	9.88E-01	1.49E+01
282	4.96E+01	1.03E+00	1.07E+00	4.20E+00	5.53E+02	3.08E+02	1.47E+01	1.09E+00	9.28E-01	1.03E+00	1.07E+00	1.50E+01
283	5.04E+01	1.03E+00	9.75E-01	4.25E+00	5.54E+02	3.07E+02	1.52E+01	9.92E-01	1.01E+00	1.15E+00	1.10E+00	1.49E+01
284	4.88E+01	1.03E+00	9.83E-01	4.32E+00	5.51E+02	3.06E+02	1.50E+01	1.28E+00	9.75E-01	9.60E-01	1.04E+00	1.50E+01
285	4.97E+01	1.04E+00	1.01E+00	4.18E+00	5.55E+02	3.09E+02	1.51E+01	7.91E-01	9.02E-01	1.10E+00	9.14E-01	1.50E+01
286	4.86E+01	1.05E+00	9.59E-01	4.26E+00	5.57E+02	3.07E+02	1.50E+01	1.01E+00	1.07E+00	1.13E+00	1.17E+00	1.47E+01
287	4.95E+01	1.07E+00	9.88E-01	4.31E+00	5.59E+02	3.09E+02	1.50E+01	1.09E+00	9.91E-01	1.04E+00	1.00E+00	1.47E+01
288	4.87E+01	1.07E+00	1.07E+00	4.20E+00	5.58E+02	3.07E+02	1.50E+01	1.11E+00	9.85E-01	1.13E+00	1.01E+00	1.48E+01
289	4.94E+01	1.07E+00	9.01E-01	4.15E+00	5.51E+02	3.06E+02	1.51E+01	1.18E+00	9.02E-01	1.09E+00	9.26E-01	1.48E+01
290	4.88E+01	1.04E+00	1.00E+00	4.10E+00	5.56E+02	3.07E+02	1.51E+01	8.69E-01	1.12E+00	1.07E+00	1.07E+00	1.49E+01
291	4.89E+01	1.03E+00	9.48E-01	4.35E+00	5.53E+02	3.07E+02	1.52E+01	1.21E+00	9.62E-01	1.07E+00	1.12E+00	1.49E+01
292	4.86E+01	1.04E+00	9.58E-01	4.24E+00	5.52E+02	3.09E+02	1.48E+01	7.12E-01	9.21E-01	1.02E+00	9.78E-01	1.48E+01
293	4.90E+01	1.07E+00	9.85E-01	4.14E+00	5.51E+02	3.09E+02	1.49E+01	8.00E-01	1.10E+00	8.56E-01	9.92E-01	1.49E+01
294	4.87E+01	1.01E+00	1.04E+00	4.15E+00	5.53E+02	3.09E+02	1.48E+01	8.72E-01	1.01E+00	1.02E+00	9.33E-01	1.48E+01
295	4.91E+01	1.01E+00	1.07E+00	4.22E+00	5.57E+02	3.07E+02	1.49E+01	1.02E+00	9.10E-01	1.06E+00	1.14E+00	1.50E+01
296	4.90E+01	1.02E+00	9.78E-01	4.19E+00	5.59E+02	3.07E+02	1.49E+01	8.25E-01	1.11E+00	8.99E-01	1.12E+00	1.48E+01
297	4.96E+01	1.00E+00	1.10E+00	4.20E+00	5.54E+02	3.07E+02	1.53E+01	1.09E+00	1.05E+00	1.04E+00	1.01E+00	1.49E+01
298	4.82E+01	1.02E+00	9.17E-01	4.20E+00	5.51E+02	3.08E+02	1.48E+01	1.13E+00	9.35E-01	1.04E+00	1.11E+00	1.50E+01
299	4.83E+01	1.07E+00	1.02E+00	4.22E+00	5.53E+02	3.06E+02	1.49E+01	9.51E-01	1.11E+00	1.01E+00	1.04E+00	1.50E+01
300	5.04E+01	1.01E+00	1.00E+00	4.20E+00	5.54E+02	3.06E+02	1.49E+01	1.28E+00	8.93E-01	1.08E+00	9.07E-01	1.48E+01

TableE-2: Correlation Matrix of Design

Correlation Matrix of Design

	1	2	3	4	5	6	7	8	9	10	11	12	13	14
1	1.00E+00	-7.29E-03	4.17E-03	2.61E-02	8.11E-03	1.31E-02	-9.08E-05	3.87E-03	2.09E-03	3.06E-03	2.45E-03	5.58E-03	2.36E-02	8.22E-03
2	-7.29E-03	1.00E+00	2.65E-03	-7.74E-03	4.15E-03	-2.54E-02	-1.13E-01	-2.63E-03	-1.45E-03	1.93E-03	7.41E-04	4.46E-03	7.17E-03	5.10E-03
3	4.17E-03	2.65E-03	1.00E+00	-2.78E-02	2.88E-01	1.25E-02	4.03E-03	4.50E-03	-1.49E-02	1.51E-02	-3.44E-04	-4.16E-03	-8.68E-03	-8.65E-03
4	2.61E-02	-7.74E-03	-2.78E-02	1.00E+00	-1.67E-03	-2.24E-02	-1.27E-02	2.57E-02	-9.18E-03	2.87E-02	-1.77E-03	-2.95E-03	-1.82E-02	2.32E-02
5	8.11E-03	4.15E-03	2.88E-01	-1.67E-03	1.00E+00	1.98E-02	9.80E-04	1.25E-02	-3.95E-04	1.57E-02	3.83E-03	-5.78E-03	8.79E-04	7.81E-03
6	1.31E-02	-2.54E-02	1.25E-02	-2.24E-02	1.98E-02	1.00E+00	1.21E-02	1.60E-02	1.32E-02	2.46E-02	1.28E-02	-6.67E-03	-1.63E-02	4.60E-03
7	-9.08E-05	-1.13E-01	4.03E-03	-1.27E-02	9.80E-04	1.21E-02	1.00E+00	2.51E-03	7.86E-03	1.12E-02	-9.65E-03	-6.59E-03	1.91E-03	-7.10E-03
8	3.87E-03	-2.63E-03	4.50E-03	2.57E-02	1.25E-02	1.60E-02	2.51E-03	1.00E+00	-9.76E-03	-6.94E-03	-5.65E-03	8.98E-03	-1.64E-02	-2.01E-02
9	2.09E-03	-1.45E-03	-1.49E-02	-9.18E-03	-3.95E-04	1.32E-02	7.86E-03	-9.76E-03	1.00E+00	-6.64E-03	1.30E-02	-8.17E-03	5.05E-03	-4.24E-03
10	3.06E-03	1.93E-03	1.51E-02	2.87E-02	1.57E-02	2.46E-02	1.12E-02	-6.94E-03	-6.64E-03	1.00E+00	-1.45E-02	-4.23E-03	-9.40E-03	6.78E-03
11	2.45E-03	7.41E-04	-3.44E-04	-1.77E-03	3.83E-03	1.28E-02	-9.65E-03	-5.65E-03	1.30E-02	-1.45E-02	1.00E+00	-7.79E-03	-3.95E-03	-5.87E-03
12	5.58E-03	4.46E-03	-4.16E-03	-2.95E-03	-5.78E-03	-6.67E-03	-6.59E-03	8.98E-03	-8.17E-03	-4.23E-03	-7.79E-03	1.00E+00	5.67E-03	5.40E-03
13	2.36E-02	7.17E-03	-8.68E-03	-1.82E-02	8.79E-04	-1.63E-02	1.91E-03	-1.64E-02	5.05E-03	-9.40E-03	-3.95E-03	5.67E-03	1.00E+00	-2.95E-03
14	8.22E-03	5.10E-03	-8.65E-03	2.32E-02	7.81E-03	4.60E-03	-7.10E-03	-2.01E-02	-4.24E-03	6.78E-03	-5.87E-03	5.40E-03	-2.95E-03	1.00E+00

REFERENCES

Aksan S.N., at el, (1993), "User Effects on the Thermal-Hydraulic Transient System Code Calculations", Nuclear Engineering and Design 14(1993)159-174.

Aksan SN, at el, (1995), "User Effects on the Transient System Code Calculation", NEA/CSNI/R(94)35.

Apostolakis G.(1999), "The Distinction between Aleatory and Epistemic Uncertainties Is Important: An Example From the Inclusion of Aging Effects into PSA", Proceedings of PSA "99, Washington, DC, 1999.

Bari, R.A., Park C.K. (1989), "Uncertainty Characterization of Data for Probabilistic Risk Assessment, Reliability Engineering and System Safety 26(1989)163-172.

Barre F., (1996), "The Role of Uncertainty in Code Develop ment", Proceedings of OECD/CSNI Workshop on Transient Thermal hydraulic and Neutronic Codes Requirements, Annapolis, Md, USA, 1996.

Barre F., at el (1995), "The Sensitivity Analysis by Adjoint Method for the Uncertainty Evaluation of the CATHARE 2 Code", Proceedings of 7th International Meeting on Nuclear Reactor Thermal hydraulic (NURETH 7), Saratoga Springs, NY USA.

Bayless P.D., Divine J.M. (1982), "Experiment Data Report for LOFT Large Break Loss-of-Coolant Experiment L2-5", NUREG/CR-2826, EGG-2210.

Benedetti, et al., "Potential influence of Three-Dimensional effects on PWR LOCA Behavior"

Benerjee S., at el (1997), "Top-Down Scaling Analyses Methodology for AP600 Integral Tests", INEL-96/0040

Bhattacharyya, A. K. and Amed, S. (1982)"Establishing data requirements for plant probabilistic risk assessment", Transaction of the American Nuclear Society, 43(1982) 477-478.

Bier, V.M., (1983)"A measure of uncertainty importance for components in fault trees", Transaction of American Nuclear Society 1983, pp384-385.

Birnbaum H., Zuckerman H.S., (1949), "A Graphical Determination of Sample Size for Wilks" Tolerance Limits", Annals of Mathematical Statistics, Vol. 20, Issue 2 (1949)313-316.

Borgonovo E., at el (2003), "Comparison of Global Sensitivity Analysis Techniques and Importance Measures in PSA" Reliability Engineering and System Safety 79(2003)175-185.

Borgonovo E., Apostolakis G.E. (2001), "A New Importance Measure for Risk-Informed Decision Making", Reliability Engineering and System Safety 72(2001)193-212.

Bovalini R., D"Auria F. (1993), "Scaling of the Accuracy of the Relap5/mod2 Code", Nuclear Engineering and Design 139(1993)187-203.

Bowker A., (1946), "Computation of Factors for Tolerance Limits on a Normal Distribution when the sample is Large", Annals of Mathematical Statistics, Vol. 17, Issue 2 (1946)238-240.

Boyack B.E., et al (2001), "Phenomenon Identification and Ranking Tables (PIRTs) for Loss-of-Coolant Accidents in Pressurized and Boiling Water Reactors Containing High Burnup Fuel", NUREG/CR-6744 LA-UR-00-5079, 2001.

Boyack B.E., at el (1990), "Quantifying Reactor Safety Margins Part 1: An Overview of the Code Scaling, Applicability, and Uncertainty Evaluation Methodology", Nuclear Engineering and Design 119(1990)1-15.

Brittain, I. and Aksan S.N., (1990) "OECD LOFT Large Break LOCA Experiments: Phenomenology and Computer Code Analyses," PSI Bericht Nr. 72, AEEW-TRS-1003, 1990

Burrows G.L., (1963), "Statistical Tolerance Limits-What Are They?" Applied Statistics, Vol 12, Issue 2 (1963)133-144.

Catton I., at el (1990), "Quantifying Reactor Safety Margins Part 6: Physically Based Method of Estimating PWR Large Break Loss of Coolant Accident PCT", Nuclear Engineering and Design 119(1990)109-117

Catton I, Lim H, (1994), "The impact of phenomenological uncertainties on an accident management strategy", Reliability Engineering and System Safety 45 (1994) 175-194.

Chen E.J., Kelton W.D., (2006) "Quantile and tolerance-interval estimation in simulation" European Journal of Operational Research 168 (2006) 520–540.

Cho J.G., Yum B.J.(1997), "Development and Evaluation of an Uncertainty Importance Measure in Fault Tree Analysis. Reliability Engineering and System Safety 57(1997)143-157.

Chun M H, at el, (2000), "An Uncertainty Importance Measure Using a Distance Metric for the Change in a Cumulative Distribution Function", Reliability Engineering and System Safety 70(2000)313-321.

CSNI-NEA, Uncertainty Methods Study, Report NEA-CSNI/R (97)35, 1998

CSNI-NEA, "Coolant System Behavior (PWG2) Separate Effects Test Matrix for Thermal-Hydraulic Code Validation Volume I, Phenomena Characterization and Selection of Facilities and Tests, OECD/GD(94)82 (July 1994)

Code of Federal Regulations 10, Parts 1 to 50, U.S. Government Printing Office, Washington D.C. (2003).

Congdon P., (2003), "Applied Bayesian Modeling", Wiley & sons, West Sussex, UK.

Conover W J. (1971), "Practical nonparametric statistics", New York, Wiley; 1971. p. 99–105.

D'Auria F. at el, (1998), "UMAE Uncertainty Methodology," NEA-CSNI report, Nuclear Energy Agency-Committee on the Safety of Nuclear Installations.

D'Auria F. et al, (1998), "Overview of Uncertainty Issues and Methodologies Proceeding ECD/CSNI Seminar on Best Estimate Methods in Thermal Hydraulic Analysis, Ankara 1, pp437-458.

D'Auria F. et al, (2006), "State of the Art in Using Best Estimate Calculation Tools in Nuclear Technology, Nuclear Engineering and Technology, 38 (2006)1.

D'Auria F., Giannotti W. (2000), "Development of a Code with the Capability of Internal Assessment of Uncertainty", Journal of Nuclear Technology, 131(2000)159-196.

D'Auria F., Marsili P. (2000), "The Capability of Internal Assessment of Uncertainty", CSNI Workshop on Advanced TH and Neutronic Codes: Current and Future Applications, Barcelona, Spain

.D'Auria F. et al., "Advancements in Planning of an IAU-Code, University of Pisa Report".

D'Auria F., at el (1991), "Scaling of Natural Circulation in PWR Systems", Nuclear Engineering and Design 132(1991)187-205.

Devooght J., (1994), :Uncertainty Analysis in Dynamic Reliability", Proceedings of PSAM - 4, Berlin: Springer.

Droguett E.L., (1999), "Methodology for the Treatment of Model Uncertainty, Ph.D Thesis; University of Maryland-College Park.

Droguett EL, Mosleh A. (2001)"Assessment of model uncertainty - a Bayesian approach". Proceedings of ESREL 2001 Conference, Torino, Italy.

Efron B., Tibshirani R.J., (1993), "An Introduction to the Bootstrap", Chapman and Hill, New York.

Expert Choice V.11, "Analytic Hierarchy Process (AHP), http://www.expertchoice.com.

Fei L., (2000), "Probabilistic Modeling for Fracture Mechanics Studies of Reactor Vessel with Characterization of Uncertainties" Ph.D Dissertation, University of Maryland, College park.

Ferson S, Ginzburg L.R., "Different Methods are Needed to Propagate Ignorance and Variability", Reliability Engineering and System Safety 54(1996)133-144.

Frank M. (1998)"Assessment of the Cassini Mission Nuclear Risk with Aleatory and Epistemic Uncertainties", Proceedings of PSAM -4, Berlin: Springer.

Frey H.C., (1993), "Separating Variability and Uncertainty in Exposure Assessment: Motivations and Methods", Proceedings of the 86th Annual Meeting Air and Waste Management Association, Pittsburgh PA.

Glaeser H., at el, (1998), "NEA-CSNI report; GRS Analyses for CSNI Uncertainty Methods Study (UMS)". Nuclear Energy Agency-Committee on the Safety of Nuclear Installations, 1998.

Griffith M .., “Discussion on CSUA PIRT Results”, 2003, Massachusetts Institute of Technology

Guba A, Makai M, Pa´l L. Statistical aspects of best estimate method-I. Reliability Engineering and System Safety 80 (2003) 217–32.

Hanson R.G ., at el (1992), “Development of a Phenomena Identification and Ranking Table (PIRT) for a Postulated Double-Ended Guillotine Break in a Production Reactor”, Nuclear Engineering and Design 136 (1992) 335-346.

Haskin FE , at el (1996), “Efficient Uncertainty Analysis Using Fast Probability Integration”, Nuclear Engineering and Design 166 (1996) 225-248

Helton, J.C. (1996), "Probability, Conditional Probability and Complementary Cumulative distribution Functions in Performance Assessment for Radioactive Waste Disposal." Reliability Engineering and System Safety 54: 145-163.

Helton J.C ., (2006), “Survey of Sampling-Based Methods for Uncertainty and Sensitivity Analysis”, Sandia Report SAND 2006-2901.

Helton J.C ., (2000), “Sampling-Based Methods for Uncertainty and Sensitivity Analysis”, Sandia Report:SAND99-2240.

Helton J.C., (2003), “Latin Hypercube Sampling and the Propagation of Uncertainty Analysis of Complex Systems”, Reliability Engineering and System Safety 81(2003)23-69.

Helton J.C ., (2002), “Latin Hypercube Sampling and the Propagation of Uncertainty Analysis of Complex Systems”, Sandia Report SAND 2001-0417.

Helton J.C . at el, (2004), “Alternative Representations of Epistemic Uncertainty”, Reliability Engineering and System Safety 85(2004)1-10.

Helton J.C. (1993), "Uncertainty and Sensitivity Analysis Techniques for Use in Performance Assessment for Radioactive Waste Disposal", Reliability Engineering and System Safety 42(1993)327-367.

Hofer H. (2002) "approximate epistemic uncertainty analyses approach in the presence of epistemic and aleatory uncertainties". Reliability Engineering and System Safety 77 (2002) 229–238.

Hofer E. (1996), "When to separate uncertainties and when not to separate", Reliability Engineering and System Safety 1996; 54:113–8.

Hoffman, F.O., and Hammonds, J.S. (1994), "Propagation of Uncertainty in Risk Assessments: The Need to Distinguish between Uncertainty due to Lack of Knowledge and Uncertainty due to Variability", Risk Analysis 14(5):707-712.

Hora S. "Aleatory and epistemic uncertainty in probability elicitation with an example from hazardous waste management". Reliability Engineering and System safety 54 (1996) 217-233.

Iman, R.L. & Hora, S.C. (1990), "A robust measure of uncertainty importance for use in fault tree system analysis." Risk analysis 10(1990)3:401-406.

Iman RL, at el, (1984), "A Fortran 77 Program and User"s Guide for the Generation of Latin Hypercube and Random Samples for Use With Computer Models", NUREG/CR-3624, SAND83-2365.

Iman RL, Conover WJ, (1982) A Distribution-Free Approach to Inducing Rank Correlation "among Input Variables

Iman RL, at el, (2002), "Assessing Hurricane Effects Part 1. Sensitivity Analysis", Reliability Engineering and System Safety 78 (2002) 131-145.

Iman R.L., at el, (2002), "Assessing Hurricane Effects Part 1. Uncertainty Analysis", Rliability Engineering and System Safety 78 (2002) 146-178.

Iman R.L., (1987), "A Matrix Based Approach to Uncertainty and Sensitivity Analysis for fault Trees", Risk Analysis Vol. 7, No. 1.

Isukapalli S.S., at el, "Stochastic Response Surface Methods (SRSMs) for Uncertainty Propagation: Application to Environmental and Biological Systems", Journal of Risk Analysis.

Joucla J., Probst P. (2006), "Rank Statistics and Bootstrap: A more Precise Evaluation of the 95th Percentile in Nuclear Safety LB-LOCA Calculations", Proceedings of ICONE 14 Conference, Miami FL, USA.

Kampas F.J., (1998), "Deconvolution of Variability and Uncertainty in the Cassini Safety Analysis. Proceedings of PSAM-4, Berlin: Springer.

Klein S.A., (2006), "EES Engineering Equation Solver for Microsoft Windows Operating Systems Commercial and Professional Versions".

Kloos M., "Discussion on GRS Methodology for TH Uncertainty Analysis", April 2006, University of Maryland.

Kljenak I., Prosek A., (1997), "Development of a Phenomena Identification and ranking Table for a Small-Break Loss-Of Coolant Accident Scenario", Proceeding of 4th Regional Meeting of Nuclear Energy in Central Europe, Bled, Slovenia.

Krzykacz-Hausmann B., (2005) "Sensitivity Analysis of Monte Carlo Estimates from Computer Models in the Presence of Epistemic and Aleatory Uncertainties" Report to Los Alamos National Laboratory.

Kurowicka D. and Cooke R., Uncertainty Analysis with High Dimensional Dependence Modeling", John Wiley & Sons, Ltd, New York 2006

Lawson A.B., (2003) "Disease Mapping with Winbugs and MLwin, John Wiley & Sons, ltd., San Francisco.

Lelloche C.S.., at el (1990), "Quantifying Reactor Safety Margins Part 4: Uncertainty Evaluation of LBLOCA Analysis Based on TRAC-PF1/MOD1", Nuclear Engineering and Design 119(1990)67-95.

Lee SY and Ban CH (2004), "Code-Accuracy Based Uncertainty Estimation (CABUE) Methodology for large-Break Loss-of-Coolant Accidents", Nuclear Technology 148(2004)335-347.

Lubbesmeyer, D., Post-Test Analysis and Nodalization Studies of OECD LOFT Experiment LP-LB-1 with RELAP5/MOD2 cy36-02, PSI-Bericht Nr. 91, Paul Scherrer Institute, Villigen, Switzerland, March 1991.

Madeira A., Giannotti W., D"Auria F. (1999), "Sample Use of CIAU for a Two Loop Pressurized Water Reactor", Proceedings of Nureth-9, San-Francisco, CA

Makai M, Pa´l L. Reply to contribution of Graham B. Wallis. Reliability Engineering and System Safety 80 (2003)313–317

Makai M, Pa´l L. Best Estimate Method and Safety Analysis II. Reliability Engineering and System Safety 91 (2006)222–32

Martin R. P., O"Dell L. D., AREVA"s Realistic Large Break LOCA Analyses Methodology, Nuclear Engineering and Design 235(2005)1713-1725

Massoud M., "Discussion on Code Structure Complexity", November 2005, University of Maryland

Modarres M. (1999) "Reliability Engineering and Risk Analysis: A Practical Guide. Marcel Dekker INC. New York

Modarres M., "Risk Analysis in Engineering; Techniques, Tools, and Trends", Springer, New York, 2006

Mosleh, A., Siu N., at el. (1995) "Model Uncertainty: Its Characterization and Quantification", Center for Reliability Engineering - University of Maryland.

Murphy R.B., (1948), "Non-Parametric Tolerance Limits", Annals of Mathematical Statistics, Vol. 19, Issue 4 (1948)581-589.

Nalezny C.L., (1985), "Summary of the Nuclear Regulatory Commission"s LOFT Program Research Findings", NUREG/CR-3005, EGG-2231.

Newland D.B., "The developing Roles of "Best-Estimate" Thermal-Hydraulics Calculations and Uncertainty Analysis in Licensing in Canada", Proceedings of OECD/CSNI Seminar on Best-Estimate Methods in Thermal Hydraulic Safety Analysis, Turkey 1998.

Neal RM., (1993), "Probabilistic Inference Using Markov Chain Monte Carlo Methods", Technical Report CRG-TR-93-1, University of Toronto.

Nilsen T, Aven T, (2003), "Models and Model Uncertainty in the Context of Risk Analysis", Reliability Engineering and System Safety 79 (2003)309-317

Nissley M.E., "Realistic Large-Break LOCA Evaluation Methodology Using the Automated Statistical Treatment of Uncertainty Method (ASTRUM)", Westinghouse Propriety Report, WCAP-1 6009-P, 2003

Nutt W.T., Wallis G.B., Evaluation of nuclear safety from the outputs of computer codes in the presence of uncertainties. Reliability Engineering and System Safety 83 (2004) 57–77

Oberkampf W L, (2002), "Error and Uncertainty in Modeling and Simulation", Iman R L, at el, (2002), "Assessing Hurricane Effects Part 1. Sensitivity Analysis", Reliability Engineering and System Safety 75 (2002)333-357.

Oberkampf W L, (2004), "Challenge Problems: Uncertainty in System Response Given Uncertain Parameters" Reliability Engineering and System Safety 85(2004)11-19.

O'Hagan A., Oakley J.E., Probability is Perfect, but We Can't Elicit it Pefectly, 2002

Orechwa Y., (2004)"Best Estimate Analysis and Decision Making Under Uncertainty", Proceedings of International Meeting on Updates in Best Estimate Methods in Nuclear Installation Safety Analysis, Washington, D.C., 2004

Orechwa Y. (2005), "Comments on evaluation of nuclear safety from the outputs of computer codes in the presence of uncertainties by W.T. Nutt, G.B. Wallis. Reliability Engineering and System Safety 87 (2005) 133–135.

OECD/GD (94)82)

OECD/NEA (1994), "Separate Effects Test Matrix for Thermal-Hydraulics Validation, Volume1-Phenomena Characterization and Selection of facilities and Tests-". NEA/CSNI/R(94)82

OECD/NEA (1984), "LOFT Experiment LP-LB-1 Data Results", Report-09010002.

NRC Databank, (2005), "LOFT Nodalization for LB-1 Test of LOFT test facility".

OECD/NEA-CSNI, (19096),"CSNI Integral test facility validation matrix for the assessment of thermal-hydraulic codes for LWR LOCA and transients", OCDE/GD(97)12.

Pal L., Makai M., (2004) "Remarks on statistical aspects of safety analysis of complex systems". arXiv:physics/0308086

Pal L., Makai M., (2005), "Statistical Considerations of safety analysis". arXiv:physics/0511140 v1

Park, C. K. & Bari, R. A., (1985), "An information-theoretic approach to uncertainty importance", BNL-NUREG-35236.

Porn K., (1997), "A Decision-Oriented Measure of Uncertainty Importance for Use in PSA", Reliability Engineering and System Safety 56(1997)17-27.

Pourgol-Mohamad M, Modarres M., Mosleh A., (2006)"A General Thermal Hydraulics Uncertainty Analysis Methodology", Proceedings of PSAM 8 conference, May 2006, New Orleans, LA

Pourgol-Mohamad M, Modarres M., Mosleh A., (2007) "Integrated Methodology for Thermal Hydraulics Uncertainty Analysis with Application", To be Submitted to Nuclear Technology Journal

Pourgol-Mohamad M., Mosleh M., Modarres M., (2006), " Treatment of Uncertainties; Output Updating in Complex thermal-hydraulics (TH) Computational Codes, ,Proceedings of ICONE14 Conference, July 2006, Miami, FL

Pourgol-Mohamad M., Mosleh A., Modarres M., (2006) "Modified Phenomena Identification and Ranking Table (PIRT) for Uncertainty Analysis; Proceedings of ICONE14 Conference, July 2006, Miami, FL

Pretel C., at el, (2001), "Qualifying, Validating and Documenting a Thermal-Hydraulic Code Input Deck", NEA/CSNI/R(2001)2/Vol.2.

Prosek A., (2000), "Optimal Statistical Estimator for Efficient Generation of the Response Surface", Proceedings of Meeting on "Best Estimate Methods in Nuclear Installation Safety Analysis (BE-2000), Washington DC, 2000.

Prosek, A., D'Auria F, Mavko, B., Review of quantitative accuracy assessments with fast Fourier transform based method (FFTBM), Nuclear Engineering and Design, 217 (2002) 179-206

Reeder D.L., "Loft System and Test Description", NUREG/CR-0247, TREE-1208, July 1978.

Reiss R.D., Ruschendorf L., (1976), "On Wilks' Distribution-Free Confidence Intervals for Quantile Intervals", Journal of the American Statistical Association, Vol. 71, Issue 356(1976)940-944.

RELAP5 Code Development Team, "RELAP5/MOD 3.3 Code Manual", NUREG/CR-5535/Rev1.

Rohatghi U.S., at el, (198?), "Uncertainty in Modeling and Scaling of Critical Flow in TRAC-PF1/MOD1", Report to Brookhaven National Laboratory.

Ronen Y ED, (1988), "Uncertainty Analysis", CRC Press, Inc, Boca Raton, FL, 1988

Rust S., McMillan N., and Iroz-Elardo N., A Bayesian Approach for Assessing SHEDS-Wood Model Uncertainty. Report to the USEPA Office of Research and Development, 2005

Saaty T.L., (2001) "Models, methods, concepts & applications of the analytic hierarchy process", Kluwer Academic Publishers, Boston 2001.

Saltelli A., at el, Sensitivity Analysis, John Willey, New York, 2001

Scheffe H., Tukey J.W. (1944), "A Formula for Sample Sizes for Population Tolerance Limits", Annals of Mathematical Statistics, Vol. 15, Issue 2 (1944)217.

Shaw, R.A., et al., Development of a Phenomena Identification and Ranking Table (PIRT) for Thermal-Hydraulic Phenomena during a PWR Large-Break LOCA, NUREG/CR-5074.

Somerville P.N. (1958), "Tables for Obtaining Non-Parametric Tolerance Limits", Annals of Mathematical Statistics, Vol. 29, Issue 2 (1958)599-601.

Song J.H., Bae K.H., (2000), "Evaluation of Analytically scaled models of a pressurized water reactor using the Relap5/Mod3 Computer Code, Nuclear Engineering and Design 199(2000)215-225

Studsvik Energiteknik, (1979a)"The Marviken Full Scale Critical Tests; Description of the Test Facility", Joint Reactor Safety Experiments in the Marviken, MXC-101.

Studsvik Energiteknik, (1979b), "The Marviken Full Scale Critical Tests; Data Accuracy", Joint Reactor Safety Experiments in the Marviken, MXC-103.

Studsvik Energiteknik, (1979c), "The Marviken Full Scale Critical Tests; Measurement System", Joint Reactor Safety Experiments in the Marviken, MXC-102.

Technical Program Group, "Quantifying Reactor Safety margins: Application of Code Scaling, Applicability, and Uncertainty Evaluation Methodology to a Large Break Loss of Coolant Accident," Technical report NUREG/CR-5249 EG&G Idaho, Inc, 1989

Trunaco T., (1998), "Prediction and Uncertainty in Computational Modeling of Complex Phenomena: A Whitepaper", SAND 98-2776

UMD-AHP

USNRC, "Emergency Core Cooling Systems, Revisions to Acceptance Criteria, "Federal Register, 53, 180, September 16, 1988.

USNRC Regulatory Guidance 1.157., "Best-Estimate Calculations of Emergency Core Cooling System Performance," May 1989

Wald A. (1943), "An extension of Wilks method for setting tolerance limits", Ann Math Stat 1943;14(1):45–55.

Wald A. (1946a), "Tolerance Limits for a Normal Distribution", The Annals of Mathematical Statistics, Vol. 17, No. 2. 1946 pp. 208-215

Wald A. (1946b), "Setting of Tolerance Limits When the Sample is Large", Annals of Mathematical Statistics, Vol. 13, Issue 4 (1946)389-399.

Wang D., Shumway R.W. (2004), "TRACE Simulations of LOFT Large Break Tests", ISL-NSAD-TR-04-23.

Wallis G.B., Ransom V.R. (2002), "Assessing Uncertainty in Code Predictions", A White paper for USNRC.

Wallis G B. (2003), "Contribution to the paper Statistical aspects of best estimate method-1 by Attila Guba, Makai M., Pa´l L", Reliability Engineering and System Safety 80 (2003)309–11.

Wallis G B, Nutt W T. Reply to „Comments on „Evaluation of nuclear safety from the outputs of computer codes in the presence of uncertainties. Reliability Engineering and System Safety 83 (2004) 57–77.

Wallis G.B., (2005), "Evaluating the probability that the outputs of a computer code with random inputs will meet a set of evaluation criteria. Reliability Engineering and System Safety xx (2005) 1-8.

Wickett A.J., at el, "Quantification of Large LOCA Uncertainties", AEA Report No. LHT 1.1.8, Nov. 1991

Wickett AJ, Neill AP, (1990), "Advanced LOCA Code Uncertainty Assessment: A Pilot Study", AEEW -R2508, Nov. 1990.

Wilks SS. (1941), "Determination of sample sizes for setting tolerance limits", Ann Math Stat 1941;12:91–6.

Wilks SS. Statistical prediction with special reference to the problem of tolerance limits. Ann Math Stat 1942;13:400–409.

Wilson G.E. and Boyack B.E., (1998), "The role of the PIRT process in experiments, code development and code applications associated with reactor safety analysis. Nuclear Engineering and Design," 186 (1998) 23-37.

Wilson G.E., et.al, (1997), "Phenomena Identification and Ranking Tables for Westinghouse AP600 Small Break Loss-of-Coolant Accident, Main Steam Line Break, and Steam Generator Tube Rupture Scenarios". INEL-94/0061, Rev.2 or NUREG/CR-6541.

Winkler, R. L. (1996). "Uncertainty in Probabilistic Risk Assessment." Reliability Engineering and System Safety 54(2-3): 95-111

Wulff W., at el(1990), "Quantifying Reactor Safety Margins Part 3: Assessmen and Ranging of Parameters", Nuclear Engineering and Design 119(1990)33-65.

Wulff W., (1996), "Scaling of Thermal-Hydraulic Systems", Nuclear Engineering and Design 163(1996)359-395.

XU D., (1999), "Energy, Entropy and Information Potential for Neural Computation", Ph.D Dissertation; University of Florida.

Young M.Y., at el, (1998a), "Application of code scaling applicability and uncertainty methodology to

Young M.Y., at el, (1998b), "Best Estimate Analysis of the Large Break Loss of Coolant Accident", Proceedings of ICODE-6.

Zio E., Apostolakis GE., "Two Methods for the Structured Assessment of Model Uncertainty by Experts in Performance Assessment of Radioactive Waste Repositories", Reliability Engineering and System Safety 54(1996)225-241.

Zuber N., at el (1990), "Quantifying Reactor Safety Margins Part5: Evaluation of Scale-Up Capabilities of Best Estimate Codes", Nuclear Engineering and Design 119(1990)97-10715.

.